THE

PHYSICAL REVIEW

A Journal of Experimental and Theoretical Physics Established by E. L. Nichols in 1893

VOL. 53, NO. 1 JANUARY 1, 1938 SECOND SERIES

Edward Leamington Nichols

EDWARD LEAMINGTON NICHOLS was born in Leamington, England, on September 14, 1854, of American parents. After his graduation at Cornell in 1875 he studied at the universities of Leipzig, Berlin and Göttingen, and from the latter university received the degree of doctor of philosophy in 1879. During the year 1879–80 he held a fellowship in the Johns Hopkins University and in the following year was one of the assistants of Edison in the famous Menlo Park Laboratory. His first teaching position was that of professor of physics and chemistry in Central University, Kentucky, where he remained for two years. In 1883 he went to the University of Kansas as professor of physics and astronomy. In 1887 he returned to Cornell, where he remained as head of the department of physics until his retirement from teaching in 1919. He died in West Palm Beach, Florida, on November 10, 1937.

Nichols' activity as an investigator began while he was still a student and extended to within only a few years of his death. Neither lack of facilities nor pressure of other duties could lessen his interest or greatly reduce his activity. A firm believer in the value of scientific research to humanity, he contributed through his experimental work to almost every branch of the physics of his day. His chief interest, however, was in problems connected with light. In the early years his work in the fields of physiological optics and of illumination was of especial importance. During the last thirty years he devoted himself to the experimental study of the luminescence of solids and liquids. In recognition of his work in these fields, in each of which he was a pioneer, he was awarded the Elliot Cresson Medal of the Franklin Institute, the Ives Medal of the Optical Society, and the Rumford Medal of the American Academy and was made an honorary member of the Illuminating Engineering Society and of the Optical Society of America. In the case of the former society Nichols and Edison were for many years the only recipients of this honor.

Nichols' work as an investigator represents only one part of his service to American physics. In many other ways his stimulating influence has been important and far-reaching. Readers of this journal will think first of the influence he has exerted through the establishment of the *Physical Review*. It was Nichols who founded the Review in 1893 and it was he who served as its editor-in-chief during the difficult early years.

Previous to 1893 there was no journal in this country devoted exclusively—or even primarily—to physics and the need of more adequate provision for publication had been keenly felt. It was obvious that at that time a journal of physics could not be self-supporting; and the number of active physicists fifty years ago was too small to make any cooperative plan of publication practicable. Having convinced himself that the physicists of the country would welcome the establishment of a journal, and with the encouragement and understanding support

of the president of the university, Jacob Gould Schurman, Nichols made an appeal to the trustees of Cornell University for financial aid. This was granted and the first number of the *Physical Review* was published in July, 1893.

Nichols remained editor-in-chief for twenty years and during this period the growth of the Review, both in circulation and in size, was rapid and continuous. Even before the organization of the Physical Society the material to be published increased more rapidly than the income and it was not until 1910 that the journal became self-supporting. In 1913, after a balanced budget had been maintained for two years and when the American Physical Society, with six hundred members, had become strong enough to ensure its continued support, Nichols retired from his duties as editor and the Review was transferred to the Society.

To estimate the importance of Nichols' service to American physics we must recall the conditions in this country at the time he began his scientific career in 1880. There was no general interest in physics, or in science generally, and very little appreciation of the importance of scientific work. Very few universities were equipped for anything more than undergraduate instruction in the sciences; and in the minds of many there existed a feeling that scientific investigation was hardly a proper function of the college teacher. Not only was there no journal of physics for the publication of results but except for the annual meeting of the American Association for the Advancement of Science there was no opportunity for physicists to get together for discussion. Even when conditions otherwise were favorable it was almost impossible to obtain financial support for scientific work.

Nichols was one of the small group of enthusiastic physicists who went ahead in spite of these conditions; and no member of this group was more active or more successful than he in stimulating research activity in physics and in developing a more general appreciation of its importance. At every gathering of physicists Nichols was present and contributed not only the results of his experimental work but the inspiration of his own enthusiasm. Through his students his influence was carried far and wide. Shortly before the time of his retirement the heads of the departments of physics in thirty-five colleges in this country and in Canada, fifteen of them state universities, were men who had received their physics training from him—and with it his firm belief in the value of scientific research and some measure of his enthusiasm. He was one of the small group that organized the American Physical Society in 1899 and later one of the society's most active members. As president of the Physical Society, of Sigma Xi, and of the American Association for the Advancement of Science he kept continually before the public the importance of scientific work and in this way also helped to prepare the way for the remarkable progress of recent years. American physicists can give no better testimony of their indebtedness to him than by striving to increase still further the usefulness of the journal which he founded and by keeping alive the enthusiasm and the high scientific ideals which were so characteristic of his life and work.

ERNEST MERRITT

Nuclear Disintegrations Produced by Cosmic Rays

ROBERT B. BRODE AND MERLE A. STARR
Department of Physics, University of California, Berkeley, California
(Received November 4, 1937)

From a study of 20,500 Wilson cloud chamber photographs, ten nuclear disintegrations have been identified in which heavily ionizing tracks are produced. These disintegrations are associated with the cosmic radiation as they are usually observed in time coincidence with the passage of other cosmic-ray particles through the chamber. The ejection of a number of heavy particles from a single source is interpreted as an "evaporation" from a highly excited nucleus.

NUCLEAR disintegrations and strongly ionizing particles have been found in the cosmic radiation by a number of observers.[1–6] Anderson and Neddermeyer[1] reported from a study of 10,543 pictures taken at sea level, 11 unambiguous cases of strongly ionizing cosmic-ray particles. Their observations at 4300 meters elevation indicated a large increase in the number of strongly ionizing particles. At both sea level and 4300 meters elevation several cases of disintegrations were observed.

From a study of 8500 photographs we reported 87 heavy tracks.[4] The greater yield of strongly ionizing tracks found in our photographs can be explained by the large volume of our chamber which was 30 cm in diameter and 10 cm deep. Anderson and Neddermeyer's chamber was 15 cm in diameter and 2 cm deep. It took about one second for the clearing field to sweep the ions out of the illuminated region of our chamber and this greatly increased the chance of observing a heavy particle that did not trip the Geiger counters.

A total of 20,500 counter tripped photographs have now been taken. In these pictures we found 161 heavy tracks that passed through the chamber a short time before the Geiger counters were tripped by some other particle. Thirty-two sharp heavy tracks were observed that apparently tripped the counters. Ten disintegrations were found with a total of 22 heavy tracks associated with them. Altogether 215 heavy tracks were observed or an average of about one heavy track to 100 photographs. All of the disintegrations observed occurred in the walls of the chamber or in pieces of metal placed in the chamber.

The disintegration shown in Fig. 1 originated in the rear of the lead plate near its lower surface. The tracks seen are due to particles projected forward through the illuminated region of the chamber and into the front glass. The apparent disappearance of the tracks near the plate is due to the location of the source behind the illuminated region. As the disintegration was near the bottom of the lead plate the two heavy tracks above the plate have passed through more than two centimeters of lead before entering the chamber. In this disintegration there are at least 4 charged particles with a mass apparently greater than that of an electron. The nature of the 17 light tracks radiating from the disintegration is uncertain. They could be electrons and positrons, or particles of heavier mass with velocities near the velocity of light.

In Fig. 2 a heavy particle is apparently the result of the passage of a penetrating particle through the lead plate. Three disintegrations of this type have been observed. This could have been a disintegration produced by a photon in which one heavy and two light tracks emerge from the lead plate. The light track below the plate is nearly a linear continuation of the light track above the plate. Because of this it seems possible that this type of disintegration is produced by a high speed charged particle that knocks out of an atom a single heavy charged particle.

[1] C. D. Anderson and S. H. Neddermeyer, Phys. Rev. **50**, 263 (1937).
[2] P. Auger and P. Ehrenfest Jr., J. de phys. et rad. **8**, 204 (1937).
[3] P. M. S. Blackett (see E. Bretscher, *Kernphysik* (J. Springer, 1936) p. 108).
[4] R. B. Brode, H. G. MacPherson and M. A. Starr, Phys. Rev. **50**, 581 (1936).
[5] J. Crussard and L. Leprince-Ringuet, J. de phys. et rad. **8**, 213 (1937).
[6] P. Kunze, Zeits. f. Physik **83**, 1 (1933).

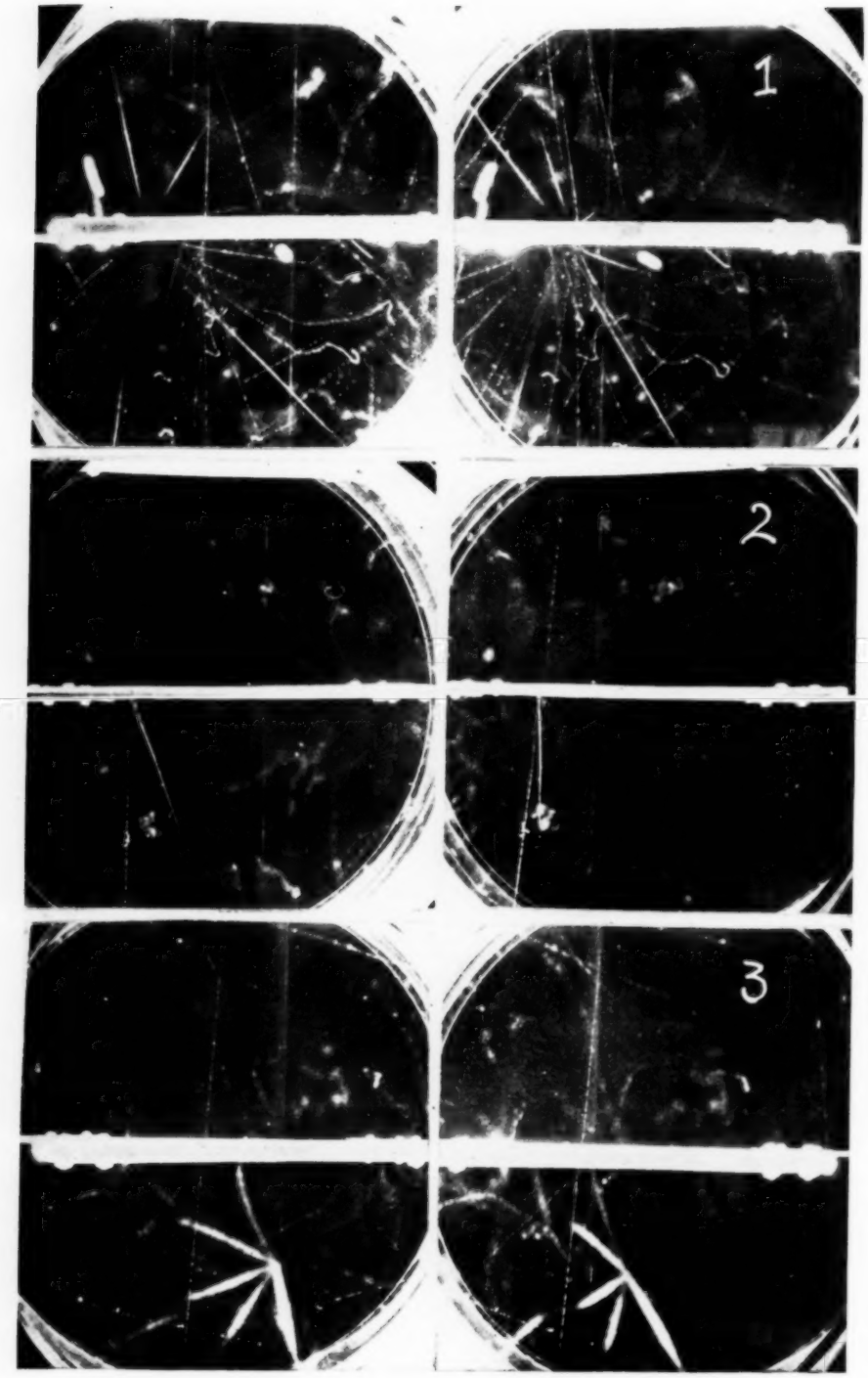

FIG. 1. A nuclear disintegration from an atom in a lead plate. Four heavy tracks and seventeen light tracks originate near the bottom of the plate and behind the illuminated region of the cloud chamber.

FIG. 2. A high speed light particle has apparently produced a disintegration in which a single heavy particle is sent out of the lead plate.

FIG. 3. A nuclear disintegration occurring in the glass plate at the front of the chamber. The breadth and distortion of the tracks are due to the fact that the disintegration occurred about a second before the expansion of the chamber.

Because of the small clearing field a heavy track can be seen in the chamber if it was formed within a second before the expansion. Fig. 3 shows a disintegration that was produced at the surface of the glass plate about a second before the expansion was produced by a penetrating particle. In this time the negative ions have been drawn to the center of the illuminated part of the chamber. Any lightly ionizing particles that might have accompanied this disintegration would have diffused so as to be no longer visible against the general chamber background.

In another chamber (18 cm in diameter and 8 cm deep) experiments are in progress for the measurement of the specific ionization of the cosmic-ray particles. The expansion has been intentionally delayed about $\frac{1}{2}$ second after the arrival of the cosmic ray to permit the ions to diffuse. In this way the individual drops can be counted. A picture taken in the course of adjustment of this chamber is shown in Fig. 4. The disintegration shows 2 heavy, 2 medium and 7 light tracks. This chamber was in a magnetic field of 1600 gauss. Except for two electron tracks, $H\rho = 18{,}000$ and 6000, none of the particles has an $H\rho$ of less than 5×10^5.

If the particles ejected by a disintegration are distributed at random in direction, less than half of them would be seen in the chamber if they started at the wall. The number of particles per disintegration should in these cases be at least twice the number observed. In Fig. 3 five heavy tracks are directed into the chamber and hence the probable number of heavy tracks sent out from this disintegrating atom is of the order of ten. The cloud chamber gives no estimate of the number of neutrons ejected by disintegrations. Since neutrons are more abundant than protons in the nuclei of all but the lightest elements, the number of neutrons ejected is quite possibly equal to or greater than the number of protons.

The time coincidence of most of these disintegrations with other cosmic-ray particles indicates that they are produced by some component of the cosmic radiation. In some cases the heavy particle appears to be directly ejected by the action of a charged particle. The observation of atoms disintegrating into a number of lighter particles is consistent with the "evaporation" model of nuclear disintegration discussed by Bohr.[7] In this model a nucleus that acquires a great excess of energy soon shares this energy among the elementary particles in the nucleus. This excess of energy leaves the nucleus by the "evaporation" of a number of particles, all with about the same energy.

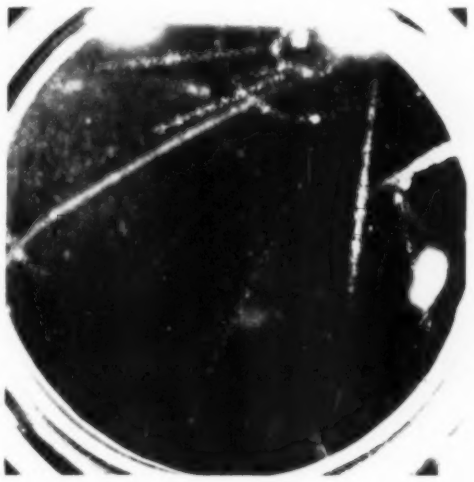

FIG. 4. In the photographing of this disintegration the expansion of the chamber was delayed about $\frac{1}{2}$ second. A magnetic field of 1600 gauss deflects appreciably only two of the electrons.

[7] N. Bohr, Science **86**, 161 (1937).

The Production of Cosmic-Ray Showers in Lead

MERLE A. STARR
University of California, Berkeley, California
(Received November 4, 1937)

Photographs were taken of cosmic-ray showers arising in lead plates of various thickness placed in turn inside a Geiger counter controlled cloud chamber. These showers are classified according to the number of particles in the shower and according to the manner of production, whether by an ionizing particle or by nonionizing radiation. The average size of showers was found to increase with the plate thickness. Studies of the frequencies of showers of different sizes as a function of plate thickness show that electron-produced and photon-produced showers occur in approximately equal numbers and are of the same character. These facts give support to the theories of Carlson and Oppenheimer and of Bhabha and Heitler. They consider the shower to be the result of repeated subdivision of incident radiation through pair production by gamma-rays and through radiative losses of high energy electrons giving rise to other gamma-rays. Eight percent of the electrons striking lead plates near seven millimeters thick gave rise to showers. About an equal number of showers from gamma-rays were present.

INTRODUCTION

A NUMBER of cloud chamber photographs[1] have been published showing large cosmic-ray showers in which electrons and γ-rays passing through lead plates have given rise to secondary particles. Many such showers are so complex that the great bulk of the tracks cannot be traced to a definite source. Others contain one or more shower centers produced either by ionizing or nonionizing radiation, or by a mixture of the two. With several thin lead plates in the cloud chamber, the progress of the shower can be followed in its passage through matter, and from these experiments it appears that no single event constitutes the origin of a large shower. Rather, a cascade of electrons and γ-rays gradually increases in size as it strikes each successive layer of lead. The large complex showers observed are simply late stages of showers originating in the walls or atmosphere surrounding the cloud chamber. Additional evidence for the multiplicative nature of shower formation is found in measurements of shower frequency as a function of absorber thickness. Both ionization chamber[2] and Geiger counter[3] methods show that the thickness of lead which gives the greatest frequency of showers of a given size increases with the size of the shower considered. Such a shift of optimum thickness with shower size is a consequence of multiplication, whatever the process by which secondaries may be emitted.

The presence of nonionizing radiation and the absorption of shower-producing radiation according to a Z^2 mass-absorption law,[4] as for the degradation of γ-rays by pair production, indicates that pair production is an important factor in shower formation. The primary electron loses a large fraction of its energy in creating a quantum of radiation. The resulting radiation forms electron pairs, and these electrons like the primary electron create more γ-radiation. The process continues until the energy is dissipated through ionization losses of many secondaries. Calculations[5] formulated on this basis lead to plausible explanations for most shower phenomena where only electrons and γ-rays are involved. Showers containing heavily ionizing particles appear to come from a disintegrative process and are not treated in the theory.

Rough calculations as shown by Carlson and Oppenheimer give the relation $n=2^t$ for the number of shower electrons to be expected at a depth t, the unit in t being 0.5 cm for lead, 1.7 cm

[1] C. D. Anderson and S. H. Nedermeyer, Phys. Rev. **50**, 263 (1936); E. C. Stevenson and J. C. Street, Phys. Rev. **49**, 425 (1936); P. Auger and P. Ehrenfest, Jr., J. de phys. et rad. **8**, 204 (1937); J. Crussard and L. Leprince-Ringuet, J. de phys. et rad. **8**, 213 (1937).

[2] R. T. Young, Jr., Phys. Rev. **52**, 559 (1937); J. K. Boggild, *Über die Sekundaren Wirkungen der Hohenstrahlung* (Kopenhagen, 1937).

[3] D. K. Froman and J. C. Stearns, Phys. Rev. **52**, 382 (1937).

[4] J. E. Morgan and W. M. Nielsen, Phys. Rev. **50**, 882 (1936); **52**, 568 (1937).

[5] J. F. Carlson and J. R. Oppenheimer, Phys. Rev. **51**, 220 (1937); H. J. Bhabha and W. Heitler, Proc. Roy. Soc. **A159**, 432 (1937).

for iron, 40 cm for water. Choice of t in these units makes the description of the shower identical for all substances. The expression above is obtained on the assumptions that the probabilities of radiation and of pair production are equal and independent of energy, and that none of the particles is stopped. Actually the probability of pair production is less than that of radiation, and both probabilities are inversely proportional to the energy. Hence small showers will occur with a maximum frequency for absorber thickness somewhat greater than the rough estimate, and large showers, because of the increased probabilities of conversion as the energy decreases, will become most frequent at a thickness smaller than estimated. In the present series of observations this rough approximation is about as good as the data. Therefore more precise solutions of the multiplication equations will not be used since such solutions are not in the most convenient form for experimental comparison. What is desired is a check for the optimum thickness of lead for showers of only a few electrons, because in the thin lead plates where these will be most plentiful there is small chance that electrons will be stopped, and agreement between theory and experiment should be best.

Since shower frequencies measured by means of Geiger counters arranged in multiple are likely to indicate too few small showers, counters are not suited to the experiments. As the simplest case consider the counting of two-particle showers. Three counters placed at the corners of a triangle with the apex just beneath a block of absorber, require at least two particles to excite all three counters simultaneously. All large showers produce counts, but there is a good chance that many small showers, especially those of two electrons, miss one of the two lower counters. Consequently, the data obtained represent an average for a shower containing substantially more than two electrons. Likewise, arrangements of counters that require higher orders of coincidence register but few of the showers containing just the minimum number of electrons. In order to check the radiation pair production theory it is desirable to obtain more accurate information concerning individual small showers than can be gotten from Geiger counters or from ionization chambers. Although operation of a cloud chamber requires considerable time to accumulate sufficient counts, the completeness of the data obtained seems to justify the effort. A record is made of every shower, and selection of those fulfilling certain requirements becomes possible.

Apparatus

A cloud chamber[6] of the moving diaphragm type 30 cm in diameter and 10 cm deep was employed in a vertical position. The shower source consisted of a lead plate suspended across the center of the chamber by means of two brass bands in contact with the glass cylindrical wall. Several different plates 8×22 cm^2 in area and of thicknesses from 0.15 to 1.6 cm were used. Another lead plate 0.63 cm thick, 7×15 cm^2 in area, was fastened to these same bands at the top inside of the chamber during part of the experiments, and replaced by an aluminum plate 0.2 cm thick for the remainder. Cemented to the upper plate with paraffin was a small glass dish containing a mixture of two parts ethyl alcohol and one part water. Previous work had shown the necessity of keeping excess liquid at the top of the chamber if expansions as close as one minute apart were to show tracks. Argon, being a monatomic gas, was chosen to fill the chamber because it requires a smaller expansion ratio than most other gases to give the same adiabatic cooling, and, since it has a fairly high atomic number, electron tracks produced in it are less diffuse than at the same age in a gas like nitrogen. When assembled with a lead plate just put in place, the chamber was flushed with tank argon until less than 10 percent air remained, and filled to a pressure of about 1.8 atmospheres. According to the exact amount of air left, between 8.0 and 8.5 percent volume expansion gave the clearest tracks. With this small expansion there is very little distortion and consequent lack of resolving power produced by gas slipping past the edges of the lead plates.

Although the most reliable data would be obtained from expansions of the cloud chamber taken at random, the number of successful pictures, that is, pictures in which a cosmic-ray track of any sort could be seen, amounts to about

[6] R. B. Brode, H. G. MacPherson, and M. A. Starr, Phys. Rev. **50**, 581 (1936).

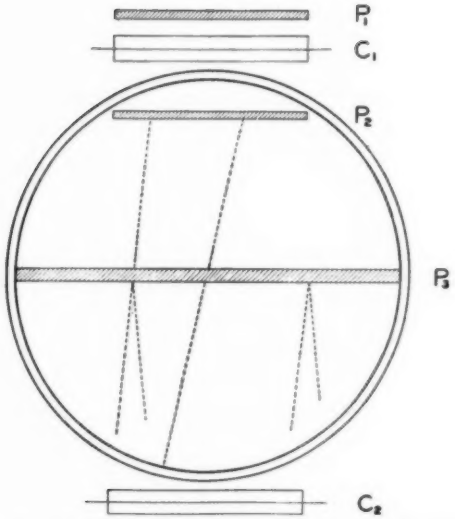

FIG. 1. C_1 and C_2 are Geiger counters; P_3 the shower source; P_1, 0.36 cm lead; P_2, 0.36 cm lead.

three percent of all the pictures. In order to speed the process of taking usable pictures, expansions of the chamber were controlled from a coincidence counter set. Two Geiger counters connected in parallel were placed at the top of the chamber and similar counters at the bottom, so as to cover a fairly large area. Each counter was two cm in diameter and fifteen cm long, and the two overlapped to present an area of about 3.5×15 cm^2 to the vertical. This was slightly less than the illuminated section of the chamber, through which a beam of light about five cm broad was projected by means of cylindrical lenses. The counting rate of either pair of counters alone was 120 per minute. In vertical coincidence with the two pairs separated by forty cm the rate was about 60 per hour.

Objection may be raised to the use of counters, but the same arguments do not apply to double coincidence as to triple. Every shower passing through the chamber can be recorded, because only one particle is required to pass through the lower counter. There are two other faults, however, which tend to select data. One is that those showers in which some particle does not have an energy great enough to penetrate the glass wall of the chamber and the walls of the second Geiger counter will not be counted. This energy, as estimated from calculations of Bethe,[7] is about five million volts, a value below the average energy of secondaries in showers. Thus, in general, we can expect very few showers to terminate inside the chamber and thereby escape detection. A more serious fault is that showers produced by γ-rays will not register unless accompanied by an ionizing particle passing through the upper counter. An attempt was made to find the magnitude of this selection by measuring shower frequencies with and without

[7] H. Bethe, *Handbuch der Physik*, Vol. 24/1, (1933), p. 522.

TABLE I. *General summary of tracks observed.*

Plate Thickness	Number of Pictures	Penetrating Electrons	Absorbed Electrons	Total Tracks Above Plate	Total Tracks Below Plate	Ratio Below/Above	Number of Electron Showers	Total Tracks	Average in Electron Shower	Number of Photon Showers	Total Tracks	Average in Photon Shower	Unresolved Showers	Tracks Above	Tracks Below	Measure of Incident Radiation
1.0 cm of lead above																
0.15	1163	971	113	1247	1182	1.05	43	98	2.3	39	82	2.1	13	55	86	1014
0.4	1650	1128	185	1633	2055	1.26	102	275	2.7	83	193	2.3	35	218	459	1230
0.65	1603	1032	213	1466	1847	1.26	94	262	2.8	89	215	2.4	32	127	307	1126
0.9	1680	1154	300	1647	1999	1.21	93	285	3.1	87	221	2.6	27	100	339	1247
1.65	1788	1255	328	1476	1847	1.25	73	281	4.0	54	192	3.6	31	105	430	1328
No lead above																
0.65	1263	960	114	1172	1341	1.15	89	254	2.9	42	95	2.3	4	9	32	1049
0.9	1302	930	104	1144	1526	1.33	92	322	3.5	34	99	2.9	7	18	75	1026
1.65	1368	1013	142	1271	1716	1.35	91	426	4.7	50	197	3.9	9	25	90	1104

additional lead plates present above the plates in which the observed showers originated. This point will be discussed in more detail below.

Five different lead plates were placed in turn at the center of the cloud chamber, and a set of pictures taken for each. The apparatus was entirely automatic, taking a picture for the first coincidence after each resetting. The time of reset could be controlled by a resistance in series with a motor which wound the film and operated relays to put everything in readiness for the next expansion. This time was set at forty-five seconds in order to allow the chamber to reach temperature equilibrium and to reduce turbulent motion of the gas. In addition to the central plate there was a total of one cm of lead arranged as shown in Fig. 1.

The experiments were carried out at an elevation of about 100 m under a thin sheet iron roof so that the incident radiation is essentially the normal sea-level cosmic radiation. Because no magnetic field was available to produce an energy spectrum, the results are to be interpreted as the average behavior of cosmic radiation, with no differentiation as to initial energy of the rays. Since showers of different sizes may be produced by incident rays of different energies, this lack of information is a handicap, but it is to be expected that the distribution of energy for each run with a given plate is about the same within statistical errors. As over a thousand pictures were taken for every thickness of lead, the incident rays are assumed to be identical at all times.

Classification of Tracks

Comparison of results for the various plates requires a systematic classification of the tracks photographed and a measure of the incident radiation. Only those electrons have been tabulated which excited the counters or at least were coincident in time with counter excitation. Also the condition was imposed that the track be included within the solid angle subtended by the counters. Stereoscopic photographs aided in locating tracks. Tracks of different ages can be identified by two means. Positive and negative ions in the track are separated by the clearing field and in a short time give the track a double appearance. An equally good estimate of age is made from the width and density of the track. These methods fail when background fog is present. For this reason the cloud chamber was

Table II. *Numbers of showers.*

Particles per shower	2	3	4	5	6	7	8	9	10	Others
Electron										
1 cm Pb above										
0.15	35	5	2	1						
0.40	63	20	12	3	2	2				
0.65	59	19	6	5	1	2	1		1	
0.90	63	12	4	5	2	2	1		2	11, 17
1.65	47	9	3	1	2	1	4	1	1	11, 13, 25, 32
Zero cm Pb above										
0.65	54	20	6	2	3	1	1	1	1	
0.90	52	15	10	6	6	3			2	13, 13
1.65	41	16	4	3	5	7	1	2	3	11, 11, 11, 13, 13, 14, 15, 20, 22
Photon										
1 cm Pb above										
0.15	37		2							
0.40	67	8	6	1	1					
0.65	66	13	2	5	1	1	1			
0.90	64	9	9	2	1	2				
1.65	34	8	1	3	2	3				14, 14, 20
Zero cm Pb above										
0.65	36	4	1			1				
0.90	22	3	4	2	1	2		1		11
1.65	33	5	3		1	2	1		1	12, 12, 12, 30

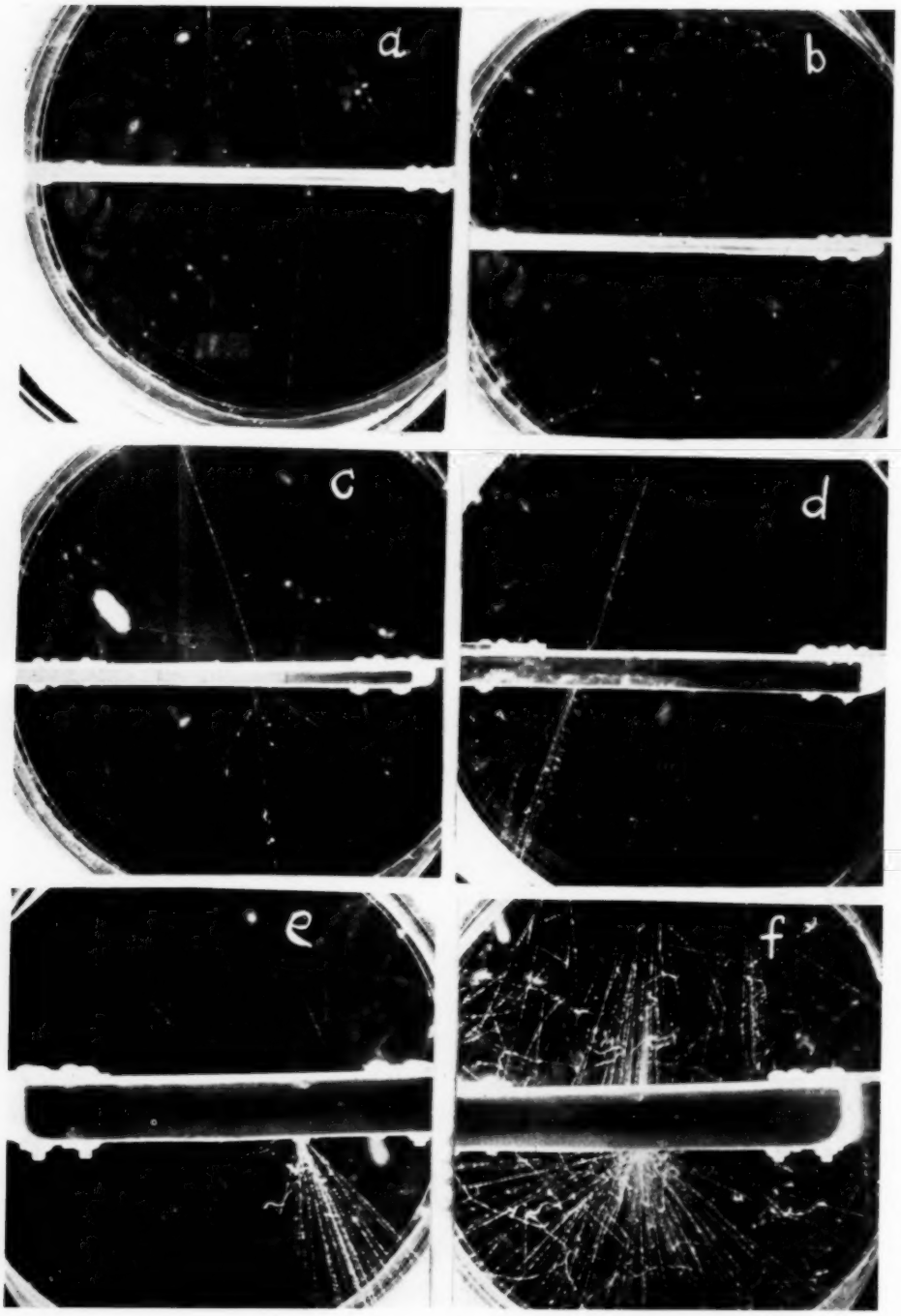

FIG. 2. *a*, Two-particle shower from an incident electron. The fuzzy vertical line is a wire used in stereoscopic measurements. *b*, Two-particle shower from an incident gamma-ray. The fuzziness and displacement of tracks in this and other photographs are caused by turbulent motion of the gas during expansion. *c*, Six electrons are produced by the incident electron, and four electrons by a gamma-ray. *d*, An unresolved shower showing absorption of deflected electrons. *e*, A few pictures were taken with a 3 cm plate. This is one of the larger showers; two-particle showers are most plentiful even for this plate. *f*, An exceptionally good example of the apparent origin of a shower in the last few millimeters of the absorber. Practically all the incident electrons stop in the plate.

thoroughly cleaned each time it was taken apart to introduce a new lead plate, and the expansion was checked visually at the beginning of every run of some forty pictures. Altogether, only a few tracks of doubtful age were photographed. Application of these two conditions to the selection of tracks assures us of obtaining consistent incident radiation, and of counting phenomena produced under comparable conditions.

A large percentage of the photographs show that a single particle has been responsible for the expansion, and has passed through the central lead plate unaffected. These particles are listed in Table I as penetrating electrons. Other particles striking the plate each produce a shower of two or more electrons, of which it is extremely probable that at least one will be contained in the solid angle covered by the lower counter, and thus complete the coincidence necessary to set off the expansion. The total number of tracks in electron-produced showers and the average per shower are listed, also the same numbers for photon-produced showers. A detailed list of showers produced by single incident electrons and γ-rays is given in Table II. Another type of shower occurred whenever a shower from the lead at the top of the chamber was increased in size by passage through the central plate. Most of these have been classified in Table I as unresolved because it is impossible to assign the electrons below the plate to a shower produced by some one particular incident electron or γ-ray. The relatively small number of unresolved showers obtained when the upper lead plates are removed is due to the fact that small angle showers are not present above the central plate to the same extent as with the lead in place. Typical examples of showers are shown in Fig. 2. Particles reaching the end of their range in the plate are called absorbed electrons.

The average number of tracks in showers is shown in Fig. 3 for the various arrangements of lead. In agreement with the theory proposed by Carlson and Oppenheimer, the average increases with the thickness of lead through which the radiation has passed. In every case the average for electron-produced showers is greater than for the corresponding photon-produced showers. This may or may not be significant. When the distribution of showers according to size is taken into consideration, it might be interpreted as meaning that the average electron has more energy than the average photon. Such increase in average size with increasing thickness of lead points to a process which does not take place at one assigned point. Out of a total of eighty-two showers originating in the thinnest plate, only one had as many as five electrons. Nine had three or four. All the rest were pairs. In comparison, with approximately twice as much incident radiation, the thickest plate gave rise to twenty showers containing more than ten tracks. The largest of these had thirty-two. There were forty-three showers of from five to ten electrons each. The fact that the thin plate gives no large showers while the thicker plates do, is fairly conclusive evidence for the verification of a multiplicative process of shower formation.

Discussion

In the multiplicative theory, an electron does not lose so large a fraction of its energy by radiation as to change its penetrating power to any great extent. Electrons and γ-rays will move along more or less in the direction of the initial radiation. Consequently wherever there is a γ-ray there is a good chance of finding an electron nearby. The centimeter of lead at the top of the chamber is sufficient to filter out most of the air γ-rays and replace them with lead γ-rays. Hence photon showers observed in the lower half of the chamber must for the most part have come from a γ-ray radiated in the lead by the same electron which excited the upper counter. On such argu-

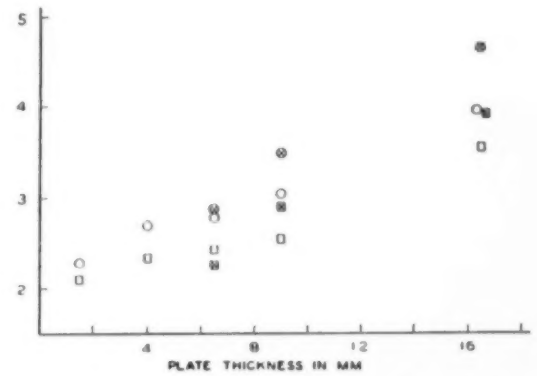

Fig. 3. Average number of electrons in showers. Circles for electron produced showers; squares for photon-produced showers. Open figures for showers with 1 cm lead above chamber; crossed figures, without lead above.

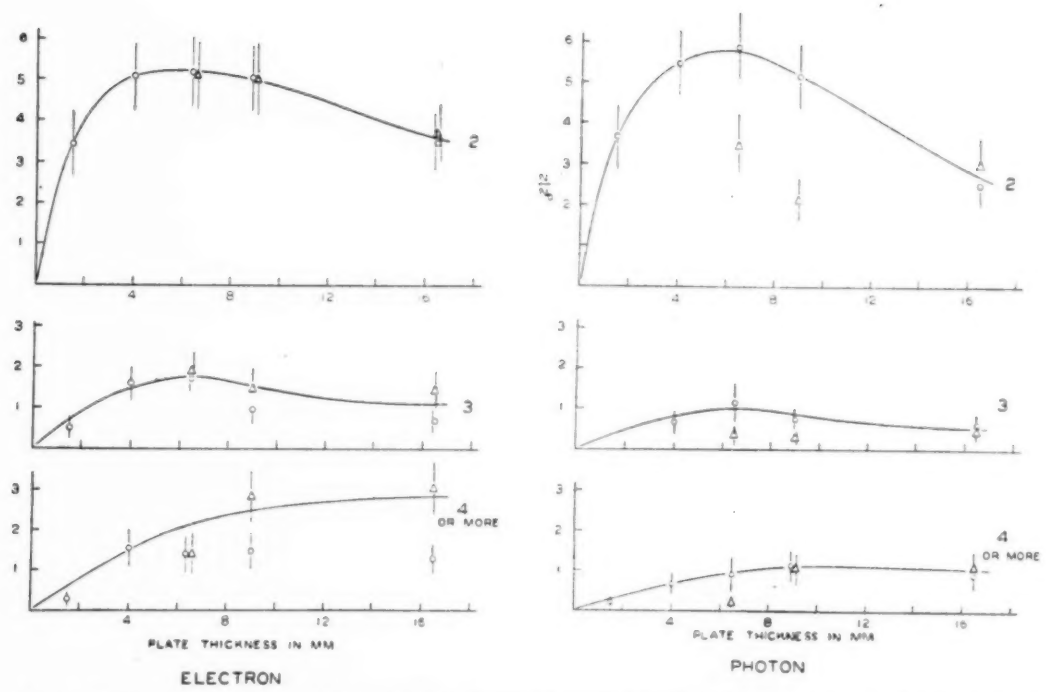

FIG. 4. Frequencies of showers of 2, 3, and 4 or more electrons plotted as percent of the incident radiation against absorber thickness. These are the showers that could be traced to a single entering electron or to a gamma-ray. Circles are for showers observed with one cm lead above the shower source: triangles without lead above.

ments it appears that a correct count of the number of showers from photon encounters is obtained from pictures taken with the upper lead present. Photographs taken at random by Anderson and others do not show more showers produced by photons than observed here. Old tracks also give a check in that they are effectively random, and they do not indicate large numbers of unrecorded photon showers. During the second part of the experiment, in which the upper lead plates were removed, relatively fewer showers from photons occurred in the photographs. This reduction is to be expected, since the source is spread over a long vertical path in air, unit t for air being about 300 m. If the process giving rise to photons takes place at some distance from the cloud chamber, there is a possibility that no electron will pass through the chamber along with a photon, because electrons and their secondary photons may go off at slightly divergent angles. Although transition effects will occur between air and lead, absorption of cosmic radiation in lead will not increase to any great extent the proportion of γ-rays. The difference in numbers of photon showers observed with and without lead above the chamber is attributed to a difference in counting efficiency rather than to an actual difference in numbers of γ-rays present.

Since the ionization produced by an electron of cosmic-ray energy is practically independent of energy, the total number of electron tracks counted in a given volume is a measure of the total ionization in that volume. By counting all tracks below and above the central plate, we derive a ratio of ionization in these two volumes. According to ionization chamber measurements, up to two cm of lead has very little effect. The ratio first rises a little and then falls slowly with increasing absorber thickness. In Table I are the results of adding all recorded tracks. It is seen that the ratio is much larger than the expected value. The discrepancy very likely is caused by the selective action of the Geiger counters. Many electrons of only a few million volts energy, which would be effective in an ionization chamber, are absorbed in the central plate and cannot reach the lower counter. Therefore, they are not photographed. About the only tracks unrecorded below the plate are in photon showers.

Lack of these low energy electrons in the

statistics is not a serious loss, because they have too small an energy to create showers and hence are of little interest in the problem. As the most appropriate measure of the incident radiation it was decided to take only those electrons which penetrated the plate plus those which produced showers. In this way incident electrons of fairly high energy are selected without the use of a magnetic field. Single electrons unable to pass through the system do not appear in the photographs, but in unresolved showers there are usually several electrons stopped by the center lead plate, which come off at rather large angles to the main bundle of particles. It is not at all surprising that the outermost portions of the shower are absorbed, since only secondaries of low energy have a chance of being deflected in nuclear fields. This absorption frequently gives large showers the appearance of coming from the bottom millimeter of absorber, as though all particles radiated from a single point. In discarding unresolved showers and low energy electrons, we obtain a slightly distorted measure of incident radiation because of the difference in stopping power of the various lead plates. An electron loses roughly 50 to 100 Mev by ionization in passing through the thicker plates, and on the average, those photographed will have this much more energy than those striking the thinner plates. It is exactly such selection, however, which gives electrons equivalent energy distributions below the different plates, and makes possible the comparison of the numbers of showers observed. There is no accurate method of determining the number of γ-rays present. We must simply assume that their number is proportional to the number of electrons.

In Table I are given the measures of incident radiation as described above. The frequencies of showers of two, three and four or more electrons in terms of this measure are plotted against plate thickness in Fig. 4. Electron showers of two particles occur at the same rate with and without the presence of the upper lead plates. Larger showers occur more frequently when a small shower strikes the central plate, and cannot be resolved as easily as two-particle showers. With the removal of the top lead there are fewer such groups of tracks to confuse interpretation, and practically all large showers can be identified as being produced by single electrons, or γ-rays. Taking into consideration the shifting of about half of the larger showers into the unresolved class when lead is placed above, we are led to the conclusion that the number of showers produced by electrons is not noticeably affected by the passage of cosmic radiation through one centimeter of lead. As already mentioned, absence of lead above the chamber reduces the efficiency of recording showers produced by photons by say one-half. When use is made of this factor, we see that showers from γ-rays occur with the same frequency as those from electrons. Theory predicts 1.5 times as many γ-rays as electrons, and about the same preponderance of showers from γ-rays over showers from electrons. Since the recording of photon showers is dependent on the presence of an electron in the upper counter and not on the number of electrons in the shower, photographs taken under the conditions of the experiment may indicate too few showers from γ-rays, but the relative frequencies should be correct. Therefore, although the absolute magnitude of measured frequencies may be in error, the similarity of photon and electron excitation curves for showers of two particles indicates that the mechanism of shower production does not depend upon the manner in which energy is supplied. In good agreement with the theory, the optimum thickness of lead for producing these showers is about six millimeters. Larger showers occur in too small numbers to give very reliable curves. Even these, however, are similar in that the maximum number of showers occurs at a greater thickness of lead than for two-particle showers.

Similarity of electron and photon excitation of showers and the good agreement of optimum thickness with calculations, indicate that showers are formed by a succession of radiation and pair production transformations. Since the theory is based on an extension from medium to high energies of the formulae for the interaction of high speed electrons and γ-rays with matter, it appears that the formulae are valid throughout the cosmic-ray energy spectrum. If this is true, we are at a loss to explain why less than ten percent of the electrons passing through a six millimeter lead plate produce showers. At sea level this thickness is the most efficient in producing

showers; the number falls off to about five percent for thicker plates. A statistical treatment of the problem by Furry[8] predicts that over twenty percent of the electrons passing through five mm of lead will give showers, forty percent at one cm, etc. Since we have reason to accept the calculated probabilities of radiation and pair production, we are left with about half or two-thirds of the incident radiation behaving in an anomolous manner. This is more than can be explained by statistical fluctuations. We may assume either that electrons and quanta of extremely high energy do not react readily with nuclei, or that the radiation is composed in large part of particles which ionize like electrons, but which do not radiate quanta. Measurements of energy loss in heavy metals as found by Nedermeyer and Anderson[9] seem to indicate the presence of such nonradiating particles. Photographs taken by Street and Stevenson[10] indicate that these penetrating particles are not protons because they do not ionize heavily enough at the end of their range. In order to account for their great penetrating power and their low ionization, the existence of a new particle with electronic charge and the mass of 100 to 200 electrons has been proposed. Further experiments by Fussell[11] and experiments in progress at Berkeley on the specific ionization of cosmic-ray particles may shed more light on the question of the existence of such a particle.

The author wishes to express his gratitude to Professor Robert B. Brode under whose helpful guidance these experiments were carried out, and to Professor J. R. Oppenheimer for his continued interest in the problem.

[8] W. H. Furry, Phys. Rev. **52**, 569 (1937).
[9] S. H. Nedermeyer and C. D. Anderson, Phys. Rev. **51**, 884 (1937).
[10] J. C. Street and E. C. Stevenson, Phys. Rev. **51**, 1005 (1937).
[11] L. Fussell, Jr., Phys. Rev. **51**, 1005 (1937).

JANUARY 1, 1938 PHYSICAL REVIEW VOLUME 5

The Latitude Effect in Cosmic Radiation at High Altitudes

S. A. KORFF
Department of Terrestrial Magnetism, Carnegie Institution of Washington, Washington, D. C.
L. F. CURTISS AND A. V. ASTIN
National Bureau of Standards, Washington, D. C.

(Received November 2, 1937)

Measurements of cosmic-ray intensities in the equatorial and temperate regions are reported, and the instrument described. The apparatus consists of a single Geiger counter, the impulses of which are transmitted by radio to a ground station. The results are compared with high altitude electroscope measurements and are found to agree satisfactorily. Flights up to 70,000 feet were obtained in Peru. The results indicate that the intensity of cosmic radiation in the upper atmosphere in Peru is about half that at Washington. The component which produces about one-half the maximum total intensity of ionization at high altitudes over Washington is cut out by the earth's magnetic field and does not reach the top of the atmosphere in Peru. The energy of this component lies between 3 and 12×10^9 ev. Analysis of the data shows agreement with the Carlson-Oppenheimer curves. The ionization at high altitudes is shown to be in large part due to secondaries.

INTRODUCTION

THE latitude effect in cosmic radiation has been one of our chief aids in determining the energy spectrum of the incoming radiation. It has long been realized that one of the most important parts of this study has been that of the latitude effect at high altitudes. Hitherto high altitude work has necessitated the use of recording equipment which depended upon recovery of the instrument after the balloon flight to obtain the record of the intensity. With the development of radio transmission of balloon-data, a new method, useful for this work, has made its appearance. It is clear that recovery of recording instruments presupposes an inhabited country and literate populace. Where the topog-

raphy is chiefly desert or ocean, the radio method has proved especially useful.

Counters and Transmitter

In order to measure the total intensity of cosmic radiation at various altitudes, a single counter was used. Except for Cosyns[1] relatively few observers have used single counters for total intensity measures, and hence the details are described. It is clear that the method to be described may also be modified for coincidence counting; indeed such coincidence sets are already being reported on by T. H. Johnson.[2]

The desiderata for counter equipment for balloon work are: (*a*) Light weight; (*b*) strong pulse with minimum number of tubes; (*c*) a sea-level counting rate such that at highest altitudes the vastly increased rate will still be within the response time-constant of the relay, or whatever other device is the slowest in the circuit; (*d*) ruggedness; and (*e*) proper operation under conditions of varying temperature and pressure.

These desiderata determine the design of the instrument. Consider factor (*c*). Since, as will be detailed below, the entire equipment was found to work accurately at counting rates up to 200 per minute, and since the cosmic-ray intensity in temperate latitudes is known to be some 200 times more intense at the high point on the intensity-altitude curve, the counter should at sea level have a counting rate of less than one count per minute. The counter was therefore made small. The cylinder was made one cm long and one cm in diameter. The cross section of the counter to radiation from any direction was therefore between 0.75 and 1 square cm. Such a counter (see Fig. 1) will normally operate at sea level at less than one count per minute.

Considering factor (*a*), we see that the counter must operate at a low voltage in order to save battery weight. Two possible types of construction may combine to give low counter operating voltage. These are (*a*) filling the counter with helium, argon, or other noble gas, and (*b*) operating at a somewhat lower pressure than

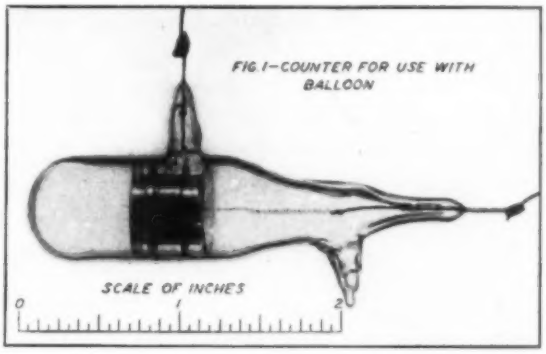

Fig. 1.

usual. In this work the counters were filled, some with helium, some with argon, at pressures from 2.5 to 3.8 cm Hg, and were found to have a stable operating plateau at between 350 and 550 volts, depending on the gas and pressure chosen. As we will see later the conditions were selected to meet various problems concerning the shape of the intensity pressure curve at high altitudes.

The counter circuit employed a single type 32 screen grid tube fed through a coupling condenser of 0.00005 mf. This tube was chosen inasmuch as it has a low filament current (60 milliamperes) and a high mutual conductance. The characteristic curve of this tube has a hump at low voltages and advantage was taken of this fact. The tube was operated at 135-volt plate potential, 2-milliampere plate current, 90-volt screen grid potential, and 3.5-milliampere screen current. The filament, rated at 2 volts, 60 milliamperes, was operated on a single cell, giving 1.4 volts over a period and supplying between 48 and 50 milliamperes. These several factors combine to produce the desired result. The circuit diagram is given in Fig. 2.

The tube is operated with a very high resistance grid leak or none at all, and with a plate load resistance of 25,000 ohms. In this condition, the plate current flows at its full (saturated) value. However, when a count occurs in the counter tube, the plate current shuts off entirely. As ions flow to the grid, the grid returns quickly to a normal potential and the full plate current flows again. As a result a cosmic-ray impulse causes a 2-milliampere deflection in the plate current of the first tube. This is a greater swing than can be obtained in the conventional manner. The output of this one tube was sufficient to

[1] M. Cosyns, Bull. Tech. de l'Assoc. Ing. sortis de l'École Polytech. de Bruxelles (1936).
[2] T. H. Johnson, Phys. Rev. **51**, 385–386 (1937) and J. Frank. Inst. **223**, 339–354 (1937).

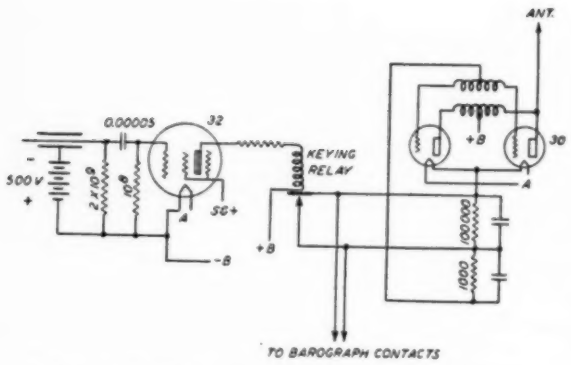

FIG. 2. Circuit of cosmic-ray balloon apparatus.

operate a Western Electric G-26 relay in the plate circuit which keyed the transmitter.

The counter and amplifier described above were put through the following tests to determine whether this arrangement was suitable for work under the conditions expected to be encountered.

(a) Counting rate

The counting rate was found to be 0.4 count per minute at sea level (ground level). An increase of a factor of 200 in the rate between the ground and the top of the flight was expected. Therefore it was necessary to ascertain that the apparatus would respond to 100 counts per minute.

The relay in the plate circuit was therefore connected to an impulse counter. The plate output was independently connected to a "scale-of-8" thyratron counter, which recorded one count for every eight pulses which the tube gave. A strong source of radium was then brought near the tube. The counting rate rose as the radium approached. The relay operated satisfactorily up to a rate of 250 counts per minute; that is, the mechanical counter and the thyratron agreed up to this point. As the rate was increased to 600 per minute, as measured on the thyratron set, the relay began to chatter, and only recorded 200. This was very satisfactory operation, since the maximum rate to be expected was something over 100, and the relay worked properly over 250.

(b) Time factor of counter and tube

A cathode-ray oscillograph was connected to the counter and amplifier tube to determine the the length of each pulse. It was found that the pulses lasted 0.005 second. The pulse was of the proper shape, starting fast, reaching a peak with less than observable lag, and falling off exponentially from this peak at the rate indicated. Thus it was established that the counter and the amplifier were not introducing any undesirable electrical characteristics, such as flat-topped pulses, which some circuits give, and that the slowest electrical part of the circuit did not introduce any delays which would result in missing counts when operating at a fast counting rate.

(c) Temperature effects on resistances

In order to determine whether the temperature variation during the flight would affect the counting rate by changing the resistances in the circuit, a high resistance, five times as great as the output resistance used, was introduced. The counting rate changed by less than ten percent. Similarly, changing the plate resistance by a large factor made small difference in the counting rate.

(d) Battery tests

For counter voltage the Eveready type X-180 battery was used. This battery weighs about 2 ounces and delivers 45 volts. It was tested by putting a resistance and meter across it, and was found to deliver 1.5 milliamperes for 4 hours with but a ten percent drop in terminal voltage. Inasmuch as this was far in excess of the load to be used, it was satisfactory. Moreover, it was found that an increase of 45 volts in the counter potential only changed the counting rate by ten percent, and thus the effect of possible temperature change on the rate due to changing battery voltage was negligible.

For filament supply an Eveready 935 single cell weighing 1.5 ounces was used. This cell was tested and delivered 50 milliamperes for 5 hours, or for five times the length of the ascending part of the flight.

For plate supply, General batteries type V-30-M were used. These deliver 45 volts, weigh about 6 ounces and have a capacity of about 65 milliampere hours.

The relay in the plate circuit of the type 32 tube was a Western Electric type G-26 telephone relay. The contacts of this relay directly keyed the oscillator, so that each time the counter counted the transmitter emitted a signal.

The transmitter was a simple oscillator, consisting of two type 30 tubes connected in push-pull. The circuit used was that described by Curtiss.[3] Effort was made to have all the oscillators identical. This oscillator, without batteries weighs 80 grams; and requires 135 volts for plate supply and 4 volts for filament power. The oscillator is overloaded and uses an instantaneous plate current of about 50 milliamperes. Since the pulse lasts but 0.1 second and long life is no object, strong signals are thus obtained.

Barograph

The altitude or pressure at which the instrument may be, is signaled by a barograph designed as a part of a radiometeorograph. This instrument is described in detail in a following paper. The models assembled by the American Instrument Co. after this design were found to work excellently, and operated without failure on all of the flights.

Receiver

The receiver used was the receiver portion of a transceiver, made by the Transceiver Corporation. The unit is of the superregenerative type. A tuned antenna of 5/2 the wave-length was extended vertically. The transmitting antenna was 1/2 the wave-length in length and also vertical. The frequency chosen was 58 megacycles. This frequency was selected considering the absence of reflections and interference, and was found satisfactory.

The output was taken from across the loudspeaker terminals, and passed through coupling condensers of 0.01 mf capacity to the grid of a 6*C*6. In the plate circuit of the latter was placed a telephone relay. This relay was then connected to a telegraph tape recorder.

The loudspeaker was left connected. The set was so adjusted that the regeneration "hiss" was heard. If the regeneration control was turned until the set was just regenerating, then when the signal came in the regeneration ceased. When regeneration ceased, the load across the 6*C*6 swung to a positive potential, and plate current flowed. The plate relay closed and the telegraph tape recorder registered a signal.

[3] L. F. Curtiss and A. V. Astin, J. Aero. Sci. 3, 35–39 (1935).

Noise has relatively little effect on a receiver of this type. A cathode-ray oscillograph was connected to the output and showed a broad noise pattern when the set was regenerating. As soon as regeneration ceased, the noise pattern collapsed into a flat horizontal line. In other words the signal resulted in the absence of regenerative noise. Other noise is merely added to the background noise and except for extraordinary bursts of static occasionally encountered in the tropics, also collapses and shows no effect when the signal comes in.

Observations

With the equipment described above, a series of flights was made. Balloons made by the Dewey and Almy Chemical Company were used. The entire single equipment weighed between 2500 and 2900 grams, depending on the batteries used. Altitudes of 50,000 to 70,000 feet (15 to 22 km) were obtained.

Four flights were made during March and April, 1937, at Washington, D. C., geomagnetic latitude 50°. The cosmic-ray counts per minute are plotted against pressure in Fig. 3. It will be noticed that a rapid increase in counting rate is observed at pressures below 400 millibars. As the instrument rises, the intensity rises to what we will call the main peak. This main peak lies at about 100 millibars. Above this elevation the intensity drops.

The instruments continued to work on the descent, and gave points approximately checking those obtained on the rise. These points are generally farther apart in terms of pressure since the descent was usually faster than the ascent. In flights 1 and 3 only a few points were so obtained since a high wind carried the balloons far enough away (estimated 150 to 200 miles) to attenuate the signals below workable levels.

Flight 2 gave an excellent proof of the reliability of the instrument. Both lifting balloons burst simultaneously and the instrument dropped in free fall from about 56,000 feet. The barograph-signals showed that the velocity attained was about 100 miles per hour at first, and this slowed down to about 60 miles per hour as the instrument entered the denser atmosphere below 15,000 feet. During all this time the cosmic-ray signals continued to come in. On the descent

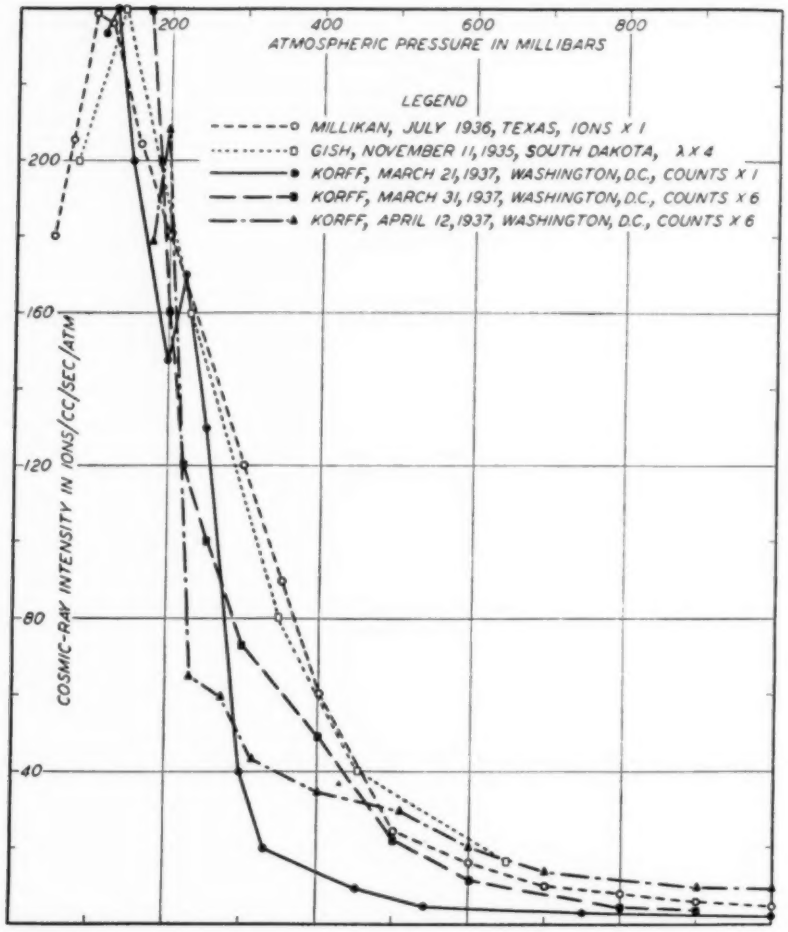

FIG. 3. Cosmic-ray counter results for Washington, compared with results of Millikan and of Gish.

the instrument accurately repeated the up-going curve, even to indicating a narrow secondary peak on the radiation.

The ascending and descending values obtained for each flight are averaged in Fig. 1, and the resultant curve is drawn through the points. The "plops" which the cosmic-ray counter gives can be plainly heard in headphones or loud-speaker and are quite unmistakable. Practice was always made to listen by ear to the signal and simultaneously watch the tape recorder.

The counting rates were adjusted to various rates initially, so that various final rates might be obtained. In one flight the rate was set quite high in order to obtain detailed information about the main peak. The maximum rate observed was as high as 250 per minute, a secondary maximum was 180, and the sea-level rate was about one. In the next flight, the rates were so set that the maximum was about 40 per minute at the top and about 0.2 at sea level. The resulting curve shows that the same observations are obtained with either rate, though obviously the faster rate allows a greater total number of counts to be gathered and therefore reduces the accidental scatter. In other words, fractions of a count being impossible, a small variation will show up more readily on a high rate than on a low rate, on which latter it might be confused with accidentals. By varying the rate by a factor of six, it was shown that the observed increase with altitude is not a function of counting rate. The repetition of the points on the downward curve indicates that the instrument is responding to radiation coming from outside.

A series of five flights was made in Lima, Peru, magnetic latitude 0°. The cosmic-ray intensities obtained in these flights are shown in Fig. 4. The intensity altitude curve is, essentially, the same shape as that obtained in Washington.

However, the maximum intensity over Peru is about half that over Washington. Moreover, this maximum intensity is attained lower down, that is, at higher pressures. The latitude effect, which is about eight percent at sea level between Washington and Peru, rises to 50 percent at about 45,000 feet.

Each point on the curves represents the average counting rate for periods of four to seven minutes. Since fewer counts were received from the lower portions of the flight, these lower points generally represent averages for a greater number of minutes than the higher ones. The counts per minute scatter more on the rapidly changing ascent portion of the curve between pressures of 400 and 150 millibars. At the top of the curve the scatter tends to diminish markedly. This same distribution of scatter is found by other observers. The vertical lines in Fig. 5 represent the amounts of this scatter. Those on Swann's curve are taken from his diagram. Those on the curve of the flight above Washington were averaged, as indicated above, every four to seven minutes. The vertical lines in this case represent the extent of the scatter, practically no points falling outside the limits thus set. The averages at the top of the flight are generally for four points, each representing the number of counts received in one minute. Toward the top of the flight the counting rate becomes high but quite uniform.

Discussion of the Results

(A) Comparison of the counter and electroscope techniques

These observations give us an opportunity to compare several different instruments and observing techniques. Four methods are considered. These are: The electroscope; the single counter; the coincidence counter; and the various devices for measuring atmospheric electricity.

In order to determine whether counters and electroscopes measure similar increases in radiation, the electroscope observations made up to 29,000 feet in Peru by Millikan and Korff[4] in 1935 are plotted on the same diagram as the counter-flight curves. Inspection shows that the two techniques yield similar results. Since "counts per minute" is an arbitrary scale, the different counter-rates are multiplied by constant factors from 1 to 4, to bring them to the same scale as the electroscope ordinate of ions per cc per atmosphere per second at a pressure of 500 millibars. This is essentially the procedure followed by Regener[5] in his comparisons of work with electroscopes and counters. It will be observed that satisfactory agreement can be obtained, and hence it may be concluded that the single counter can be regarded as an instrument capable of measuring the total intensity of cosmic radiation.

[4] I. S. Bowen, R. A. Millikan, S. A. Korff, and H. V. Neher, Phys. Rev. **50**, 579–581 (1936).
[5] E. Regener and G. Pfotzer, Physik. Zeits. **35**, 779–784 (1934).

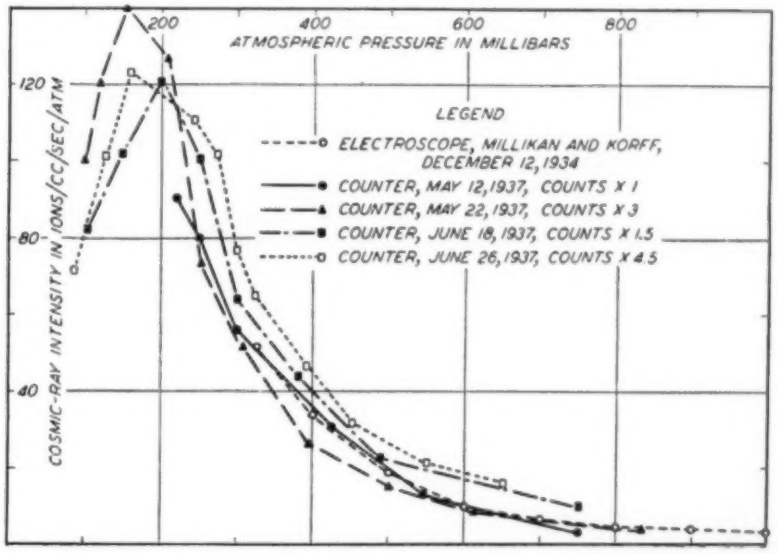

FIG. 4. Cosmic-ray intensity as a function of altitude in Peru; points obtained with electroscopes and with counters.

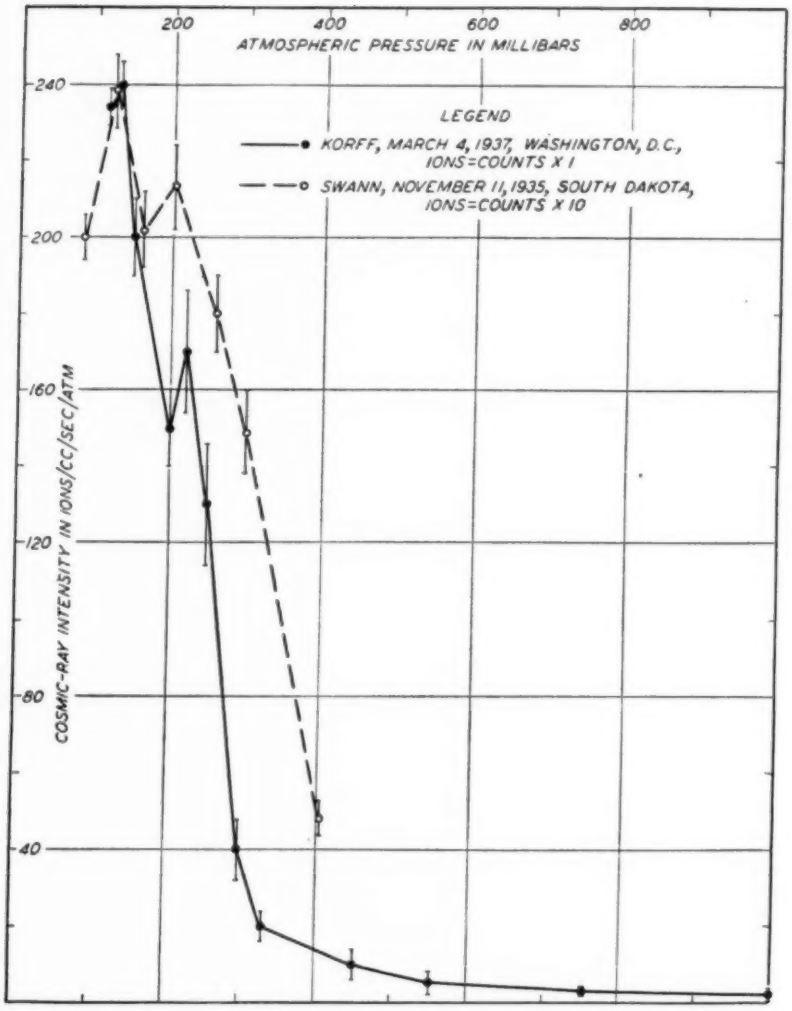

FIG. 5. Individual flight with single counter in Washington, compared with coincidence counter flight by Swann.

Similarly the counter observations at Washington are compared with the excellent results obtained by Millikan[6] in his balloon flights in Texas. In this case the curves can be compared right up to the top of the intensity rise. From this comparison it will be seen that the electroscope does not show small secondary dips as well as counters do. The electroscope tends to integrate over these dips, though they may be surmised from the readings. The counters, on the other hand, give a continuous record of the intensity between any two elevations.

Consider now the single counter as compared with the coincidence counter. In Fig. 5 are plotted the single counter rates obtained on a typical flight and the vertical coincidences obtained by Swann[7] on the manned stratosphere-flight. It will be seen that the coincidence counters tend to integrate somewhat more than the single counter does. Further, the departure of the coincidence curves from the single counter curves at lower elevations is in accordance with the theoretical analysis of Gross,[8] who shows that the vertical component of the radiation will fall off less fast than the total radiation. Minor secondary humps in the curve are also found.

Turning next to the problem of comparing the cosmic-ray results with those obtained in the atmospheric electric work, we find that if the

[6] I. S. Bowen, R. A. Millikan, and H. V. Neher, Phys. Rev. **52**, 81–88 (1937).

[7] W. F. G. Swann, G. Locher, and W. Danforth, Nation. Geog. Soc., Contrib. Tech. Papers **2**, 16–25 (1936); Phys. Rev. **51**, 389–390 (1937). (Points taken from Fig. 10, curve *A*, p. 22.)

[8] B. Gross, Zeits. f. Physik **83**, 214–221 (1933).

results of Gish and Sherman[9] be plotted together with the cosmic-ray intensity curves, the results will run very nearly exactly parallel. In Fig. 3 the results by Gish are plotted for positive air conductivity, his values of λ in units of 10^{-4} e.s.u. being multiplied by 4 to bring them onto the same scale as the cosmic-ray intensities. It will be seen that these results, which are for roughly the same latitude, agree well with the cosmic-ray curve. In the past comparisons have been made between the atmospheric electric curves and the ionization curves of Regener, which latter, in consequence of the latitude and longitude effect, have higher intensities at high altitudes. We may conclude that cosmic rays are the principal agent responsible for that ionization and conductivity in the upper atmosphere which Gish measures.

(B) Shift of peak

Inspection of the curves will show that the peak at which the maximum intensity is reached tends to move to higher pressures at low latitudes. This is due to the fact that the softer part of the incoming radiation is cut off by the earth's magnetic field and does not reach the top of the atmosphere at the equator. Those rays which produce ionization in the upper atmosphere at low latitudes are therefore harder and penetrate further into the atmosphere before they come into equilibrium with their secondaries.

The shift of the peak is also seen in the curves of Millikan,[6] where comparisons are made between the flights they made at Chicago, in Texas, and at Madras. It will be further seen that the curve which the senior author obtained in Peru fits in between those which Millikan obtained in Texas and India. This is to be expected since the longitude-effect operates between Peru and Madras, both of which places lie close to the magnetic equator, in such a way as to reduce the intensity at Madras.

Between Washington and Lima, Peru, the peaks shift by about one-half meter of water toward higher pressures. Since the earth's field will cut out all particles of energy less than 12,000 Mev entering at Peru, and about 4000 Mev entering at Washington, the shift of the peak may be interpreted as indicating that a group of rays of energy not less than 12×10^9 ev will reach equilibrium with their secondaries after penetrating about 0.5 meter of water more than is needed to bring those of 4×10^9 ev to equilibrium. This is in accord with the theoretical curves of Carlson and Oppenheimer.[10] They find a shift of peak owing to the production of multiplicative showers, by a difference in energy of 2700 Mev (lower limit of energy entering at northern latitudes) and 20,000 Mev (energy entering at Madras), of about 100 percent in abscissae of thickness of matter. The peak shift observed in the experiments reported on herein is just about half this, and the energy limit of the southern peak is also about half the second figure, or about 10^4 Mev, entering at Peru.

(C) Heights of peaks

The heights of the principal peaks of the intensity altitude curves determine the latitude-effect at high altitudes. Since the peak for Washington lies at 240 on the scale of ions per cc per atmosphere per second and the Peru peak at 120, or about half, we may conclude that one-half the radiation reaching the top of the atmosphere in Washington is cut off by the field and does not reach the atmosphere in Peru. This fraction of the radiation lies, according to the latitude effect calculations, between about 4 and 12,000 Mev.

However, it must be remembered that the interpretation of the latitude effect as directly indicating what fraction of the energy lies in any given energy band depends on the assumption that one cosmic ray, of whatever nature or energy, passing through the counter, produces a count. This behavior is true only for ionizing radiation. All cosmic-ray measuring instruments work on this principle. The agreement between the counters, the electroscope, and the other methods indicates that we are indeed measuring the ionizing component of the radiation plus the ionization due to secondaries. We must remember that non-ionizing radiation would not excite the counter. The glass and metal of the counter are equivalent to about one cm of water. Since the maximum secondary formation takes place after the penetration of about 100 cm of water, we

[9] O. H. Gish and K. L. Sherman, Nation. Geog. Soc., Contrib. Tech. Papers 2, 94–116 (1936). (Points taken from Fig. 4, curve *B*, p. 106.)

[10] J. F. Carlson and J. R. Oppenheimer, Phys. Rev. 51, 220–231 (1937).

see that few ionizing secondaries will be formed in the counter itself. Regener's tests confirm[5] this conclusion.

The cosmic-ray intensity drops at very high altitudes below the maximum value, reached at about 50,000 feet. It is therefore clear that much of the ionization produced in measuring instruments at high altitudes is due to secondaries. In the Peru flights this drop was found to be about 30 percent of the total. Since the main peaks represent ionization primarily due to secondaries, the experiments show that the component of the primary radiation cut off by the earth's field was responsible for about half the total secondary production in the upper atmosphere. It does not follow that half the primary energy, or even that half the total number of incident rays, was involved. A large latitude effect proves that most of the incident rays are charged particles only if the same absorption law is followed by charged particles and by other forms of radiation, which we know is not true. We have tacitly assumed that the ionization in any measuring instrument is proportional to the amount of the incident radiation. Such an assumption would hold true only for a homogeneous radiation. It appears possible that the component of the radiation which is cut off by the earth's field is a powerful producer of secondaries, and that most of its energy is absorbed in the upper atmosphere. It is principally a more penetrating component which produces sea-level effects.

(D) Shape of curve

At high altitudes, beyond the primary peak, the intensity falls off sharply. In the flight of *Explorer II*, Swann finds a decrease[7] of about 20 percent between the maximum at about 0.8 meter of water and the top of the flight. Millikan[6] similarly finds a drop of about 25 percent between the maximum of his Texas flight and the top of his flight. Like results are obtained with the counter flights in Peru. Nor do any of these flights reach very high altitudes. The important question is: To what value will the measured intensity fall at the limit of the atmosphere? An extrapolation of the various curves to zero-pressure indicates that the ionization shown in a counter or electroscope may be quite low. This gives rise to the question of whether a component of the primary radiation may be perhaps only very slightly ionizing. Should Millikan's suggestion regarding a non-ionizing component of the radiation be substantially correct, this would be the effect we would observe. Photons or neutrons would excite the counter only if they knock secondary electrons out of the walls, the surrounding atmosphere being assumed absent. In other words, a counter is not capable of distinguishing whether a count was due to a primary ionizing particle or to a secondary electron ejected by the primary from the surrounding molecules of air or the counter wall.

By removing the surrounding air, that is, by attaining high altitudes, we remove the biggest source of secondaries. From these measurements at extreme altitudes we shall see whether the primaries are ionizing or not. As we will show in a following paper, preliminary high-altitude counter flights show a marked falling off beyond the "primary maximum," and that possibly some of the radiation is non-ionizing. The curve for dip of the intensity at extreme altitudes found in the flights in Peru shows that at least 30 percent of the total ionization at high altitudes is due to secondaries. This value is merely a lower limit. Further flights are being undertaken to settle this point.

ACKNOWLEDGMENTS

The work described above was undertaken as a cooperative project. Thanks for financial support are primarily due the Cosmic-Ray Committee of the Carnegie Institution of Washington and to Dr. John A. Fleming, Director of the Department of Terrestrial Magnetism. Cooperation was received from Dr. Briggs, Director of the National Bureau of Standards. Advisory assistance with balloon-technique was received from the United States Weather Bureau. Work in Peru was greatly aided by Dr. G. A. Wagner, Chief of the Peruvian Meteorological Service, and from Dr. Santiago Bedoya of the Ministry of Foreign Affairs. For assistance in Panama the author is particularly indebted to Dr. James Zetek. Thanks are also extended to the many other persons who have helped the work, but whose names the limitations of space prevent listing.

Cosmic-Ray Observations in the Stratosphere*

L. F. CURTISS, A. V. ASTIN, L. L. STOCKMANN, B. W. BROWN
National Bureau of Standards, Washington, D. C.

AND

S. A. KORFF
Department of Terrestial Magnetism, Washington, D. C.

(Received November 8, 1937)

With radio methods devised as a part of a program for development of radiometeorographs, it has been found possible to record the response of a Geiger-Müller tube counter to cosmic rays at altitudes up to 116,000 feet. Records were made automatically by means of a recording receiver at a ground station. The results show a gradual rise in cosmic-ray intensity which is clearly evident at a pressure of about 500 millibars and then decreases slightly at a pressure of about 300 millibars after which the rise to maximum intensity at a pressure of about 100 millibars is very rapid. This maximum is about 150 times the count recorded near the ground level and is followed by a rapid decrease in counting rate at pressures below 100 millibars. At the highest altitude reached, approximately 116,000 feet, where the pressure is only 5 millibars, the counting rate falls to a value which is about the same as that observed at a pressure of 600 millibars. The general trend of these observations indicates that as the limit of the atmosphere is approached the counts continue to decrease, confirming the view which has been put forward by other observers that the greater part of cosmic-ray phenomena are due to secondary effects generated within our atmosphere.

I. INTRODUCTION

SINCE an important part of our knowledge of cosmic rays is to be obtained from information at high altitudes in the stratosphere at various latitudes, a ready means of obtaining such information should prove valuable. In the opinion of the authors the most promising method which has so far been conceived is that of automatic radio equipment attached to small balloons arranged to transmit the data to a ground station. Recovery of equipment is not necessary to secure the record so that observations may be made at any point where a satisfactory receiving station can be erected. Our experience with radiometeorographs[1] has revealed that the radio problems involved are very simple and that transmitting and receiving equipment can be made to function with a considerable degree of reliability. We have been able to demonstrate that it is readily possible to set up a receiving station of ample sensitivity which will respond only to signals from a transmitter operating at the desired wave-length. All problems of electrical interference, atmospheric and similar disturbances have been overcome under the conditions of our experiments so that the records obtained are absolutely clear and unambiguous.

The following paper gives the result of 18 successful ascensions from the National Bureau of Standards during the last six months. These ascensions were undertaken to test the equipment under all usual operating conditions and to secure data at this latitude to compare with similar data obtained near the magnetic equator and reported in the adjoining paper. In addition we were also fortunate in obtaining data on cosmic-ray counts at a new high altitude, approximately 116,000 feet, corresponding to a pressure of about 5 millibars or to within $\frac{1}{2}$ of 1 percent of the top of the atmosphere.

II. DESCRIPTION OF EQUIPMENT

The first requirement in designing equipment for this work is that it shall not have excessive weight. To attain really high altitudes in the stratosphere the difficulties are much lessened if the load does not exceed about 5 pounds. Larger loads require the use of extra size balloons or of a large number of small balloons. In either case the launching except under most favorable conditions is a problem, and the expense of an ascension is considerable.

* Publication approved by the director of the National Bureau of Standards of the U. S. Department of Commerce.

[1] L. F. Curtiss and A. V. Astin, J. Aero. Sci. 3, 35 (1935).

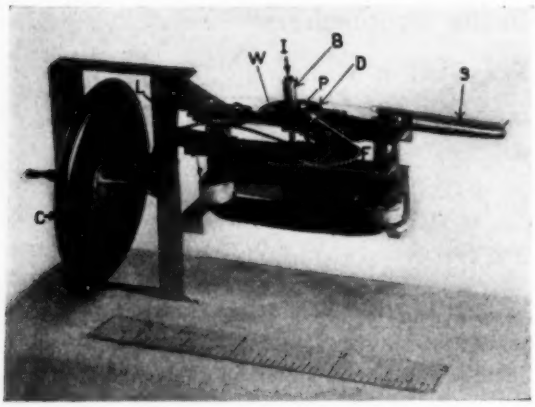

FIG. 1. Olland type radiobarograph for cosmic-ray balloon observations.

It is also desirable to utilize the "hot-house" arrangement devised by Regener and Pfotzer[2] to keep batteries and instruments at a fairly constant temperature. This led us to adopt a double-walled Cellophane inclosure similar to that used in early trials with radiometeorographs for which we have records of inside temperatures showing that they rarely fall below 20°C.

Within the inclosure were mounted the following items of equipment: transmitter, counter with its associated vacuum tube circuit and relay, barograph, and necessary batteries.

The transmitter used is essentially the same as the push-pull 5-meter transmitter described in an earlier paper,[1] with the substitution of a voltage fed for a current fed antenna. This change eliminated the trailing half of the doublet-antenna and made launching much simpler. No difference in transmitting efficiency was observed in making this change.

The Geiger-Müller tube counter and circuit is described in detail in the adjoining paper.[3] The counters were filled with argon to a pressure of about 4 cm and operated at 400 to 500 volts. This voltage was supplied by 10 units of the new 45-volt radio batteries, weighing about 2 oz. each, recently developed for radiometeorographs.

An important part of the equipment is the barograph which is a modified radiometeorograph which has been designed at the National Bureau of Standards. Since for cosmic-ray observations the pressure alone is of interest this instrument is arranged to give pressure readings by radio employing the well-known Olland principle. A photograph is shown in Fig. 1. A tiny radiometeorograph electric motor carries a Bakelite disk *D* on its output shaft, which turns at a speed of 4 r.p.m. Collar *B* turns freely on the same shaft and is provided with an external thread and an internal insulating sleeve, *I*.

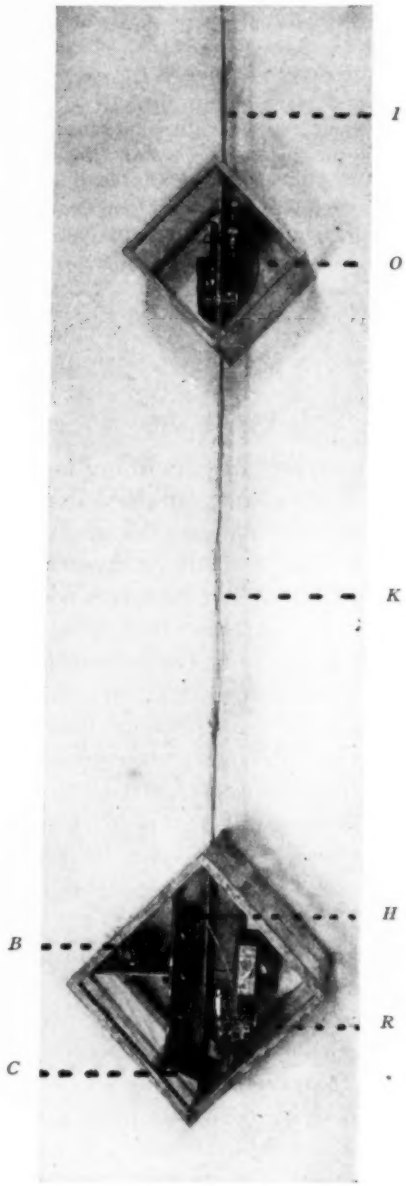

FIG. 2. Complete balloon equipment mounted in Cellophane inclosure. *I*, Antenna. *O*, 5-meter oscillator with batteries. *K*, Keying wires. *H*, 400 volt battery for counter. *B*, Barograph. *R*, Relay. *C*, Geiger-Müller tube counter in light-tight shield.

[2] E. Regener and Pfotzer, Physik. Zeits. **35**, 779 (1934).
[3] Korff, Curtiss and Astin, Phys. Rev. **53**, 14 (1938).

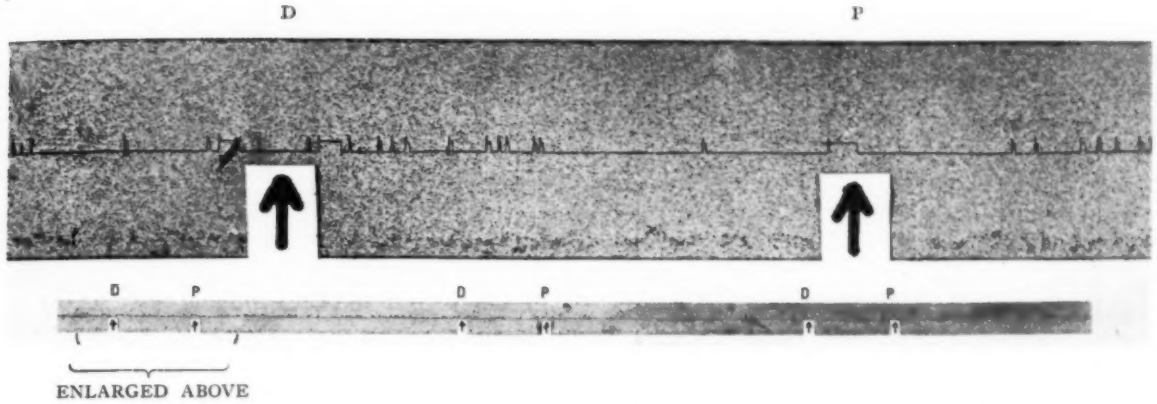

FIG. 3. Sample of tape from actual record showing barograph signals and cosmic-ray counts.

A fine Nichrome wire, approximately 3 mil in diameter extends from the spring, *S*, around the threads of the collar, *B*, and is attached to an insulating lever, *L*, which magnifies the motion of the aneroid capsule *C*. This motion causes the collar *B* to rotate and as it does so the platinum-iridium arm, *P*, rotates with it about the motor shaft as an axis. As this platinum arm turns it contacts a similar wire *W*, imbedded in the Bakelite disk, *D*, once for each revolution of the motor shaft. There are also two fixed contacts, *F*, which give a reference point for measuring pressures on the tape of the ground recorder. As the platinum wires, *W*, *P* and *F*, come in contact they key the transmitter by means of a pair of wires running up to it. These wires are attached, one to the frame of the barograph and the other to the insulated metal support for the spring, *S*. This contact causes the transmitter to emit a short signal which is picked up by the ground station. This arrangement requires the transmitter to be energized for a very small fraction of the total time so that a relatively strong signal can be used without increasing the weight of the *B* batteries. These strong signals are easy to locate and the problem of keeping the receiver tuned is much simplified.

The complete equipment is shown in Fig. 2 in which the transmitter and its batteries are in the upper compartment, and the counter and its batteries in the lower. This separation of $\frac{1}{4}$ wavelength was found necessary to prevent a feedback of the 5-meter signal into the vacuum tube circuit of the counter rendering the counting circuit inoperative. With all parts in place ready to be released this outfit weighed about 2100 grams or a little less than 5 pounds.

The receiver used in the observations reported here was a commercial superregenerative 5-meter receiver altered for satisfactory operation of a relay and tape recorder. This was accomplished by adding a rectifier tube much as described by Bent.[4] Our modifications resulted in a receiver which would actuate a relay only in response to a signal in the 5-meter band. Electrical interference, atmospherics and similar disturbances had no effect, since, to operate the relay, a train of 5-meter waves of sufficient duration to silence the regenerative oscillator is required.

The relay connected to the output of the receiver was used to actuate a tape recorder using waxed paper tape. A sample of actual record taken at an altitude of about 64,000 feet is shown in Fig. 3. *D* represents the fixed double signal of the barograph and *P* the contact of the pressure arm. All other shorter signals are pulses from the Geiger counter. The enlarged section is the left-hand end of the lower strip which shows how the pressure signals repeat every 15 seconds, with the shorter cosmic-ray signals distributed in a random manner between them.

III. Results Obtained from Balloon Ascensions

There are many factors which affect the altitude to which a rubber balloon, of the type used in this work, will rise before bursting.

[4] A. E. Bent, Bull. Am. Meteor. Soc. **18**, 99 (1937).

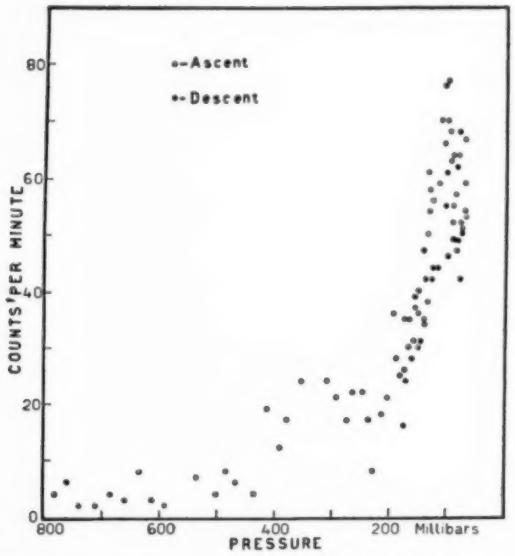

FIG. 4. Graphical representation of data from a single flight to 56,000 feet.

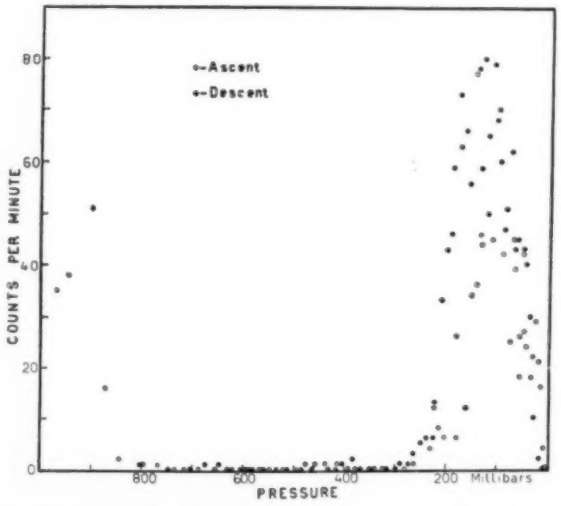

FIG. 5. Complete data from single flight to 116,000 feet showing low counting rate near the top of the atmosphere.

These factors do not seem to be very well known or understood at present. We have been able to show to our own satisfaction that some of the ideas on the subject which are prevalent do not hold. For example, it is assumed that the lower the inflation the higher the altitude to which a rubber balloon can go. As the result of repeated trials we have found this not to be true. This unexpected result can be explained we believe by the effect of the sun on the rubber. A fairly rapid ascensional rate seems to be required to prevent local over-heating and premature bursting. We also have found a wide difference in behavior of individual balloons so that at best the attainment of the maximum altitude of which these balloons should be capable is a matter of chance. For the most part we have used rubber balloons weighing about 650 grams with a nominal bursting diameter of 20 feet. Three to five such balloons inflated to a diameter of about 1.8 meters and having a free lift of about 1380 grams were used on each flight. The total free lift was thus nearly 4000 grams or about 1800 grams more than the load attached.

A total of 24 ascensions have been made between June and November, 1937. The balloons were released from the roof of one of the buildings of the National Bureau of Standards.

The penthouse containing the receiver was on the same roof facilitating last minute adjustments of the receiver. There was usually a slight shift in tuning directly after the take-off. For the remainder of the ascension retuning was rarely required. In the course of this work several difficulties were encountered and eliminated so that of the total number only 18 ascensions gave results on which we could rely. The first difficulty was traced to electrical leakage over the outside of the glass envelope of the Geiger-Müller counter. This was remedied by careful washing in alcohol and ether and dipping in molten Superla wax. It was soon found that some of the counters were sensitive to ultraviolet light. It was finally found necessary to inclose them in light-tight thin walled hard rubber cylinders. Thorough electrical insulation of all parts of the equipment was attained by dipping all supports in molten Superla wax.

In order to determine the behavior of our counting circuit at the very low pressures encountered in the upper stratosphere, we mounted an exact duplicate of our equipment under a large glass bell jar and pumped it down to 5 millibars residual pressure. We then compared its counting rate with a radium preparation at a fixed distance with that obtained at atmospheric pressure and also tested its recovery from a very rapid counting rate by bringing the radium close and quickly removing it to a distance. As a result we found the behavior of the equipment to

be the same at reduced pressure as at atmospheric pressure.

Our Washington results are illustrated by the two curves in Figs. 4 and 5. In each case the values for the number of counts per minute is taken directly from the wax-tape record. In arriving at a value of the count per minute for a given pressure we took the count for each successive minute and the average of the 4 pressure readings obtained in the same interval. The results shown in Fig. 4 are those of an average ascension. The minimum pressure is 65 millibars corresponding to an altitude of about 56,000 feet. A secondary maximum obtained in nearly all ascensions at about 350 millibars is shown as well as the principal maximum at about 100 millibars. The values obtained for a part of the descent are also shown. In most cases we were able to follow the signals until the balloon was only a mile or so high when the horizon cut the signals since by this time the balloon would be from 100 to 200 miles distant. We know the point of landing for about 3 of every 4 ascensions since the equipment was found and returned to us. Unless two or more balloons broke simultaneously, which happened occasionally, the descending record agreed well with the ascending record. This fact shows particularly well in Fig. 5 where we show the result of the highest ascension to a pressure of 5 millibars or about 116,000 feet. We succeeded in making 3 ascensions to near this pressure, which is lower than that attained in a previous ascension[5] to a pressure of 8 millibars which at that time was considered an altitude record for this country. The difference in altitudes associated with the pressures is accounted for by the fact that at that time an incorrect altitude table was used. The altitudes quoted in this paper are based on the "standard atmosphere."[6]

As is evident from the arrangement of the circles which show the counting rate at various pressures, the counter used to obtain the data represented in Fig. 5 had an exceptionally low blank. For several minutes its counting rate after passing an altitude of about 3000 feet was considerably less than 1 per minute. However, it is interesting to note that at the beginning of this ascension from the ground up to 3000 feet a counting rate of 30 or 40 per minute was observed falling abruptly at about the 3000 foot level. This ascension was made early on a morning when the air was unusually free from any evidence of motion. A misty haze blanketed the region and the atmosphere had been stagnant throughout the preceding night. We attribute this high activity to a layer of radium emanation which had slowly diffused to the height of 3000 feet during the stagnant period. This effect was never observed on clear, windy days.

The interesting result of the cosmic-ray observations on this ascension is the low value which the cosmic-ray count also rapidly reaches at the maximum altitude. During the 14 minutes the equipment was below the 15 millibar pressure the average cosmic-ray count was 0.5 per minute indicating a cosmic-ray intensity as low as that at 600 millibars, and about 1 percent of that at the maximum of the curve. We regard this as a striking confirmation of the view that most of the observed cosmic-ray phenomena are secondary effects produced within our atmosphere. The primary rays are either of such a nature that the type of equipment which is generally used does not detect them or are relatively few in number when compared with the secondaries.

The net results of observations covered by this

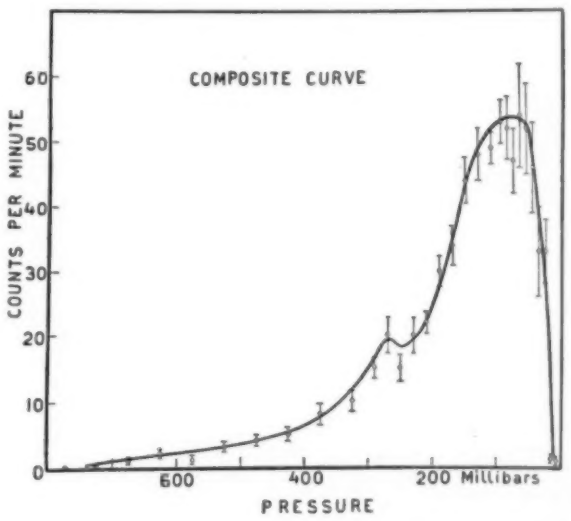

FIG. 6. A composite curve showing average value of cosmic-ray counts obtained from the 10 highest flights. Vertical lines represent the probable error of the arithmetic mean.

[5] L. F. Curtiss and A. V. Astin, Science **83**, 411 (1936).
[6] N. A. C. A. Technical Report No. 538. Annual Report 1935.

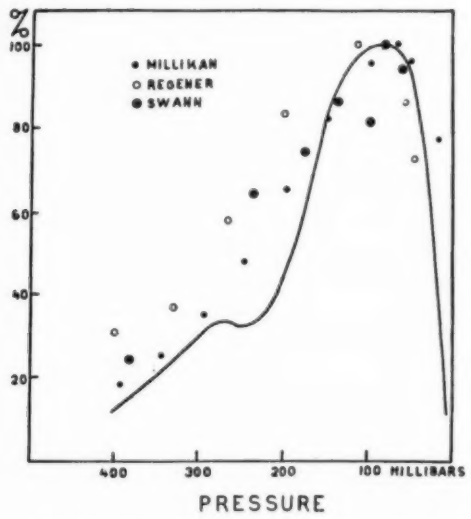

FIG. 7. Our composite curve shown in comparison with measurements reported by other observers.

paper are conveniently shown by a curve representing the average values of counting rates plotted against pressure as a composite curve for our ten highest flights. This is shown in Fig. 6. The counters by which these data were obtained were made as nearly alike as possible and the counting rates and counting voltages were consequently very similar. The blank or accidental discharge rate for each counter was determined from the counting rate at 800 millibars and subtracted from the counting rates at all lower pressures. The counts were then averaged directly without any multiplicative factor. This was not the case in the adjoining paper in which counting rates varied by as much as six to one due to intentional differences in the counters. The vertical lines show the value of the probable error of the arithmetic mean for each point. Below 50 millibars 4 records were available for averaging and the last two points were averaged from 18 minutes of a record of a single flight during which the apparatus was in the pressure range indicated.

IV. DISCUSSION

The precision of the measurements reported is from their very nature not great. By counting methods observations over many minutes at each altitude would be required to give an accuracy of even a few percent. For this reason too great weight cannot be given to these preliminary observations in discussing their bearing on cosmic-ray problems. However, one or two points do stand out perhaps with sufficient clarity to warrant a comparison with results obtained in other ways.

One interesting feature is that the general trend of our single counter measurements agrees well with coincidence measurements obtained by Regener and Pfotzer[7] using a triple counter arrangement and, therefore, taking in a limited solid angle of rays in the vertical direction. Earlier measurements with ionization chambers by Regener[8] and others indicated a leveling of the cosmic-ray intensity at the maximum. Since coincidence counters revealed a marked decrease beyond the maximum it was assumed that this difference was due to the fact that coincidence counters took in a definite solid angle whereas ionization chambers were nonselective as regards direction. That this conception is in error is also shown by the results published by Millikan, Neher and Haynes[9] where measurements to a pressure of 17 millibars are reported. The same rapid descent in intensity beyond the maximum is shown to be obtained with an ionization chamber. Our results merely trace this curve to about one-third the lowest pressure which they attained and indicate that this downward descent continues as the limit of the atmosphere is approached.

Attention should also be called to a difference which seems to exist between our single counter measurements and those by ionization chambers, namely, that the rise of the intensity of curve with decreasing pressure is more rapid in our measurements and also falls more sharply after passing the maximum. This is shown in Fig. 7, where our composite curve is drawn for comparison with measurements by other investigators. The solid circles represent the measurements with an electroscope by Millikan in July, 1936 at San Antonio, Texas and reveal the difference in steepness of the rise and fall of cosmic-ray intensity, when compared with our curve.

---

[7] E. Regener and G. Pfotzer, Nature **136**, 718 (1935).
[8] E. Regener, Naturwiss. **25**, 1 (1937).
[9] R. A. Millikan, H. V. Neher and S. K. Haynes, Phys. Rev. **50**, 992 (1936).

The rapid decrease in intensity below a pressure of about 100 millibars presents something of a paradox since it must mean that the primary radiation is of such high energy that it affects counters and ionization chambers to a moderate degree compared with the secondary radiation. On the other hand this radiation is so absorbable in the atmosphere that it is nearly all converted into secondaries within a layer equivalent to 2 meters of water and results in an intense emission of secondary particles at a very high altitude after traversing a comparatively thin layer of the atmosphere. There are several ways to explain this paradox qualitatively on the basis of knowledge we already have regarding the possible nature of the primary radiation. The simplest is to assume that much of the primary radiation is of the nature of heavy charged particles. Such particles will have the requisite energy associated with them at much lower velocities than would electrons or positrons. As a result of their electrical charge they would experience a magnetic deflection in the earth's field which could be made to agree with that experienced by electrons by assuming that they carry multiple charges. Since these particles would be like alpha-particles of very high velocity they would be converted quite rapidly into secondary radiation in the upper atmosphere. At the same time, since their number in comparison with that of the secondary particles would be small, the low value of cosmic-ray intensity in the upper stratosphere would be explained. This hypothesis might also help to explain the principal difference which appears between our single counter measurements and those by ionization chambers, namely, that the rise of the intensity curve with decreasing pressure is more rapid in the former case and also falls more sharply after passing the maximum. If heavy particles are involved in the primary beam or in the secondaries originating from it, one might expect the ionization chambers to show higher values than counters. As already mentioned, such an effect is visible in our composite curve since our results lie below those obtained by Millikan with an electroscope on both sides of the maximum.

We should also like to point out a second point of difference between our results and those of Millikan which is a definite indication of a secondary maximum of intensity at a pressure of about 300 millibars. This is revealed in our composite curve, Fig. 7, and is even more clearly evident on many of the individual records. Since this peak in the curve does not occur in results reported from Peru in the adjoining paper, the radiation contributing to this secondary maximum must be considerably affected by the earth's field. If this explanation for its appearance in our results is correct, observations at higher latitudes should reveal this secondary maximum more clearly.

The chief value of this report, however, is believed to be that it shows that automatic observations in the stratosphere to altitudes of at least 120,000 feet can be made with ease and reliability as far as transmission of data is concerned. Thus at a comparatively low cost frequent observations are possible which will greatly improve the accuracy of the combined results. This seems to offer a way to obtain the much-needed information regarding the nature of the main group of primary particles entering our atmosphere and the processes which lead to their conversion into secondary radiation.

V. Acknowledgments

We take great pleasure in expressing our appreciation to Dr. Lyman J. Briggs, Director of the National Bureau of Standards, and to Dr. J. A. Fleming, Director of the Department of Terrestial Magnetism, Carnegie Institution, Washington, D. C., for their encouragement and support in this work which otherwise would have been impossible.

Collisions of Alpha-Particles with Neon and Deuterium Nuclei*

JOHN T. MCCARTHY
Sloane Physics Laboratory, Yale University, New Haven, Connecticut
(Received November 12, 1937)

The tracks of about 600,000 Th C and C′ alpha-particle tracks were photographed in a Wilson cloud chamber filled with a mixture of neon and deuterium. An analysis of the elastic collisions with neon atoms gave points on a range-velocity diagram which fitted Eaton's curve fairly well except at the lower end. Reasons are given for thinking that this curve should be lowered slightly in the region of small velocities. A range-velocity curve is obtained from the collisions with deuterons. On the very reasonable assumption that, for a given velocity, the ranges of two isotopes are proportional to their masses, this curve indicates that Mano's calculations for protons are correct even for small velocities. It is shown that these collisions are elastic even when a high energy alpha-particle imparts considerable energy to a deuteron. No sign of inelastic collisions with either deuterons or neon atoms was obtained, although some were expected for the latter. The possible reasons for their nonappearance are discussed.

INTRODUCTION

THE cloud-chamber method has often been used to study the passage of alpha-particles and other atomic nuclei through gases. When a nucleus is struck by an alpha-particle with sufficient violence to produce a visible track, the velocity of the former can be computed from measurements made upon the forked tracks. Since the range of the nucleus can also be measured, an analysis of a number of collisions, on the assumption that energy and momentum are conserved, allows the construction of a range-velocity curve for the kind of atom in question. Various authors[1] have obtained such curves for a number of different elements, the work being limited somewhat by the difficulty in obtaining a desired element in a suitable gaseous form. Besides being essential for a full numerical investigation of the energy changes in transmutation experiments, these curves are also a part of our general knowledge of the manner in which heavy charged particles travel through gases.

All of the collisions between alpha-particles and atomic nuclei which have been observed in a cloud chamber have been found to be elastic except a few with nitrogen nuclei. Blackett[2] and others[3] obtained photographs in which an alpha-particle had disintegrated a nitrogen nucleus. These photographs are the most convincing evidence that the alpha-particle is captured in a proton disintegration.

In the present work a mixture of neon and deuterium was put in a cloud chamber and bombarded with alpha-particles from Th C and C′. The reasons for the investigation and the possibilities of its outcome were many:

(1) It was desired to study the collisions between alpha-particles and deuterons. The low stopping power of deuterium demanded the mixture of a heavier gas with it.

(2) Neon was chosen as this heavier gas because, although Eaton[4] failed to obtain a photograph of its disintegration by alpha-particles, recent experiments[5] have shown that the yield of this disintegration process is nearly as large as the yield for nitrogen. The photography of a proton disintegration would give further proof of the capture of the alpha-particle and would allow a calculation of the nuclear energy change which takes place in the reaction:

$$_{10}Ne^{20}+{}_{2}He^{4}\rightarrow{}_{11}Na^{23}+{}_{1}H^{1}.$$

(3) Protons and deuterons are the only two isotopes accessible to study in this way. There is every reason to suppose the range of a particle to be proportional to its mass.[6] From the range-

* Part of a dissertation presented to the faculty of the Graduate School of Yale University in candidacy for the degree of Doctor of Philosophy.

[1] P. M. S. Blackett, Proc. Roy. Soc. **A102**, 294 (1922); **103**, 62 (1923); P. M. S. Blackett and D. S. Lees, Proc. Roy. Soc. **A134**, 658 (1932); N. Feather, Proc. Roy. Soc. **A141**, 194 (1933); W. W. Eaton, Phys. Rev. **48**, 921 (1935); R. L. Anthony, Phys. Rev. **50**, 726 (1935).

[2] P. M. S. Blackett, Proc. Roy. Soc. **A107**, 349 (1925).

[3] P. M. S. Blackett and D. S. Lees, Proc. Roy. Soc. **A136**, 325 (1932); W. D. Harkins, Zeits. f. Physik **50**, 97 (1928); W. D. Harkins and A. E. Schuh, Phys. Rev. **35**, 809 (1930).

[4] W. W. Eaton, reference 1.

[5] E. Pollard and C. J. Brasefield, Phys. Rev. **51**, 8 (1937).

[6] H. Neuert, Physik. Zeits. **36** (1935), footnote p. 642.

velocity curves for two isotopes it is possible to test this proportionality and, in the present case, also to test the validity of the proton curve in the region of small velocities where some published curves are considered to be dubious.

(4) Although there has not been much need of a deuteron range-velocity curve in the past, the increasing use of these particles as bombarding particles for transmutations suggests the value of such a curve in the future.

(5) Schultz[7] has recently observed the emission of neutrons by deuterium under bombardment by the alpha-particles of Ra C′ or Th C′. Although the very low yields obtainable discourage the hope of observing this reaction in a cloud chamber, there is a slight possibility that one of the alpha-particle deuteron collisions might prove to be of this inelastic type.

Experimental Procedure

The cloud chamber used was of the conventional sylphon type built according to plans published by Dahl, Hafstad and Tuve.[8] It was filled with a gas mixture containing about equal parts of neon and deuterium at a pressure of about 90 cm of Hg.

Stereoscopic photographs were taken of the tracks by a camera of a type originally designed by Kurie.[9] This camera, by the use of mirrors and a single lens, takes two photographs side by side on the same film which are equivalent to photographs taken by two cameras at right angles. The photographs are reprojected by replacing the developed film in the camera and using it as a projection apparatus. The technique used for photography, reprojection and final analysis of the tracks was the same as that used and described by Eaton.[4]

The source of alpha-particles was a monel metal button having on its surface thorium active deposit obtained by radioactive recoil from a source of radiothorium. The alpha-particles were introduced into the chamber through a very thin sheet of mica, the space between the source button and the mica being evacuated at all times. When disintegration photographs are hoped for, the alpha-particles should be retarded as little as possible before entering the chamber. A sheet of mica equivalent to 5 mm of air (as determined by weighing) was finally chosen as the thinnest which would not break under the strain of gas pressure.

The measured lengths of the forks of a collision were reduced to the corresponding lengths in standard air (76 cm pressure at 15°) by multiplication by the stopping power of the gas. Since the exact composition of the gas was not known, the mean stopping power was determined by measuring the average range of alpha-particles in the gas and comparing it with the known range of the particles in air under standard conditions. The stopping power for recoil atoms is arbitrarily assumed to be the same as that for alpha-particles. This assumption is probably valid for deuterons but is admittedly questionable for heavy atoms.

The range-velocity curve for alpha-particles necessary for the analysis of the collisions was

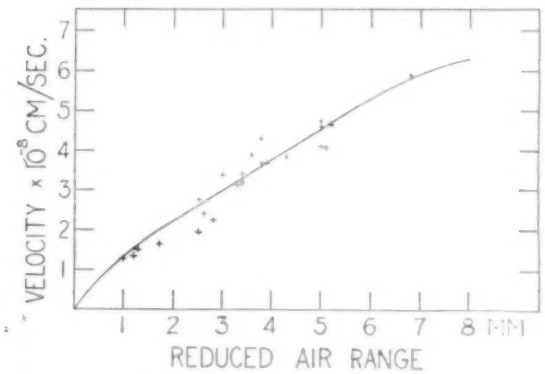

Fig. 1. Range velocity curve for neon.

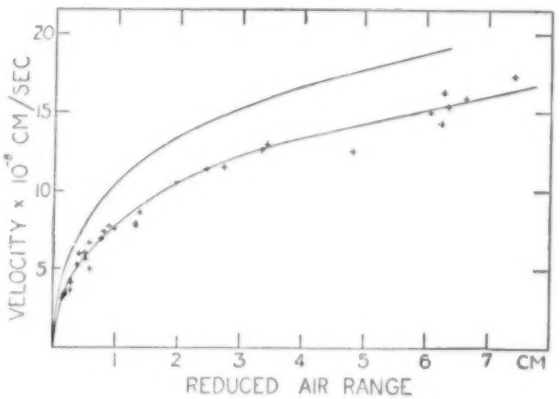

Fig. 2. Range velocity curves for protons and deuterons.

[7] H. L. Schultz, Washington Meeting, American Physical Society, April 1937.
[8] O. Dahl, L. R. Hafstad and M. A. Tuve, Rev. Sci. Inst. **4**, 373 (1933).
[9] F. N. D. Kurie, Rev. Sci. Inst. **3**, 655 (1932).

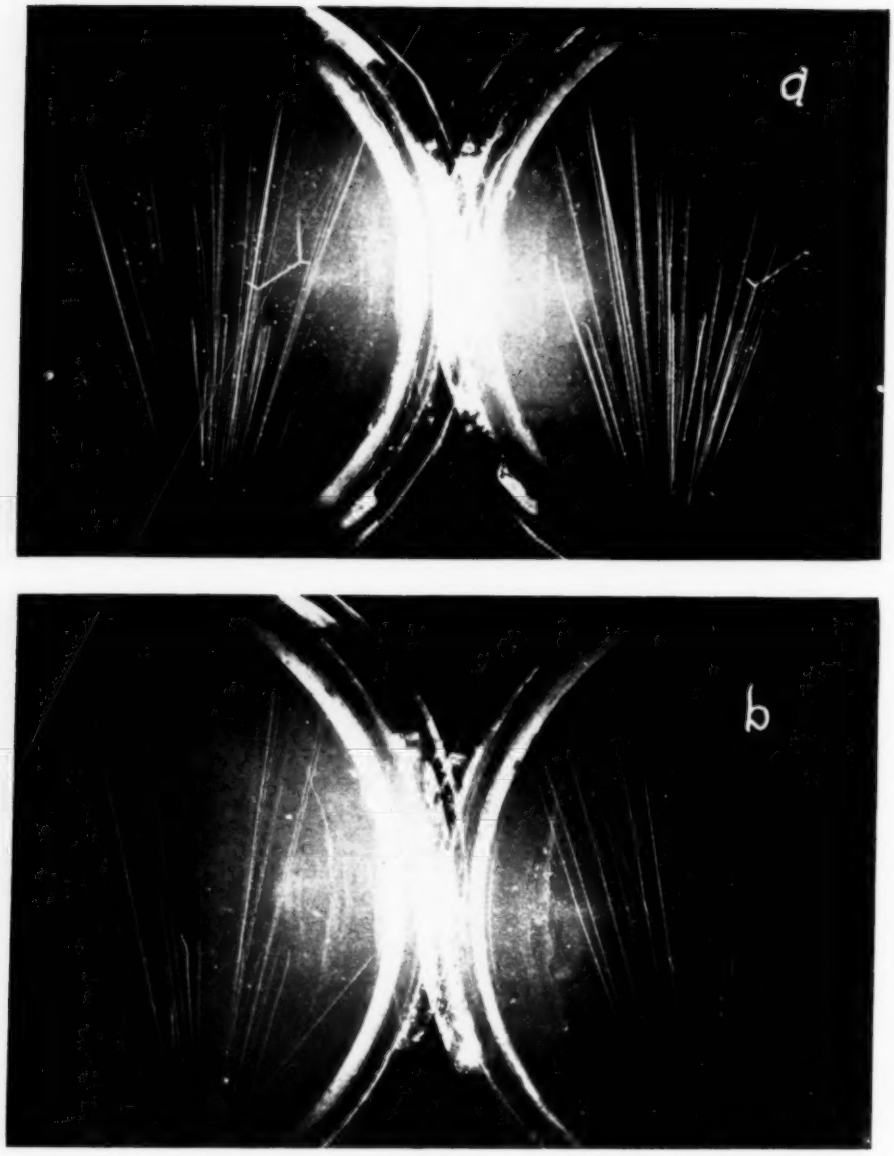

FIG. 3. a. Unusual event: an alpha-particle suffers two successive collisions with neon nuclei. b, c, and d. Examples of collisions of alpha-particles with deuterons.

one constructed from the work of Blackett and Lees[1] and Mano.[10] The results of the former seem to be the most reliable for particles of small ranges, and Mano's curve is probably the best for large ranges.

RESULTS

Of the 15,000 stereoscopic photographs taken of alpha-ray tracks in a mixture of neon and deuterium it is roughly estimated that there were on the average 40 tracks per photograph. Hence a total of 600,000 tracks were studied, of which approximately two-thirds were of the long range type from Th C′. Of the neon collisions which were analyzed, 25 were chosen for velocity calculation. The points corresponding to these collisions are plotted together with Eaton's curve in Fig. 1. It is seen that these points group about the curve fairly closely but seem to suggest that the first part of the curve should be

[10] G. Mano, Ann. de physique **1**, 407 (1934).

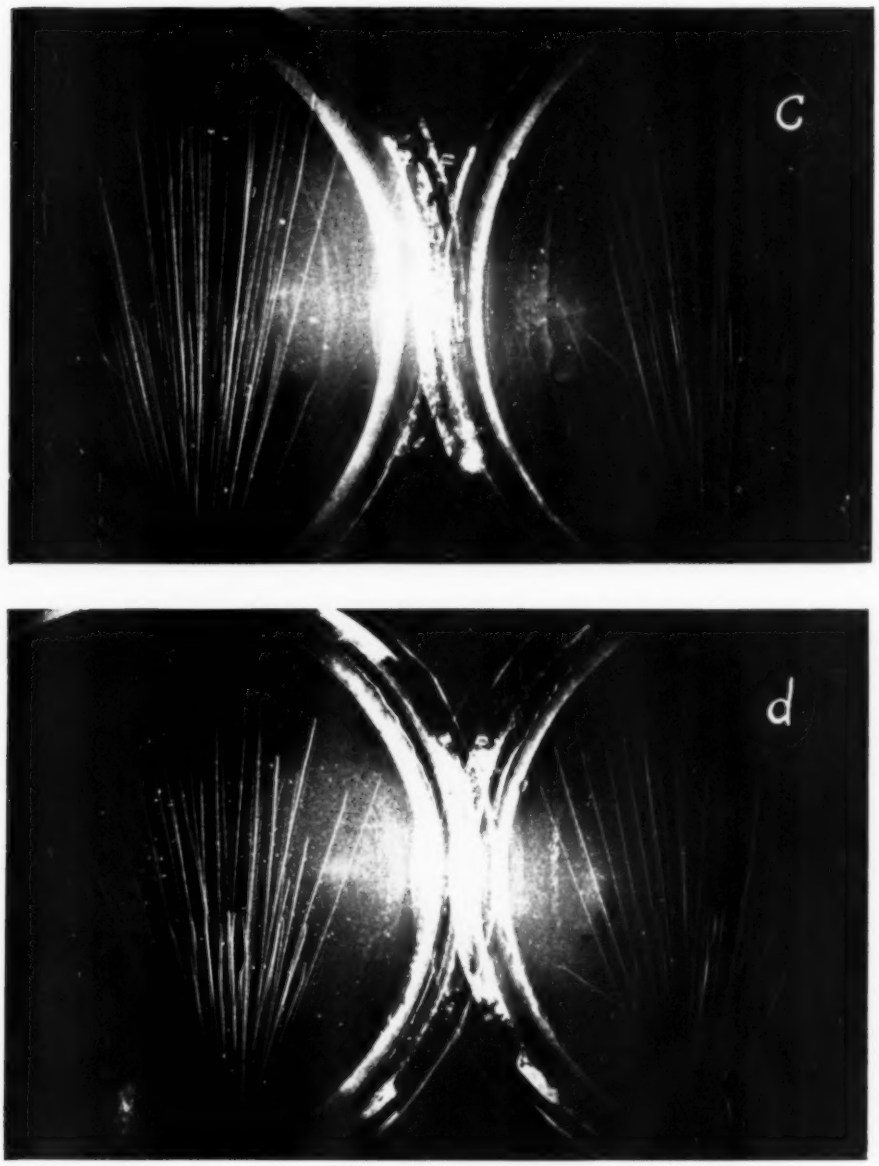

FIG 3. c and d.

lower. Two other considerations seem to make the same suggestion:

(1) The neon curve crosses the curve for fluorine at the lower end. This crossing is unexpected and has been ascribed by Eaton to a spurious effect arising from the different methods of calculating stopping powers. Eaton took account of the variation of stopping power with velocity, while in Feather's work on fluorine and in the present work the mean value of the stopping power was used. This difference of procedure would be expected to show slightly different results for small ranges.

(2) Anthony[1] found that, for large velocities, the ratio of the ranges of neon atoms and alpha-particles for the same velocity was a constant for points along the two curves. This situation is true for smaller velocities also if the neon curve is dropped slightly below the fluorine curve in this region. The constancy of this ratio probably has some significance, since it has been found to hold true for the curves of any pair of

elements which are in the same column of the periodic table.

In Fig. 3a is shown an unusual type of event: an alpha-particle suffered two successive collisions with neon nuclei, striking both of them hard enough to produce recoil spurs.

Although deuteron collisions were relatively infrequent and were occasionally poorly photographed because of the long thin character of the deuteron track, finally about 30 alpha-particle deuteron collisions were obtained which were good enough for complete analysis. The points plotted on the graph in Fig. 2 are those obtained from these collisions. The upper curve is the range-velocity curve for protons, plotted from the calculations of Mano.[11] The lower curve applies to deuterons and is drawn from the proton curve on the assumption that the range of a deuteron is twice that of a proton of the same velocity. The experimental points are seen to fit this curve very well.

This good agreement is in divergence with the results of Parkinson, Herb, Bellamy and Hudson[12] who, by means of a two million volt generator, have measured the range of protons in air as a function of energy. Their data disagree considerably with the theoretical values of Mano at energies below 0.7 Mev. The "visual" range-energy curve obtained in somewhat the same manner by Tuve, Heydenburg and Hafstad,[13] disagrees even more. At high velocities and energies the calculations of different theoretical authors agree and are probably correct, because the hypotheses on which the theories are based are better satisfied at higher velocities.

Examples of deuteron collisions are given in Fig. 3b, c, d. The characteristic appearance of these collisions usually makes them easy to identify.

Three of the highest points on the deuteron graph represent collisions in which the deuteron has been given a kinetic energy greater than its binding energy. The collision corresponding to one of these points is shown in Fig. 3b. A deuteron with a velocity of 16×10^8 cm per sec. has a kinetic energy of 2.66 Mev, while the binding energy is only 2.14 Mev. Furthermore, in these collisions the impinging alpha-particle had an initial energy of 7.11, 7.19 and 7.83 Mev in the three cases. In order to disintegrate a deuteron an incident alpha-particle must possess a kinetic energy of at least three times the binding energy of the deuteron.[14] This condition is fulfilled in each of the three above cases and yet the collisions were elastic. Likewise with other elements it has been found by other investigators that in certain collisions the alpha-particle can approach very closely to the nucleus and impart considerable energy to it without causing a disintegration.

No inelastic collisions with either a deuteron or a neon nucleus were photographed. This might be expected for the deuterons but is surprising and disappointing for neon in view of the large number of tracks photographed both in the present work and in Eaton's work. Altogether it is estimated that about a million effective tracks have been photographed in neon. Since the yield from neon is about two-thirds that from nitrogen, about eight disintegration processes would be expected to occur in the course of the combined work. That not one of these events was observed is indeed unfortunate. Although the films were inspected carefully several times and all suspicious collisions were completely analyzed, it is possible that an inelastic collision was overlooked. Fig. 3c illustrates the kind of collision which was often suspected to be a neon disintegration, the long fine track being a possible proton. Analysis showed that in reality it is a deuteron collision with a short recoil alpha-ray track.

In conclusion, the author is pleased to express gratitude to Professor A. F. Kovarik for his advice and assistance during the course of the present work and to Dr. Ernest Pollard for many helpful discussions.

[11] G. Mano, J. de phys. et rad. **5**, 628 (1934).
[12] D. B. Parkinson, R. G. Herb, J. C. Bellamy and C. M. Hudson, Phys. Rev. **52**, 75 (1937).
[13] M. A. Tuve, N. P. Heydenburg and L. R. Hafstad, Phys. Rev. **50**, 806 (1936).
[14] H. S. W. Massey and C. B. O. Mohr, Proc. Roy. Soc. **A148**, 206 (1935).

Artificial Radioactivity of Tantalum

O. OLDENBERG*
Radiation Laboratory, Department of Physics, University of California, Berkeley, California
(Received October 22, 1937)

Radioactivity has been induced in tantalum by slow neutrons, fast neutrons, and fast deuterons. (1) Slow neutron capture leads to Ta^{182} with a lifetime of 97 days. (2) Fast neutron bombardment excites, in addition, an 8.2-hour period with the emission of electrons, K radiation of Ta, and γ-rays. The process responsible for these effects is probably the capture of one neutron with the ejection of two neutrons. The product nucleus, Ta^{180}, goes over to Hf^{180} largely by K electron capture; in this process either γ-rays are emitted or by their internal conversion extranuclear electrons ejected. (3) Deuteron bombardment of tantalum leads to a decay curve affected to such an extent by impurities that the tantalum activity can not be observed clearly.

PROBLEM

THE present paper deals with artificial radioactivity in tantalum bombarded with slow neutrons, fast neutrons, or fast deuterons. Tantalum has only one isotope, $_{73}Ta^{181}$, so that the attribution of radioactive nuclei artificially produced is comparatively simple.

Two periods produced in tantalum are known. A very weak activity with a long period of 200 ± 100 days, produced by slow neutrons from a radon—beryllium source, was observed by Fomin and Houtermans[1] and attributed to Ta^{182}. Heyn[2] reported another very weak activity produced by fast neutrons in Ta. Its half-life was determined by Pool, Cork, and Thornton[3] to 9.1 hours.

In the present investigation tantalum was bombarded with slow neutrons, fast neutrons from lithium, and 5.5 Mev deuterons in the cyclotron of the Radiation Laboratory of the University of California. Sheet tantalum furnished by the Fansteel Metallurgical Corporation was used. Its surface was carefully cleaned by scraping and washing in acids and distilled water. For experiments with deuteron bombardment surface impurities are most troublesome; therefore the tantalum samples were baked out at red heat in high vacuum in an induction oven. A thin platinum foil protected the tantalum in the chamber of the cyclotron from possible impurities knocked out by the deuteron beam from the metal walls. The platinum foil was baked in high vacuum in the same way as the tantalum. The decay curves of the radioactive products were measured with a Lauritsen electroscope.

(1) Slow neutrons

The long period of 200 days ±100 given by Fomin and Houtermans was confirmed. A more accurate value of the half-life is 97 ± 8 days. As there exists only one stable isotope, Ta^{181}, capture of slow neutrons must lead to Ta^{182}. The particles emitted are negative; this was determined by the Thibaud trochoid method. I am indebted to Mr. Ernest M. Lyman for the use of his apparatus. By the observed electron emission Ta^{182} goes over to the stable W^{182}. A very faint period of a few minutes probably belongs to an impurity.

(2) Fast neutrons

Fast neutrons were produced from lithium bombarded with deuterons of 5.5 Mev. The tantalum sample was protected from slow neutrons by a cadmium chamber filled with borax. The same long period as for slow neutrons resulted, due to neutron capture leading to Ta^{182}. In addition, an 8.2 ± 0.2-hour period was observed. (Fig. 1.) A very weak period of approximately 21 minutes may belong to an impurity and may be identical with the short period observed with tantalum bombarded by slow neutrons.

The 8.2-hour period is likewise excited if the lithium target is protected by a copper foil of 1/1000 inch which reduces the energy of the

* On leave of absence from Harvard University.
[1] V. Fomin and F. G. Houtermans, Physik. Zeits Sowjetunion **9**, 273 (1936).
[2] F. A. Heyn, Nature **139**, 842 (1937).
[3] M. L. Pool, J. M. Cork, and R. L. Thornton, Phys. Rev. **52**, 239 (1937); see Zeits. f. Physik **106**, 238 (1937).

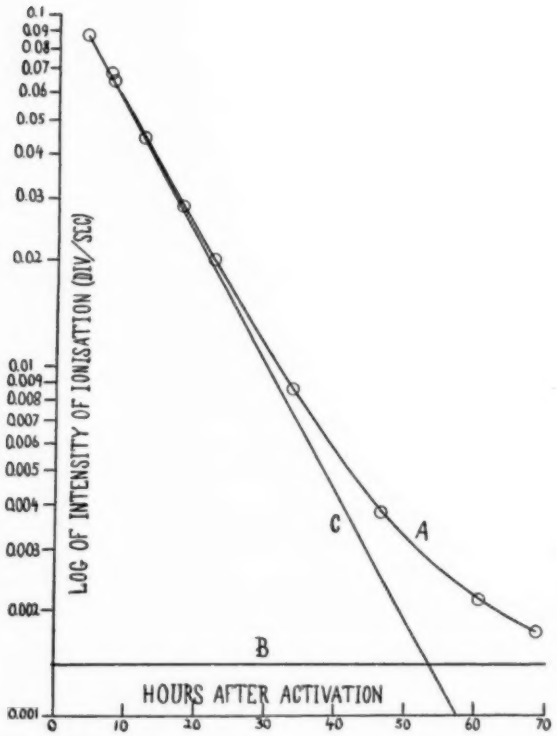

FIG. 1. Decay curves for tantalum bombarded by fast neutrons. Curve *A*, observed; curve *B*, 97-day period applied as correction; curve *C*, corrected curve, 8.2-hour period.

deuteron beam to a small fraction of its original value. This proves that neutrons as they emerge from Li without an appreciable contribution of kinetic energy from the beam are sufficient to excite the nuclear reaction.

The 8.2-hour β-particles have an absorption curve in aluminum with an end point at about 0.54 mm, corresponding to an upper limit of 0.48 Mev according to Feather's formula.

In order to determine at least a relative value for the yield of radioactive Ta excited by fast neutrons Ta samples were bombarded together with Cu samples arbitrarily chosen as a standard. Cu was bombarded for so short a time that the 10-min. period prevailed. By bombarding several sheets of Ta and Cu in touch with each other it was checked that no one sheet appreciably absorbed the neutrons and so reduced the effect on the following sheets. The saturation activity for Ta is 0.08 if the value for Cu is assumed to be one.[4] (This figure does not exactly express the probabilities of the effects of fast neutrons on Ta and Cu nuclei since it is not taken into account that in Cu electrons are able to emerge from greater depths than in Ta, both metals being uniformly affected through their whole bodies by neutrons.)

The 8.2-hour period is undoubtedly identical with the 9.1-hour period reported by Pool, Cork, and Thornton. A correction made for the superimposed long period of 97 days is responsible for the difference.

The 8.2-hour period must be attributed to tantalum itself and not to an impurity for the following reasons. First, its intensity is comparable with the intensity of the 97 day period induced in tantalum at the same bombardment. The ratio of the saturation activities for the short and the long period is approximately 1 : 3. Secondly, the possible impurities fail to show such a period. The Fansteel Metallurgical Corporation kindly informed us that the tantalum sample might contain 0.25 percent columbium and much smaller percentages of Fe, C, Li, Sn, Mn, and Mg. In a separate experiment, a piece of columbium was bombarded with fast neutrons. It failed to show the 8.2-hour period; in fact, columbium is almost completely inactive. None of the other impurities mentioned lead to an 8.2-hour period. It is to be concluded that this period belongs to tantalum itself.

The particles emitted by the 8.2-hour activity are negative; no positive particles could be observed.

The established processes caused by fast neutron bombardment are as follows (see Table I showing the stable isotopes).

(a) *Capture of the neutron.* This process is induced in tantalum by fast neutrons as well as by slow neutrons (Section 1). This is indicated by the 97-day period. Because the Li target gives off neutrons of a certain energy distribution the

TABLE I. *Stable isotopes.*

$_{71}$Cp	$_{72}$Hf	$_{73}$Ta	$_{74}$W
			183
	180	181	182
	179		
	178		
	177		
175	176		

[4] E. McMillan, M. Kamen, and S. Ruben, Phys. Rev. 52, 375 (1937), footnote 3.

energy of the neutrons actually captured remains uncertain. It is only certain that thermal neutrons are excluded by borax and cadmium.

(b) *Capture of the neutron with ejection of a proton.* This would lead to Hf^{181}, an isotope known to have a lifetime of more than 30 days. Hence, this process is ruled out.

(c) *Capture of the neutron with emission of an α particle.* This process would lead to an isotope of cassiopeium, Cp^{178}, which would go to Hf^{178} with electron emission.

(d) *Capture of the neutron with emission of two neutrons.*[5] This process would lead to Ta^{180}.

Between the alternative Cp^{178} and Ta^{180} the decision was made on the basis of a chemical separation. I am much obliged to Dr. G. T. Seaborg for his detailed advice regarding the chemical method. Tantalum metal and a small amount of rare earth oxalate added to act as a carrier were treated with a mixture of hydrofluoric and nitric acids. This mixture was fumed with 9 normal perchloric acid. The T_2O_5 was filtered out. The rare earth remaining in the filtrate was precipitated by the addition of hydrofluoric acid and filtered out. The result was that the activity was concentrated in the tantalum, the rare earth scarcely showing an activity above background. It is concluded that the active isotope is Ta^{180} produced by the capture of the neutron with emission of two neutrons.

Ta^{180} is expected to go over to the neighboring Hf^{180} by either positron emission or capture of a K electron. This last process has been predicted on the basis of Fermi's theory of β disintegration. The first experimental evidence for this process was recently obtained by Alvarez[6] who observed that a certain radioactive vanadium isotope emits $K\alpha$ radiation as well as positrons. This indicates that this isotope may decrease its nuclear charge as well by K electron capture as positron emission. Theoretically it is known[7] that the ratio of these two alternative processes changes in favor of K electron capture for the heavier elements because of the stronger Coulomb force and the consequent closer approach of K electrons to the heavy nuclei. In agreement with this theoretical

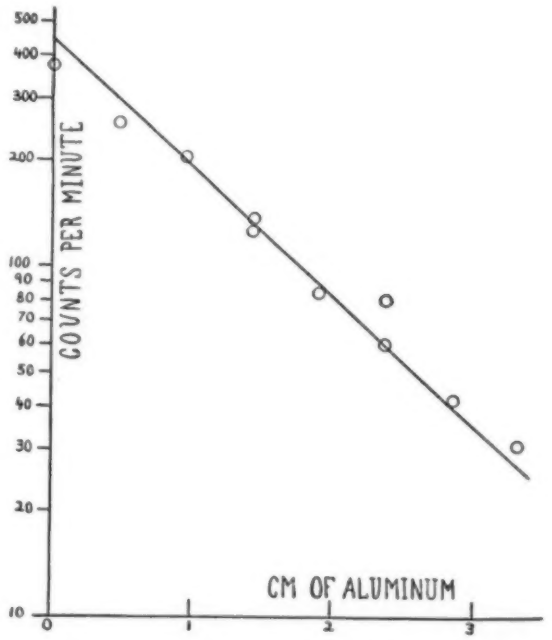

FIG. 2. Absorption curve for tantalum bombarded by fast neutrons. Circles indicate observations, solid line the absorption curve predicted for $K\alpha$ of hafnium.

argument, the survey reported by Pool, Cork, and Thornton[8] shows that positron emission is observed for many light nuclei, for a few nuclei of medium weight, but for no heavy nuclei. Therefore, it is not surprising that in Ta no positron emission is observed. In order to check the $K\alpha$ emission from the active tantalum the method of Alvarez was applied, that is, the absorption curve in aluminum was observed with a Geiger counter. The curve is given in Fig. 2. (Corrections are made for the background of the counter and, in addition, for a background of 40 counts per sec. due to a harder γ radiation.) The solid line represents the absorption curve as one might expect it from the $K\alpha$ line of hafnium, the next lighter element. The agreement seems sufficient to prove the emission of K radiation. It is inferred that K electron capture takes place. This result confirms the attribution of the activity to the Ta^{180} nucleus since K electron capture is not to be expected for the alternative Cp^{178} nucleus which presumably would be an electron emitter. The hard γ-rays are so weak that it is not possible to measure an absorption curve in order to determine their energy.

[5] M. L. Pool, J. M. Cork, R. L. Thornton, Phys. Rev. **51**, 890 (1937).
[6] L. W. Alvarez, Phys. Rev. **52**, 134 (1937).
[7] C. Møller, Phys. Rev. **52**, 84 (1937).
[8] M. L. Pool, J. M. Cork, and R. L. Thornton, Phys. Rev. **52**, 239 (1937).

The K radiation belongs to the electron emission of the 8.2-hour period, observed with the electroscope, and not to the 97-day period; it disappears completely after a few days. The 8.2-hour period is observed very sharply as a straight line on the semi-logarithmic diagram indicating the presence of only one period (Fig. 1). It follows that electrons and K radiation emerge from the same active nucleus. One may assume a branching disintegration leading to Hf^{180} by K electron capture or instead to W^{180} by electron emission.[9] But this interpretation would lead to the difficulty that W^{180} is not known as a stable isotope so that one would have to assume this isotope either as stable with a very small concentration or as unstable with a long life. (Since one might expect W^{180} to go over to Hf^{178} by α-emission, this emission was checked with ionization chamber and linear amplifier; no such α-emission could be observed. Thanks are due to Mr. Dean B. Cowie for his cooperation and the use of his apparatus.) More plausible than the idea of a branching reaction leading to an unknown W^{180} is the assumption that the electrons are emitted by a secondary process connected with K electron capture. Such a process would be the emission of a γ-ray which may be replaced by internal conversion, that is ejection of one of the extranuclear electrons (Auger process) as it is well known from the β-ray line spectrum. Such a γ-ray emission (or its alternative) is to be expected combined with K electron capture because, in general, the K electron capture must lead to an excited level of the new nucleus, the energy of which is available for radiation. (The conversion of the $K\alpha$ radiation into electron emission by an Auger process would be observed as emission of much softer β-rays, practically not to be separated from the β-rays with the harder limit just described.)

(3) Deuterons

The activity of tantalum, excited by 5.5 Mev deuterons was investigated with all possible accuracy and followed through several months. Mr. J. R. Richardson kindly took a series of cloud chamber photographs. Yet no definite conclusions can be drawn as the decay curve is too complicated. It seems to be a superposition of at least five or six periods. Most of them differ so widely that an analysis of the observed curve may be attempted. Almost all of them are sure to belong to impurities. This follows from a consideration of the established deuteron reactions. The stable isotopes are given in Table I. The reaction, Ta^{181} (d, n) W^{182}, would lead to the *stable* isotope W^{182}. Likewise, the reaction, Ta^{181} (d, α) Hf^{179}, would lead to a *stable* isotope, Hf^{179}. The only *radioactive* isotope to be expected[10] would be due to the Oppenheimer-Philipps reaction Ta^{181} (d, p) Ta^{182}. The resulting isotope Ta^{182} is known to have a lifetime of 97 days.

The overwhelming contribution of impurities observed after deuteron bombardment, in spite of the extreme care with which the sample was cleaned, is certainly due to the closer approach the deuteron has to light nuclei than to the heavy Ta nucleus.

After the gradual decay of some of the superimposed periods the 97-day period is actually apparent. The thick target yield is of the order of magnitude 10^9 deuterons per activated Ta atom provided that the activity observed for this period is not partly due to impurities with equal or longer periods. The masking is so strong that at present no more accurate figure for the Ta^{180} period can be obtained from deuteron bombardment, although with deuterons a much stronger activity can easily be induced than with slow neutrons. The superimposed periods can be attributed to definite impurities as far as it is possible to measure their lifetimes. Very intense is the 10-min. period of N^{13} due to the bombardment of carbon. Its intensity is not even materially reduced by the careful cleaning process described above. Hence the carbon impurity is probably contained in the body of the metal unless one assumes that the residual gas in the cyclotron deposits carbon from decomposed oil vapor on all surfaces. On the other hand, a period of 15 hours, emitting electrons, is materially reduced by the cleaning process; it probably belongs to Na. Several other periods are so much fainter that they cannot be measured with an accuracy sufficient for identification.

[9] See S. N. Van Voorhis, Phys. Rev. **50**, 895 (1936).

[10] In any such argument (Sections 2 and 3) the possibility of isomers is disregarded. So few isomers are known that this is plausible although by no means certain.

The author takes pleasure in expressing his gratitude to Professor E. O. Lawrence for the hospitality with which he was received at the Radiation Laboratory of the University of California and for the spirit of cooperation among his collaborators which makes the work at Berkeley so pleasant and profitable. The research has been aided by grants to the laboratory from the Research Corporation, The Chemical Foundation, and the Josiah Macy, Jr. Foundation.

Note added in proof: In the above argument for the disintegration of Ta^{180} no stable W^{180} is assumed to exist. Professor A. J. Dempster kindly informed me of his recent discovery of this isotope (Phys. Rev. **52**, 1074 (1937)). This removes the objection to the negative electron emission from Ta^{180}. This process must be considered as possible in addition to K electron capture, either due to a branching reaction or an isomer of Ta^{180}, both isomers disintegrating with periods of little difference.

JANUARY 1, 1938 PHYSICAL REVIEW VOLUME 53

The Oppenheimer-Phillips Process

H. A. BETHE
Cornell University, Ithaca, New York

(Received November 15, 1937)

The mechanism proposed by Oppenheimer and Phillips for the disintegration of nuclei by deuterons with proton emission (d-p reaction) is examined. A formula is derived which expresses the probability of this process in terms of the sticking probability of the neutron (§2) and the penetrability of the potential barrier. The importance of the finite (rather than zero) nuclear radius for the penetrability is pointed out and the penetrability is calculated for various values of the radius (§3). The energy distribution of the emitted protons is found to be given directly by the sticking probability of the neutron (§5). Therefore it may differ considerably from the distribution in "ordinary" nuclear reactions by containing relatively more high energy protons. A measurement of the energy distribution would allow direct conclusions about the width of low nuclear levels which is of importance for the theory of the α-decay and therefore of the nuclear radius (§5). The probability of the O-P reaction is compared with that of ordinary nuclear reactions. The O-P mechanism is found to prevail in the d-p reactions for nuclear charges of about 25 and higher; if the reaction leads to a nucleus which emits fast β-rays, the O-P mechanism will be valid at still lower charges. The relative probability of d-p as compared to d-n reactions is found to be (on the average) unity for very light nuclei, to decrease with increasing atomic number until the O-P process becomes prevalent, and to increase from there on. The excitation function of reactions with nuclei up to $Z\sim30$ is found to be an inadequate test for the O-P mechanism (§6). The question of secondary (cascade) disintegration following the d-p reaction is discussed and it is found that such disintegrations (e.g. d-pn or d-$p\alpha$) should be rare with deuteron energies below the top of the potential barrier (§7).

§1. GENERAL

IN any ordinary nuclear reaction the first step is the entry of the incident particle as a whole into the initial nucleus. In the "compound nucleus" thus formed, the nuclear particles rearrange themselves until the compound nucleus breaks up into final nucleus and produced particle. However, according to Oppenheimer and Phillips,[1] this general scheme does not apply to reactions of the d-p type:[2] Here the incident deuteron does not enter the nucleus as a whole but splits up outside the nucleus into a proton which leaves as the "produced particle," and a neutron which is absorbed by the nucleus.

The Oppenheimer Phillips (O-P) process is, therefore, in principle *simpler* than the ordinary type of nuclear reactions. While the ordinary reactions are double processes, consisting of the formation and disintegration of the compound nucleus, the O-P process is a simple absorption, i.e. formation of the compound nucleus which is in this case identical with the final nucleus. The proton does not enter the reaction at all except by carrying away the surplus energy and momentum, this latter function being, of course, quite essential because otherwise a simple absorption process could never occur. Since the O-P process differs essentially from all other

[1] Oppenheimer and Phillips, Phys. Rev. **48**, 500 (1935).
[2] I.e., reactions produced by deuterons (d) with emission of a proton (p). For the nomenclature, see Livingston and Bethe, Rev. Mod. Phys. **9**, 245 (1937).

nuclear reactions, the usual "dispersion theory"[3-5] does not apply to it but a special theory must be developed which will be done in §2. In this theory, the cross section of the O-P process will be expressed in terms of the neutron width of the states of the final nucleus[4, 5] or of the "sticking probability" of the neutron.[5]

It is, of course, a matter of primary importance whether a *d-p* disintegration will occur more easily according to the O-P scheme or to the ordinary scheme, i.e., with the deuteron entering as a whole. It was first believed[1] that the O-P process was favored mainly because the neutron, being uncharged, penetrates more easily into the nucleus than the whole deuteron. However, while this effect is certainly important for heavy nuclei, it appears negligible for light ones ($Z\sim 20$). The essential point in favor of the O-P process seems to be that in the ordinary scheme the *d-p* reaction would have to compete with other processes, notably the *d-n* reaction, while in the O-P scheme there would be no such competition (reference 5, §80).

Even so, the O-P process will be restricted to fairly heavy nuclei. For the lightest nuclei, the potential barrier is so low that it presents no obstacle to the entering deuteron nor to the outgoing proton, the latter fact being important for the question of the competition of the proton emission with the neutron emission. (cf. §6).

§2. Oppenheimer-Phillips Process and Compound Nucleus

Since the O-P process is a simple quantum process, its cross section is given by

$$\sigma=\frac{2\pi}{\hbar}|\int V_{AN}\,\chi_A\,\chi_D\,\chi_B^*\,\psi_D^c\,\psi_P^{e*}\,d\tau|^2, \quad (1)$$

where A denotes the initial, B the final nucleus, D the deuteron, P the proton, N the neutron. V_{AN} is the interaction between initial nucleus and neutron, the χ's are the internal wave functions (discrete states) and the ψ's the wave functions describing the motion in space (continuous spectrum). The upperscript c denotes normalization per unit current, e per unit energy and a per unit amplitude. The relation between these normalizations is

$$\psi^e=v^{-\frac{1}{2}}\psi^a, \quad (2a)$$

$$\psi^e=(M^2v/2\pi^2\hbar^3)^{\frac{1}{2}}\psi^a, \quad (2b)$$

where v is the velocity, M the mass of the particle in question.

The expression (1) is related to the neutron width of nucleus B which is defined by[6]

$$\Gamma_N=2\pi|\int V_{AN}\,\chi_A\,\chi_B^*\,\psi_N^e\,d\tau'|^2 \times(2i+1)(2s+1)/(2j+1), \quad (3)$$

where the integration goes over the same coordinates as in (1) except those of the proton, and i, s, j are the spins of nucleus A, neutron N and nucleus B. In order to correlate (1) and (3), we shall assume that the nuclear wave functions χ_A and χ_B are rapidly varying in comparison with the particle wave functions ψ_N etc. Then, e.g. the integral in (3) may be written approximately

$$|\int V_{AN}\,\chi_A\,\chi_B^*\,d\tau'|^2|\psi_N^e|^2_{Av}, \quad (3a)$$

the average being taken over the positions of the neutron important in the integral (3). According to reference 4, §4, the main contribution to (3) comes from positions of the neutron at the surface of the nucleus; therefore the average should be taken over these positions.

Combining now (1) with (3), we find

$$\sigma=\frac{\Gamma_N}{|\psi_N^e|^2_{Av}}\frac{2j+1}{(2i+1)(2s+1)}\frac{1}{\hbar} \times|\int\psi_D^c\,\psi_P^{e*}\,\chi_D\,d\tau_P|^2_{Av}. \quad (4)$$

In the last expression, the integration goes over the positions of the proton; its result depends on the coordinates of the neutron and should be averaged over the surface of the nucleus. (Moreover, an average should be taken with respect to the directions of the outgoing proton, cf. §4.)

[3] Breit and Wigner, Phys. Rev. **49**, 519 (1936).
[4] Bethe and Placzek, Phys. Rev. **51**, 450 (1937).
[5] Bethe, Rev. Mod. Phys. **9**, 69 (1937).

[6] For the statistical weight factors, cf. reference 4, appendix. An elementary derivation is this: In the capture cross section (1), we are interested in the transition from a state with given orientation of the spins of neutron and initial nucleus A, to a compound state with any spin orientation. The neutron width (3), on the other hand, gives the transition probability from a compound state with given spin orientation to any separated state. Compared to the capture cross section, the neutron width must therefore contain a factor which gives the number of orientations of the neutron spin, $2s+1$, times the number of spin orientations for the initial nucleus, $2i+1$, divided by that number for the final nucleus, $2j+1$.

The quantity $\Gamma_N/|\psi_N|^2$ which is just the first factor in (3a), no longer contains any reference to the neutron wave function. It may be expressed in terms of the sticking probability of neutron and initial nucleus if the definition of a sticking probability is extended to negative kinetic energies of the neutron. Such an extension is necessary because most final states B reached in the d-p process have less energy than the initial nucleus A plus a free neutron (cf. §7). For fast neutrons, the connection between neutron width and sticking probability is[7]

$$\frac{\Gamma_N}{|\psi_N{}^e|^2}=(2s+1)(2i+1)h\,D'\,\xi_N\,\pi R^2\,v_N, \quad (5)$$

where v_N is the velocity of the neutron, ξ_N its sticking probability, R the radius of the nucleus and D' the spacing of the levels[8] of nucleus B. For our neutrons, the velocity v_N would become imaginary. To avoid this difficulty, we arbitrarily replace the neutron energy $E_N=\frac{1}{2}M_N\,v_N{}^2$ by the deuteron energy $E_D=\frac{1}{2}M_D\,v_D{}^2$ and obtain

$$G_N{}^*=\Gamma_N/|\psi_N{}^e|^2=(2s+1)(2i+1)h\,D'\times\xi_N{}'\,\pi R^2\,v_D\sqrt{2}. \quad (6)$$

The modified sticking probability $\xi_N{}'$ will be identical with ξ_N for high energies and will be somewhat smaller than ξ_N for low energies.[9]

Inserting (6) into (4) and introducing wave functions normalized per unit amplitude for deuteron and proton with the help of (2a, b), the cross section (4) reduces to

$$\sigma=\frac{(2j+1)}{\sqrt{2}\pi}\,\frac{M_P{}^2\,v_P\,R^2}{\hbar^3}\,D'\,\xi_N{}'\,|\int\psi_D{}^a\,\psi_P{}^{a*}\chi_d\,d\tau_P|^2_{av}. \quad (7)$$

The integral over the proton coordinates must be calculated with the neutron kept fixed.

§3. The Penetrability of the Potential Barriers

The integral in (7) which determines the cross section contains three factors:

1. The proton wave function ψ_P. This function will have almost constant amplitude provided the proton is energetic enough not to be appreciably affected by the potential barrier. This will always be true for the fastest protons emitted, i.e. those corresponding to low states of the final nucleus B (cf. also §5, 7).

2. The wave function of the center of gravity of the deuteron, ψ_D, will fall off in an exponential fashion as the deuteron approaches the nucleus, due to the Coulomb potential barrier.

3. The internal wave function of the deuteron, χ_D, will fall off exponentially with the distance between proton and neutron. Therefore, if the neutron is kept fixed at the surface of the nucleus, this function will decrease with increasing distance of the center of the deuteron from the nucleus. This factor varies therefore in the opposite direction than the second; thus there will be an optimum distance r_0 (of the deuteron from the nucleus) at which the product $\psi_D\,\chi_D$ will be a maximum. We may say that at this distance the deuteron will ordinarily "break up" into its constituents.

The wave functions ψ_D and χ_D may be calculated using the WKB (Wentzel-Kramers-Brillouin) method.[10] This has been done by Oppenheimer and Phillips,[1] and their results may be taken over directly. The only point in which we differ from their treatment is that it does not seem legitimate to us to set the radius R of the nucleus equal to zero. Especially if the deuteron energy approaches the height of the potential

[7] Konopinski and Bethe, to appear shortly, §2. See also reference 5, §54D.

[8] More accurately, $1/D'$ is the total number of levels per unit energy, counting each level according to its statistical weight $2j+1$.

[9] When applied to slow neutrons, (6) gives

$$\xi_N{}'=\frac{\pi}{2}\,\frac{\Gamma'}{D}\,\frac{\hbar^2}{MR^2}\,Q^{-\frac{1}{2}}, \quad (6a)$$

where $D=\frac{1}{2}D'(2i+1)(2s+1)$ is the actual spacing of neutron resonance levels, $\Gamma'=\Gamma_N\,E_N{}^{-\frac{1}{2}}$ and Q is the energy evolution in a $d-p$ reaction. Taking $R=10^{-12}$ for radioactive nuclei (§5, 6), we have for atomic weights around 100, approximately $\hbar^2/MR^2=0.7$ MV. Q is about 5 MV, D may be estimated to be about 5 volts (reference 5, Chapter X) and Γ' about 10^{-3} volts$^{\frac{1}{2}}$ (reference 5, §62). This would make $\xi_N{}'$ about 0.1 from slow neutron experiments.

[10] To the wave function ψ_D of the center of the deuteron, the WKB is directly applicable, since the corresponding wave equation is separable in polar coordinates and thus the problem reduces to a one-dimensional one. The wave equation for χ_D, however, is not separable; if we introduce polar coordinates s, ϑ, φ for the position of the proton relative to the center of the deuteron, the interaction between neutron and proton will depend only on s while the Coulomb interaction between proton and nucleus depends also on ϑ. In order to apply the WKB to such a nonseparable problem, the direction of grad ψ must first be known. This direction is given by symmetry considerations if nucleus, neutron and proton all lie on a straight line. Then grad ψ will obviously also be along that line. Thus we can find ψ for all these "straight-line positions." This is sufficient since, for given distances R and r of neutron and deuteron center from the nucleus, χ will be largest when the neutron is closest to the deuteron, i.e. when all particles lie on a straight line.

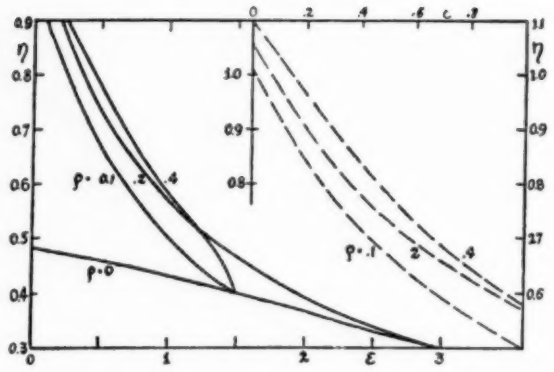

FIG. 1. The break-up distance r_0 of the deuteron as a function of its kinetic energy E for various values of the nuclear radius R. Abscissa $\epsilon=E/I$ (I=deuteron binding energy). Ordinate $\eta=Ir_0/Ze^2$. Curves for various values of $\rho=IR/Ze^2$.

barrier, it is necessary to consider the finite nuclear radius. This is the case for practically all experiments carried out with light nuclei such as Na, Mg, Al;[11] and even for Cu bombarded by deuterons of 3–5 MV, the finite nuclear radius is important.

Using the WKB method, we obtain for the wave functions

$$\psi_D(r)\sim\exp\left\{-\frac{(2M_D)^{\frac{1}{2}}}{\hbar}\int_r^{r_E}\left(\frac{Ze^2}{x}-E\right)^{\frac{1}{2}}dx\right\}, \quad (8)$$

$$\chi_D(r,R)\sim\exp\left\{-\frac{(2\mu_D)^{\frac{1}{2}}}{\hbar}\times\int_0^{2(r-R)}\left(I-\frac{Ze^2}{r}+\frac{Ze^2}{r+\frac{1}{2}\zeta}\right)d\zeta\right\}. \quad (9)$$

Here $M_D=2M$ is the mass of the deuteron, $\mu_D=\frac{1}{2}M$ the reduced mass of proton and neutron in the deuteron, M the neutron (= proton) mass. I is the binding energy of the deuteron, ζ the distance between proton and neutron in the deuteron, and

$$r_E=Ze^2/E. \quad (8a)$$

The equations (10), (11) may be re-written:

$$\psi_D\,\chi_D\sim\exp\left\{-\frac{2M^{\frac{1}{2}}}{\hbar}\frac{Ze^2}{I^{\frac{1}{2}}}F(\epsilon,\eta,\rho)\right\}, \quad (10)$$

where

$$F(\epsilon,\eta,\rho)=\epsilon^{-\frac{1}{2}}f(\epsilon\eta)+(\eta/1-\eta)^{\frac{1}{2}}\times[f(1-\eta)-f(\{1-\eta\}\{2-\rho\eta^{-1}\})], \quad (11)$$

$$f(x)=\arccos x^{\frac{1}{2}}-x^{\frac{1}{2}}(1-x)^{\frac{1}{2}}, \quad (12)$$

$$\eta=Ir/Ze^2, \quad (11a)$$

$$\rho=IR/Ze^2, \quad (11b)$$

$$\epsilon=E/I. \quad (11c)$$

Of the two terms in (11), the first represents the penetration of the deuteron through the Coulomb potential barrier (ψ_D), the second the penetration of the neutron through the "potential barrier" due to its binding to the proton.

As already mentioned, the product $\psi\chi$ will have a sharp maximum for some value r_0 of the deuteron distance r, i.e., F will have a minimum for a certain value η_0 of η. The contributions to the integral in (7) will come mainly from the neighborhood of r_0; therefore, to the accuracy attempted in this paper, it will suffice to calculate F at its minimum η_0. The condition $\partial F/\partial\eta=0$ gives the following equation for η_0:

$$(1-\epsilon\eta_0)^{\frac{1}{2}}=\eta_0(1-\eta_0)^{-\frac{1}{2}}[-f'(1-\eta_0)+(2-\rho\eta_0^{-2})\times f'(\{1-\eta_0\}\{2-\rho\eta_0^{-1}\})]+\tfrac{1}{2}(1-\eta_0)^{-\frac{1}{2}}\times[f(1-\eta_0)-f(\{1-\eta_0\}\{2-\rho\eta_0^{-1}\})]. \quad (13)$$

From this equation, ϵ can easily be obtained as a function of η_0 for given ρ.

The result is given in Fig. 1 for some values of ρ which are important experimentally. According to (11b), ρ is the ratio of the deuteron binding energy $I=2.2$ MV to the height of the potential barrier Ze^2/R. With the large nuclear radii proposed by the author,[12] the potential barrier for deuterons varies from about 3 MV for Na to 10 MV for U (reference 5, Table XXXIII) corresponding to a variation of ρ from 0.7 for Na to 0.2 for U. With the small radii of Gamow, ρ would be about three-quarters of these values (0.5 to 0.15).

As is seen from Fig. 1, the "break-up distance" η_0 is not very sensitive to the nuclear radius which is represented by ρ. For zero deuteron energy, η_0 is slightly larger than unity which means that the deuteron breaks up at a point at

[11] Lawrence, McMillan and Thornton, Phys. Rev. **48**, 493 (1935); Henderson, Phys. Rev. **48**, 480 (1935).

[12] Bethe, Phys. Rev. **50**, 977 (1936).

which the Coulomb potential is slightly less than the binding energy I of the deuteron. With increasing deuteron energy, the break-up position shifts to points of higher Coulomb potential, i.e., to smaller values of η_0. This continues until the break-up occurs at the surface of the nucleus itself, i.e., until $\eta_0=\rho$. From then on, the deuteron penetrates as a whole into the nucleus and the penetration probability is given by the ordinary Gamow theory (reference 5, §68). The deuteron energy for which the deuteron breaks up just at the surface of the nucleus (i.e., for which $\eta_0=\rho$), is equal to the height of the potential barrier minus the deuteron binding energy

$$E_0=Ze^2/R-I. \tag{14}$$

In addition to the experimentally important values $\rho=0.2$ and 0.4, there is also given in Fig. 1 a curve for $\rho=0$. This curve which corresponds to the assumption of Oppenheimer and Phillips behaves rather differently from the others. The reason is connected with the behavior of the "potential barrier for the neutron"

$$V_N=I+\frac{Ze^2}{r}-\frac{Ze^2}{2r-x} \tag{15}$$

(cf. (9); x=distance between neutron and nucleus, $2r-x$ distance proton-nucleus). For small nuclear radii ($\rho<\frac{1}{6}$), this potential may become negative for positions of the neutron just outside the nucleus so that the barrier does not quite extend to the surface of the nucleus; for larger nuclear radii, V_N remains always positive right down to $x=R$. This constitutes a qualitative difference between the assumption of zero radius and the actual situation.

After the break-up distance η_0 has been determined, the value of $F(\epsilon, \rho, \eta_0)$ may be found by direct insertion into (11) (12). The result is given in Fig. 2 where this minimum value of F is plotted against the deuteron energy for various values of ρ. It is seen that the various curves are approximately parallel so that we may write approximately

$$F(\epsilon, \rho, \eta_0)\approx F(\epsilon, 0)-g(\rho). \tag{16}$$

Inserting this into (10), we find that the energy dependence of the penetration function $\psi_D\chi_D$ is almost the same for all values of the nuclear

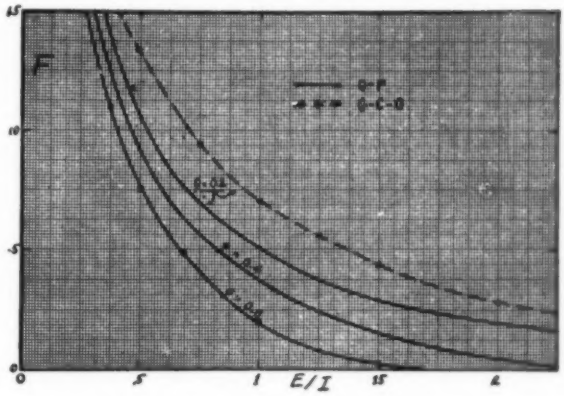

FIG. 2. The Oppenheimer-Phillips penetration function F. The penetrability of the potential barrier is $P=\exp.(-0.6\,ZF)$ where Z is the nuclear charge. Abscissa E/I = kinetic energy of deuteron/deuteron binding energy. Curves for different values of $\rho=IR/Ze^2$ = deuteron binding energy/nuclear potential barrier. $\rho=0.6$, 0.4, 0.2 correspond to $Z=13$, 25 and 70, respectively. The broken curve gives the penetration function F in the ordinary Gamow-Condon-Gurney theory for $\rho=0.2$; for $\rho=0.6$ the G-C-G function (represented by the dots) practically coincides with the O-P function.

radius and that this radius is only important for the absolute value of $\psi\chi$, and therefore for the absolute yield. (The yield will, of course, increase with increasing radius.) The approximate validity of (16) is the reason why the penetration function with zero radius, as calculated by Oppenheimer and Phillips, agrees with the observed excitation functions of reactions of the d-p type.[11]

For comparison, we have also given in Fig. 2 the penetrability of the deuteron as a whole according to the ordinary Gamow-Condon-Gurney (G-C-G) theory which is

$$\psi_D(R)\sim\exp\left\{-\frac{2M^{\frac{1}{2}}}{\hbar}\frac{Ze^2}{I^{\frac{1}{2}}}\epsilon^{-\frac{1}{2}}f(\epsilon\rho)\right\}. \tag{17}$$

This penetrability coincides, of course, with the O-P penetrability above the critical energy (14). The figure shows that for low potential barrier ($\rho=0.6$) the G-C-G curve is practically identical with the O-P curve even at low energies while for high barrier ($\rho=0.2$) there is a considerable difference, the G-C-G curve being considerably steeper. For $\rho=0.4$, the result would be nearer to that for $\rho=0.6$ than to that for $\rho=0.2$. Thus it is necessary to go to fairly heavy nuclei in order to find an appreciable difference between the O-P and the G-C-G excitation functions (cf. Fig. 3). This fact does not preclude the possibility

that the O-P *mechanism* is valid for much lighter nuclei (cf. §6).

§4. Integration and Normalization

Compared to the exponential in (10), all other factors in the cross section (7) are relatively unimportant. We shall therefore use crude methods for their determination so that our final result can only give the order of magnitude of the cross section. Any attempt at greater accuracy seems unwarranted in view of the use of the WKB method for the calculation of deuteron wave function, and of the approximations made in §2.

The normalization condition on the internal wave function χ_D of the deuteron is $\int \chi_D^2 d\tau = 1$, the integration being over the position of the neutron relative to the proton.[13] For this normalization, it is sufficient to replace χ_D by the wave function of a free deuteron, which amounts to neglecting the polarization of the deuteron by the Coulomb field of the nucleus. The normalized wave function of a free deuteron is

$$\chi_D^0 = (\alpha/2\pi)^{\frac{1}{2}} e^{-\alpha s}/s \tag{18}$$

with

$$\alpha = (MI)^{\frac{1}{2}}/\hbar \tag{18a}$$

and s the distance between neutron and proton. Thus (9) must be multiplied by $\alpha^{\frac{1}{2}}/(2\pi)^{\frac{1}{2}}s$.

The required integration over the proton coordinates, especially the angles, is facilitated by the fact that the square of the integral must be averaged over all directions of the motion of the proton, and all positions of the neutron at the surface of the nucleus. We shall introduce polar coordinates with the direction from the center of the nucleus to the neutron as axis; the angular coordinates of deuteron and proton in this system may be $\vartheta_D\varphi_D$, $\vartheta_P\varphi_P$ whereas the directions of motion of the two particles (at infinity) may be specified by $\Theta_D\Phi_D$, $\Theta_P\Phi_P$. If the distance of the proton from the nucleus is large compared to that of the neutron (nuclear radius) which will be true whenever the deuteron energy is small compared to the potential barrier, we may put $\vartheta_D = \vartheta_P = \vartheta$, $\varphi_D = \varphi_P = \varphi$. We have then to integrate (7) over $\vartheta\varphi$ and to average the square of the integral over $\Theta_D\Phi_D\Theta_P\Phi_P$.

We expand, in the usual way, the wave functions of deuteron and proton in polar coordinates. If ϑ' is the angle between $\mathbf{r}_P$ and the direction of motion of the proton, we have

$$\begin{aligned}\psi_P &= (k_P r_P)^{-1}\sum_{l'}(2l'+1) f_{l'}(r_P) P_{l'}(\cos\vartheta') \\ &= 4\pi(\lambda_P/r_P)\sum_{l'm'} f_{l'}(r_P)\, Y_{l'm'}(\vartheta_P\varphi_P)\, Y_{l'm'}^*(\Theta_P\Phi_P)\end{aligned} \tag{19}$$

and a similar expression for the deuteron. Here $f_{l'}$ is a radial wave function which, at large distances from the nucleus, has the form

$$f_{l'} = e^{i\delta_{l'}} \sin(k_P r_P - \tfrac{1}{2}l'\pi + \delta_{l'}). \tag{19a}$$

The last factor in (7) becomes then

$$\begin{aligned}|\int \chi_D \psi_D^a \psi_P^{a*} d\tau_P|^2_{Av} &= (4\pi)^{-2}\sum_{lm l'm'}\int \sin\Theta_P d\Theta_P \\ &\times \sin\Theta_D d\Theta_D d\Phi_P d\Phi_D |\, Y_{l'm'}(\Theta_P\Phi_P)|^2 |\, Y_{lm}(\Theta_D\Phi_D)|^2 \\ &\times |(4\pi)^2 \lambda_P\lambda_D \int dr_P (r_P^2/r_P r_D) f_l(r_D) f_{l'}(r_P) \chi_D(r_P, 0) \\ &\times \int \sin\vartheta d\vartheta d\varphi [\chi_D(r_P,\vartheta)/\chi_D(r_P,0)] \\ &\qquad \times Y_{lm}(\vartheta\varphi)\, Y_{l'm'}^*(\vartheta\varphi)|^2.\end{aligned} \tag{20}$$

Here $\chi_D(r_P, 0)$ is the value of the internal wave function of the deuteron if nucleus, neutron and proton lie on a straight line, as calculated in §3. The last (angular) integral will be a slowly varying function of r_P, therefore we may write

$$\begin{aligned}&|\int dr_P \cdots \int \sin\vartheta d\vartheta d\varphi \cdots|^2 \\ &\qquad \approx |\int dr_P \cdots|^2 |\int \sin\vartheta d\vartheta d\varphi \cdots|^2_{\max},\end{aligned}$$

the value of the last integral being taken at that value of r_P which makes the integrand of the first integral a maximum, i.e. at $r_P = 2r_0 - R$ (cf. §3).

The integrations over $\Theta_D\Phi_D\Theta_P\Phi_P$ can be carried out immediately, they give unity for any $lml'm'$. To evaluate the remaining integrals, we observe that $f_{l'}$ has about the same form for all important values of l'; therefore we re-write (20)

$$\begin{aligned}&(4\pi)^2\lambda_P^2\lambda_D^2 \sum_l |\int dr_P (r_P/r_D) f_l(r_D) f_{l'}(r_P) \\ &\qquad \times \chi_D(r_D, 0)|^2_{Av(l')} \times \sum_{l'm'm} |\int \sin\vartheta d\vartheta d\varphi \\ &\qquad \times [\chi_D(\vartheta)/\chi_D(0)] Y_{lm}(\vartheta\varphi)\, Y_{l'm'}^*(\vartheta\varphi)|^2.\end{aligned} \tag{21}$$

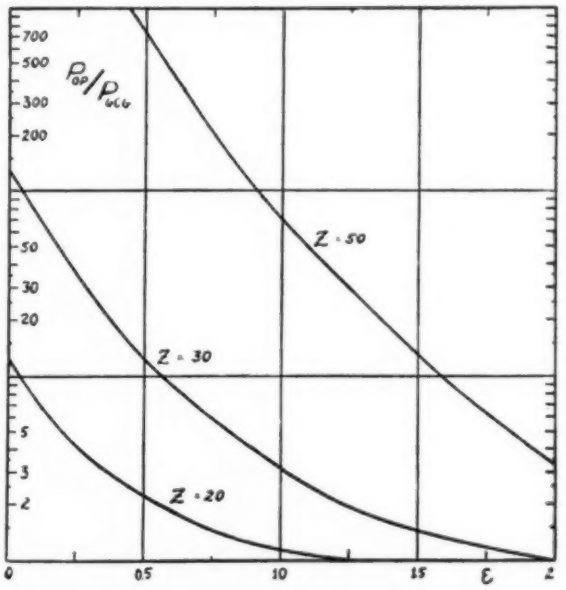

FIG. 3. The ratio of the penetrabilities of the potential barrier in the Oppenheimer-Phillips and the Gamow-Condon-Gurney theories for various nuclear charges as a function of E/I=kinetic energy of deuteron/binding energy.

[13] Then $|\psi_D\,\chi_D|^2 d\tau_D\, d\tau_{\rm rel}$ gives the probability of finding the deuteron in the volume element $d\tau_D$ and the relative coordinates between the limits indicated by $d\tau_{\rm rel}$. In order to obtain the probability for given neutron and proton coordinates, we must multiply $|\psi_D\,\chi_D|^2$ by the Jacobian

$$\frac{\partial(\mathbf{r}_D, \mathbf{r}_{\rm rel})}{\partial(\mathbf{r}_N, \mathbf{r}_P)} = \begin{vmatrix} \frac{1}{2} & \frac{1}{2} \\ -1 & 1 \end{vmatrix} = 1.$$

The sum over $l'm'$ can be carried out immediately using the completeness relation for the spherical harmonics; then the sum over m is found using the addition theorem

$$\sum_m |Y_{lm}|^2=(2l+1)/4\pi,$$

so that the last sum in (21) reduces to

$$\int \sin\vartheta d\vartheta d\varphi[\chi_D(\vartheta)/\chi_D(0)]^2. \tag{22}$$

Here we use again the wave function (18) of the free deuteron, and the geometrical relation

$$\begin{aligned} &s^2=R^2+r_P^2-2Rr_P\cos\vartheta;\\ &sds=Rr_P\sin\vartheta d\vartheta; \qquad s(\vartheta=0)=s_0=r_P-R. \end{aligned} \tag{23}$$

Then (22) becomes

$$\begin{aligned} &2\pi(s_0^2/Rr_P)\int(ds/s)e^{-2\alpha(s-s_0)}\\ &\qquad\approx(2\pi s_0^2/2\alpha Rr_P^2)(1-e^{-4\alpha R}) \end{aligned} \tag{24}$$

since r_P is the average value of s. Since $1/\alpha=4.5\cdot10^{-13}$ cm, $e^{-4\alpha R}$ is negligible even for fairly light nuclei.

The integral over r_P contains the factor $f_l(r_D)\chi_D$ which has a sharp maximum for $r_P=2r_0-R$ (§3), and the factor $f_{l'}(r_P)$. The latter function oscillates rapidly with a period of $2\pi\lambda\!\!\!^{-}_P$ and has the amplitude unity. It can be shown that the change of $f_{l'}$ with r_P is more rapid near $r_P=2r_0-R$ than that of the product $f_l\chi_D$, except for very large proton wave-length $\lambda\!\!\!^{-}_P$. Therefore we assume that the main contribution to the integral comes from a region of extension $\lambda\!\!\!^{-}$ on either side of the maximum of $f_l\chi_D$, and replace the integral by $2\lambda\!\!\!^{-}$ times the value of the integrand at $r_P=2r_0-R$. Putting the average of $f_{l'}^2(2r_0-R)$, averaged over l', equal to one-half, (21) becomes finally

$$\begin{aligned} &(4\pi)^2\lambda\!\!\!^{-}_P{}^4\lambda\!\!\!^{-}_D{}^2(r_P/r_D)^2\sum_l P_{\mathrm{OP}l}(\alpha/2\pi s_0^2)\times[2l+1/4\pi]\\ &\times(2\pi s_0^2/2\alpha Rr_P^2)=4\pi(\lambda\!\!\!^{-}_P{}^4\lambda\!\!\!^{-}_D{}^2/Rr_0^2)\sum_l(2l+1)P_{\mathrm{OP}l}. \end{aligned} \tag{25}$$

Here $P_{\mathrm{OP}l}$ is the square of $f_l\chi_D$, the latter being taken without the factor $\alpha^{\frac{1}{2}}/(2\pi)^{\frac{1}{2}}s$ (cf. 18). Thus, for $l=0$, $P_{\mathrm{OP}l}$ is simply the square of (10), the Oppenheimer-Phillips penetrability

$$\begin{aligned} P_{\mathrm{OP}}&=\exp\left\{-\frac{4M^{\frac{1}{2}}}{\hbar}\frac{Ze^2}{I^{\frac{1}{2}}}F(\epsilon,\eta_0,\rho)\right\}\\ &=\exp\left(-0.6ZF(\epsilon,\rho)\right). \end{aligned} \tag{26}$$

For $l\neq0$, slightly smaller results are obtained because of the additional potential barrier due to the centrifugal force (ref. 5, §72, and ref. 7). As for ordinary disintegrations, we replace the sum over l by $Pl_e'^2$ where l_e' is a "critical orbital momentum."

Inserting these results into (7), we obtain the final formula

$$\sigma_{\mathrm{OP}}=2\sqrt{2}(2j+1)M\hbar^{-2}R\lambda\!\!\!^{-}_P{}^3\lambda\!\!\!^{-}_D{}^2l_e'^2r_0^{-2}D'\xi_N'P_{\mathrm{OP}}. \tag{27}$$

§5. Energy Distribution of the Emitted Protons

The cross section (27) may be written

$$\sigma_{\mathrm{OP}}=\sigma_0(2j+1)D'\,\xi_N'\,E_P^{-\frac{1}{2}}, \tag{28}$$

where σ_0 does not depend on the energy E_P of the proton. The excitation energy of the final nucleus being a constant minus the proton energy, the number of protons with an energy between E and $E+dE$, $\sigma(E)dE$, is obtained by summing (28) over all the nuclear states in the energy interval dE. Since dE/D' is the number of levels counting each level according to its degeneracy $2j+1$, we must simply replace $(2j+1)D'$ by dE:

$$\sigma_{\mathrm{OP}}(E)dE=\sigma_0\,\xi_N'\,E^{-\frac{1}{2}}\,dE. \tag{29}$$

In this formula, the factor $E^{-\frac{1}{2}}$ varies relatively slowly with the energy and is, moreover, theoretically rather uncertain. The number of protons per unit energy is given primarily by the sticking probability ξ_N'. This is in striking contrast to disintegrations of the ordinary type in which the number of outgoing particles per unit energy is determined by the number of energy levels of the final nucleus in the corresponding energy interval (ref. 5, §54). This latter relation leads, as is well known, to the Maxwell-Boltzmann law

$$\sigma_{\mathrm{ord}}(E)dE\sim e^{-E/T}\,dE \tag{30}$$

for the energy distribution of the outgoing particles in an ordinary nuclear reaction such as the d-n reaction.

While the energy distribution in an ordinary reaction can thus be predicted from the "evaporation model," not much can be said about the sticking probability ξ_N' which determines the distribution of the Oppenheimer-Phillips protons. Two extreme views may be taken

(a) *The sticking probability may have the same order of magnitude for all levels* of the compound nucleus (in our case ≡ final nucleus), including the lowest ones.[14] Then the protons from the d-p reaction should be *uniformly distributed in energy* between two limits [see below, (31), (32)].

(b) *The sticking probability may decrease for low compound levels* in such a way as to leave the *reduced neutron width* Γ^* (cf. 6) approximately *constant*. This would mean that ξ_N' varies inversely as the spacing D' of levels: In this case, therefore, the energy distribution of the protons would be the same as in an ordinary nuclear reaction,

[14] Grave theoretical reasons are against this assumption because it would mean the validity of the one-body model for the low states of nuclei.

showing a very sharp drop in intensity towards higher proton energies.

(c) Any intermediate assumption may be made; e.g., we think it plausible that for relatively high excitation of the compound nucleus, ξ is almost constant, while near the lowest level the reduced width G^* becomes constant, with a transition region between.

In view of these uncertainties and of the great theoretical importance of the sticking probability, it would be very interesting to measure experimentally the energy distribution of the emitted protons. In order to make the O-P mechanism certainly valid, the experiment should be carried out with heavy nuclei and preferably with an element with only one isotope. The deuteron energy is rather immaterial, but the deuterons should be fairly monochromatic (thin target). Owing to the large density of nuclear levels, the protons will, of course, not show any "group structure" as with light nuclei, except possibly near the high energy limit (corresponding to low states of the residual nucleus). The spectrum would extend to an upper limit

$$E_{\max}=E_D+Q, \tag{31}$$

where Q is the reaction energy (about 4–6 MV). At the low energy end, the proton spectrum will break off at an energy approximately equal to the Coulomb potential at the distance $2r_0-R$ from the nucleus, i.e. the distance at which the proton is found when the deuteron breaks up. With the notations of §3, we have

$$E_{\min}=\frac{Ze^2}{2r_0-R}=\frac{I}{2\eta_0-\rho}. \tag{32}$$

For zero deuteron energy, we have about $2\eta_0-\rho=1.9$ so that $E_{\min}=1.2$ MV; for $E_D=I=2.2$ MV, $E_{\min}$ is about I; and if the deuteron energy becomes equal to or greater than the height of the potential barrier, $E_{\min}$ will be equal to the potential barrier. In practically all cases, $E_{\min}$ is large enough so that the corresponding proton range $R_{\min}$ is considerably greater than the range of the incident deuteron. Therefore the whole proton distribution should be easily observable without disturbance by the scattered deuterons.

It is of particular importance that these measurements would give the width of nuclear levels right down to the lowest states of the compound (= final) nucleus, states which could never be examined by ordinary neutron bombardment. The d-p reaction supplies neutrons of "negative kinetic energy." The importance of the width of these low levels lies mainly in the theory of the α-decay. It can probably be assumed that the α-width without barrier is of the same order as the neutron width[15] for a given level. Thus the measurement of the proton distribution from the O-P reaction should settle the problem of the nuclear radii. If assumption (a) above (constant sticking probability down to the lowest levels, uniform proton distribution) proves true, the width of the low levels would, according to (6), be very large due to their large spacing. This would make the radii of radioactive nuclei almost as small as in the one-body model of Gamow (about $9\cdot10^{-13}$ cm). If, on the other hand, assumption (b) proves to be correct (constant G^*, proton distribution showing rapid decrease towards high energies), the large nuclear radii proposed by the author ($12\cdot10^{-13}$ cm) would result. Assumption (c), which we consider most likely at the moment, would lead to an intermediate value for the radius.

§6. Comparison of Oppenheimer-Phillips and "Ordinary" Processes

Integrating (27) over the proton energy from $E_{\min}$ to $E_{\max}$, we find

$$\sigma_{OP}=2^{\frac{1}{2}}\lambda_D^2 l_c'^{\frac{1}{2}} r_0^{-2} R(\lambda_{\min}-\lambda_{\max}) P_{OP}\xi_{NB}', \tag{33}$$

where $\lambda_{\min}$ and $\lambda_{\max}$ are the proton wave-lengths corresponding to the energies $E_{\min}$ and $E_{\max}$ (cf. 31, 32). (Of course, $\lambda_{\min}>\lambda_{\max}$.) ξ_{NB}' is the average of the sticking probability over the levels of nucleus B between ground state and excitation energy $E_{\max}\dots E_{\min}$, slightly greater weight being given to the higher states. The taking of such an average is, of course, adequate only if ξ changes slowly with the energy (assumption (a) in §5); if, on the other hand, the reduced neutron width G^* (cf. 6) remains approximately constant (assumption b), we may write

$$\sigma_{OP}=\sqrt{2}R\,\lambda_D^2\, l_c'^{\frac{1}{2}}\, r_0^{-2}\,\lambda_{\min} \times T'\,E_{\min}^{-1}\,P_{OP}\,\xi_N', \tag{33a}$$

[15] The "neutron width" G^* deduced for levels below the neutron dissociation energy is, of course, not an actual width but only a convenient measure of the matrix element.

where T' is the temperature of nucleus B corresponding to the excitation energy $E_{max}-E_{min}$ and ξ_N' the corresponding sticking probability of the neutron. T' is in general considerably smaller than E_{min}.

The O-P cross section (33) may be compared with the cross section of an ordinary nuclear reaction produced by a deuteron (reference 5, Eq. (681a))

$$\sigma_{GCG}=\pi\lambda_D^2\, l_c^2\, P_{GCG}\, \xi_D\, \Gamma_Q/\Gamma. \qquad (34)$$

Here Γ is the total width of the levels of the compound nucleus formed by adding the deuteron to the initial nucleus, Γ_Q the partial width referring to the outgoing particle, P_{GCG} the penetrability of the potential barrier for the deuteron as a whole, according to the ordinary theory of Gamow, Condon and Gurney, ξ_D the deuteron sticking probability and l_c the critical orbital momentum for the "ordinary" disintegration. The ratio of (34) to (33) is

$$\frac{\sigma_{GCG}}{\sigma_{OP}}=\frac{\pi}{2^{\frac{1}{2}}}\frac{l_c^2}{l_c'^2}\frac{r_0^2}{R(\lambda_{min}-\lambda_{max})}\frac{\xi_D}{\xi_{NN}}\frac{P_{GCG}}{P_{OP}}\frac{\Gamma_Q}{\Gamma}. \qquad (35)$$

The critical orbital momentum l_c is discussed in reference 5, §72. For deuteron energies well below the top of the barrier, we have (Eq. 633) $l_c^2=\frac{1}{2}g$ where g is given in (600a) of reference 5. Analogous considerations for the O-P process give $l_c'^2=\frac{1}{2}g'$ where g' differs from g in that the nuclear radius R is replaced by the break-up distance r_0 of the deuteron. Since $g\sim R^{\frac{1}{2}}$, we have $l_c^2/l_c'^2=(R/r_0)^{\frac{1}{2}}$. Then we may write

$$\frac{\sigma_{GCG}}{\sigma_{OP}}=k(E_D, Z)\frac{\xi_D}{\xi_{NN}}\frac{P_{GCG}}{P_{OP}}\frac{\Gamma_Q}{\Gamma}, \qquad (36)$$

where k is a relatively unimportant factor which is given by

$$k=\frac{\pi}{2^{\frac{1}{2}}}\frac{r_0^{\frac{1}{2}}}{R^{\frac{1}{2}}(\lambda_{min}-\lambda_{max})}. \qquad (37)$$

Assuming the nuclear radius to be 10^{-12} cm for radioactive nuclei, and to be proportional to $A^{\frac{1}{3}}$ (A = atomic weight) otherwise, we find

$$k=0.14_5\, Z^{\frac{1}{2}} A^{-\frac{1}{6}}\, \eta_0^{\frac{1}{2}} \times[(2\eta_0-\rho)^{\frac{1}{2}}-(\epsilon+q)^{-\frac{1}{2}}]^{-1}, \qquad (37a)$$

where $q=Q/I\approx 2$ to 3. The factor k turns out to be almost independent of the deuteron energy, decreasing by 10 to 20 percent when the deuteron energy increases from I to $2I$. For $E_D=I$, the values of k are approximately

$Z=$	10	20	30	50	70	92
$k=$	4.7	8.8	13.5	26	39	57.

In view of the many approximations made, the numerical values of k should not be trusted; they may easily be wrong by a factor of 5 either way. However, the tendency of k to increase with increasing Z seems to be real. Moreover, k may actually depend more strongly on the deuteron energy.

The second factor in (36), *viz.* the ratio of the sticking probabilities of deuteron and neutron, is very difficult to estimate. It is likely that ξ_D is considerably larger than ξ_N'; in fact, ξ_D will be approximately unity while the "modified sticking probability" ξ_N', may be about 0.1 (footnote 9).

The penetrabilities of the potential barrier can be found from Fig. 2; e.g. for $\rho=0.2$, $Z=70$, $E_D=2I=4.4$ MV, we have from that figure $F_{OP}=0.19_5$, $F_{GCG}=0.28$ which gives, according to (26), $P_{OP}=3.5\cdot 10^{-4}$ and $P_{GCG}=0.8\cdot 10^{-5}$, corresponding to a ratio of 45 in favor of the O-P penetration. With $E_D=I=2.2$ MV the ratio would be 5000. Altogether, the factors beside Γ_Q/Γ in (33), will be about unity for moderate energies ($\sim$3–4 MV), decreasing with increasing energy.

This means first of all that *the d-p reaction will practically always follow the O-P mechanism for heavy nuclei.* For the proton width of heavy nuclei is known to be extremely small compared to the neutron (and therefore the total) width (ref. 5, §79), so that $\Gamma_Q/\Gamma\ll 1$ if Q is a proton. The ratio Γ_Q/Γ can be estimated to be about 10^{-4} for heavy nuclei and medium excitation energies so that only one *d-p* process in 10,000 would follow the "ordinary" instead of the O-P mechanism.

Furthermore, we see that for heavy nuclei and moderate deuteron energies *the O-P process will be about equally as probable as the d-n reaction.* (The *d-n* reaction follows the G-C-G mechanism with Γ_Q practically equal to Γ.) A more accurate experimental determination of the relative probabilities of *d-p* and *d-n* process could be used to determine the relative sticking probabilities of

deuteron and neutron according to (33). However, it must be considered that the d-n reaction is, in the case of heavy nuclei, often followed by the emission of an α-particle or a second neutron (cascade disintegration, cf. ref. 5, §79 E). The yields of these reactions must, for our purpose, be added to that of the d-n reaction itself.

For lighter elements, the probability of the O-P process will decrease as compared to the "ordinary" processes owing to the change in the relative penetrabilities. This decrease will be partly compensated by the decrease of k (cf. (37)). Nevertheless, the "ordinary type" d-p reaction will ultimately become as probable as the O-P process so that we reach the limit of validity of the O-P mechanism. As we shall show, this limit occurs for Z about 25, so that $k \approx 10$. Setting, as before, $\xi_N = \frac{1}{10}\xi_D$, the limit of validity of the O-P mechanism is given by

$$\frac{\Gamma}{\Gamma_{\text{proton}}} \frac{P_{OP}}{P_{GCG}} \approx 100. \tag{38}$$

The figure 100 is of course very uncertain, and a possible error of at least a factor 5 either way must be admitted.

To estimate $\Gamma/\Gamma_{\text{proton}}$, we note (1) that even for medium heavy nuclei Γ is practically equal to the neutron width, (2) that the width for each kind of particles is supposed to be proportional to the number of available states of the respective final nuclei (ref. 5, §54, §79). The latter depends on the available energy (ref. 5, §79) which is

$$U = E_D + Q - B, \tag{39}$$

where Q is the reaction energy and B the potential barrier. The difference of the available energies for the d-n and the d-p reactions is thus

$$U_N - U_P = Q_N - Q_P + B_P$$
$$= \epsilon_- - 0.8 \text{ MV} + B_P, \tag{40}$$

where B_P is the proton potential barrier, 0.8 MV the difference of the masses of neutron and hydrogen atom, and ϵ_- the energy difference between the (isobaric) nuclei formed in the d-p and the d-n reaction. If the former nucleus is heavier, ϵ_- would be equal to the maximum energy of the β-particles emitted (plus the energy of the subsequent γ-ray if the β-emission leads to an excited state). If the d-n nucleus is heavier, ϵ_- is negative; and if in particular the d-n nucleus emits positrons, $\epsilon_- = -1.02 - \epsilon_+$ where ϵ_+ is the maximum energy of the positrons. The relative number of available states, and therefore the ratio of the widths, is given by the statistical formula

$$\frac{\Gamma_N}{\Gamma_P} = \exp\left(\frac{U_N - U_P}{T}\right), \tag{41}$$

where T is the nuclear temperature corresponding to some average excitation energy between U_N and U_P. Now for medium heavy nuclei Q_N is about 5 MV (difference of mass excesses of deuteron and neutron), $Q_P - B_P$ will turn out to be about zero (§7), so that $\frac{1}{2}(U_N + U_P)$ will be 5–7 MV, depending on the deuteron energy. The corresponding nuclear temperature would be about 1.3 MV according to reference 5, Table XXI.

The solution of (38) is approximately

$$U_N - U_P \approx 4T. \tag{42}$$

To verify this, we show that P_{OP}/P_{GCG} is not very different from unity under the conditions given by (42). On the average, ϵ_- in (40) will be zero (see below for a more detailed discussion); therefore (42) corresponds to a proton barrier of $4T + 0.8$ MV ≈ 6 MV $= 2.7\ I$, i.e. (cf. (11b)) to $\rho = 0.37$. For $\rho = 0.4$ and a deuteron energy of 2.2 MV ($= I$), we have $F_{OP} = 0.37$ (cf. Fig. 2) and $F_{GCG} = 0.39_5$ (cf. (19)). With $R = 10^{-12}$ cm for the natural radioactive nuclei, a barrier height of 6 MV corresponds about to $Z = 25$. This would give (cf. (26))

$$P_{OP}/P_{GCG} = e^{0.6 \cdot 25 \cdot 0.02_5} = 1.4.$$

With a higher deuteron energy, we should find an even smaller ratio P_{OP}/P_{GCG}. Therefore $\Gamma_N/\Gamma_P = \exp.(U_N - U_P/T)$ is only slightly less than 100 (cf. (38)), so that (42) follows immediately.

According to (36), the limit of validity of the O-P mechanism is therefore given by

$$B_P = 4T + 0.8 \text{ MV} - \epsilon_-. \tag{43}$$

Assuming $T = 1.3$, this gives

$$B_P = 6 \text{ MV} - \epsilon_-. \tag{43a}$$

The limit of validity depends therefore on the relative stability of the nuclei formed in the d-n

and d-p reactions. If the product of the d-p reaction is radioactive, the reaction will follow the O-P mechanism even for relatively light nuclei; if it is stable, the "ordinary" type of reaction will persist to somewhat heavier nuclei. This is due to the competition of the ordinary type with the d-n reaction; this competition will be easier when the product of the d-p reaction is more stable than that of the d-n reaction.

The exact value of the critical nuclear charge above which the O-P mechanism is valid, depends also on the assumed nuclear radii. With the large radii, $B_P=6$ corresponds (reference 5, Table XXXIII) to about $Z=36$; with the small (Gamow) radii, the limit would be $Z=20$ (for $\epsilon_-=0$), and with the intermediate radii assumed in this paper, we have $Z=25$. In a case such as Na^{23} d-p where the product nucleus (Na^{24}) emits β-rays of as much as 4.6 MV (including γ-ray energy), the O-P mechanism may be valid in spite of the exceedingly low nuclear charge $Z=11$.

These estimates of the limit of validity are very crude, mainly because of the uncertainty in the numerical value 100 in (38), but also because the nuclear temperature T is not very certain (it is probably much higher for light nuclei such as Na which works against the O-P mechanism in such cases). If, e.g., the correct figure in (38) is 10 instead of 100, we should have $2.3T$ in (39) and assuming now $T=1.6$ MV (generally lighter nuclei!) 4.5 MV in (39a). This would shift the limit of validity to $Z=17$ (with the medium radius), if $\epsilon_-=0$, and to still lower Z when the product nucleus of the d-p reaction is radioactive ($\epsilon_->0$).

Much more information on these problems could be obtained from experimental investigations of the relative yields of d-n and d-p reactions. For very light atoms, the probabilities of the two reactions should vary from case to case and should, on the average, be about equal. For higher atomic weight (perhaps $10<Z<25$), the probability of the proton reaction should show, on the average, a slow decrease because the competition between d-n and d-p process becomes more and more favorable for d-n. The minimum is reached at the limit of validity of the O-P mechanism; further increase of the atomic number will increase the relative probability of proton emission because the O-P penetrability increases compared to the G-C-G penetrability. Moreover, the fluctuations from case to case should become much less pronounced in the O-P region because the competition has stopped. For very heavy nuclei, as already mentioned, the d-p reaction is presumably about equally probable as the d-n reaction for energies of about 4 MV.

While all the problems mentioned thus far have not yet received much attention experimentally, a rather large amount of work has been done on excitation functions of d-p as compared to d-n and d-α reactions. Here the theory gives much less striking results. Large differences between the O-P and the G-C-G type of reaction can be expected only for rather heavy nuclei for which no experiments are available. In Fig. 3 we have plotted the ratio P_{OP}/P_{GCG} as a function of the deuteron energy for various nuclear charges. The nuclear radius was assumed to be 10^{-12} for naturally radioactive nuclei. It is seen that for $Z=20$ the ratio of the excitation functions is practically unity for all energies above 2 MV ($\epsilon=1$), for $Z=30$ it decreases only from about 3 at 2 MV to 1 at and above 4 MV, and only for $Z\geqslant 50$ the ratio changes rapidly above 2 MV. Therefore we believe that the validity of the O-P mechanism can scarcely be proved by comparing the excitation functions of d-p and other reactions for nuclei of $Z\leqslant 30$.

§7. Secondary (Cascade) Disintegrations

As any nuclear process, a d-p reaction may in principle be followed by a break-up of the residual nucleus provided sufficient energy is available. If the residual nucleus is sufficiently heavy, it will always disintegrate with neutron emission whenever this is energetically possible (cf. reference 5, §79 and §65). In our case, neutron emission leads back to the original nucleus; it is therefore energetically possible if

$$E_D-E_{\min}-I>0, \tag{44}$$

where $E_{\min}$ is the minimum proton energy given in (32). From Fig. 1, it can be shown that the expression in (44) is always negative for deuteron energies below $B+I$ where B is the height of the potential barrier. Thus a d-pn reaction can only occur[16] when the deuteron can go over the

[16] Strictly speaking, there are always some protons of smaller energy than $E_{\min}$. When such slow protons are emitted, a d-pn reaction is possible. However, the number of these protons is small because they have to penetrate the potential barrier, and therefore the probability of the d-pn reaction will also be small.

potential barrier, and in this case the primary *d-p* reaction is relatively improbable compared to a primary *d-n* reaction, since it is no longer favored by a greater penetrability. Therefore the *d-pn* reaction (which would be hard to observe) will be of rather minor importance.

The question of *d-pα* reactions is rather harder to decide because in this case the energy evolution cannot be determined so accurately. However, it can be said with certainty that the *d-pα* reaction can only have an appreciable probability with a given nucleus if slow neutrons give an *n-α* reaction with the same nucleus. For we have shown above that the product nucleus of the *d-p* reaction will, in general, not have sufficient energy to emit a neutron; it has therefore less excitation energy than the compound nucleus formed by adding a slow neutron to the target nucleus. If that latter compound nucleus emits γ-rays rather than α-particles, i.e., if the capture of slow neutrons is more probable than a *n-α* reaction, the same will be *a fortiori* true of the final nucleus formed in the *d-p* reaction, because the probability of α-emission decreases rapidly with decreasing excitation energy. *n-α* reactions with slow neutrons and heavy nuclei have only been observed for Th and U (reference 2, Table LX); therefore we may expect that only these extremely heavy elements give *d-pα* reactions to any appreciable extent. (A *small* yield of the *d-pα* reaction will, of course, always be obtained; it may be calculated from the penetrability of the potential barrier for α-particles if the energy evolution in the reaction is known). This seems to make unlikely the reaction *Au-d-pα* which was reported by Cork and Thornton[17] and was previously considered probable by the author (reference 5, p. 205).

The rarity of *d-pα* reactions may also be understood if we consider that the *d-p* reaction produces a nucleus with too many neutrons which will naturally have no tendency to lose further charge by emission of an α-particle. This is in contrast to the *d-n* reaction which produces a nucleus of too high charge so that a subsequent α-emission seems favorable.

Our considerations show that *d-p* reactions with deuteron energies below the potential barrier should rarely lead to any cascade disintegration.

[17] Cork and Thornton, Phys. Rev. **51**, 59 (1937).

JANUARY 1, 1938 PHYSICAL REVIEW VOLUME 53

A New Method for Investigating Atomic Electron Velocities

A. L. HUGHES AND MARVIN M. MANN, JR.
Wayman Crow Laboratory of Physics, Washington University, St. Louis

(Received November 13, 1937)

When electrons of sufficient speed pass through helium under conditions favorable to single scattering, the electrons scattered through a suitable angle fall into two distinct classes, those scattered elastically and those scattered inelastically. The former have been scattered by nuclei and the latter by atomic electrons. Because the atomic electrons are in random motion, those electrons which have been scattered by them through a definite angle have a distribution of energies, the most probable energy being that corresponding to a collision with an atomic electron at rest. Jauncey has shown that when a fast electron of energy V_0 collides with an atomic electron having a component velocity u in a certain direction, the electron will have energy given by $V = V_0 \cos^2\theta + u(2mV_0/e)^{\frac{1}{2}} \sin\theta$, where θ is the angle of scattering. It can be shown to follow from this relation that the *distribution of energy* among the scattered electrons is identical with the *distribution of component velocities* among the atomic electrons. Moreover, since the last mentioned distribution is closely related to, and identical in shape with, the profile of the Compton modified band in x-ray scattering, measurements of the energy distribution of the scattered electrons will give an experimental determination of the profile of the band. Wave mechanical computations lead to a definite shape for this profile which can now be tested by experiments on electron scattering. A beam of electrons, with energies between 1000 and 4000 volts, was directed into helium at a low pressure and the distribution of energies of electrons scattered at 34.2° measured. It was found that the experimental results gave a profile for the Compton modified band in excellent agreement with the profiles calculated by Hicks and in good agreement with those calculated by Kirkpatrick, Ross and Ritland. Values for the probability of the various component velocities of the atomic electrons are tabulated.

Introduction

THIS paper gives an account of a new method for measuring the distribution of velocities of the electrons in an atom. It is based on the remarkable similarity between the scattering of photons by electrons and the scattering of electrons by electrons, and is therefore intimately related to the Compton effect. Ever since Jauncey gave the essential theory in 1924–25 it has been known that the profile of the modified line in the Compton effect gives, in principle, direct information as to the distribution of velocities among the electrons in the atoms of the scattering material. Although the theory is simple and straightforward, it has been quite difficult to secure reliable experimental x-ray data to which to apply the theory. Only in the last few years have reliable experimental data been secured for solids, and only in the last two years have successful measurements been made on gases. The corresponding measurements in electron scattering are, in certain respects at least, more easily made. (1) The probability of scattering of electrons by electrons is far greater than that of photons by electrons. (This is illustrated by the fact that Debye-Hull-Scherrer photographs require exposures running into hours, while the corresponding electron diffraction photographs are obtainable in seconds.) (2) The width of the band representing the distribution of energy among the inelastically scattered electrons relative to their mean energy is ten to twenty times greater than the width of the Compton band relative to the wave-length of its center. Since both these widths lead to values for the atomic electron velocities, the values determined by electron scattering measurements should be the more accurate. It may well be that electron scattering measurements will surpass x-ray scattering measurements as a means of studying atomic electron velocities.

Theory

X-ray scattering

When a monochromatic beam of x-rays is scattered by matter, there is found in the scattered radiation, some radiation of longer wave-length than the primary (the "modified" radiation) as well as radiation of the same wave-length as that of the primary (the "unmodified" radiation). The presence of the modified radiation, quite unexplainable on the classical theory of x-ray scattering, was accounted for by a new point of view due to A. H. Compton. He postulated that the radiation is made up of photons to which the conservation laws apply. On carrying through the calculation, it is found that, when a photon is scattered in a definite direction from its original direction by collision with an electron, originally at rest, the energy of the photon is reduced by a definite amount (depending on the original energy of the photon and on the scattering angle θ) which manifests itself by a change in wave-length (depending only on θ and not at all on the original wave-length). The wave-length of the modified radiation, λ', is given by

$$\lambda' = \lambda + (2h/mc) \sin^2 (\theta/2) \qquad (1)$$

where λ is the wave-length of the original radiation, h is Planck's constant, m is the mass of the electron and c is the velocity of light.

According to the theory as outlined in the foregoing paragraph, the modified radiation would be just as monochromatic as the primary radiation. However it was noticed, even in the early days of the Compton effect, that the modified radiation was more diffuse than either the primary radiation or the unmodified radiation. Jauncey[1] proposed a quantitative explanation of the diffuseness of the modified radiation. The essential point in his theory is this. The electrons in the atom with which the photons collide are not at rest, but, on the contrary, are in random motion, so that the energy with which the photon comes away from a collision in a direction θ depends on the magnitude and direction of motion of the electron at the moment of impact. The wave-length of the modified radiation differs from λ', defined by Eq. (1) by an amount λ'' which is given by

$$\lambda'' = u(2\lambda/c) \sin (\theta/2), \qquad (2)$$

where u is the component of the initial velocity of the atomic electron along the bisector of the angle between the direction of motion of the primary radiation and the reverse of that of

[1] G. E. M. Jauncey, Phil. Mag. **49**, 427 (1925); Phys. Rev. **25**, 723 (1925); Phys. Rev. **46**, 667 (1934).

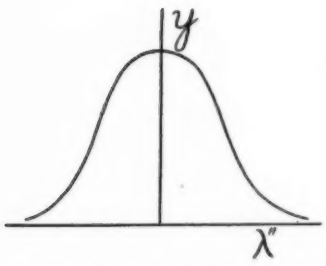

FIG. 1. Profile of the Compton modified band.

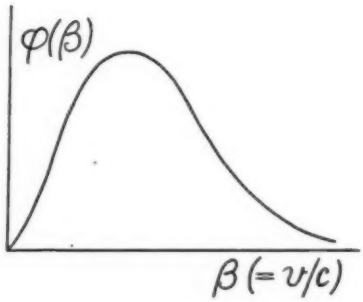

FIG. 2. Distribution of resultant speeds of atomic electrons.

the scattered radiation. Thus, corresponding to each value of the component of velocity u, which the electron had just before impact, there will be modified radiation whose wave-length is displaced from the value λ' by the amount λ''. Since, in general, u may have any value whose probability diminishes monotonically on both sides from $u=0$, we should expect to find the modified radiation to be a band instead of a line. Conversely, a measurement of the distribution of intensity in the modified band, gives information as to the velocity of the electrons in the atom. The importance of this was first realized by Jauncey, who showed how the then accepted values of the velocities of the electrons in the Bohr circular orbit theory and in the Bohr-Sommerfeld elliptical orbit theory could be used to predict the distribution of intensity across the Compton modified band. Comparison with experiment would then afford a decisive test of these theories of the atom insofar as they predict atomic electron velocities.

When Jauncey first proposed his theory of the modified radiation, the most recent atomic theory available was the Bohr-Sommerfeld theory of elliptical orbits, and it was perfectly natural to discuss the application of his theory to this model. It is entirely incorrect to imply, as DuMond[2] has done, that Jauncey's theory became obsolescent with the replacement of the Bohr-Sommerfeld atom by the wave mechanics atom. Jauncey's theory is quite independent of any particular atomic model; on the contrary, its purpose is to provide a test of whatever distribution of velocities the prevailing atomic theory predicts, whether this theory be the Bohr-Sommerfeld theory, the wave mechanics theory, or the post wave mechanics theory when it comes. In fact, the essence of Jauncey's theory is that it provides a method for finding the distribution of velocities of the atomic electrons from observations on the distribution of intensity in the Compton modified band. DuMond also comments on Jauncey's theory adversely because Jauncey places "an unfortunate emphasis" on the energy of the electron rather than on the momentum, and again because he stresses position rather than momentum. This criticism seems to be without much point, for in the atoms discussed by Jauncey there is surely a one to one correspondence between electron energy probability and electron momentum probability. Any experimental approach which directly measures one of these probabilities provides a test of the theory and indirectly of its predictions as to the other probability. Quite apart from these considerations, it is quite evident from the vector diagrams, used by Jauncey in his original papers to illustrate his derivations, that he was relating wave-lengths in the modified band directly to the velocities of the atomic electrons.

A brief comment on the methods by which the experimental data may be used to give the distribution of speeds among the atomic electrons is in order at this point. If the distribution of intensity across the Compton modified band be represented by Fig. 1, then the distribution of atomic electron speeds (i.e., resultant velocities assuming of course that they are isotropic as to direction) is given as $\phi(\beta)$ in Fig. 2 by means of the relation

$$\phi(\beta)=K\lambda dy/d\lambda. \qquad (3)$$

This relation in this explicit form is due to DuMond. However, substantially the same idea was used by Jauncey in 1925 in the reverse

[2] Jesse W. M. DuMond, Rev. Mod. Phys. **5**, 1 (1933); Phys. Rev. **52**, 419 (1937).

order. He assumed certain speed distributions among the atomic electrons and calculated the shape of the Compton modified band. A far more elegant and general method of handling the experimental data was developed later by Jauncey.[3] He noticed that the linear relation between λ'' and u in Eq. (2) immediately led to the following result. If $f(u)du$ is the number of electrons with velocity components between u and $u+du$, then the number of scattered photons with wave-lengths between λ'' and $\lambda''+d\lambda''$ (note that λ'' is measured from the center of the Compton modified band) is $f(\lambda''c/2\lambda \sin(\theta/2))d\lambda''$, or $f(\lambda'' \times \text{const.})d\lambda''$ when λ and θ are given. In other words, this states that the *shape of the Compton modified band is identical with the shape of the component velocity distribution function* of the atomic electrons producing the band. Thus Fig. 1, which is obtained directly from experiment, gives at once the shape of the component velocity distribution function which can then be compared with curves obtained theoretically. It is no longer necessary to go through the laborious process of computing the resultant velocities to test a theory.

Electron scattering

It will be shown that the inelastic scattering of electrons by atoms may be identified with the scattering of the electrons by one or other of the atomic electrons, and that the cooperation of two or more scattering centers (be the other center the nucleus or another atomic electron) plays a negligible part if the impinging electrons have sufficient speed. When an electron approaches a center of force, repelling or attracting according to the inverse square law, the resulting deflection, θ, is determined by what, in simple orbit theory, is called the "collision parameter." For the case of an electron of mass m and speed v moving towards an isolated nucleus of charge Ze,

TABLE I. *Collision parameters.*

V	p_n	p_e
1,000 volts	0.047×10^{-8} cm	0.021×10^{-8} cm
2,000	0.023	0.0105
5,000	0.0094	0.0045
10,000	0.0047	0.0021

[3] G. E. M. Jauncey, Phys. Rev. **46**, 667 (1934).

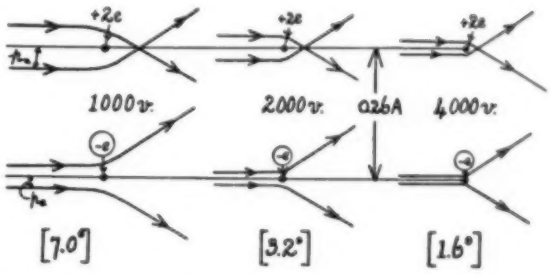

FIG. 3. Collision parameters for the scattering of an electron by a nucleus and by an atomic electron, calculated for a 34.2° deflection.

the relation between the collision parameter p_n and the deflection θ is

$$p_n=(Ze^2/mv^2)\cot(\theta/2)=(300Ze/2V)\cot(\theta/2) \quad (4)$$

when the energy of the impinging electron is V electron volts. For the case of an electron moving towards another electron (initially at rest) the relation between the collision parameter p_e and θ is

$$p_e=(2e^2/mv^2)\cot\theta=(300e/V)\cot\theta. \quad (5)$$

For the specific case experimentally investigated in this paper, *viz.*, a deflection of electrons through 34° on collision with helium atoms, Table I gives values of p_n and p_e for various electron energies. In Fig. 3 we compare the collision parameters with the most probable distance between the helium nucleus and an atomic electron, which is 0.26×10^{-8} cm. It is evident from this diagram that we are justified in regarding the scattering of electrons through a moderately large angle (e.g., 34°) by an atom of helium as being due *either* to the nucleus *or* to one of the atomic electrons, whenever the collision parameters are sufficiently small in comparison with the atomic electron-to-nucleus distance.[4] We may therefore regard helium gas as providing a mixture of nuclei and atomic electrons which scatter independently of one another, when the impinging electrons have enough speed.

[4] It is probably superfluous to mention that the atomic electron-to-nucleus line is not always perpendicular to the line of approach of the impinging electron, as in Fig. 3. On relatively rare occasions the nucleus and one atomic electron may be so orientated that both contribute deflections of the same order of magnitude to give the observed deflection. The contention is merely that the faster the impinging electron the smaller are the collision parameters and the less often do we have any departure from what may conveniently be called "single center scattering."

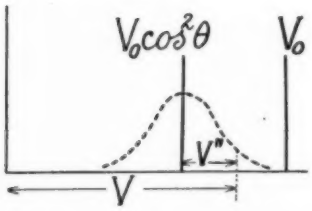

FIG. 4. Division of scattered electrons into an elastically scattered group and an inelastically scattered group.

The atom as a whole plays no part in the scattering of individual electrons. All that the atom, as such, does is to provide the distribution of velocities among the electrons which do the scattering.

Scattering by a nucleus is distinguished from scattering by an atomic electron by the fact that in the first case the collision is "elastic," that is the electron loses no energy, while in the second case the collision is "inelastic," that is, the electron loses some of its energy to the atomic electron during the scattering process. If the atomic electron is initially at rest, the energy which the impinging electron retains is

$$V = V_0 \cos^2\theta = V_0 - V_0 \sin^2\theta. \quad (6)$$

This is clearly analogous to Eq. (1), which gives the wave-length of the photon after colliding with an electron. We should expect to find the electrons scattered through a selected angle by a gas such as helium to be divided into two distinct groups, those which have been scattered by the nuclei and which have lost no energy, and those which have been scattered by the atomic electrons and which, if the atomic electrons were initially at rest, would all have one and the same energy, $V = V_0 \cos^2\theta$. If the atomic electrons are moving at random with various speeds the electrons scattered inelastically will have a distribution of energies centered around $V_0 \cos^2\theta$ (shown as a dotted line in Fig. 4).

The next step is to show how an experimental determination of the distribution of energy among the inelastically scattered electrons may be used to find the distribution of velocities among the atomic electrons. The argument is due to Jauncey[5] and runs closely parallel to his theory of photon scattering. An electron moving with a velocity v_0, in the direction shown in

[5] G. E. M. Jauncey, Phys. Rev. **50**, 326 (1936).

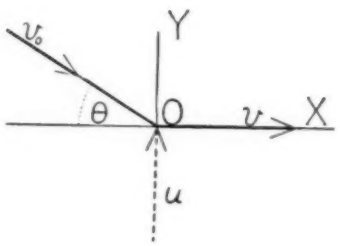

FIG. 5. Collision between a fast electron and an atomic electron.

Fig. 5 is deviated through an angle θ by a collision with an atomic electron at O, so that after collision it has a velocity v. The atomic electron may be moving with any velocity and in any direction. Jauncey finds that the *energy* of the impinging electron after collision is

$$V = V_0 \cos^2\theta + u(2mV_0/e)^{\frac{1}{2}} \sin\theta - u^2(m/2eV_0) \tan^2\theta, \quad (7)$$

where u is the *component of velocity* of the atomic electron in a direction which, to a first approximation, coincides with OY (Fig. 5).

On carrying the analysis to a second approximation it is found that the direction of the component of velocity to be used in Eq. (7) makes a small angle δ with OY such that

$$V\cos^2\delta = V_0\cos^2(\theta+\delta).$$

We may illustrate the application of this to a particular case, for which $V_0 = 2000$ volts, and $V_0\cos^2 34° = 1377$ volts. The values of δ corresponding to V (or to V'') are as shown in Table II. While this result is of interest, it has no direct bearing on our investigation on the scattering by helium, for the distribution of velocities is isotropic and the component velocity has the same value irrespective of direction. However, in principle though possibly not in practice, it would be necessary to consider it in the application of the method of electron scattering to the study of the probably asymmetrical distribution of electron velocities in the surfaces of solids.

Neglecting the third term in Eq. (7) we may rewrite it as

$$V'' = V - V_0\cos^2\theta = u(2mV_0/e)^{\frac{1}{2}} \sin\theta, \quad (8)$$

TABLE II. *Location of component velocity vector.*

V	V''	δ
1177 volts	−200 volts	+6° 21′
1277	−100	+3° 03′
1377	0	0°
1477	+100	−3° 33′
1577	+200	−7° 31′

where V'' is the surplus energy which the scattered electron acquires on collision with an atomic electron having a component velocity u, over what it would have been had the component velocity been zero. (The "surplus" may be positive or negative.) Attention is called to the striking parallelism between Eq. (8) for electron scattering and Eq. (2) for photon scattering. The significant implication discovered by Jauncey for the linear relation between λ'' and u in Eq. (2) applies to Eq. (8) in precisely the same way. According to Eq. (8), an atomic electron with a component velocity u, gives rise to an inelastically scattered electron, moving in a direction θ, with energy V, or what amounts to the same thing with energy differing from $V_0 \cos^2 \theta$, the value for a collision with an atomic electron at rest, by an amount V''. Let the number of atomic electrons with component velocities between u and $u+du$ be $f(u)du$, and let these give rise to $F(V'')dV''$ inelastically scattered electrons (in the direction θ). Then

$$f(u)du = F(V'')dV'' \times \text{const.} \qquad (9)$$

Because of the *linear* relations between V'' and u in Eq. (8), we can write $dV'' = du(2mV_0/e)^{\frac{1}{2}} \sin\theta$, and so change Eq. (9) to

$$f(u) = F(V'') \times \text{const.} \qquad (10)$$

where the quantity $(2mV_0/e)^{\frac{1}{2}} \sin\theta$ is absorbed in the constant, since we can treat V_0 and θ as constants. The importance and usefulness of this relation can hardly be overestimated. It tells us that the shape of the experimentally measured *distribution of energies* among the inelastically scattered electrons, *viz.*, $F(V'')$, gives simultaneously the shape of $f(u'')$, the *distribution of component velocities* of the atomic electrons. Any theory of the atom which gives a definite prediction as to the distribution of component velocities among its atomic electrons, can be tested by direct comparison with the experimentally obtained distribution of energies among the inelastically scattered electrons.

Approximations

Certain approximations have been made in deriving the formulas which are to be applied to the experimental data. These will now be discussed with special reference to the particular angle of scattering and electron energies used in the experimental work.

Although a rigorous investigation of the effect of disregarding relativity has not been made, it seems safe to conclude that the fractional change which would be introduced into any formula because of relativity would be of the order of v^2/c^2, or less. Even with the fastest electrons used in these experiments (4000 volts), v^2/c^2 amounts to only 0.016, and may therefore be neglected.

In the derivation of Eq. (6), the atomic electrons were regarded as free, i.e., the binding energy of the atom was not taken into account. The effect of taking the binding energy into account may be estimated by considering the special case in which the atomic electron is at rest. We shall assume that the energy and momentum imparted to the atom may be neglected and that the energy for ionization is supplied by the impinging electron. We then have

$$mv_0^2/2 = mv^2/2 + mw^2/2 + E \qquad (11)$$

for the energy balance, and

$$mv_0 = mv\cos\theta + mw\cos\phi, \qquad (12)$$

$$0 = mv\sin\theta - mw\sin\phi, \qquad (13)$$

for the momentum. Here v_0, v, and w are the velocities of the impinging electron before and after the collision and of the recoil electron after collision, E is the energy of binding (corresponding to the ionization potential), and θ and ϕ are the directions in which the two electrons move after collision. Except for the appearance of E in the energy equation, these equations are identical with those from which Eq. (6) was derived. An approximate solution is

$$V = V_0 \cos^2\theta - E. \qquad (14)$$

This means that the effect of taking the binding energy into account is to shift the center of the inelastic band towards the origin, i.e., away from the elastic band, by an amount E. A shift in the position of the center of the Compton modified band has been attributed to the effect of binding by DuMond, Ross, Kappeler, and Burkhardt, though the method of taking it into account differs from that used here. For 2000 volt electrons impinging on helium atoms (for

which E is 25 electron volts) the effect of allowing for E is to shift the center of the band of inelastically scattered electrons from 1368 to 1343 volts. A shift of this amount could be produced by an error in the scattering angle of 0.8°, without bringing E in at all, so that to establish, with certainty, the effect of binding requires the angle of scattering to be known to better than about 0.2°. This is not easy for one has to evaluate correctly the effect of the slight spread (±0.3°) in the angle of scattering, due to the finite width of the slits defining the electron beam entering the analyzer, in addition to determining the angle exactly.

The assumption that "single center scattering" occurs, that is, that the scattering of a sufficiently fast electron is the result of its interaction with a single center (a nucleus or one atomic electron) is an approximation which needs to be examined. The angles in parentheses in Fig. 3 are those through which the attraction of the nucleus would deflect an electron passing close to the atomic electron which is assumed to be 0.26×10^{-8} cm away. The observed deflection, *viz.*, 34°, is really due to the joint action of the atomic electron and the nucleus (and also the other atomic electron which we shall neglect). If we may assume, merely as a rough approximation, that the observed deflection is the sum of what the nucleus and the atomic electron would produce if acting separately, then the actual deflection of a 4000 volt electron by an atomic electron would be 34°±1.6°, i.e., 35.6° and 32.4° (two values because the atomic electron may be on either side of the nucleus). If, in addition, it be assumed that the energy change is associated with only that part of the deflection attributed to the atomic electron, we shall have two values, $V_0 \cos^2 35.6°$ and $V_0 \cos^2 32.4°$ for the energy after collision. In this extremely simplified picture, in which the atomic electron is at rest and located either as shown in Fig. 3, or on the opposite side of the nucleus, we should expect to find inelastically scattered electrons with energies differing by ±3.8 percent from that found on the assumption that the atomic electron acts strictly alone. As an alternative mode of approach, we may assume that the departure from ideal "single center scattering" in the case of inelastic scattering is of the same order of magnitude as for elastic scattering. It will be recalled that, in elastic scattering, a quantity $(Z-F)$, where Z is the atomic number and F the atom form factor, enters in place of Z, which would appear by itself if nothing but the nucleus were to be considered. For $\theta=34°$, and 4000 volt electrons impinging on helium atoms, F is 1.3 percent of Z. Conversely we may assume that the effect of the nucleus and the other atomic electron in modifying the deflection produced by the atomic electron near which the incoming electron passes, is of the same order of magnitude. It is not difficult to see in a general way, that this will result in replacing inelastically scattered electrons of one and the same energy, *viz.*, $V_0 \cos^2 \theta$ by a group whose half-width will be of the order of the first or second power of the 1.3 percent. Both lines of argument lead to the result that 4000 volt electrons, scattered at 34°, by atomic electrons *at rest* will have energies distributed over a band whose half-width is of the order of a few percent of the energy corresponding to the center of the band. When, however, the atomic electrons are in motion, as they must be in actual atoms, this motion of itself results in the energy of the inelastically scattered electrons being spread out over a band of considerable width, so that the effect of the departure from ideal "single center scattering," considered in this paragraph, on the *shape* of the band may be considered almost negligibly small.

The error resulting from neglecting the term in u^2 in Eq. (7) will now be considered. On writing $V''=V-V_0 \cos^2 \theta$, and solving Eq. (7) for u, we obtain

$$u=(V_0e/2m)^{\frac{1}{2}}(\cos^2\theta/\sin\theta)\{V''/V_0\cos^2\theta + (\tfrac{1}{4})(V''/V\cos^2\theta)^2\}, \quad (15)$$

or

$$u=Ax(1+x/4), \quad (16)$$

where A and x are $(V_0e/2m)^{\frac{1}{2}}(\cos^2\theta/\sin\theta)$ and $V''/V_0\cos^2\theta$, respectively. The number of atomic electrons with *component velocities* between u and $u+du$ is $f(u)du$. These will scatter a certain number, $F(V'')dV''$ of the impinging electrons through an angle θ into an *energy* range dV'' at V''. (V'', being defined as $V-V_0\cos^2\theta$, is the excess energy which the scattered electron has as a result of the atomic electron having a com-

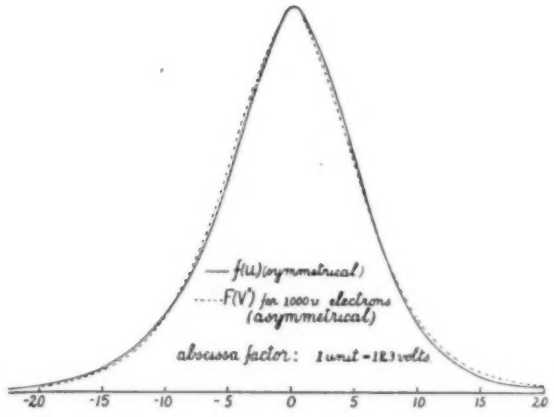

FIG. 6. Modification of the energy distribution curve due to a second-order term.

ponent velocity u over the value $V_0 \cos^2 \theta$ which it would have for the case $u=0$.) We can write

$$f(u)du = \text{const. } F(V'')dV''$$
$$= \text{const. } V_0 \cos^2 \theta \cdot F(x \cdot V_0 \cos^2 \theta)dx,$$

when V_0 and θ are held constant. Since Eq. (16) yields

$$du = A(1+x/2)dx$$

we have

$$f(u) = F(x \cdot V_0 \cos^2 \theta)(1+x/2)$$
$$= F(V'')/(1+x/2), \quad (17)$$

where constant quantities are ignored. To obtain $f(u)$ from $F(V'')$ which is given directly by experiment, we must divide each ordinate by $(1+x/2)$. However the new curve gives $f(u)$ in terms of x as abscissa and we need it in terms of u. The u value for each x can be obtained by writing $u = Ax(1+x/4)$ which gives a nonuniform scale in u. To get a uniform scale in u, all that is necessary is to take each point on the new curve, $F(V'')/(1+x/2)$, and displace it horizontally by an amount $(1+x/4)$. Thus to get $f(u)$ in terms of u uniformly spaced along the abscissa, we first contract each ordinate of $F(V'')$ in the ratio $1 : (1+x/2)$ and then expand each abscissa in the ratio $1 : (1+x/4)$. We shall illustrate the effect of neglecting the term in u^2 in the case where it should be most noticeable in our experiments, i.e., for the slowest electrons, of 1000 volts energy. We shall assume $f(u)$ to have the shape shown in Fig. 6, a shape given by wave mechanics and shown to be substantially accurate by our experiments. Since $f(u)$ represents the distribution of component velocities in the atom it must be symmetrical about the origin. We have seen that if we neglect the u^2 term, the shape of the $F(V'')$ curve giving the distribution of energies among the scattered electrons is identical with that of $f(u)$. But if we take account of the u^2 term, we can get $F(V'')$ from $f(u)$ by reversing the procedure outlined in the previous paragraph. The result is that $F(V'')$ is no longer identical in shape with $f(u)$ but has a shape like that of $f(u)$ slightly warped, as shown in Fig. 6. The predicted asymmetry in $F(V'')$ is probably too small to be detected experimentally at present.[6]

The errors introduced by the various approximations discussed above are of the order of the experimental uncertainties in the present measurements and may therefore be disregarded. However, they are not negligibly small. If the precision of measurement could be improved by a factor of five or ten, it would probably be necessary to allow for them in comparing theory with experiment.[7]

All sources of error in the accuracy of the simple formula, Eq. (10), except the one due to the neglect of relativity, become less the greater the energy of the impinging electron. Unfortunately, the *number* of electrons scattered diminishes as the square of their initial energy, so that the scattered electron currents are too small to measure accurately when the electron energy is increased beyond a certain value. With our present apparatus and methods of measurement this point is reached when the electron energy exceeds about 5000 volts.

Energy distribution curves: theoretical

We have seen that, on Jauncey's theory, $f(u)$ is identical in shape with $F(V'')$, the experi-

[6] This kind of asymmetry should, in principle, be found in the shape of the Compton band. Professor Jauncey has shown how it leads to a slight displacement in the position of the maximum from that given by the simple theory. A displacement has been observed experimentally by Ross and Kirkpatrick and by DuMond and Kirkpatrick, who however have not taken the effect discussed here into account in their explanation of the displacement.

[7] While the error introduced by the neglect of the u^2 term can be taken into account quantitatively, that arising from the lack of perfect "single center scattering" can only be estimated qualitatively. This indicates that, even if the precision were improved, it might not be possible to check the first effect quantitatively, because it would always be more or less masked by the second effect. In principle such a check could be made in x-ray scattering insofar as perfect "single center scattering" prevails.

mentally determined distribution of energies among the inelastically scattered electrons about the center of the band. The shape of $f(u)$ is given at once merely by re-labeling the abscissas in terms of u instead of V'', the conversion being effected by means of Eq. (8). The curve so obtained gives us what may be regarded as an experimentally determined distribution of atomic electron component velocities, which may, if one desires, be compared with curves predicted by theory. However the results of the two available theoretical investigations give, not $f(u)$, but $f(\lambda)$, the closely related profile of the Compton modified band. It is necessary to show how such profiles can be related to our electron energy distributions. On eliminating u between Eqs. (2) and (8), we get

$$V''=(\lambda''/\lambda)\cos(\theta/2)(2mV_0/e)^{\frac{1}{2}} \quad (18)$$

$$=1011(\lambda''/\lambda)\cos(\theta/2)V_0^{\frac{1}{2}} \quad (19)$$

when V'' and V_0 are in volts. By means of this equation we can change from abscissas in λ'', used in plotting the profile of the Compton band, to abscissas in V'' used in giving the results of electron scattering experiments.

Kirkpatrick, Ross and Ritland,[8] using screening data from Slater, have calculated the profiles of the Compton modified bands for the first eighteen elements. They give the profiles, $f(\lambda'')$, for various values of λ'' (in XU) for the case of $\lambda=695$ XU and $\theta=90°$. To get the values of λ'' appropriate to scattering at 34.2°, the angle used in our experiments, a consideration of Eq. (2) shows that the values of λ'' used by these authors in $f(\lambda'')$ for 90° must all be multiplied by $\sin(34.2°/2)/\sin(90°/2)$. Hence to get the values of V'' for 34.2° electron scattering from the values of λ'' for 90° x-ray scattering, we must use

$$V''=1011(\lambda''/695)\cos(34.2°/2)V_0 \times\sin(34.2°/2)/\sin(90°/2)$$
$$=0.5782\lambda''V_0^{\frac{1}{2}}. \quad (20)$$

Hicks[9] has calculated the shape of the Compton modified band for helium and hydrogen by methods which are considered to be more satisfactory in principle than those using screening data. He gives his values in terms of a non-dimensional quantity, β, which is defined by DuMond's equation

$$\lambda''=\beta(\lambda'^2+\lambda^2-2\lambda'\lambda\cos\theta)^{\frac{1}{2}}. \quad (21)$$

β is also u/c, the ratio between the component electron velocity and the velocity of light. To a close approximation Eq. (21) may be written

$$\lambda''=\beta 2\lambda\sin(\theta/2), \quad (22)$$

which is equivalent to Eq. (2).

To compare Hicks' values with those given by Kirkpatrick, Ross and Ritland for the special case calculated by the latter, we put $\lambda=695$ XU and $\theta=90°$ into Eqs. (1) and (21), and get

$$\lambda''=999.4\times\beta\ (\text{XU}). \quad (23)$$

(The approximate formula, Eq. (22), gives a result only 1.7 percent less.) Since the values of β used by Hicks in his graph are 2, 4, 6, $\cdots\times10^{-3}$, Eq. (23) gives the corresponding sequence $\lambda''=2, 4, 6, \cdots$ in XU. Table III gives (1) the values (denoted by K.R.R.) of $f(\lambda'')$ calculated by Kirkpatrick, Ross, and Ritland for $\lambda=695$ XU and $\theta=90°$, (2) those (denoted by "H-4") computed from Hicks' data for the same λ and θ as outlined above, and (3) the corresponding abscissas in V'' for electron scattering through 34.2° of electrons whose initial energy is V_0 electron volts. Thus, by plotting $f(\lambda'')$ against V'' for the values of V_0 used in our experiments, we

TABLE III. *X-ray and electron scattering: theoretical.*

X-RAY SCATTERING $\lambda=695$ XU, $\theta=90°$			ELECTRON SCATTERING FOR ELECTRON ENERGY V_0 AND $\theta=34.2°$
λ''	$f(\lambda'')$ K.R.R.	$f(\lambda'')$ H-4	V''
0 XU	60.0	60.0	0
1	56.3	58.7	$0.578\times V_0^{\frac{1}{2}}$ volts
2	52.2	54.5	1.156
3	47.0	48.5	1.735
4	41.0	41.6	2.313
5	34.8	34.6	2.890
6	28.2	28.2	3.469
7	23.0	22.5	4.047
8	18.1	17.9	4.626
9	14.1	14.2	5.204
10	11.4	11.2	5.782
12	6.95	7.04	6.938
14	4.03	4.52	8.095
16	2.46		9.250
18	1.34		10.407
20	0.90	1.34	11.563

[8] P. Kirkpatrick, P. A. Ross and H. O. Ritland, Phys. Rev. **50**, 928 (1936).
[9] B. Hicks, Phys. Rev. **52**, 436 (1937).

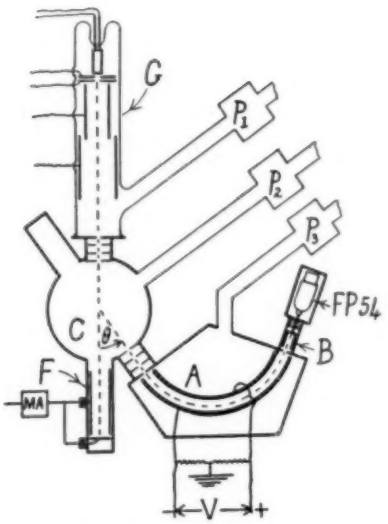

FIG. 7. Apparatus.

can compare the form of the curve predicted by theory with that found by experiment.

EXPERIMENTAL

Apparatus

The apparatus consists essentially of three parts, an electron gun G, a collision chamber C, and an electrostatic analyzer, A (Fig. 7). Several types of electron gun were tried. The one finally used consists of an indirectly heated cylindrical cathode emitting electrons from the flat end which is perpendicular to the axis of the tube.[10] The focusing arrangement consists of two plates, each with a circular hole, and two cylindrical anodes, arranged co-axially. By carefully choosing the voltages applied to the plates and anodes, it is possible, with 4000 volts potential on the second anode, to obtain electron currents up to 150 microamperes through 1.5 mm holes into the collision chamber. With helium at about 0.005 mm pressure in the collision chamber, the path of the electron beam is clearly seen as a narrow pencil of light, not more than about 2 mm in diameter, and showing no visible divergence. The total electron current passing across the chamber into the Faraday cage F is measured by a microammeter. The bottom of the Faraday cage can be moved aside by means of a ground glass joint (not shown) so as to allow the electron beam to strike a fluorescent screen. This is helpful in making adjustments of the voltages to give the best possible beam. A set of four slits, spaced over a length of 52 mm, serves to define the direction of the scattered electron beam entering the analyzer. The scattering angle, i.e., the angle between this direction and that of the primary beam from the gun is 34.2°. Owing to the finite width of the slits, the electrons which are accepted by the slit system have been scattered through $34.2° \pm 0.3°$. The electrostatic analyzer has been described before,[11] and so merely the dimensions of this particular one will be given. The radii of the deflecting plates are 5.50 cm and 6.50 cm. The entrance slit is 0.3 mm by 5 mm, and the exit slit (i.e., into the collector B) 0.47 mm by 8 mm. The collector is connected to an FP-54 tube which is mounted in a vacuum and as close to it as possible. The associated circuit is that described by DuBridge and Brown.[12] A resistor of 5×10^{11} ohms is used to shunt the control grid of the tube to the filament. The output is measured by means of a Leeds and Northrup, type R, galvanometer. The sensitivity of the system is 50,000 divisions per volt, so that with the resistor referred to above, 1 division deflection corresponds to 4×10^{-17} amp. The high sensitivity was necessary because even the largest inelastic current obtained under the most favorable conditions did not exceed 5×10^{-15} amp.

While it is necessary to have helium at a pressure of about 0.008 mm in the collision chamber to scatter enough electrons to measure, it is very necessary to maintain as high a vacuum as possible in the electron gun and analyzer. The gun is separated from the collision chamber by four discs, each with a hole 1.5 mm in diameter through which the electrons pass into the collision chamber. The analyzer is likewise separated from the collision chamber by a set of four slits, the two outermost, 0.3 mm by 5 mm, defining the scattered electron beam and the two innermost, somewhat larger, helping to retard the flow of gas. When the electron gun, the collision chamber, and the analyzer are pumped out by separate pumps and when gas is

[10] We take pleasure in acknowledging our thanks to Dr. R. G. Hergenrother for supplying us with the electron gun used in most of the measurements.

[11] A. L. Hughes and J. H. McMillen, Phys. Rev. **34**, 291 (1929); **39**, 585 (1932).

[12] L. A. DuBridge and Hart Brown, Rev. Sci. Inst. **4**, 532 (1933).

allowed to leak directly into the collision chamber, it is possible, because of the restricted communicating passages between the various regions, to obtain a vacuum in the gun and analyzer one hundred times better than that in the collision chamber. Three two-stage oil diffusion pumps, containing Apiezon oil, are connected respectively to the electron gun, the collision chamber, and the analyzer, by means of short tubes, 3 cm wide. Each pump has a speed of 9.5 liters per second, measured at its intake. Cooled traps, located between the pumps and the parts to which they are connected, prevent oil vapors diffusing into the apparatus. The three two-stage pumps are backed by a common one-stage Apiezon oil pump, which in turn is backed by a fast mechanical pump. To control the pressure in the collision chamber, a specially designed stopcock, whose opening can be changed from about 1 cm² down to zero, is placed between the collision chamber and its pump. Helium, carefully purified by passing through two charcoal tubes in liquid air, is stored in a sylphon reservoir, whose maximum volume is about 2 liters. The helium passes into the collision chamber through a very fine capillary glass tube and then through a well outgassed charcoal tube immersed in liquid air. The driving pressure can be varied over a limited range by altering the size of the sylphon reservoir. With all pumps in action it is possible to obtain a pressure below 5×10^{-5} mm in both gun and analyzer while maintaining a useful working pressure of about 5×10^{-3} mm in the collision chamber.

The high voltages necessary to operate the electron gun are supplied by suitable power packs. At first the voltage for the deflecting plates in the analyzer was obtained from a power pack, but as this proved to be rather unsteady it was replaced by a stack of heavy duty Burgess "B" batteries and a set of 30 flashlight batteries so that any voltage up to 1200 volts could be obtained in steps of 1.5 volts. The steadiness of the deflecting voltage is excellent.

Results

Next we shall describe the procedure followed in taking observations. The first thing is to obtain the best possible vacuum conditions,

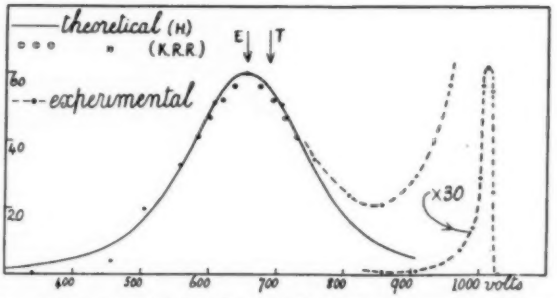

FIG. 8. Energy distribution of 1010 volt electrons scattered at 34.2°.

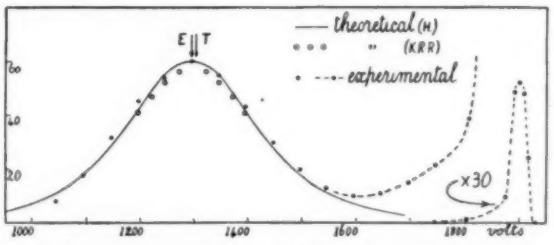

FIG. 9. Energy distribution of 1900 volt electrons scattered at 34.2°.

which may take several hours pumping if the apparatus has been opened to the atmosphere. Then the cathode of the electron gun is heated and the voltages adjusted to give a large electron current through the collision chamber. After conditions have become steady the helium is allowed to flow in, the rate being controlled by changing the size of the sylphon reservoir and the aperture of the stopcock used as a choke. The electron current to the Faraday cage B is measured as the deflecting voltage in the analyzer is altered in small steps over the whole range over which scattered electrons are observed. The maximum of the elastic peak is located and the energy of the electrons is given by the value of the deflecting voltage, multiplied by a factor depending on the geometry of the analyzer. This is found to check well with the value of the voltage accelerating the electrons into the collision chamber, as of course it should. It is found that it is better to complete the exploration of the inelastic peak before making any measurements on the elastic peak. The relatively large currents found at the elastic peak tend to produce a temporary unsteadiness during which it is very difficult to measure the very small inelastic currents. It may be that a large current disturbs the conditions in the FP-54 tube and its associated circuit for an appreciable length of time, or

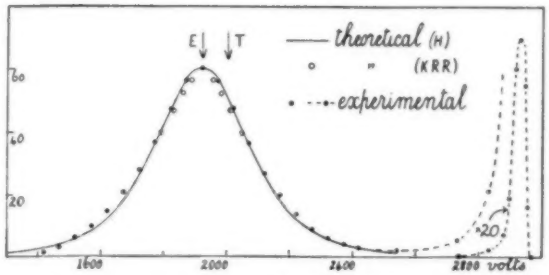

FIG. 10. Energy distribution of 2930 volt electrons scattered at 34.2°.

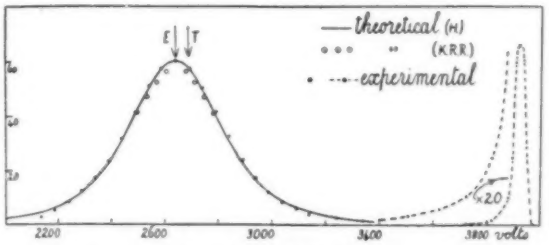

FIG. 11. Energy distribution of 3922 volt electrons scattered at 34.2°.

it may be that, in locating the elastic peak, relatively large electron currents are brushed over one or other of the deflecting plates giving rise to a pseudo contact potential which dies away slowly and irregularly. Whatever may be the explanation, the difficulty is avoided by completing the exploration of the inelastic peak before beginning measurements on the elastic peak.

The experimental independent variable is the deflecting voltage applied to the curved plates in the analyzer. We use, however, in Figs. 8–11, as abscissas for the distribution of energy curves, not the deflecting voltage, but the corresponding voltage which measures the actual energy possessed by the scattered electrons. To get the curve giving the true distribution of energy among the inelastically scattered electrons, it is necessary to divide the value of the electron current obtained at each deflecting voltage, by that voltage. This is because the range dV, of energies admitted by the analyzer, increases in proportion to V.[13] Our results for the scattering of electrons with energies close to 1000, 2000, 3000 and 4000 volts, respectively, are shown in Figs. 8–11. The dots in these diagrams are mean experimental values and were obtained in the following way. With the primary electron energy adjusted to a value close to one of the four listed above, the scattered electron current was measured as the deflecting voltage was raised in small steps from the lowest to the highest value at which measurable currents were obtained. This constituted one "run." Several such runs, requiring about three hours each, were made for approximately the same primary electron energy. The scale of ordinates for each run was adjusted so that the maximum of the inelastic band was always 60 units, and the curves were then shifted laterally (when necessary) by small amounts so as to have them centered as nearly as possible about the same voltage value, which was taken to be the center of the distribution curve. From the individual curves, so superposed, it was possible to draw a mean curve, and the dots shown in Figs. 8–11 were taken off the mean curves for the different primary energies. The number of dots shown in the figures referred to represents a much larger number of experimental measurements (e.g., the 23 dots on the inelastic portion of the 2930 volt curve were obtained by combining four separate runs involving 77 separate measurements).

Since this investigation has to do with the profile of the Compton modified band as determined from inelastic electron scattering, the location and shape of the elastic peak is not of primary importance. However, it is desirable to record how the mean elastic curves plotted in Figs. 8–11 were obtained. The elastic peak was plotted separately for each run and its height, width, and distance from the inelastic maximum was measured. Then a composite elastic peak having the average height and the average width, was placed at the average separation from the inelastic peak. Thus the elastic peaks in Figs. 8–11 were constructed and located. The theoretical resolution, determined by the dimensions of the analyzer, is $dV/V=0.015$, while the experimental resolution, given by the width of the peak at one-fifth of its height is about 0.02. (One-fifth is taken arbitrarily because below this the elastic peak broadens asymmetrically.)

Theoretically, the inelastic maximum should be found at $V=V_0\cos^2\theta$. Actually it is always found at a slightly smaller value (see Table IV and also E and T in Figs. 8–11). The irregularity in the differences suggest some inconstant experimental condition. It is possible that temporary pseudo contact potentials are set up when the strong beam

[13] Similarly when an electron velocity spectrum is obtained by means of a magnetic field, each reading must be divided by the value of the magnetic field, H, at which it was obtained, to give a true distribution of velocities. The need for this step (division by V or H) has been overlooked by many investigators who have taken the measured electron currents as a function of the deflecting voltage to be the true distribution of energies (or velocities). For a very complete discussion of the matter, see a paper by R. Kollath, Ann. d. Physik **27**, 721 (1936).

TABLE IV. *Location of the maximum of the inelastic band.*

Elastic Peak V_0	Inelastic Peak		Difference
	Theor.	Exp.	
3922v	2683v	2640	43
2930	2002	1920	83
1900	1302	1295	7
1010	690	658	32

of electrons is swept across the deflecting plates in the process of locating the elastic peak with the result that the deflecting potentials necessary to bring the peak on the exit slit will be affected. Had the differences in the last column of Table IV been constant and of the order of 25 volts, one would have been tempted to attribute it to the effect of binding of the electrons in the helium atom, as outlined above in the section on "Approximations."

Discussion

The main purpose of this investigation is to determine the distribution of component velocities of the atomic electrons in the helium atom, which, as we have seen, gives simultaneously the profile of the Compton modified band. Investigations by Kirkpatrick, Ross and Ritland,[8] and by Hicks,[9] have led to theoretical predictions as to the shape of the profile of the band. To check these theoretical profiles against our experimental results it is necessary to convert the profiles ($f(\lambda'')$ plotted against λ'') into curves giving the theoretical distribution of energies among the inelastically scattered electrons by replacing abscissas in λ'' by abscissas in V''. The conversion factors are given in Table III. In Figs. 8–11, the continuous lines give the curves so calculated from Hicks' data. (Hicks gives two curves He-2 and He-4 which differ slightly. As the latter is believed to be the more nearly correct on theoretical grounds, we use it to compare with our results.) The open circles give the values calculated from the data of Kirkpatrick, Ross and Ritland in the region where they differ perceptibly from those of Hicks. It is clear that our experimental points fit the theoretical curves remarkably well, and that the fit improves with increasing electron energy. It may therefore be concluded that the theory as to the nature of inelastic scattering of fast electrons is satisfactory. This being so, the next step is to invert the procedure, and assume the theory to be true and use as many experimental measurements as possible to determine the most probable shape of the distribution of component velocities of the electrons in the helium atom. We shall arbitrarily exclude the measurements made with 1010 and 1900 volt electrons since theory suggests that the data with the faster electrons will lead to more accurate results, and since we have plenty of measurements with 2930 and 3922 volt electrons to give dependable mean values. We get the distribution of component velocities among the atomic electrons from the distribution of energies among the inelastically scattered electrons by changing the abscissas in the latter from V'' to λ'' by means of Eq. (20) which gives us

$$\lambda'' = V'' \div (0.5782\, V_0^{\frac{1}{2}}), \qquad (24)$$

where λ'' is computed for $\lambda = 695$ XU and $\theta = 90°$ (the case for which Kirkpatrick, Ross and Ritland calculated their profiles) and V'' is for electrons of energy V_0 scattered at 34.2°. Eq. (23) then allows us to write

$$\beta(=u/c)\times 10^3 = \lambda'' = V'' \div (0.5782\, V_0^{\frac{1}{2}}), \qquad (25)$$

which gives us the abscissas in terms of u, the component velocity of the atomic electron. By means of this equation, the ordinates of the dots representing experimental points in Figs. 10 and 11 for various values of V'' are re-plotted against β, and the best mean curve is drawn through the four sets of dots.[14] (There are four sets because we use the two halves of both the 2930 and 3922 volt curves.) From this mean curve we pick off the dots shown in Fig. 12. In Fig. 12 we also have the two curves computed theoretically by Hicks (who considers the "H-4" curve to be the more accurate) and the curve computed by Kirkpatrick, Ross and Ritland, which is represented by a broken line. (The last curve agrees so well with the "H-4" curve over the middle part that it is difficult to show the small differences between them because of the necessary finite thickness of the line in the drawing.) It is clear that our experimentally determined values are in excellent agreement with the "H-4" curve, and also with that due to Kirkpatrick, Ross and Ritland, except in the region below about $\beta = 3\times 10^{-3}$. It appears that the K.R.R. curve is not sufficiently

[14] To secure the best possible mean curves, the individual curves were drawn carefully on a large scale. This was necessary because they were all close to each other.

rounded at the maximum to account for the experimental results.[15] At the other end, the last two experimental points are decidedly below the theoretical curves. It may be that this represents a real disagreement, but we must remember that the electron currents from which these points are derived are of the order of 1 or 2×10^{-16} amp., values which are difficult to measure with any degree of accuracy. Finally it should be mentioned that the experimental dots plotted in Fig. 12 are based on seven distinct runs in which a total of 134 separate measurements of electron currents were made. In view of the closeness of fit between the mean experimental points and the "H-4" theoretical curve it is desirable to supplement Fig. 12 by Table V in which the numerical values are listed.

It is clear that the scattered electrons are divided into two well marked groups, those scattered elastically and those scattered inelastically. The division becomes more definite the higher the energy of the electrons before scattering. Even at our highest voltage, the elastic peak has a "foot" on its low voltage side, indicating the presence of electrons which have lost a small amount of energy. (The "feet" are shown on two scales in Figs. 8–11.) An obvious explanation is that the foot is due to the lack of perfect "single center scattering" as defined earlier in the paper. It is easy to see, by allowing the atomic electron in Fig. 3 to take any position on a sphere around the nucleus, that occasionally a deflection observed at the selected angle will be due to a deflection by the nucleus followed (or preceded) by a small but not negligible deflection by an atomic electron. The more unequal the contribution of one or other scattering center to the resulting deflection, the more frequent is this kind of scattering. We may assume that, when the deflection is due chiefly to the nucleus, the smaller the deviation attributed to the atomic electron, the less energy is taken from the impinging electron. Thus the shape of the "feet" in Figs. 8–11 is qualitatively accounted for. The approximation to ideal "single center scattering" improves as the square of the energy of the impinging electron. This consideration by itself suggests that we should carry out experiments with faster electrons than we have used. However, as the number of electrons scattered diminishes as the square of their energy, a point is reached when the scattered electron currents are too small to be measured accurately.

TABLE V. *Theoretical and experimental profiles for the modified band, and the equivalent component velocity distribution of the atomic electrons.*

λ''	u	$f(u)$ (K.R.R.)	$f(u)$ (H-2)	$f(u)$ (H-4)	$f(u)$ EXPERIMENTAL
0 XU	0×10^7 cm/sec	60.0	60.0	60.0	60.0
1	3	56.3	58.9	58.7	58.5
2	6	52.2	55.6	54.5	54.6
3	9	47.0	50.6	48.5	48.9
4	12	41.0	44.6	41.6	41.9
5	15	34.8	38.2	34.6	34.9
6	18	28.2	32.0	28.2	28.6
7	21	23.0	26.2	22.5	23.3
8	24	18.1	21.2	17.9	19.0
9	27	14.1	16.9	14.2	15.2
10	30	11.4	13.4	11.2	11.8
12	36	6.95	8.3	7.03	6.8
14	42	4.03	5.2	4.53	3.5
16	48	2.46	(3.5)	(3.0)	1.4

The last four columns could also be labeled $f(\lambda'')$ the profile of the Compton modified band for $\lambda=695$ XU and $\theta=90°$.

[15] Lack of perfect resolution would of course flatten the experimental curves near the maximum, but it is considered that this explanation is not sufficient to account for the difference between the experimental values and the K.R.R. curve.

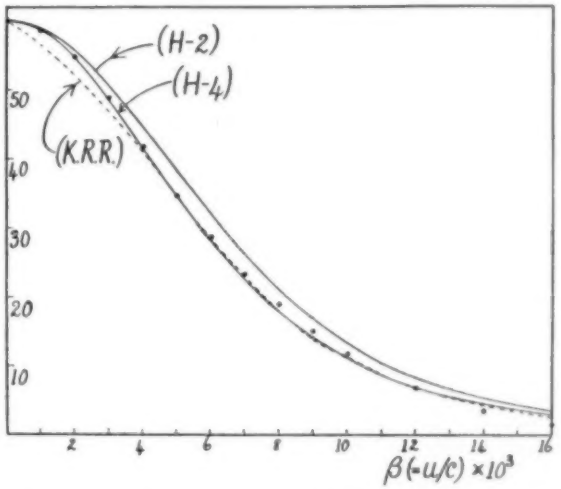

FIG. 12. Theoretical and experimental distributions of component velocities of atomic electrons in helium. Continuous lines: theoretical curves due to Hicks. Broken line: theoretical curve due to Kirkpatrick, Ross, and Ritland. Dots: experimental values. Abscissas: each unit $=\beta\times10^3=u/(3\times10^7)=\lambda''$ in XU (for $\lambda=695$ XU and $\theta=90°$).

It is planned to use this new technique to the study of the distribution of velocities of the atomic electrons in the atoms of various gases. An attempt will be made to see if it can be applied to the analogous problem in solids, where we may be prepared to find anisotropy in the distributions, particularly in certain crystals.

We take great pleasure in acknowledging our indebtedness to Drs. Kirkpatrick and Hicks who very kindly let us have the numerical data from which their published curves were drawn, thereby allowing us to make a better comparison between theory and experiment. We also desire to express our appreciation of the great interest shown by Professor G. E. M. Jauncey in this problem.

The Atomic Masses of the Heavy Elements*

A. J. DEMPSTER
University of Chicago, Chicago, Ill.

(Received November 6, 1937)

Comparisons have been made between a series of different atomic masses by means of a double-focusing mass spectrograph. The small displacement between the positions of multiply charged ions of one mass and atoms of another mass is measured and gives a value for the difference in the packing fractions of the two atomic masses. The following pairs of ions have been compared: O^{+}-Ti^{+3}, C^{+}-Ti^{+4}, N^{+}-Fe^{+4}, O^{+}-Cu^{+4}, Al^{+}-Ag^{+4}, Cu^{+}-Au^{+3}, Ti^{+}-Au^{+4}, Cu^{+}-Pt^{+3}, Sn^{+}-Th^{+2}, Sn^{+}-U^{+2}, Sn^{+}-AcU^{+2}, Zr^{+}-W^{+2}(91, 92), Mo^{+}-Pt^{+2}(96, 97, 98), Mo^{+}-Ir^{+2}, Pd^{+}-Pb^{+2}(102, 104), Rh^{+}-Pb^{+2}, Pd^{+}-Tl^{+2}, Pd^{+}-Bi^{+2}, Ru^{+}-Os^{+2}(96), Ru^{+}-Pt^{+2}(99), Pd-Ga^{+}. Less exact comparisons have also been made between the following pairs: Mo^{+}-Os^{+2}(94, 95, 96), Ag^{+5}-Zn^{+3}, Na^{+}-Zn^{+3}, Sn^{+}-Ta^{+3}, K^{+2}-Ru^{+5}, Ni^{+2}-Ru^{+5}, Al^{+}-Pd^{+4}, Fe^{+}-Ag^{+2}. The values deduced for the packing fractions of titanium, iron, and copper, and the probable values for zinc, silver, gold, and platinum are higher than those to be expected from Dr. Aston's packing fraction curve by about 2 parts in 10,000.

DURING the last year, several redeterminations of the masses of the light elements have been made by Aston[1] and by Bainbridge and Jordan.[2] These now give excellent agreement with the masses deduced from nuclear disintegration experiments.[3] In the present paper, some comparisons of the atomic masses of heavier elements not previously measured will be presented. These have been made possible by the development of the new source of ions referred to in the following section.

Apparatus and Method

In the mass spectrograph used, the rays after passing a narrow slit are deviated through 90° in a cylindrical condenser. A divergent bundle of rays of one velocity is brought to a focus by the electric field at the entrance to a magnetic field in which the rays are then deviated through 180° and brought to a focus on a photographic plate. The velocity dispersion produced by the electrostatic field is compensated by the velocity dispersion in the magnetic field, so that the original divergent bundle may contain rays of slightly different energies. The theory of this type of double-focusing mass spectrograph has been given in a previous paper.[4] A general description with a photograph of the instrument showing the method of mounting the various parts was given in a paper in the *Proceedings of the American Philosophical Society*.[5] The electrostatic stray field at the beginning and end of the cylindrical condenser was computed, and the extra deviation of the ions that would have occurred in these stray fields was avoided by shortening the outer charged cylindrical plate at each end by about 2 mm.

The source of ions was a high frequency spark between solid electrodes as previously described.[5, 6] A study of the types of ions obtainable in this manner has recently been made by Sheng-Lin Ch'u.[7] The ions were accelerated by a potential of 3000 to 10,000 volts obtained from a transformer and rectified by a kenotron and condenser. The electrostatic deflecting field was obtained either from a battery of storage cells or from a transformer and two kenotrons with large condensers, followed by a stabilizing circuit as described by Evans.[8] For

* A paper delivered in part at the Tercentenary Conference of Arts and Sciences at Harvard University, September, 1936. This investigation was supported by a grant from the Penrose Fund of the American Philosophical Society.

[1] F. W. Aston, Nature **137**, 357, 613 (1936).

[2] K. T. Bainbridge and E. B. Jordan, Phys. Rev. **49**, 883 (1936); **51**, 384 (1937).

[3] M. S. Livingston and H. A. Bethe, Rev. Mod. Phys. **9**, 373 (1937).

[4] A. J. Dempster, Phys. Rev. **51**, 67 (1937). Two typographical errors should be corrected. At the bottom of the first column, p. 67, the symbol C is an abbreviation for $V \log_e r_2/r_1$, and in the eighth line from the bottom of the second column, p. 67, k^2 is an abbreviation for $e/mC = e/m\ V \log_e r_2/r_1$.

[5] A. J. Dempster, Proc. Am. Phil. Soc. **75**, 762 (1935).

[6] A. J. Dempster, Rev. Sci. Inst. **7**, 46 (1936).

[7] Sheng-Lin Ch'u, Phys. Rev. **50**, 212 (1936).

[8] R. Evans, Rev. Sci. Inst. **5**, 371 (1934).

several months this circuit proved quite satisfactory but was finally discarded on account of irregularities.

Method

It has been found that the spark sources give a considerable proportion of multiply charged atoms. This makes possible the extension of the "doublet" and "bracket" methods of mass comparison to many elements not hitherto studied by ions from a gas discharge. Because of the small divergence of the masses of the elements from exactly integral values, narrow "doublets" are formed when a multiply charged heavy atom is brought into approximate coincidence with a lighter atom having a smaller charge in the ratio of the masses. If the atomic mass (oxygen 16 = 16.000) of one type of atoms is $I_1(1+f_1)$ where f_1 is the packing fraction, and I_1 an integer, and that of the other is $I_2(1+f_2)$, and if the charge on the first is n_1e and that on the second n_2e, then the two atoms appear on the plate as though they were singly charged atoms of masses $(I_1/n_1)(1+f_1)$ and $(I_2/n_2)(1+f_2)$. We pick cases where $I_1/n_1=I_2/n_2=m$. Then a doublet appears with the mass difference $m(f_2-f_1)$ and from this, f_2-f_1 may be deduced. The same relation is found when we allow for the mass decrease of the ions due to the loss of n_1 electrons from the first and n_2 from the second type of atoms. To calculate the mass difference from the observed spacing on the plate, we must know the separation due to a known mass difference. The accuracy with which this mass scale need be found is usually small. In this paper we wish the error due to the mass scale to be less than 0.1×10^{-4} m, in measuring a mass difference $(f_2-f_1)m$. In nearly all cases of the doublets measured (see Table II), this latter mass difference is less than 10×10^{-4} m. The maximum permissible error due to the mass scale is thus one percent or more of the measured difference. The accuracy of the mass scale need not then be greater than one percent. This large tolerance makes it permissible to assume integral spacing between isotopes of the heavy elements for the purpose of calibration. Direct measurement of the mass difference between successive isotopes has been carried out as yet only for the lighter elements, and for bromine for which Aston determined a difference of 1.9983 mass units,[9] with a possible error of 0.0015. The divergence from 2.000 is thus only of 0.08 percent of the mass difference, and the difference in the packing fractions is only 0.04×10^{-4}. Between other pairs of light isotopes, Ne(20, 22); Mg(24, 26); Si(28, 30); S(30, 32); Cl(35, 37), the mass difference differs from 2.000 by much less than one percent, and the difference in the packing fractions is less than 0.2×10^{-4}. In the series of radioactive elements where the mass differences may be accurately computed, the difference from integral spacing is always less than one percent. In cases of neutron absorption leading to a new isotope, the mass added (1.009) might possibly differ from unity by as much as 0.9 percent, but in these cases γ-ray emission is observed, resulting in a much smaller difference from unity. In the elements between mass number 100 and 200, the added mass is approximately 100.1 giving an average mass difference of 0.1 percent more than unity between successive atomic masses. The packing fraction increases on the average over this range by 0.16×10^{-4} for masses separated by two units. The small mass differences observed in this paper will be computed by assuming integral spacing between the isotopes, usually of heavy elements, used as the mass scale. The error in the mass scale required to give an error of 0.1×10^{-4} in the differences of the packing fractions will be computed in many cases, and if later observations should show an unexpected large divergence (amounting to several percent) from integral spacing in any case used, the results reported can be readily corrected.

The theoretical connection between mass and distance on the plate is given by the proportionality of the radius of curvature in the magnetic field to the square root of the mass of the ion. That is $M^{\frac{1}{2}}=a+cx$ where x is the distance measured on the plate and a and c are constants. From the masses used to give the mass scale, c is computed and the unknown mass M at x is then found from $M^{\frac{1}{2}}-(M_1)^{\frac{1}{2}}=c(x-x_1)$. The accuracy of this relation between mass and position on the plate was tested very carefully with several photographs of the series of molyb-

[9] F. W Aston, Nature **137**, 357 (1936).

denum isotopes 92 to 100 at different positions, and no deviation could be found as large as the experimental error. In case the masses used to give the scale are two units apart, c may be found from $((M+2)^{\frac{1}{2}}-M^{\frac{1}{2}})=c(x'-x)$. As the packing fractions for the masses used are always less than 10^{-3}, we may replace this by $(I+2)^{\frac{1}{2}}-I^{\frac{1}{2}}=c(x'-x)$, and determine c with more than the one percent accuracy desired. The small separation x_2-x_1 between the components of a doublet then gives the difference in the packing fractions by the relation

$$c(x_2-x_1)=m^{\frac{1}{2}}(1+\tfrac{1}{2}f_2)-m^{\frac{1}{2}}(1+\tfrac{1}{2}f_1)=\tfrac{1}{2}m^{\frac{1}{2}}(f_2-f_1).$$

In cases of "bracketing" two isotopes of one element with masses $ni_1(1+f_1)$ and $ni_2(1+f_2)$ with n charges give lines at the masses $i_1(1+f_1)$ and $i_2(1+f_2)$ on either side of an isotope of another element at $i(1+f)$. As we can make only two accurate independent measurements x_2-x_1 and $x-x_1$, it is not possible to determine the three f's involved. However if we calculate

$$a=(x-x_1)/(x_2-x_1)[i_2^{\frac{1}{2}}-i_1^{\frac{1}{2}}]$$

and compute $\Delta M=[i_1^{\frac{1}{2}}+a]^2-i$, we may easily show that

$$\frac{\Delta M}{i}=f-\frac{i^{\frac{1}{2}}-i_1^{\frac{1}{2}}}{i_2^{\frac{1}{2}}-i_1^{\frac{1}{2}}}f_2-\frac{i_2^{\frac{1}{2}}-i^{\frac{1}{2}}}{i_2^{\frac{1}{2}}-i_1^{\frac{1}{2}}}f_1 \qquad (1)$$

to an accuracy much greater than that attained in the measurements.[10] In most of the cases discussed in this paper $i_2^{\frac{1}{2}}-i^{\frac{1}{2}}$ is very nearly equal to $i^{\frac{1}{2}}-i_1^{\frac{1}{2}}$ so that the value of $\Delta M/i$ as computed is $f-\frac{1}{2}(f_1+f_2)$, that is the difference between the packing fraction f of the one element and the arithmetic mean of the fractions for the two isotopes of the other. As discussed above, it is unlikely that the packing fractions f_1 and f_2 of two isotopes differing by two units should differ by more than 0.2×10^{-4}.

[10] From the relations above $i^{\frac{1}{2}}=cy(1-\frac{1}{2}f)$ where $y=x+a/c$ with similar expressions for $i_1^{\frac{1}{2}}$ and $i_2^{\frac{1}{2}}$. Substituting these in the expression for a, we find

$$[i_1^{\frac{1}{2}}+a]^2=i+i^{\frac{1}{2}}\left(f-\frac{f_2y_2-f_1y_1}{y_2-y_1}\right)+i_1^{\frac{1}{2}}(f_2-f_1)\frac{y_2}{y_2-y_1}$$

neglecting a^2. Thus

$$\frac{\Delta M}{i}=f-\frac{y-y_1}{y_2-y_1}\cdot\frac{y_2}{y}f_2-\frac{y_2-y}{y_2-y_1}\cdot\frac{y_1}{y}\cdot f_1$$

giving relation (1) as a sufficient approximation by the substitution of $i^{\frac{1}{2}}$ for y.

Technique of Mass Comparisons

It has been emphasized by Aston that the reliability of the measurements of doublets on the photographic plate is much increased when the doublets are of equal intensity. This is particularly true if the lines to be measured are not perfectly symmetrical or are curved. Some of the difficulties of mass spectroscopy are similar to those met with in the measurement of optical spectrum lines. The theoretical resolving power of the mass spectrograph may however be reduced by a new series of experimental troubles not met with in optical spectroscopy. The electric and magnetic fields may change slightly during an exposure giving rise to unsymmetrically broadened lines. In this case the centers of lines of different intensities may appear displaced by various amounts. For this reason there is a great advantage in a source with which exposures may be made in a few seconds. Aston has noticed that comparisons of molecule ions and atom ions are often unsatisfactory. If a source is intermittent or periodic it is possible that the ions to be compared are formed most strongly at different parts of the cycle. A periodic alteration of gas pressure may accompany a periodic gas discharge and may lead to one ion appearing as a slightly broadened line while another formed during an earlier part of the discharge may be sharper. Possibly the passage of the ions into the electric field may give rise to a space charge or surface polarization which reduces the field acting on the ions by various amounts at different times during the discharge. In the present experiments, it was noticed that lines of unequal sharpness were often obtained in comparisons of a metal ion and an ion formed from the gas in the tube, such as copper with oxygen or iron with nitrogen. With sparks between two metals of high melting points, the lines appeared equally sharp and even in many cases of metals with great differences in their boiling points, such as platinum and lead, no difference in sharpness was observed. In these cases both ions probably pass the field simultaneously immediately after the spark has passed. A further cause of error may be the formation of insulating layers on metal surfaces bombarded by the rays[11]

[11] R. Lariviere Stewart, Phys. Rev. **45**, 488–90 (1934).

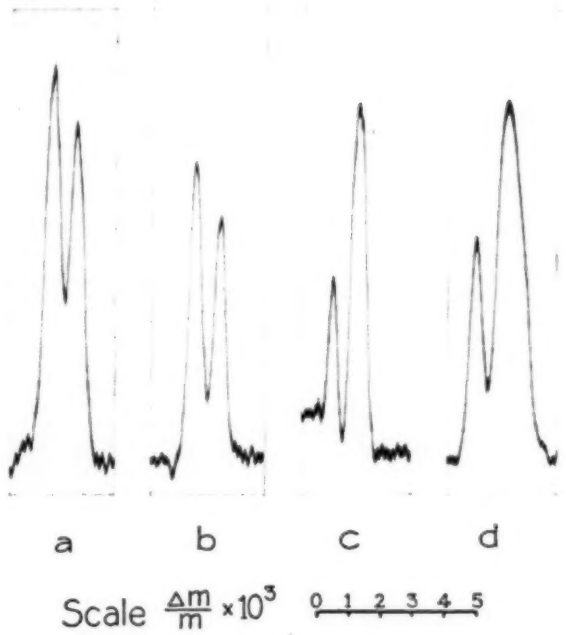

FIG. 1. Microphotometer traces of doublets. (a) Titanium-oxygen at mass 16, (b) rhodium-lead at mass 103, (c) molybdenum-platinum at mass 98, (d) tin-thorium at mass 116. The scale shows the displacements corresponding to mass changes of 1, 2, 3, 4, and 5 parts in 1000.

or the occurrence of insulating dust particles on the surfaces.[12] The formation of insulating patches on metallic surfaces is specially liable to occur when hydrocarbons are present.[11] These surfaces or particles become charged and may cause spurious deflections and curved or sloping lines.[13] Provided both ions pass the electric field and charged surfaces simultaneously and follow almost identical paths it is likely that any variation in the spacing due to surface charges is very small. This is one reason for preferring close doublets to brackets which are more widely spaced.

A difficulty common to mass spectroscopy and to optical spectroscopy is the actual measurement of the separation of the two lines forming a close doublet on the photographic plate. A discussion of the errors that may occur in measuring doublets in the solar spectrum has been given by St. John and Ware.[14] On page 21 of that paper, photometer traces are given of lines reproduced on the plate facing page 20, and errors of 7 to 10 percent were made by trained observers in visual measurements of the separations. However, the doublets used in the present measurements were in nearly all cases much sharper and more completely separated than those shown in St. John and Ware's paper. Microphotometer traces of most of the doublets reported in this paper were made on process films with a Moll recording microphotometer. On the same trace was recorded for calibration the light transmitted through a fifth millimeter scale carefully ruled on a silvered glass plate. The separations computed from the traces were compared with the direct measurements. Examples of photometer traces of doublets are given in Fig. 1, (a) Ti^{+3}-O^{+}, (b) Rh^{+}-Pb^{+2}, (c) Mo^{+}-Pt^{+2} (98), (d) Sn^{+}-Th^{+2}, the larger mass being to the right. The displacements corresponding to a mass change of 1 in 1000 are indicated on the mass scale. The last trace shows a broadening of the over-exposed thorium line. Between positions of half the maximum intensity, the widths of some lines correspond to mass changes as small as 1 in 2500.

The direct visual measurements were first made with a Geneva measuring instrument using two fibers in the eyepiece. The magnification was adjusted so that the part of the line included between the two fibers corresponded roughly to the center half or free portion of the line as recorded on the trace. In this way any residual intensity between the lines would not be expected to affect the setting on one line. All the measurements in this paper were later repeated with a Gaertner measuring instrument, which was tested for absence of error by an accurate scale having twenty rulings to the millimeter. In the eyepiece, a circular opaque diaphragm made of a silvered piece of glass was often used. It had a clear sector across the top and a narrow vertical space 0.2 mm wide, in which the magnified image of the central part of the line appeared. In this way, any lack of symmetry in the field of view due to the second component of the doublet was avoided. The doublets to be measured were usually selected from a larger number;

[12] A. J. Dempster, Proc. Am. Phil. Soc. **76**, 492 (1936).

[13] F. W. Aston (Nature **138**, 1094 (1936)) points out that his measurement of the CH_4-O doublet gives a value that differs from Bainbridge and Jordan's value by much more than the experimental error. In the reproduction of the doublet given in the Phys. Rev. **50**, 287 (1936), Fig. 9, it is apparent that the two lines forming the doublet are not parallel.

[14] Charles E. St. John and L. W. Ware, "Accuracy in Separation of Close Solar Lines," J. Astr. **44**, 17 (1916).

any doublets with unsymmetrical lines, due to variations in the electric or magnetic field, being discarded. In many cases, doublets with overexposed lines, which may conceal a small dissymmetry, were also discarded. Most of the lines photographed were, however, remarkably straight and symmetrical. With the best lines settings could be reproduced with a probable error of 0.001 mm. This corresponds to a probable error of 0.1×10^{-4} in the packing fraction. However, in most cases the error was greater than this. A slight broadening became noticeable if the pressure in the analyzing chamber was above 2×10^{-5} mm of mercury. The pressure in the spark chamber was usually several times as high due to evolution of gas from the electrodes.

Experimental Results

The masses of many of the light elements have recently been compared with the mass of the lightest oxygen isotope (16.000) with a high degree of accuracy.[15] Also by observing the energy set free in nuclear transformations, the masses of most of the nuclei up to argon may be found with very great accuracy.[16] Among the mass comparisons reported in this paper, there are only a few which have been made directly with these accurately known masses (Ti, Fe, Cu, Pd, Ag). A second group of comparisons have been made, with these latter as secondary standards (Au, Pt, Zn, Ga, Pb, Bi, Tl). A third group includes comparisons of masses of elements neither of which has as yet been compared with known masses. In these cases, the measurements give the difference between the packing fractions of the two elements. As the investigation proceeds, it is expected that many more secondary standards will be established and that it will be possible to refer more and more of these masses back to oxygen as the primary standard. This last group, which includes many of the most accurate mass comparisons, is, however, of immediate interest in connection with the packing fraction curve, as the measurements give a series of differences between pairs of points on this curve. The packing fraction curve that is in best agreement with these observations will be discussed in a later paper. All of the mass comparisons reported in this paper are new. The comparisons are all between atomic masses, since molecules occur very rarely in the spark sources.

Oxygen-Titanium (48)

Triply-charged titanium ions are produced by a spark between titanium electrodes, and the strongest isotope at 48 forms a doublet with singly-charged oxygen atoms which come either from the residual gas or from a layer of titanium oxide on the metal. Nine doublets with exposure times of 3 to 8 seconds gave an average mass difference of 0.01155 ± 0.00015. This gives a packing fraction for titanium of $(-7.22\pm0.1)\times10^{-4}$ and an atomic mass of 47.9651 ± 0.0005. The nine doublets were picked as the best out of a total of nineteen, ten were considered inferior because overexposed, diffuse or very unequal in intensity. Almost the same mass difference however was given by the rejected doublets, as the average of the whole nineteen gave a packing fraction of $(7.09\pm0.2)\times10^{-4}$ only slightly different from the value given by the nine best doublets. In this paper, the errors will be estimated as "probable errors," that is, a value of $x\pm r$ means that the probability of the true value lying in the range $x-r$ to $x+r$ is one-half. A recent paper by R. T. Birge[17] emphasizes the advantages of this method of indicating the uncertainty in a measurement, and points out the relation of this to other methods of estimating errors.

The mass scale used in evaluating the mass difference was the spacing of the titanium isotopes 47, 48, 49 which was assumed as integral. As discussed above, no error as large as 0.1×10^{-4} would occur in the packing fraction in this case unless the mass differences between these isotopes should differ from unity by more than two percent.

Carbon-Titanium

Doublets were found at mass 12 with a spark between titanium and gold electrodes. These are almost certainly due to quadruply-charged

[15] F. W. Aston, Nature **137**, 396, 613 (1936); **139**, 922 (1937); **140**, 149 (1937). Bainbridge and Jordan, Phys. Rev. **51**, 384 (1937).

[16] E. Pollard and E. J. Brasefield, Phys. Rev. **51**, 8 (1937). M. S. Livingston and H. A. Bethe, Rev. Mod. Phys. **9**, 373 (1937).

[17] R. T. Birge, Phys. Rev. **52**, 241 (1937).

titanium ions and singly-charged carbon. The carbon is probably an impurity in the titanium although it could also come from the wax used to seal the chamber. Four doublets with exposures of one to one and one-half minutes gave a difference of the packing fractions of carbon and titanium of $(9.8\pm0.4)\times10^{-4}$. If the packing fraction of carbon is taken[18] as 2.96×10^{-4}, that of titanium is -6.84×10^{-4}, in satisfactory agreement with the value determined from the oxygen comparisons.

Nitrogen-Iron

With a spark between a titanium and a cast iron electrode, doublets were formed at mass 14, which are almost certainly due to nitrogen and quadruply-charged iron atoms of mass 56. Eight doublets with exposures of 10 to 20 seconds were measured and gave a mass difference of 0.017 using as mass scale the spacing between the titanium isotopes assumed as integral. This gives a difference of 12.3×10^{-4} between the packing fractions of nitrogen and of iron. If the packing fraction of nitrogen is taken as 5.2×10^{-4}, that of iron is -7.1×10^{-4}. The large estimated error was ±0.4, as the doublets were unequal in intensity and not suitable for measurements of the highest precision.

Oxygen-Copper

Quadruply-charged copper ions appear approximately at mass numbers 15.75 and 16.25, nearly equally spaced on either side of the oxygen isotope at 16. As explained above from the positions of the two copper isotopes with masses 15.75 $(1+f_1)$ and 16.25 $(1+f_2)$, the arithmetic mean of the two packing fractions may be calculated. The difference given by three photographs with exposures of 2 minutes for the quantity ΔM was 0.011 mass units, using as mass scale the distance between the lines due to the two copper isotopes (assumed to differ by two units in mass). Thus the mean of the packing fractions of the copper isotopes, $\frac{1}{2}(f_1+f_2)$, is -6.90×10^{-4}. As the lines were not perfectly sharp and only three of the best were used, a relatively large error of $\pm0.2\times10^{-4}$ is estimated. A divergence from integral spacing in the copper isotopes amounting to 1.3 percent would be required before the mass scale would introduce an error amounting to 0.1×10^{-4} in the packing fraction.

Aluminum-Silver

Quadruply-charged ions of the silver isotopes at 26.75 and 27.25 may be compared with aluminum ions at mass 27. It was difficult to get suitable lines for comparison as the singly-charged aluminum ions are generally much stronger than the silver ions. This difficulty was overcome by evaporating in vacuum a thin coating of aluminum on to a sheet of silver, and making an electrode by rolling up the sheet into a small pencil. For some of the photographs, the second electrode was palladium, and for others an alloy of silver with ten percent of zinc. The average mass difference ΔM for seven photographs with exposure times of 15 to 20 seconds was 0.0032, giving a difference between the packing fraction of aluminium and the mean of the fractions for the silver isotopes of 1.18×10^{-4} with an estimated probable error of 0.2×10^{-4}. A scale error of 0.1×10^{-4} would result from a difference from integral spacing in the silver isotopes used as the mass scale of eight percent. Aston has recently given -3.4×10^{-4} as a provisional value for the packing fraction of aluminum. It is probable however that the packing fraction for aluminum is slightly greater than Aston's provisional value. From the maximum energy of the electrons emitted by Al^{28}, and the mass of silicon, the mass of Al^{28} may be calculated,[19] and from this the mass of Al^{27} may be computed from the energy of the protons set free by deuteron bombardment.[20] The mass as computed by Livingston and Bethe[21] is 26.9899 ±0.0008 giving a packing fraction equal to $(3.75\pm0.3)\times10^{-4}$. With this value the arithmetic mean of the packing fractions of the two silver isotopes is $(-4.93\pm0.5)\times10^{-4}$.

Several photographs were made with one electrode a copper-aluminum alloy and the other a copper-beryllium alloy, and strong doublets were found at atomic mass 9 between triply-

[18] F. W. Aston, Nature **139**, 922 (1937).

[19] Cork, Richardson and Curie, Phys. Rev. **49**, 208 (1936).
[20] McMillan and Lawrence, Phys. Rev. **47**, 343 (1935).
[21] Livingston and Bethe, Rev. Mod. Phys. **9**, 373 (1937).

charged aluminum ions and singly-charged beryllium atoms. Unfortunately, no reliable measurements could be made due to a lack of a suitable mass scale for the large separation at this small mass. However, it may be possible to superimpose on these doublets lines from known masses to serve as a scale and thus give an independent determination of the mass of aluminum.

Copper-Platinum

With one electrode made of platinum-iridium alloy and the other of copper-beryllium alloy, triply-charged platinum and iridium ions appeared at the masses 64.33···, 64.66···, 65, 65.33···, and 66. The triply-charged atoms at 65 formed a doublet with the singly-charged atoms of the heavier copper isotope. Five good doublets with exposure times of 20 to 60 seconds gave a mass difference of 0.058 with the difference between the lines at 64.66··· and 65.33··· as mass scale. The difference in the packing fraction of copper (65) and platinum (195) is then $(8.93\pm0.1)\times10^{-4}$. The mean of the fraction for the two copper isotopes has been determined as $(-6.9\pm0.2)\times10^{-4}$. It is very probable as discussed above that the two fractions differ by less than 0.2×10^{-4}. If the packing fraction for copper (65) is taken as $(-6.9\pm0.2)\times10^{-4}$, that for platinum 195 is $(2.03\pm0.3)\times10^{-4}$.

Copper-Gold

Triply-charged gold atoms from a spark between an 18-carat gold electrode and a platinum-iridium electrode appeared at the mass 65.66··· and were compared with the singly-charged copper atoms at 65 present as an impurity in the gold. The separation between the two copper isotopes was used as the mass scale. It was found that the gold line was displaced from the position it should have occupied if its packing fraction had been the "mean" of the fractions for the copper isotopes. The average of ten photographs with exposure times of one to two minutes gave a value of 0.058 mass units for ΔM. This gives a difference of $(8.90\pm0.2)\times10^{-4}$ between the gold packing fraction and the "mean" of the fractions for the two copper isotopes. The "mean" in this case, as given by (1) above, is quite different from the arithmetic mean. However, if the packing fractions of the two copper isotopes differ by less than 0.2×10^{-4}, no appreciable error is made in using the value previously determined for the arithmetic mean. If this latter is taken as $(-6.9\pm0.2)\times10^{-4}$, the packing fraction of gold is 2.0×10^{-4} with an estimated error of 0.4×10^{-4}. The gold line was much weaker than the copper lines, hence the large estimated error.

Titanium-Gold

With a spark between a gold electrode and a titanium electrode, quadruply-charged gold ions at mass 49.25 appeared between the two titanium isotopes at 49 and 50. Ten photographs made with 30 to 100 seconds exposure were measured and gave a value for ΔM of 0.048 mass units. This gives a difference in packing fractions of $(9.36\pm0.2)\times10^{-4}$ between that for gold and the average given by (1) for the titanium isotopes. If the packing fraction for gold is taken as 2.0×10^{-4}, as suggested by the comparison with copper, the average for the two titanium isotopes at 49 and 50 is -7.36×10^{-4}. This is in close agreement with the directly observed packing fraction -7.22 for the titanium isotope at mass 48.

In addition to the mass comparisons in which the atomic mass of one of the masses has been determined in terms of oxygen, a great many comparisons have been made between masses, neither of which has as yet been referred to the oxygen standard. These comparisons are of significance since it is probable that the reference to oxygen will become possible for one or other of the masses. Also the difference in the packing fractions of two elements allows us to make comparisons directly with any assumed packing fraction curve and to detect any unexpected irregularity in it.

Tin-Thorium

With a spark between a thorium electrode and one of tin, doubly-charged thorium atoms form a doublet[22] with the singly-charged tin atoms at

[22] A reproduction of a thorium and a uranium doublet is given in Nature **138**, 120 (1936), also in the Proc. Am. Phil. Soc. **76**, 497 (1936).

mass 116. Sixteen doublets with exposures of 7 to 30 seconds were measured using the separation of the tin isotopes at 116 and 118 to fix the mass scale. An error of one percent in the mass scale leads to an error of less than 0.1×10^{-4} in the difference of the packing fractions. A difference of 0.120 mass units was found giving a difference in the packing fractions of 10.0×10^{-4}. Seven of the sixteen doublets were, however, sharper than the others, and the average value given by these seven was $(10.12\pm0.1)\ 10^{-4}$, and is considered more probable than the average of the whole group.

Uranium-Tin

With a spark between an electrode of uranium metal and a tin electrode, a doublet[22] at mass 119 is formed by the singly-charged tin isotope and doubly-charged ions of the uranium isotope at 238. The best results were obtained after the tin had been worn completely down to the iron holder, so that the spark played between the uranium and the iron, a little tin apparently evaporating into the spark from the hole in the iron where the end of the tin electrode remained. The mass scale was taken from the separation of the two tin isotopes at 118 and 120 assumed as two mass units. The five best doublets made with exposures of one to two minutes gave a mass difference of 0.124 units, giving for the difference in the packing fractions of the tin isotope at 119 and uranium a value of $(10.41\pm0.1)\ 10^{-4}$. The position of the uranium line was also compared by the bracket method with the computed position it should have had if its packing fraction had been the average of the fractions for the two tin isotopes at 118 and 120. The difference between the average and the packing fraction of uranium was found from five photographs to be $(10.53\pm0.1)\times10^{-4}$.

Actino-Uranium-Tin

On several photographs the doubly-charged faint actinium isotope at 235, actino-uranium, appeared between the tin isotopes at 117 and 118. The mass difference between this line and a line corresponding to a mass midway between the tin isotopes was 0.123, giving a difference in packing fraction for actino-uranium and the mean of the packing fractions for the two tin isotopes of $(10.5\pm0.3)\times10^{-4}$.

Tungsten-Zirconium

With a spark between a tungsten and a zirconium electrode, doublets were obtained with exposures of one to two and a half minutes between the doubly-charged tungsten atoms of mass 182 and 184 and the singly-charged zirconium atoms at 91 and 92. Using the distance between the zirconium masses as the mass scale, three doublets at 91 gave a mass difference of 0.0714 units. This gives a difference between the packing fraction of zirconium 91 and tungsten 182 of $(7.85\pm0.2)\times10^{-4}$. Three doublets at 92 gave a mass difference of 0.0740, and a difference in the packing fractions of zirconium 92 and tungsten 184 of $(8.05\pm0.2)\ 10^{-4}$.

Platinum-Molybdenum

With a spark between a molybdenum electrode and one made of platinum-iridium alloy, doublets were obtained with one minute exposures at atomic masses 96, 97 and 98 between singly-charged molybdenum ions and doubly-charged platinum atoms of mass 192, 194 and 196. The doublets at 96 were not satisfactory. Four were measured, using the two iridium lines as mass scale, and the best two gave $(8.3\pm0.4)\times10^{-4}$ as the difference in packing fractions between molybdenum 96 and platinum 192. At mass 97, three fairly good doublets gave $(7.7\pm0.2)\times10^{-4}$ as the difference between the packing fractions of platinum 194 and molybdenum 97. At mass 98 four doublets gave $(7.68\pm0.2)\times10^{-4}$ for the difference in packing fractions of Mo 98 and Pt 196. Here the mass scale was given by the separation of the two platinum isotopes at 196 and 198.

Iridium-Molybdenum

In the photographs made with the spark between molybdenum and platinum-iridium electrodes, singly-charged molybdenum ions of mass 96 occurred between the two doubly-charged iridium isotopes[23] at 95.5 and 96.5. The measurement on nine photographs of the dis-

[22] A. J. Dempster, Nature **136**, 909 (1935).

placement of the molybdenum line from the calculated position of a mass midway between the two iridium masses gave a difference of $(7.72\pm0.2)\times10^{-4}$ between the packing fraction of molybdenum 96 and the mean of the packing fractions of the two iridium masses

On the same plates the iridium line at 95.5 was measured with respect to the two molybdenum lines at 95 and 96. The same nine photographs gave $(7.68\pm0.2)\times10^{-4}$ for the difference between the packing fraction of iridium 191, and the mean of the packing fractions of the molybdenum masses at 95 and 96.

Palladium-Lead

With a spark between a palladium electrode and a lead electrode to which a little thallium and bismuth had been added, doublets were obtained with 30 to 90 seconds exposure at mass 104 between singly-charged palladium[24] and the doubly-charged lead isotope at 208. Five of the best doublets were measured and the mass difference found to be 0.0828 mass units, taking the mass scale from the two lead isotopes at 206 and 208, and 0.0826 mass units, when the mass scale was taken from the two palladium isotopes at 104 and 105. A departure from integral spacing of the isotopes of 1.2 percent would be required before a difference as large as 0.1×10^{-4} would be produced in the packing fractions. Taking the mean of the two mass differences, we find $(7.96\pm0.15)\times10^{-4}$ as the difference between the packing fractions of palladium 104 and lead 208.

Doublets were also formed between the palladium isotope at 102 and the doubly-charged lead atoms of mass 204. Only two obtained with 15 seconds exposure were measured using the difference between the two thallium lines at 101.5 and 102.5 to give the mass scale. A difference of $(8.07\pm0.2)\times10^{-4}$ was found between the packing fraction of the two masses.

Palladium-Thallium

In several photographs made with the electrodes used in the last comparison, the palladium isotope at 102 was bracketed by the two doubly-charged thallium isotopes at 101.5 and 102.5. Two photographs with 60 seconds exposure were measured and gave a difference of $(8.03\pm0.2)\times10^{-4}$ between the packing fraction for palladium 102 and the mean of the packing fractions for the thallium isotopes.

Rhodium-Lead

With the same lead alloy electrode but with a second one of platinum-rhodium alloy (10 percent rhodium) doublets[24] were obtained at mass 103 with 20 to 40 seconds exposure between the rhodium atoms and the doubly-charged lead isotope at 206. If the distance between the masses 206 and 207 is taken as mass scale, the difference between the packing fraction of lead 206 and rhodium 103 as given by three doublets was found to be $(7.96\pm0.15)\times10^{-4}$.

Palladium-Bismuth

With the same electrodes doubly-charged bismuth ions appeared with 30 to 90 seconds exposure between the two palladium isotopes at 104 and 105. Five brackets were measured using the unit of mass between the isotopes at 104 and 105 to give the mass scale. The difference between the packing fraction of bismuth and the mean of the fractions for the two palladium isotopes was $(7.84\pm0.1)\times10^{-4}$.

Ruthenium-Platinum

With electrodes made of an alloy of platinum, gold, osmium and ruthenium, a doublet of doubly-charged platinum (198) and singly-charged ruthenium (99) was obtained with one to two minutes exposure. By using the spacing between the gold line 197 and the platinum line at 198 for the mass scale, an average mass difference for three doublets of 0.082 was found. This gives a difference between the packing fractions of platinum 198 and ruthenium 99 of $(8.26\pm0.2)\ 10^{-4}$.

Ruthenium-Osmium

With the same electrodes, a doublet was found with singly-charged ruthenium atoms at 96 and doubly-charged osmium atoms at 192. By using the osmium lines at 190 and 192 as

[24] A reproduction showing doublets at 102, 103 and 104 is given in the Proc. Am. Phil. Soc. **74**, 497 (1936).

mass scale, an average mass difference for three doublets of 0.0815 units was obtained, giving a difference between the packing fractions of ruthenium 96 and osmium 192 of $(7.9\pm0.2)\ 10^{-4}$.

Palladium-Gallium

With an alloy of lead, gallium and zinc (85 : 10 : 5) as one electrode and a palladium rod as the other, the two gallium isotopes at 69 and 71 appeared with 15 to 120 seconds exposure between the sequence of palladium isotopes at 68, 69.33···, 70, 70.66···, 72, 73.33···, that is, at two-thirds the value of the palladium masses. These lines may be attributed to palladium ions that passed the electric field with six charges and then picked up three electrons before passing the magnetic field. If the palladium isotopes at 106 and 108 are taken to give the mass scale, the gallium mass at 71 was found displaced from the computed position by an amount which gave a difference in packing fraction between the gallium 71 mass and the mean of the two palladium masses of $(1.46\pm0.2)\ 10^{-4}$. Similarly the isotope at 69 was compared with the palladium isotopes at 102 and 104 and a difference of $(1.55\pm0.2)\times10^{-4}$ was found.

In addition to the mass comparisons reported above, several provisional comparisons were made where there was a greater probable error, due to the lines not being sharp, or due to the fact that only a few doublets were obtained. They are reported here as they serve to confirm some of the other measurements and indicate comparisons that may be made with greater precision in the future.

Silver-Iron

With a spark between an iron and an eighteen carat gold electrode, doubly-charged silver atoms appeared at masses 53.5 and 54.5 bracketing the iron isotope at 54. Two photographs were measured by using the silver isotopes as mass scale. The mass difference between the iron mass and the calculated position of a mass midway between the silver masses was 0.0166 mass units. This gives a difference between the packing fraction of iron (54) and the average of the silver fractions of $(2.55\pm0.3)\times10^{-4}$. If we take the average of the silver fractions to be -4.95×10^{-4} as determined above by comparison with aluminum, we find the fraction for iron 54 to be -7.4×10^{-4}. The errors in the aluminum (0.3) and the two comparisons (0.2 and 0.3) are however so large that this value can be regarded as only approximate.

Silver-Zinc

With electrodes made from an alloy of silver (90 percent) and zinc (10 percent), triply-charged zinc ions occurred at 21.33··· and 22 close to the silver ions with five charges at 21.4 and 21.9. By using the separation of the silver ions as mass scale, the difference between the packing fraction of zinc 64 and the mean of the fractions for the silver isotopes was $(2.0\pm0.3)\ 10^{-4}$ while the difference for the zinc isotope at 66 was $(2.5\pm0.3)\ 10^{-4}$. The arithmetic mean of the fractions for the silver isotopes was determined above as $(-4.95\pm0.5)\times10^{-4}$. The "means" in the present comparisons given by (1) probably do not differ from this value by more than the estimated error. We can thus deduce an approximate value -6.9×10^{-4} for zinc 64 and -7.4×10^{-4} for zinc 66.

Osmium-Molybdenum

With a spark between an osmium and a molybdenum electrode doublets were found at masses 94, 95 and 96 between singly-charged molybdenum ions and doubly-charged osmium ions of masses 188, 190, and 192. Only one doublet was measured for each mass and the difference in the packing fractions of the three molybdenum and three osmium isotopes were found to be $(7.78\pm0.3)\ 10^{-4}$ at 94, $(7.76\pm0.3)\times10^{-4}$ at 95, and $(7.58\pm0.3)\times10^{-4}$ at 96.

Zinc-Sodium

In the comparison of triply-charged zinc atoms and silver atoms with five charges, singly-charged sodium atoms appeared on two photographs and could be compared with triply-charged zinc ions at 22.66··· and 23.33···. By using the separation of the two zinc isotopes to give the mass scale, the difference between the packing fraction

of sodium and the mean of the fractions for zinc was found to be $(4.9\pm0.5)\times10^{-4}$. If we take the packing fraction of sodium to be $(1.7\pm0.15)\times10^{-4}$ as deduced from the energy set free in the disintegration by deuterons and the mass of neon 21, then the mean of the packing fractions for zinc 68 and 70 is $(-6.6\pm0.6)\times10^{-4}$.

Nickel-Ruthenium

With an electrode made by packing a nickel tube with ruthenium powder, strong triply-charged nickel ions at mass 20 were bracketed with fainter ruthenium atoms with five charges at 19.8 and 20.2. By using the ruthenium atoms to give the mass scale, the difference between the packing fraction for the nickel isotope and the mean of the fractions for the two ruthenium isotopes was found to be $(1.1\pm0.3)\times10^{-4}$.

Potassium-Ruthenium

With the same electrode doubly charged potassium ions appeared at mass 19.5. The packing fraction difference was calculated to be $(0.4\pm0.3)\times10^{-4}$.

Aluminum-Palladium

With an electrode of copper-aluminum alloy and another of palladium, quadruply charged palladium ions appeared at 26, 26.25, 26.5 and 27.5 superimposed on a strong aluminum line at 27. The palladium line which should also appear near 27 was concealed by the stronger aluminum line, and could not be resolved. By using the separation of the palladium isotopes as mass scale the difference in packing fraction was computed to be $(1.6\pm0.4)\times10^{-4}$.

Summary

A summary of the measurements reported in this paper are given in Table I and Table II. The first gives the difference in packing fractions in cases where one atomic mass is known, so that a value may be deduced for the packing fraction of the second. The values for the heavy element all lie above Aston's packing fraction curve by about 2×10^{-4}. This curve however did not claim to give the values for the heavy elements with any great accuracy. The value found for gold by the copper comparison is confirmed to a

Table I. *Differences in packing fractions. $f=(M-I)/I$ observed, and values deduced for different elements, m = mass number near which the measurement was made, n = number of photographs measured. A bar over some of the f's indicates a mean value.*

m	Ions	n	$(f_2-f_1)10^4$	Assume	Deduce	
16	O-Ti	9	-7.22 ± 0.1	O, $f_1\times10^4=0.0$	Ti(48),	$f_2\times10^4=-7.22\pm0.1$
12	C-Ti	3	$-9.8\ \pm0.4$	C, $f_1\times10^4=2.96$	Ti(48),	$f_2\times10^4=-6.8\ \pm0.4$
14	N-Fe	8	$-12.3\ \pm0.4$	N, $f_1\times10^4=5.3$	Fe(56),	$f_2\times10^4=-7.0\ \pm0.4$
16	O-Cu	3	$-6.9\ \pm0.2$	O, $f_1\times10^4=0.0$	Cu(63–.65),	$f_2\times10^4=-6.9\ \pm0.2$
27	Al-Ag	7	$-1.2\ \pm0.2$	Al, $f_1\times10^4=-3.75\pm0.3$	Ag(107–109),	$f_2\times10^4=-4.95\pm0.5$
65	Cu-Pt	5	8.93 ± 0.1	Cu, $f_1\times10^4=-6.9\ \pm0.2$	Pt(195),	$f_2\times10^4=\ 2.03\pm0.3$
65	Cu-Au	10	8.90 ± 0.2	Cu, $f_1\times10^4=-6.9\ \pm0.2$	Au(197),	$f_2\times10^4=\ 2.0\ \pm0.4$
49	Au-Ti	10	9.36 ± 0.2	Au, $f_1\times10^4=\ 2.0\ \pm0.4$	Ti(49–50),	$f_2\times10^4=-7.36\pm0.6$
54	Ag-Fe	2	2.55 ± 0.3	Ag, $f_1\times10^4=-4.95\pm0.5$	Fe(54),	$f_2\times10^4=-7.4\ \pm0.8$
21.3	Ag-Zn	5	$2.0\ \pm0.3$	Ag, $f_1\times10^4=-4.95\pm0.5$	Zn(64),	$f_2\times10^4=-6.9\ \pm0.8$
22	Ag-Zn	6	$2.5\ \pm0.3$	Ag, $f_1\times10^4=-4.95\pm0.5$	Zn(66),	$f_2\times10^4=-7.4\ \pm0.8$
23	Na-Zn	2	$4.9\ \pm0.5$	Na, $f_1\times10^4=-1.7\ \pm0.15$	Zn(68–70),	$f_2\times10^4=-6.6\ \pm0.6$

Table II. *Differences in packing fractions observed for various pairs of isotopes.*

m	Ions	n	$(f_2-f_1)10^4$	m	Ions	n	$(f_2-f_1)10^4$	m	Ions	n	$(f_2-f_1)10^4$
116	Sn-Th	7	10.14 ± 0.1	102	Pd-Pb	2	8.07 ± 0.2	94	Mo-Os	1	7.78 ± 0.3
119	Sn-U	5	10.41 ± 0.1	103	Rh-Pb	3	7.96 ± 0.15	95	Mo-Os	1	7.76 ± 0.3
91	Zr-W	3	7.85 ± 0.2	102	Pd-Tl	2	8.03 ± 0.2	96	Mo-Os	1	7.58 ± 0.3
92	Zr-W	3	8.05 ± 0.2	104.5	Pd-Bi	5	7.84 ± 0.1	19.5	K-Ru	1	$0.4\ \pm0.3$
97	Mo-Pt	3	$7.7\ \pm0.2$	96	Ru-Os	3	7.91 ± 0.2	20	Ni-Ru	1	$1.1\ \pm0.3$
98	Mo-Pt	4	7.68 ± 0.2	99	Ru-Pt	3	8.26 ± 0.2	27	Al-Pd	3	$1.6\ \pm0.3$
96	Mo-Ir	9	7.72 ± 0.2	69	Pd-Ga	7	1.29 ± 0.3	117.5	Sn-AcU	2	$10.5\ \pm0.3$
95.5	Mo-Ir	9	7.68 ± 0.2	71	Pd-Ga	7	1.37 ± 0.3	96	Mo-Pt	4	$8.3\ \pm0.3$
104	Pd-Pb	5	7.96 ± 0.15								

certain extent by the fact that it gives a value for titanium (49) which is close to the values for titanium (48) found by direct comparisons with oxygen and carbon. The values for iron 54 and 56 deduced by different methods are close together as are also the values for zinc.

In Table II mass comparisons are given between atoms for which neither mass is known accurately at the present time. As soon as further observations give a value for one of the masses, the comparison may be used to deduce the other. The values are also of immediate interest in connection with the packing fraction curve. Theoretical curves may be tested and a probable curve drawn in which the masses agree with all the comparisons in Table II as well as with the values in Table I. A discussion of this curve will be given in a later paper.

The author is indebted to Dr. A. E. Shaw for assistance in preparing the electrodes, and to Mrs. G. S. Monk for carrying out most of the computations.

JANUARY 1, 1938 PHYSICAL REVIEW VOLUME 53

The Recombination of Ions in Pure Oxygen as a Function of Pressure and Temperature

MILTON E. GARDNER
Department of Physics, University of California, Berkeley, California
(Received October 25, 1937)

All previous investigations of the coefficient of recombination in pure gases have employed the older technique which did not allow the use of an outgassed chamber and made no corrections for initial recombination, diffusion, etc. This work was undertaken in pure oxygen in order to compare the results with existing theories. Aside from the initial drop in the curves of the recombination coefficient plotted against time due to preferential and initial recombination, the value of the coefficient of recombination in oxygen was found to be constant at a given pressure over extended intervals of time. It was, accordingly, possible to obtain a definite and probably correct value for the coefficient of recombination in pure oxygen at 76 cm pressure and 25°C. This value is $\alpha=(2.08\pm0.05)\times10^{-6}$. Comparison of the variation with pressure in the range 10 cm to 76 cm pressure was approximately in good agreement with the theory of J. J. Thomson assuming the ion to have a mass of $M=64$ and a mean free path of that given by mobility measurements. The temperature variation between the limits of -78°C to $+105$°C verified the Thomson equation quite accurately using the same data concerning the ion. At the lowest temperature a deviation was observed, indicating a possible increase of ionic mass to 96. While these results are a good confirmation of the Thomson theory they cannot be reconciled with the Langevin theory, although the Langevin theory probably holds beyond 10 atmospheres. Loeb has indicated the character of the transition between the two theories. The outstanding difficulty introduced by the change in the coefficient with time, due presumably to initial recombination, which is impossible of analysis in the less pure gases of the previous workers, is now somewhat more amenable to treatment. It is shown that if one includes the retarded diffusion of the ions created within ten times the radius of the sphere of active attraction, the time intervals involved in the x-ray flash periods, and the gradual formation of ions of mass $M=64$ from the initially ionized particles which may be accelerated by x-ray irradiation, the rough theory of initial recombination given by Loeb will account for the behavior.

INTRODUCTION

WHEN equal numbers of positive and negative ions in a gas are left in a field free space far from the walls of a container they recombine at the rate,

$$dn/dt=-\alpha n^2 \qquad (1)$$

where n is the density of ions of either sign and α is the coefficient of recombination.[1] Now experiments evaluating α have shown that under varying conditions ranging from 100 atmospheres of pressure to pressures in discharge tubes the processes giving rise to an α are of diverse types.[2]

[1] L. B. Loeb, *Kinetic Theory of Gases*, second edition, pp. 583–600. J. J. Thomson, *Conduction of Electricity through Gases*, third edition, Vol. 1, pp. 20–57.

[2] W. R. Harper, Proc. Camb. Phil. Soc. **28**, (Part II) 219 (1932); I. S. Bowen and E. F. Cox, Phys. Rev. **51**, 232 (1937).

In recent years it has therefore become desirable to classify recombination processes into one of several categories in which the value of α and the mechanisms involved may be very different. In order properly to present the scope of this investigation the recombination processes will be classified as follows:

1. Electron recombination; free electrons with + ions, a relatively improbable radiative process for which $\alpha \sim 10^{-10}$. It does not occur appreciably in gases ionized by x-rays due to low ion densities but may occur in discharge tubes plasma.

2. Normal or volume recombination; + and − ions randomly distributed in space, $\alpha \sim 10^{-6}$, which is the process concerned in this investigation. It predominates with ion densities of intermediate magnitudes shortly but not immediately after ionization, at pressures of one atmosphere and below. It is governed by the theory of J. J. Thomson.

3. Initial recombination occurring where x-ray or β-ray processes result in electron attachment and negative ion formation near the + ion of the initially ionized molecule. The ions are distributed in pairs which gives a fictitiously high value of the coefficient. It is important for time intervals less than 0.1 sec. after ionization in O_2 and is quite pronounced at lower pressures and lower ion densities. It disappears as an important factor with increase in time after ionization due to diffusion. This process will be discussed in this work.

4. Columnar ionization takes place chiefly with α-particle or proton ionization in gases, where high densities of ions occur in columns. This has theoretically been analyzed successfully by Jaffé[3] and the validity of the equation has been checked.[4] It does not concern this study.

5. Preferential recombination where the electrons attach to form a − ion within the sphere of active attraction d of the parent + ion. Here d is given by $d=e^2/[(\frac{3}{2})kT]$. It occurs at higher pressures, 10 atmospheres and up in O_2 and air, and follows according to Langevin's theory. At low pressures it is unimportant except for very low ion densities. It is of great importance in cosmic-ray studies and can be avoided by use of inert gases.

Two theoretical equations for α based upon entirely different assumptions have been derived. The theoretical value of α as developed by Langevin[5] assuming the motion of the ions to be largely governed by their electrical attractions gives,

$$\alpha = 4\pi e(k_+ + k_-)\epsilon, \tag{2}$$

where e is the electronic charge, k_+ and k_- are the ionic mobilities of the positive and negative ions respectively, and ϵ is a correction factor less than unity at atmospheric pressure but approaching unity at high pressures, which cannot be theoretically computed on this theory. The Langevin theory makes α depend upon the mobility k of the ions which varies inversely with the pressure, is nearly independent of the temperature at constant density and depends largely upon the mean free path L and relatively little on the mass of the ion. The factor ϵ being unknown served merely as a correction factor to make the experimental values conform to theory and could be evaluated experimentally from Langevin's method of measurement.

The theoretical value of α as derived by J. J. Thomson[6] assumes that recombination is largely governed by the random heat motions of the ions and molecules, and gives

$$\alpha = 2^{\frac{1}{2}}\pi d^2 C\epsilon. \tag{3}$$

Here C is the root-mean-square thermal velocity of the ions and $d=e^2/[(\frac{3}{2})kT]$ is the distance where the potential energy of one ion in the field of the other is equal to the kinetic energy of thermal agitation of the ions and molecules of the gas. The probability ϵ that recombination will occur after the ions have approached to within a critical distance d where active attraction sets in was derived by Thomson as

$$\epsilon = 2w - w^2, \tag{4}$$

where $$w = 1 - 2[1 - e^{-x}(x+1)]/x^2, \tag{5}$$

$x=2d/L$, and L is the mean free path of the ions.

[3] G. Jaffé, Ann. d. Physik **42**, 303 (1913).
[4] J. Schemel, Physik. Zeits. **1**, 977 (1929); **30**, 849 (1929); **85**, 137 (1928).
[5] L. B. Loeb, *Kinetic Theory of Gases*, first edition, pp. 479–483. P. Langevin, Ann. de Chim. et Phys. **28**, 433 (1903).
[6] L. B. Loeb, *Kinetic Theory of Gases*, second edition, pp. 592–598. J. J. Thomson, *Conduction of Electricity through Gases*, third edition, Vol. 1, pp. 40–47.

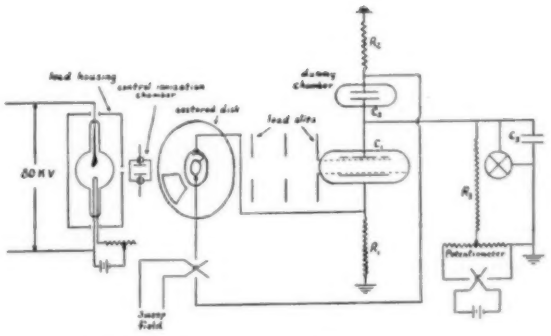

FIG. 1. Arrangement of apparatus.

The value of α as derived by Thomson depends not only upon the pressure and temperature at constant density but it is also primarily a function of the mass M of the ion. The equation as derived by Thomson, after inserting known constants, becomes,

$$\alpha = 1.90 \times 10^{-5} (273/T)^{\frac{1}{2}} (1/M)^{\frac{1}{2}} \epsilon, \qquad (6)$$

where ϵ is a function of x and

$$x = 0.810 (273/T)^{2} (P/760)(La/L) \qquad (7)$$

the factor La/L being the ratio of the mean free path of molecules in air at N.T.P. (about 1×10^{-5} cm) to the mean free path of the ions in the gas at N.T.P. This ϵ is not logically applicable to the Langevin theory although Richardson derived it for that purpose.

Several measurements in the past have been made of the recombination of ions as a function of pressure and temperature for different gases, but there is a considerable amount of discrepancy in the results obtained by the different investigators.[7] This discrepancy can be attributed to the fact that the experiments were not performed under comparable conditions. The investigators did not all work in the same region of ion age, they used different types of ionizing agents, the gases employed were far from pure, they neglected diffusion and in experiments employing air blasts there was a great deal of turbulence. Heretofore no measurements of α as a function of pressure and temperature have been made employing the modern technique of thoroughly outgassing the ionization chamber prior to the introduction of carefully purified gases of a single molecular specie in which ion formation is insured before measurements begin, and where initial recombination is eliminated.

APPARATUS AND EXPERIMENTAL PROCEDURE

The apparatus and procedure were essentially the same as those employed by Marshall[8] and Luhr[9] except for some important modifications. The essential features of the apparatus are shown in Fig. 1. First among the modifications was an ionization chamber which was placed in the beam of x-rays so that the radiation could be observed and maintained constant. To compensate for the charge induced on the electrometer system by the sweep field, a dummy chamber was employed so that a potential of opposite sign could be applied to the lower plate of this chamber. By adjusting $R_2/R_1 = C_1/C_2$ the induced charges canceled. Instead of having all metal chambers as in the earlier work, the recombination chambers were made of glass.

Two recombination chambers were used, one having an ionized volume of 190 cm³ and one an ionized volume of 700 cm³. The chambers consisted of rectangular monel metal electrodes sealed inside of Pyrex glass tubes. The lower plate was connected through a resistance R_1 to ground and to a brush in contact with the commutator. The upper electrode was connected to a capacity and a Compton electrometer. Surrounding the upper electrode was a wide guard ring directly connected to ground. Mid-potential vanes, not shown in the figure, were also installed to maintain the lines of force straight from the lower plate to the collecting electrode, and were connected to appropriate points along R. The course of the fields involved was tested electrolytically on cross-sectional models. Electrostatic shielding was accomplished by surrounding the metal electrodes with a cylindrical screen made of monel metal which fitted closely to the glass inside the tube. In the smaller chamber the ends of the screen were

[7] P. Langevin, Comptes rendus **87**, 177 (1902); R. J. McClung, Phil. Mag. **3**, 283 (1902); L. L. Hendren, Phys. Rev. **21**, 314 (1905); H. Thirkill, Proc. Roy. Soc. **A88**, 590 (1913); H. A. Erickson, Phys. Rev. **27**, 473 (1908); H. A. Erickson, Phil. Mag. **18**, 328 (1909); H. A. Erickson, Phil. Mag. **23**, 747 (1912); H. Philips, Proc. Roy. Soc. **A83**, 246 (1910).

[8] L. C. Marshall, Phys. Rev. **34**, 618 (1929).

[9] O. Luhr, Phys. Rev. **35**, 1394 (1930); O. Luhr, Phys. Rev. **36**, 24 (1930); O. Luhr and N. E. Bradbury, Phys. Rev. **37**, 998 (1931).

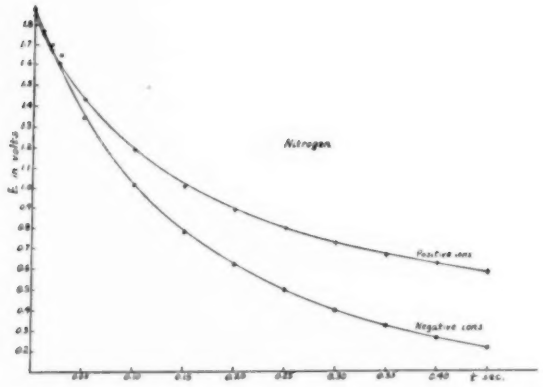

FIG. 2. Relative number of ions in the ionization chamber after a time t.

closed with thin sheet aluminum. In the later chamber the contact potentials present in the first chamber were reduced by making the electrostatic shield entirely of monel metal screen. Since the chambers were made of Pyrex glass it was possible to thoroughly outgas them at 400°C for several hours prior to the introduction of the carefully purified gas.

The oxygen employed was commercial tank oxygen which was purified in a manner similar to that used by Bradbury.[10] The oxygen which was slowly admitted to the purifying train first passed through a liquid-air trap than through a tube of heated copper oxide, then through tubes of $CaCl_2$, KOH, P_2O_5 and finally to a second liquid-air trap. At half an atmosphere of pressure liquid oxygen collected in the liquid-air traps. After pumping off the first fraction of the gas, the gas was permitted to enter the ionization chamber after passing through another liquid-air trap which separated the chamber from contamination by mercury vapor and stopcock grease from the rest of the system. The liquid oxygen was thus fractionally distilled into the recombination chamber insuring a high degree of purity. In order to make a run at atmospheric pressure, the liquid-air flask on the last trap was replaced by a flask of frozen alcohol and the oxygen allowed to distill into the tube. Below half an atmosphere pressure, a liquid-air flask could be used on the trap.

In taking measurements, the charge collected on the electrometer system was measured as a function of the age of the ions in the same manner employed by Marshall[8] and Luhr.[9] Integration of Eq. (1) gives

$$\alpha = 1/t(1/n - 1/n_0), \tag{8}$$

where t is the time during which the ions recombined after the termination of the x-ray flash, n_0 the ionic density at $t=0$ and n the ionic density after a time t.[11] Inserting the experimental constants in Eq. (8) gives,

$$\alpha = 1.59\times10^{-19}(RfV/t)(1/E - 1/E_0), \tag{9}$$

where R is the value of the high resistance, R_3, in ohms between the potentiometer and the electrometer, f the frequency of rotation of the sectored disk, V the volume of ionization and E and E_0 the potential in volts read from the potentiometer at the time $t=t$ and $t=0$, respectively.

EXPERIMENTAL RESULTS

Measurements were first made on purified nitrogen in which electrons do not attach to form negative ions but remain free.[10] The measurements were made in an attempt to determine the rate of electron recombination mentioned as process 1. With carefully purified nitrogen introduced into the outgassed glass chamber of 190 cm^3 ionized volume, electrons were found to be in profusion as evidenced by the high diffusion rate of the negative ions. A typical result obtained is shown in Fig. 2. The ordinates are the potentiometer readings in volts which are proportional to the number of ions in the chamber. The curves therefore show the proportional numbers of ions remaining in the tube after a time t. The negative ions fall off more rapidly with time than do the positive ions. Thus due to the extremely high diffusion rate of electrons, they diffused out of the space, leaving a positive space charge. The positive space charge in turn increases the rate of diffusion of the positive ions out of the chamber. Since this loss by diffusion may be comparable or even greater than the loss by recombination, this makes a calculation of α impossible. Analogous conditions obtain in

[10] N. E. Bradbury, Phys. Rev. **40**, 508 (1932).

[11] Since α is nearly constant with time in the region where data are to be used in this work this equation was used in place of the more accurate equation of Luhr, reference 9, $\alpha_t = (1/t_2 - t_1)(1/n_2 - 1/n_1)$. It gave more accurate values because of the larger differences in potentiometer readings.

the positive column of glow discharge tubes. Consequently further investigations in nitrogen were abandoned as electron recombination was obviously orders of magnitude less than diffusion losses. Attention was then turned to an accurate evaluation of α as a function of temperature and pressure in a pure molecular gas where electrons attach to form ions rapidly and where complications due to aging were a minimum, in order to test the Thomson theory.

The gas chosen was pure O_2 as Luhr[12] and Bradbury[13] have shown that the ions are relatively simple and attachment is rapid. In most of the runs with oxygen, readings were taken of both positive and negative ions and the values obtained averaged. Fig. 3 shows a series of values taken at atmospheric pressure and room temperature with the chamber of 190 cm³ ionized volume, with the sectored disk rotating at different speeds. For short time intervals there is a sharp decline in α as was observed by Marshall[8] and Luhr.[9] This is due to the nonrandom distribution of the ions shortly after being formed. This initial recombination takes place in short time intervals while the ions are diffusing to a random distribution. Since the sharp decline in α at short time intervals is due to nonrandom distribution of the ions this effect should be more pronounced at lower pressures where the ionic densities are correspondingly decreased. Fig. 4 shows a set of runs taken at half an atmosphere with the small chamber. The ionization in this case is just half that obtained at atmospheric pressure, and the

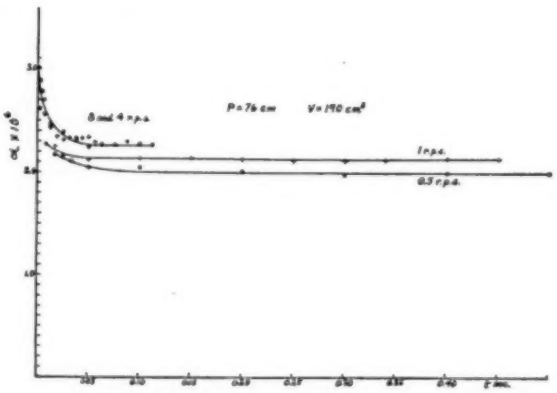

FIG. 3. Variation of the measured value of α with time. Press. 76 cm. Ion density about 10^6 ions/cm³.

[12] O. Luhr, Phys. Rev. **38**, 1730 (1931); O. Luhr, Phys. Rev. **44**, 459 (1933).
[13] N. E. Bradbury, Phys. Rev. **44**, 883 (1933).

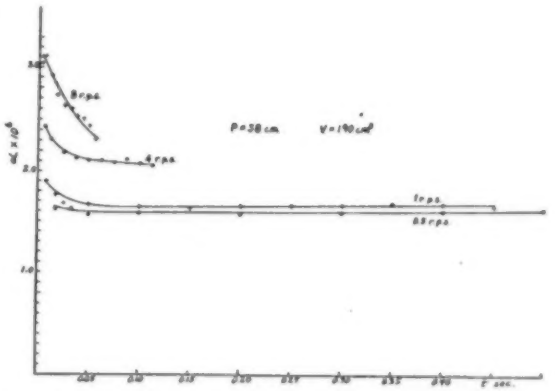

FIG. 4. Variation of the measured value of α with time. Press. 38 cm.

sharp decline in α with short time intervals is much more pronounced. In addition it will be noted that the curves taken with the sectored disk rotating at different speeds are now more widely separated, except for the curves taken at 1 and 0.5 r.p.s.

For the longer time intervals in the small chamber the value of α gradually increased with time instead of decreasing as observed by Marshall and Luhr. This small increase was probably due to loss of ions by contact potentials existing in the chamber. If this were true, then at lower pressures where the mobility and diffusion of ions has increased, this increase in α with longer time intervals should be more pronounced, which was just what was observed. With the larger chamber, constructed so as to eliminate these errors as much as possible, no such effects were observed. Instead, a very slight and continual decline of α with time was observed, which may or may not be entirely due to observational errors.

The values of α taken for the pressure variation were taken at an aging time $t=0.15$ sec. where it can be seen from the curves that the decline in α due to initial recombination has ceased and during this time the loss by diffusion to the electrodes is negligible. Fig. 5 shows the values of α as a function of pressure. The readings were all taken at room temperature which varied between 20°C and 30°C, and which for many reasons could not be maintained constant during the eight hour runs. Several readings were taken at each pressure with the small chamber and are represented by the crosses. The spread of values

shows the degree of reproducibility of the readings. The full line curves are the theoretical values of α calculated from the Thomson theoretical equation for the two temperatures shown. At 10 cm pressure the value of α is some three times what it should be according to the Thomson theory. Assuming that this high value was entirely due to loss of ions by contact potentials, calculations were made to determine what magnitude these potentials would have to be to account for this loss. This turned out to be of the order of one to two volts. Consequently the new and larger chamber was constructed to decrease this loss as much as possible. The points indicated by circles are the values obtained with the chamber of 700 cm³ ionized volume. It will be noted that the value of 10 cm pressure with the larger chamber gave a value of about half that obtained with the smaller chamber. The value of α is still 50 percent higher than the theoretical value, and the curve of α with time shows a continual decline as may be seen from Fig. 6. The values taken at 10 cm pressure with the sectored disk rotating at 4, 2, 1, and 0.5 r.p.s. are shown in Fig. 6. Here it will be noted that the decline of α with time has become much more pronounced relative to those at higher pressures (compare Figs. 3 and 4). Also the effect of ionic density on the value of α is much more pronounced, giving a value at 4 r.p.s. twice that at 2 r.p.s. Hence it was clear that at 10 cm the value at 1 r.p.s. is no longer satisfactory and since the curve at 0.5 r.p.s. is lower and the decline in α with time at 0.5 r.p.s. is practically negligible, the value of α for 0.5 r.p.s. at 10 cm should be used. From Fig. 5 it can be seen that the value of α at 10 cm pressure as taken from the values at 0.5 r.p.s. lies nearly on the Thomson theoretical curve. At 5 cm pressure, the value of α as obtained with the large chamber is some 5 times the theoretical value even at 0.5 r.p.s. However at 5 cm pressure a large proportion of the negative ions are temporarily free electrons so that loss by diffusion probably accounts for the abnormally high values. Hence free electrons again preclude a study of recombination at lower pressures.

Figures 3, 4, and 6, show that α is greatly influenced by the ionic density as pointed out by Marshall[8] and Luhr.[9] To study this, the value of α as a function of pressure was measured with the ionic density reduced to the value obtained at 5 cm pressure by filtering the x-rays through copper sheets. The value of α so obtained is given by the dotted line in Fig. 5 and is seen to be markedly increased. The effect of ionic density on the value of α will be discussed later.

The measurements of α as a function of temperature were all taken at atmospheric pressure, and with the sectored disk rotating at 1 r.p.s. In these measurements the difficulties encountered in the pressure measurements due to marked changes in ionic density as well as to the mobility and diffusion of the ions and electrons were absent. The results of the measurements of α as a function of temperature are shown in Fig. 7. The curve represents the

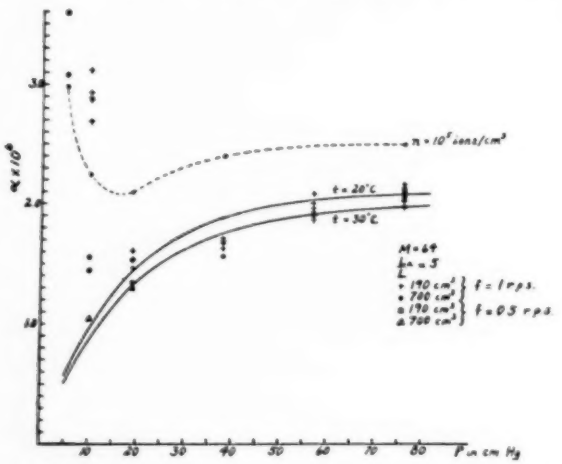

FIG. 5. Variation of α with pressure. Full lines show theoretical values of α calculated from Thomson's equation. Points about theoretical curves are for $n = 10^8$ ions per cm³.

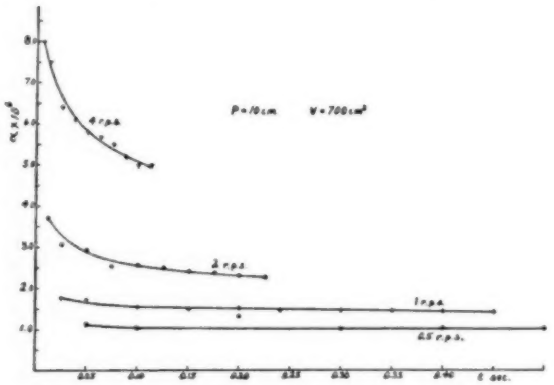

FIG. 6. Variation of α with time at different sector speeds. $P = 10$ cm. Vol. = 700 cc.

theoretical values as calculated from the Thomson equation.

The influence of impurities in the gas on α is shown by the values obtained when the tube had a slow leak of 10 microns in 12 hours when evacuated. The readings taken under these conditions are shown by the triangular points in Fig. 7. The striking change due to the minute traces of CO_2 or C_2H_5OH which diffuse into the tube filled with O_2 at atmospheric pressure for most of the time through the minute hole is obvious. These impurities also destroyed the constancy of α with time characteristic of a pure gas and the curves showed a continual decline with time. This is in beautiful accord with the observations of Marshall[8] and Luhr[9] who used metal chambers and who found that α was not a constant but continually decreased with time. On the basis of theory, α, after the initial decline, should be a constant in a pure gas. Thus the explanation of the continual decrease in α with time on the basis of impurities in Marshall's and Luhr's experiments which now appears to be confirmed.

In the present investigation the use of a glass chamber which could be thoroughly outgassed and the use of carefully purified gas showed α to be practically constant after the period of initial recombination as is seen in the curves of Figs. 3, 4, and 6. The new constant value of α found was much higher than that obtained by Luhr. It was $\alpha=(2.08\pm0.05)\times10^{-6}$ while Luhr[14] found $\alpha=1.32\times10^{-6}$. In view of the effect of impurities the character of the present curves indicates that the present value is more probably the correct value for O_2.

Discussion and Conclusion

That the Thomson theory is theoretically and experimentally the correct approach to the problem at atmospheric pressure has been shown by Loeb and Marshall[15] and later by Harper.[16] No measurements of α as a function of pressure and temperature for pressures below two atmospheres by investigators[7] of the past can be logically explained by Langevin's theory. Furthermore, the sharp decline of α at short time intervals at ordinary pressures as observed by Rümelin,[17] Plimpton,[18] Marshall,[8] and Luhr[9] can only be explained on the basis of the Thomson theory since it definitely indicates a diffusion to a more random distribution. Yet in spite of this evidence, the Langevin theory generally has been quoted as the accepted theory in texts. In a recent article by Mächler[19] and Kraus,[20] based upon high pressure measurements, ordinary atmospheric recombination is again ascribed to the Langevin process.

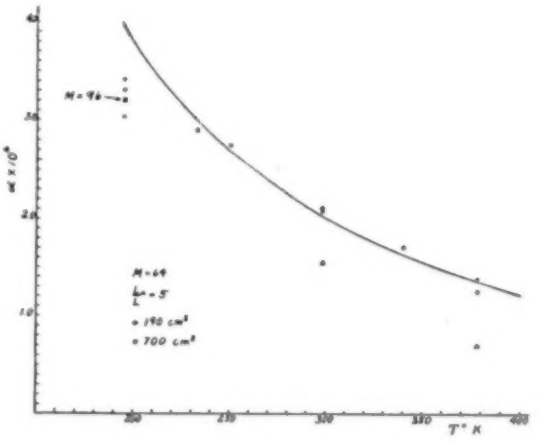

Fig. 7. Variation of α with temperature.

The theoretical curves based on Thomson's equation which are compared with the experiments reported here were calculated from Eq. (6). As can be seen, the Thomson equation has two somewhat adjustable constants, the mass M and the mean free path L of the ion. Experiments on the mobilities of ions have shown that there is, on the average, a fivefold lowering of the mean free path of the ion in comparison to the uncharged molecule due to the action of the dielectric attractive forces.[21] Thus $La/L=5$ should be used in the Thomson equation. Furthermore, mass spectrograph investigations of ion formation by Luhr[13] have shown that the mass of the ion is greater than a single molecule for high

[14] O. Luhr and N. E. Bradbury, Phys. Rev. **37**, 998 (1931).
[15] L. B. Loeb and L. C. Marshall, J. Frank. Inst. **208**, 371 (1929); L. B. Loeb, *Kinetic Theory of Gases*, second edition, pp. 587–591.
[16] W. R. Harper, Proc. Camb. Phil. Soc. **28** (Part II), 219 (1932).
[17] G. Rümelin, Ann. d. Physik **43**, 821 (1914).
[18] S. J. Plimpton, Phil. Mag. **25**, 65 (1913).
[19] W. Mächler, Zeits. f. Physik **104**, 1 (1936).
[20] P. Kraus, Ann. d. Physik **29**, 449 (1937).
[21] L. B. Loeb, *Kinetic Theory of Gases*, second edition, pp. 567–568.

pressures. It was therefore assumed that the ionic mass M is 64, that is, that the O_2^+ ion after 10^{-2} sec. consisted of two molecules. This is consistent with aging experiments. The curves of Figs. 5 and 7 were calculated using these values. Other combinations of M and L were tried but none gave as good agreement with experimental results as the values given above. It is seen that the agreement obtained for the experimental and computed values is quite good. Better agreement with the variation in pressure could not be expected due to the changes in ionic density and the mobility of the ions with decrease in pressure. The temperature variation is in excellent accord with the theory except at the lowest temperature where the deviation is greater than can be attributed to experimental error. Since at this lower temperature oxygen is not far from its critical temperature it is possible that polymers are being formed. The theoretical value of α was therefore calculated for this temperature on the assumption that the mass of the ion $M=96$, that is, the ion then consists of a group of three molecules. The point marked by the square, Fig. 7, shows the result of this calculation. Thus it is possible that the mass of the ion is increasing at these lower temperatures.

The measurement of α made in pure oxygen as a function of pressure and temperature reported here are a good confirmation of the Thomson theory and are absolutely incompatible with the Langevin theory. The numerical and experimental agreement leaves no doubt as to the applicability of the Thomson theory for O_2 in this region of measurements. The assumptions and approximations made in the deduction of the theory permit of no closer agreement than observed.

That the Langevin equation might be valid for the high pressure was already recognized by Thomson.[22] On the Thomson theory the ions will in general diffuse through the gas until they approach to within a distance d where active electrical attraction tends to bring the ions together. But if the ions are initially formed closely enough to each other (within a distance d), as they will be at high pressure by rapid electron attachment, the electrical attrac-

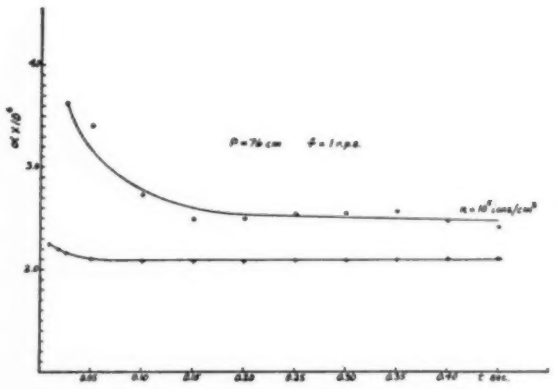

FIG. 8. Variation of α with time. Lower curve for ion density ten times that for upper curve.

tions of the ions will largely govern their motion, i.e. preferential recombination will occur. Thus for high pressures the assumptions underlying the Langevin theory become valid. Loeb[23] has shown that the transition from low pressures to high pressures can be given by an equation of the form

$$\alpha=\alpha_T f+\alpha_L(1-f), \tag{10}$$

where α_T is the Thomson value and α_L is the Langevin value of the recombination coefficient, and f is the fraction of negative ions formed within a distance d of the positive ion. The fraction f can be calculated from the rate of attachment of the liberated electrons to form negative ions and the rate of diffusion of the electrons from the parent atom before attachment takes place. This coefficient of diffusion demanded by theory as applied to experiments is surprisingly low.

The effect of ionic density on the value of α is shown in Figs. 3, 4, 5, and 6. Fig. 8 shows the apparently higher value of α obtained at atmospheric pressure when the ionic density was reduced to approximately one-tenth the value of that previously obtained at atmospheric pressure as represented by the lower curve. Curves of α as a function of time taken with shorter x-ray exposures and lower pressures, show that longer values of t are required for α to reach an apparent constant value, but in addition these same conditions appear to produce a higher value of the constant portion of the curves. This seems to indicate an apparent increase in the average

[22] J. J. Thomson, *Conduction of Electricity through Gases*, third edition, Vol. 1, pp. 47–48.

[23] L. B. Loeb, Phys. Rev. **51**, 1110 (1937).

value of α after the initial phase of recombination has ceased. Except at the longest time intervals the apparent constancy of the curves of short exposure time, low pressure, and ionic density is illusory. Loeb[24] has shown that if the ions are initially formed at a distance Δr_0 apart and diffuse to a distance Δr where random distribution of the ions is obtained, then during initial recombination the value of α as measured becomes

$$\alpha=\alpha'\left\{\frac{\Delta r}{\Delta r_0+(12Dt/\pi)^{\frac{1}{2}}}\right\}^3 \qquad (11)$$

where α' is the true coefficient, and D is the coefficient of diffusion. For practical purposes the value of Δr can roughly be taken as

$$\Delta r=(1/n)^{\frac{1}{3}} \qquad (12)$$

where n = the ionic density. This equation when calculated to take into consideration the aging of ions during the x-ray flash period, gives rise to curves following fairly closely the general shape and trend of the observed curves. It predicts, however, that, if the normal coefficient of diffusion is used, the curves would drop to a constant value in intervals of time 0.01 of those observed. This would indicate that as far as achieving random distribution is concerned, the coefficient of diffusion is apparently 0.01 as great as that for normal ions. This is not entirely unreasonable since the diffusion from the sphere of active attraction is strongly retarded at distances from d to 10 d. The equation further predicts that the point where α has a certain definite value relative to the true value α' should vary inversely with ionic density. The data taken with the x-rays filtered through copper sheets to give a tenfold reduction in n show that corresponding points are shifted in time by 50-fold, Fig. 8, while the theory predicts a shift of 4.7 without correction for the x-ray flash period.

Finally, since the concentration of ions is proportional to pressure while the coefficient of diffusion is inversely proportional to pressure it would be expected that corresponding values of the ratios α/α' in initial recombination would vary in time directly as the cube root of the pressure. This is contrary to observation, for the theory would predict an increase in t with increase in pressure for corresponding values of α/α' but Figs. 3, 4, and 6 show a decrease in t with increase in pressure. There is, however, another factor which cannot be neglected. Immediately after ionization, the ionized molecules undergo further changes in forming the stable ions existing at longer time intervals. This is the well-known aging effect observed in mobility experiments and in Luhr's[12] investigations of ion formation with the mass spectrograph. Consequently the mass of the ion in oxygen is probably undergoing changes up to some 0.01 second so that the average value of α will decrease gradually with time. Hence, part of the high values and gradual decrease of the observed α with time for the lower concentrations and pressures may be ascribed to newer and less massive ions. It is possible that in addition the products of x-ray ionization and excitation in oxygen may facilitate the rate of formation of these complexes, i.e. that aging is facilitated by dense ionization and a high concentration of ionization products. These phenomena are not included in the rough Eq. (11) of Loeb so that too much cannot be expected from this equation as regards verification of these experiments. It can be concluded, however, that making the assumptions of a decreased rate of diffusion to random distribution, taking into account the finite time of ionization, and recognizing the existence of aging effects in pure oxygen the type of curves obtained for α at shorter time intervals and lower ionic concentrations can be satisfactorily explained in a general way.

In conclusion, the writer wishes to thank Professor Loeb under whose direction the investigations were made and whose helpful criticisms made the culmination of the difficult measurements possible.

[24] L. B. Loeb, Lecture notes, "Conduction of Electricity in Gases," mimeographed edition, 1937.

The Variation of Magnetic Double Refraction with Temperature in Acetone and Certain Acetic Esters*

JOHN B. HAWKES[1]
Columbia University, New York, N. Y.
(Received October 7, 1937)

Measurement of the Cotton-Mouton coefficient at various temperatures between −60°C and 40°C were made on acetone and several normal acetic esters. Under neutral environment the relationship for these materials is best represented by a straight line with a slope of the same sign but of much larger value than can be justified by the mathematical theory. This is interpreted as indicating a larger molecular interaction in the liquid than is assumed in the theory. In the presence of a freshly cleaned surface of copper, acetone shows a reversal of sign of the birefringence with decreasing temperature. Evidence in the case of amyl acetate indicates that there is no discontinuity in the Cotton-Mouton coefficient near the freezing point.

I. INTRODUCTION

IN 1901 Kerr[2] observed that a fine suspension of iron oxide when placed in a magnetic field became birefringent. The effect disappeared when the magnetic field was removed. Later work by other investigators, among them Cotton and Mouton, demonstrated that the double refraction was associated with the particles of iron suspended in the liquid, rather than with the liquid itself.

In 1907 Cotton and Mouton[3] found that magnetic birefringence was, to a lesser degree, the property of certain organic liquids, notably nitrobenzene and others of the aromatic series. The sign of the double refraction was considered positive in the case of nitrobenzene, and negative for carbon disulphide. In 1909 the same investigators reported[4] that in nitrobenzene the variation of the magnetic double refraction over a range of temperature from room temperature upward was approximately a straight line with a slight concavity away from the temperature axis.

It was found by Cotton and Mouton that if the liquid in the magnetic field were thought of as a uniaxial crystal, of which the optic axis was parallel to the magnetic field, the magnetic double refraction could be treated exactly like a crystalline birefringence whose magnitude was proportional to the square of the magnetic field strength. If Δ represents the phase difference between the components of the emergent light parallel and perpendicular to the magnetic field, the general relationship

$$\Delta=\frac{L(n_p-n_s)}{\lambda}=C_mLH^2 \qquad (1)$$

was found to hold. Here Δ is in fractions of a wave-length; n_p and n_s are the indices of refraction parallel and perpendicular, respectively, to H; L is the length of light path in the liquid exposed to the magnetic field; λ is the wave-length in vacuum; H is the average magnetic field strength in oersteds; and C_m is the Cotton-Mouton coefficient, defined by this equation.

A mathematical theory of magnetic double refraction has been worked out by Langevin,[5] and developed and enlarged by a number of other investigators.[6] The treatment is much the same in all cases, and will not be given here. It is sufficient to point out that the orientation of the molecules by the magnetic field is assumed to be the origin of the optical anisotropy of the liquid as a whole, each molecule being assumed to have an optical anisotropy of its own which may be thought of as an ellipsoid of optical asymmetry fixed in the molecule. In addition, the important assumption is made that the intermolecular forces in the liquid are negligible.

The calculations of both Debye and Born give us, for a molecule with no permanent magnetic moment, i.e., for a molecule of a

* Publication assisted by the Ernest Kempton Adams Fund for Physical Research of Columbia University.
[1] Now at Stevens Institute of Technology, Hoboken, N. J.
[2] Kerr, Brit. Assoc. for Adv. of Sci., Reports, p. 568 (1901).
[3] Cotton and Mouton, Comptes rendus **145**, 229 (1907).
[4] Cotton and Mouton, Comptes rendus **149**, 340 (1909).
[5] Beams, Rev. Mod. Phys. **4**, 160–172 (1932).
[6] Debye, *Marx Handbuch der Radiologie*, Vol. 6, pp. 754–769; Born, *Optik*, pp. 345 ff; 360 ff.

diamagnetic substance, an expression of the form

$$C_m = A + B/T, \qquad (2)$$

in which C_m is the Cotton-Mouton coefficient; T is the absolute temperature; B is a constant which is a function *inter alia* of the magnetic polarizibility and of the optical electric polarizibility; A is similarly a function of the optical electric polarizibility, but not of the magnetic polarizibility. In Born's expression, A is small relative to B, while in Debye's relationship, A is zero.

From 1909 until 1922 little work on the variation of the Cotton-Mouton coefficient with temperature was published. In 1922 Szivessy[7] brought out the results of experiments on nitrobenzene. Szivessy's measurements were made over the range from 10°C to 60°C. These results, while confirming the theory in a general way, insofar as the value of C_m increased with decreasing temperature and showed a concavity away from the temperature axis, nevertheless were in poor quantitative agreement with the theory. The value of C_m found by Szivessy for nitrobenzene increased more rapidly with falling temperature than could be justified by Debye's equation. In Born's expression (2) Szivessy's results require the constant term to be large; a condition which this theory does not allow.

Since the work reported in this paper was begun, there has appeared[8] some data on oxygen and NO at high pressure (100 kg/cm²) and at two temperatures, 19°C and −80°C. The report cited indicates that the NO gave a thermal variation that was substantially zero between these two temperatures. The oxygen is reported as giving a variation proportional to a power of T between the inverse square and the inverse cube. The authors suggest that polymerization may play a part in the behavior of oxygen.

II. Apparatus

The apparatus employed in the present investigation consisted of the magnet and compensator described by Boorse[9] and additional equipment for controlling the temperature of the material under examination. A diagrammatic sketch of the apparatus is given in Fig. 1.

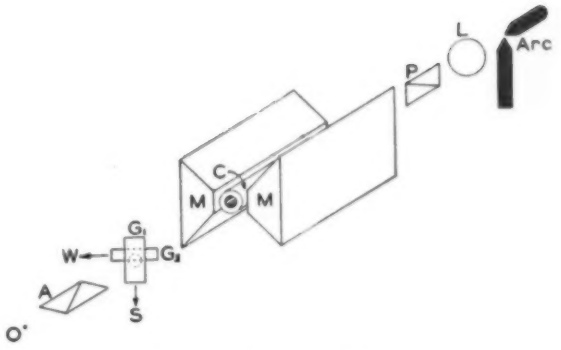

FIG. 1. Schematic diagram of the apparatus.

The source of light is the positive crater of a carbon arc. The lens system, L, produces parallel light which is polarized by a Nicol prism, P, in a plane at 45° to the axis of the magnetic field MM. The beam of light from P passes through the liquid in cell C, which is surrounded by a cooling jacket through which methanol is circulated. The means of regulating the temperature of the methanol is not shown. Upon leaving the cell, C, the light passes through the Palmer-Boorse compensator, G. This consists essentially of two glass strain-plates; G_1 covering the entire beam, and strained in a direction perpendicular to the magnetic field; and G_2 covering half the beam, and strained parallel to the magnetic field. The light finally passes through the analyzing Nicol, A, which is at right angles (optically) to P, after which it is viewed by the observer located at O. The attention of the observer is focused, by means of a telescope, on the lower edge of plate G_2.

It will be noticed that no provision has been made for providing monochromatic light for the observations. The question of what wave-length of the initial white light is effective in producing a visual image on the retina of the eye at these low intensities is one frequently raised. Under working conditions a red or a blue Wratten filter completely extinguished any trace of visual image. A good green filter of unknown history passed enough light to make the optical field barely visible, although no match could have been made at this intensity. A Wratten yellow filter (passing most of the red), produced almost no diminution in the intensity of the visual

[7] Szivessy, Ann. d. Physik **68**, 127 (1922).
[8] Bizette and Tsai, Comptes rendus **202**, 2143 (1936).
[9] Boorse, Phys. Rev. **46**, 187 (1934).

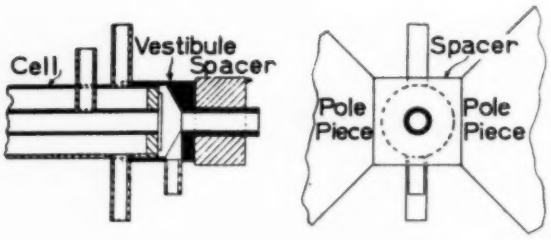

FIG. 2. Detail view of cell assembly.

field. The conclusion was reached that the effective value of the wave-length employed, even with the white source, might be taken somewhere in the green-yellow.

The manipulation of the compensator G was changed slightly from that outlined by Boorse. Briefly, the method was as follows: By means of a sliding weight on a graduated bar, the tension W on the half-shade plate G_2 could be varied continuously from zero to 250 grams. With the tension W at a convenient arbitrary value, say 100 grams, the two halves of the optical field were adjusted to match by means of the spring adjustment S on the compensator plate G_1. The two halves of the visual field then send elliptically polarized light to the analyzing Nicol. However, although the two ellipses are congruent, they are polarized in opposite directions, i.e., the conventional points tracing out the ellipses are rotating in opposite senses. The analyzer transmits only the amplitude corresponding to the direction in which it is set. In the present case it transmits a component parallel to the minor axis of the ellipse.

If we now apply the magnetic field, the two halves of the visual field become unmatched when a magnetically birefringent material is in the cell. The two halves of the field are restored to equality by sliding the weight on the bar. The amount ΔW by which the tension W is changed to restore the match is a measure of the magnetic birefringence.

The cell, by means of which the temperature of the specimen could be regulated, is shown in detail in Fig. 2. It was made of two concentric cylindrical tubes, the inner one containing the specimen, and the space between the tubes serving as a jacket for circulating the cooling methanol. The inner tube was filled through two filler-tubes passing through the jacket. One end of the cell is shown in Fig. 2 (the other end is identical). The jacket was supplied with circulating fluid through two connections at each end, as shown. The cylindrical symmetry of the cell is important in eliminating temperature inhomogeneity in the liquid specimen due to the presence of warm and cold spots in the jacket, arising from irregularities in the flow of the cooling methanol.

On the ends of the cell, which were ground parallel to each other and perpendicular to the axis of the cell, were attached thin glass windows of microscope cover glass, carefully selected for optical neutrality. The cement used to attach the windows is described by Boorse, and consists of a mixture of dextrine and *d*-mannitol. This cement remains semifluid even at relatively low temperatures, and thus does not exert an appreciable force on the windows when differential contraction between the window and the cell is brought about by a change in temperature of the cell.

Over the end of the cell is slipped a vestibule of hard rubber, shown in black in Fig. 2. This vestibule serves three purposes: (1) it provides a forespace in front of the window which is filled with evaporated liquid nitrogen introduced through the connection shown below the vestibule; (2) the opening bored in the tube, shown projecting to the right, serves as an optical stop to prevent light reflected from the inner surface of the cell from reaching the compensator and the eye of the observer; (3) the tube mentioned in (2) fits loosely into a hole drilled in the spacer-block separating the pole-pieces of the magnet, so as to support the cell properly in the magnetic field without constraint due either to the contraction arising from change of cell temperature, or due to the attraction between the pole-pieces when the magnetic field is applied.

The introduction of evaporated nitrogen into the forespace eliminates condensation of moisture on the windows, without the necessity of using double windows or other devices likely to produce optical disturbances.

The cooling methanol was introduced at one end of the cell and withdrawn at the other, thus giving the minimum of transverse temperature gradient in the specimen. The methanol was

cooled by circulating it through copper coils surrounded by solid carbon dioxide. A mixing valve enabled the amount of circulation through the coils to be regulated. The fine temperature regulation was performed by a thermostat which operated a heating coil in a reservoir through which the methanol passed.

The thermostat consisted of a resistance thermometer of 130 ohms of No. 36 nickel wire inserted in the circulating system just upstream from the cell. This thermometer formed one arm of a Wheatstone bridge, of which the adjacent arm was a variable resistor. The other two arms were fixed resistors. The temperature at which the bridge would balance was controlled by the setting of the variable resistor. The galvanometer mirror threw a spot of light onto a photoelectric cell, which in turn (through a relay circuit) reduced the current in the heating coil in the reservoir. By this means the temperature was held constant to about 0.01°C.

The temperature of the cell was determined to within a degree centigrade by means of two toluol thermometers, one located at the inlet and the other at the outlet of the cell. The difference between these two readings was less than 2°C, except at the lowest temperatures reached, at which point the difference rose to approximately 4°C. The temperature of the cell was assumed to be the mean of the inlet and outlet temperatures.

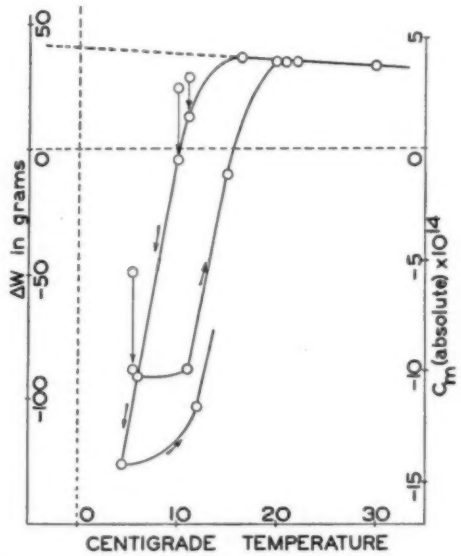

FIG. 3. C_m for acetone in the presence of freshly etched copper.

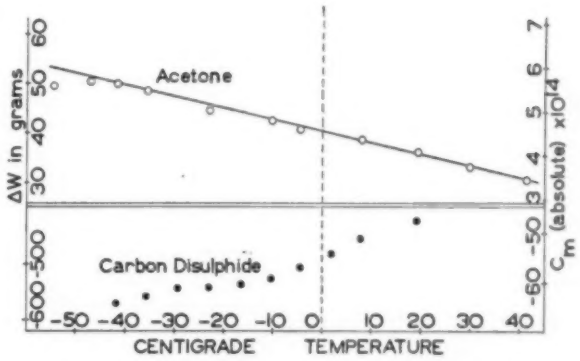

FIG. 4. C_m for acetone in aged copper and in Pyrex.

III. SPECIMEN MATERIALS

Measurements over a range of temperature from 40°C to −60°C have been made on the following organic liquids:

Acetone	Methyl Acetate	Ethyl Acetate
n-Propyl Acetate	*n*-Butyl Acetate	*n*-Amyl Acetate

A run was also made on carbon disulphide for purposes of comparison.

The acetone was technical acetone distilled three times in a Pyrex still with a refluxing column. The middle half of each run was preserved for the next distillation. The last two distillations were made over calcium chloride to remove traces of water. The esters were all from the Eastman Kodak Company Research Laboratory, and were all redistilled before using.

IV. RESULTS

The first thing to point out under this heading is the existence of an interaction between the material of the cell and the specimen. This interaction was most pronounced in the case of a copper cell carefully cleaned with a solution of hydrochloric acid and then thoroughly rinsed with distilled water, then with acetone, and finally with large amounts of the acetone to be studied. The values of C_m for acetone in the copper cell so treated, are given in Fig. 3. The fact that the two branches of the curve (one taken with decreasing temperature, and the other with rising temperature) happen to rejoin at slightly below room temperature, rather than at some other temperature, may be characteristic of acetone, as there is some indication that the other materials studied formed loops

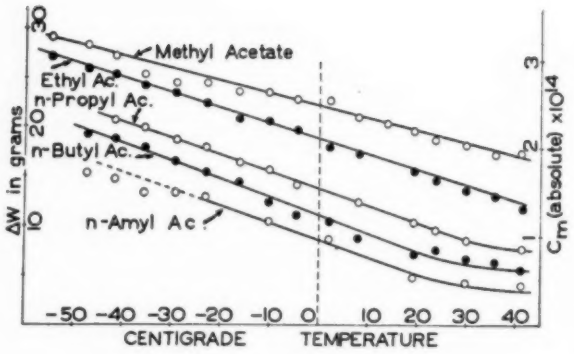

FIG. 5. C_m for certain acetic esters.

rejoining at considerably lower temperatures. This type of behavior was first noticed in a newly-made brass cell, and caused the abandonment of brass in favor of copper; the copper however showed the same effect when it was new, but gradually over a number of days of use, the loops became less and less steep until at last no reversals took place and the variation of the Cotton-Mouton coefficient with temperature took on the form shown in Fig. 4.

In order to determine which type of relationship represents the action of acetone and other materials in a neutral environment, a Pyrex cell was constructed of the same form as the metal cell described above and shown in Fig. 2. Acetone and methyl acetate were measured in this cell and gave values in agreement with the curves of Figs. 4 and 5, within the limits of experimental error (±5 percent). The experimental error was larger in the glass cell on account of a greater thermal inhomogeneity in the liquid arising from the lower thermal conductivity of the glass compared to copper. In addition, the magnetic birefringence was partly masked by a Faraday effect due to the fact that unavoidable inaccuracy in the shape of the glass cell caused it to lie with its axis not quite perpendicular to the magnetic field. Enough precision was obtained, however, to verify the agreement between the curves in glass and in aged copper.

The values upon which the curves of Figs. 4 and 5 are based are given in Table I. Each value is the mean of several determinations. No value is based on fewer than 20 determinations, and in the case of acetone the mean of as many as 130 determinations is used for several of the points. It will be noticed that with the possible exception of the higher esters, the concavity upward, which Szivessy, and Cotton and Mouton, found in nitrobenzene, is not present. In the three esters which may show such a curvature, it exists, if at all, only at the higher temperatures.

The precision of these measurements of ΔW is estimated to be better than ±0.5 gram. The total spread of the individual readings for each point is of the order of ±2.5 grams.

The values of ΔW given in Table I can be converted into C_m in absolute units for substitution in expression (1) given earlier in this article, by multiplying ΔW by the factor 0.11×10^{-14}. This factor is obtained by standardizing $\Delta W = 35.6$ grams at 20°C as equivalent to $C_m = 3.9 \times 10^{-14}$, and taking the factor of proportionality.

Amyl acetate apparently supercooled considerably to reach the lowest temperature on its curve. At −48°C the cell containing the amyl acetate was slightly disturbed, whereupon the liquid became completely opaque. The temperature of the cell was then slowly raised to approximately −30°C, at which point melting began to be apparent. A small amount of light could be seen through the liquid, but the path was partially obscured by a large number of needle-like crystals. On further warming these crystals disappeared in the neighborhood of −20°C. Recooling, after this, led to freezing in the

TABLE I. *ΔW in grams. $C_m = \Delta W \times 0.11 \times 10^{-14}$ where C_m is the Cotton-Mouton coefficient.*

DEGREES C	ACETONE	METHYL ACETATE	ETHYL ACETATE	n-PROPYL ACETATE	n-BUTYL ACETATE	n-AMYL ACETATE
41.0	30.4	17.1	11.6	7.6	5.6	4.0
35.8		17.0	12.8		6.3	
29.8	33.2	18.0	13.4	8.4	6.7	4.2
23.5		18.6	14.3	9.5	7.5	
19.1	36.2	19.4	15.3	10.2	7.1	4.8
13.5		20.2				
7.9	38.9	20.9	17.1	12.2	8.6	
1.9		22.6	17.9		10.2	8.6
−4.8	40.9	22.7	19.6	14.0	10.9	
−10.4	42.5	23.4	20.4	15.5	12.2	10.3
−16.6		23.5	20.7	16.2	14.3	
−23.2	44.7	24.3	22.2	17.7	15.1	12.7
−29.4		24.4	23.4	18.5	16.3	13.1
−35.8	48.5	25.3	24.1	19.8	17.8	13.1
−41.8	50.0	27.1	25.2	20.5	18.7	14.5
−47.4	50.5	28.2	25.9	20.2	19.1	15.1
−54.8	49.6	29.1	27.1			

neighborhood of −30°C repeatedly, without any further supercooling. It is interesting to note a suggestion of a plateau in the neighborhood of −30°C on the curve, (Fig. 5) although the magnitude of the effect is small and may not be significant.

One effect was very pronounced in the amyl acetate below −30°C, however. The lens action (due to a difference in refractive index caused by a temperature difference between the liquid near the wall of the cell, and the liquid on the axis of the cell) became very large below the apparent freezing point. In fact, on looking through the cell as the temperature was being lowered, the distant cell window, which ordinarily at such times appeared only slightly reduced in angular size, had in this case dwindled to the apparent size of a pinhole.

It is safe to say, however, that there is no marked change in the magnetic birefringence of amyl acetate in the neighborhood of its freezing point.

V. Discussion

The results of this investigation, as in the case of that of Szivessy, cannot be reconciled with the predictions of either Born or Debye, and the conclusion seems inevitable that the discrepancy between theory and experimental fact must be ascribed to intermolecular energies neglected in the theory. This thought led to the question of whether the disagreement should be ascribed to the complexity of the organic molecules involved in the action or whether it was due merely to the liquid state. To answer this, a run was taken on carbon disulphide (Eimer & Amend, C.P. redistilled). Carbon disulphide is the simplest molecule showing marked magnetic double refraction. The results are given as a part of Fig. 4. It is to be noted that C_m for carbon disulphide is large negatively, and is plotted here merely for comparison. It is clear that the agreement with the theory is, if anything, worse than for acetone. It therefore seems safe to say that the theory is not applicable to liquids.

On the subject of the loops traced by C_m for acetone and methyl acetate in the presence of etched copper, further investigation must precede an explanation. There are, however, two possibilities to be considered: (1) the formation of metal-bearing molecules with the acetone or methyl acetate; (2) the catalytic action of a fresh surface of the metal causing molecular aggregation in the acetone. In connection with these two possibilities there are several observed facts to be considered, namely: (1) when copper-oxide powder is added to the acetone showing the loop, the loop is altered so that ΔW remains positive over the entire temperature range; (2) when the curve is a loop, the time for the birefringence to disappear after the magnetic field is removed becomes quite long at low temperatures, rising in some cases to as much as 30 seconds (when the curve is a straight line, the relaxation time is quite short—of the order of $\frac{1}{2}$ second—and is apparently independent of the temperature); (3) the equilibrium values from which the upper branch of the curve in Fig. 3 was plotted were obtained only after a wait of several minutes. This is indicated by the arrows which connect the initial values with the final stable values at each temperature.

It should be pointed out here that in the work of other investigators the effect on the value of the Cotton-Mouton coefficient, of interaction between the acetone and the material of the cell has not been mentioned. Most of the measurements have been made in brass cells. While it seems likely, in the light of the present investigation, that acetone and the acetic esters give satisfactory results in a properly matured metal cell, it is possible that the disagreement between various investigators[9] on the values of C_m for the alcohols is due to an interaction between the alcohol and the material of the cell.

During the investigation of the literature for data covering the optical behavior of acetone and the esters, it was noticed that there is a large gap in the data on the index of refraction of liquids below room temperature. The experience gained in this investigation shows that technically such measurements would be difficult to make, but they should be by no means impossible, and it seems quite possible, in view of the behavior of the thermal coefficient of the refractive index of amyl acetate below −30°C, that the field would yield data of interest.

In closing I would like to express my appreciation and gratitude for the kindness of the late

Professor A. P. Wills in placing the compensator and the electromagnet at my disposal, and for his encouragement during the period of apparatus development. I wish to thank, also, Professor D. P. Mitchell whose suggestions have contributed largely to the satisfactory solution of the problem of the temperature control of the cell. Professor H. W. Farwell has been a valuable aid through his continuous interest and his technical advice on the details of the investigation.

JANUARY 1, 1938 PHYSICAL REVIEW VOLUME 53

Internal Friction in Solids

II. General Theory of Thermoelastic Internal Friction

CLARENCE ZENER*
Wayman Crow Hall of Physics, Washington University, St. Louis, Missouri
(Received July 6, 1937)

Stress inhomogeneities in a vibrating body give rise to fluctuations in temperature, and hence to local heat currents. These heat currents increase the entropy of the vibrating solid, and hence are a source of internal friction. The general theory of this internal friction is here developed. The simplest example of stress inhomogeneity is that occurring in the transverse vibrations of reeds and wires. Explicit formulae are obtained for reeds and wires, and the effect is calculated of crystal orientation in single crystal specimens. Microscopic stress inhomogeneities arise from imperfections, such as cavities, and from the elastic anisotropy of the individual crystallites. The internal friction due to spherical cavities is calculated. The internal friction due to elastic anisotropy is investigated for cubic metals, and is found to be greatest for lead, least for aluminum and tungsten.

§1. INTRODUCTION

IN a recent paper[1] the writer investigated theoretically that part of the internal friction of a vibrating reed which arises from the flow of heat back and forth across the reed. On comparing the calculated values of this thermoelastic internal friction with the experimental values of internal friction for longitudinal vibrations in rods, he predicted that over a wide frequency band the internal friction in reeds due to this thermoelastic effect was of a larger order of magnitude than that due to all other causes. In the succeeding paper an experimental verification of this prediction will be presented. The striking agreement of prediction with experiment renders it opportune to investigate more thoroughly the thermoelastic effect. Such an investigation is here undertaken.

This paper begins with a generalization of the analysis given in reference 1 for transverse vibrations (§2). It is found that for a rod of arbitrary cross section vibrating transversely, with frequency ν,

$$Q^{-1}=\frac{E_S-E_T}{E_S}\cdot\frac{\nu_0\nu}{\nu_0^2+\nu^2}. \tag{1}$$

Here E_S is the adiabatic Young's modulus, E_T the isothermal modulus, both measured along the axis of the wire. In the case of a rectangular cross section (reed), the frequency for maximum Q^{-1}, ν_0, is given by

$$\nu_0=(\pi/2)Dd^{-2}.$$

Here D is the thermal diffusion constant of the material, d is the width of the rod in the plane of vibration. In the case of circular cross section (wire),

$$\nu_0=0.539Da^{-2},$$

where a is the radius of the rod, or wire. Eq. (1) is valid for both isotropic and anisotropic rods. Tables are given to show the dependence of $(E_S-E_T)/E_S$ upon crystal orientation in single crystal rods. It is predicted that the internal friction in single crystal zinc rods will vary radically with crystal orientation, differing by a factor of seven for parallel and normal orientation.

* Now at the College of the City of New York.
[1] C. Zener, Phys. Rev. 52, 230 (1937).

The thermoelastic effect is present wherever there are inhomogeneities of stress. These inhomogeneities may be inherent in the type of vibration, as in the transverse vibrations of reeds and wires, or they may be caused by cavities, by a mixture of two phases, by the random orientation of the individual crystallites, etc. Whatever the cause of the stress inhomogeneity, the thermoelastic effect may be investigated from two viewpoints. We may seek the rate of dissipation of the mechanical energy of vibration. This dissipation is due to the slight difference in phase between the stresses and the corresponding strains. On the other hand, we may seek the rate of generation of heat. Stress inhomogeneities give rise to heat currents, which increase entropy, and an increase of entropy is inevitably associated with generation of heat. In §3 both of these points of view are investigated. The mechanical analysis for the dissipation of vibrational energy, and the thermodynamical analysis for the generation of heat, both lead to the same general expression for the Q^{-1} of a cubic metal with no internal strains, namely

$$Q^{-1}=[(C_p-C_v/)C_v]\cdot\Re\cdot\sum f_k[\nu_k\nu/(\nu_k^2+\nu^2)], \quad (2)$$

with $$\sum f_k=1.$$

C_p and C_v are the specific heats at constant pressure and constant volume, respectively. The factor $\Re$ is that fraction of the total strain energy which is associated with fluctuations in dilation.

Equation (2) may be most readily interpreted by regarding Q^{-1} not as a function of frequency ν, but of $x=\log_{10}\nu$. We then obtain

$$Q^{-1}=\tfrac{1}{2}[(C_p-C_v)/C_v]\cdot\Re\cdot\sum f_k\mathfrak{B}(x-x_k), \quad (3)$$

where $$\mathfrak{B}(x)=\operatorname{sech}\{(\log_e 10)x\}.$$

The $\mathfrak{B}$ function, first introduced by Bennewitz and Rötger,[2] is plotted in Fig. 1. It is symmetrical about its maximum at $x=0$. Each term in the summation is thus a $\mathfrak{B}$ function with the weight f_k, shifted so that its maximum is at x_k. The associated ν_k is interpreted as the reciprocal of a time of relaxation for the establishment of temperature equilibrium across a distance L_k. From the diffusion equation one finds $\nu_k\approx D/L_k^2$.

[2] K. Bennewitz and H. Rötger, Physik. Zeits. **37**, 578 (1936).

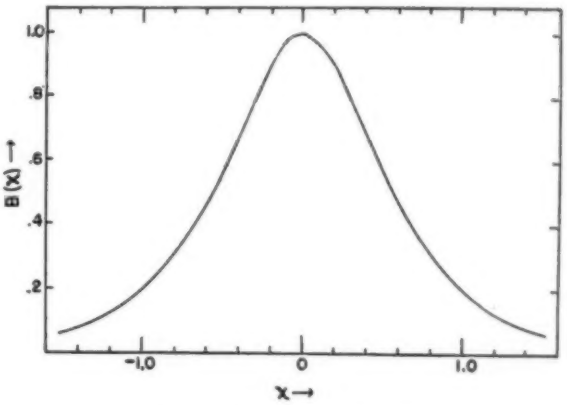

FIG. 1. Plot of the $\mathfrak{B}$ function.

A particularly simple type of stress inhomogeneity is formed by a spherical cavity in a vibrating solid. During vibrations these cavities will cause comparatively large local heat currents. The internal friction resulting therefrom is calculated in §4.

The elastic anisotropy of single crystals, combined with their random orientation, renders it impossible for strains which are macroscopically homogeneous to be also microscopically homogeneous. Hence in a vibrating polycrystalline solid heat currents flow back and forth between adjacent crystallites. The internal friction resulting therefrom may be roughly guessed at from Eq. (3) by replacing the summation by a single $\mathfrak{B}$ function, with the associated ν_k equal to D/L^2, where L is the mean diameter of the crystallites. The ratio $\Re$ is estimated in §5 for various polycrystalline metals. It is found that the Q^{-1} for aluminum is lower, for lead is higher, than for any other common metal. This is in agreement with the recent careful experiments of Wegel and Walther,[3] and of Förster and Körster,[4] who find that aluminum has the least, lead the greatest, internal friction of any nonferromagnetic metal investigated.

Two experimental methods are commonly used to measure internal friction. In the first, one determines the number N of oscillations required to reduce the amplitude of free oscillation to $1/e$'th its initial value. The quantity $\delta=1/N$ is called the logarithmic decrement of the solid. In

[3] R. L. Wegel and H. Walther, Physics **6**, 141 (1935).
[4] F. Förster and W. Köster, Zeits. f. Metallkunde **29**, 116 (1937).

the second method, one measures the width $\Delta\nu$ of a resonance curve at half-maximum (plot of square of amplitude against frequency). On dividing this width by the frequency at the maximum, one obtains a second dimensionless measure of internal friction. Internal friction may be interpreted theoretically from two points of view. If we regard the elastic modulus as complex, $M+im$, then the ratio m/M is a dimensionless measure of internal friction. Again, if we denote by E the energy of vibration, and by ΔE the loss per cycle of the energy of vibration, then $\Delta E/E$ is also a dimensionless measure of internal friction. These theoretical measures are related to each other, and to the experimental measures, by the equation

$$Q^{-1}=(1/2\pi)\cdot(\Delta E/E)=m/M.$$

§2. Transverse Vibrations of Reeds and Wires

When the width of a rod (wire or reed) is small compared with the wave-length in transverse vibrations, the only stress of importance is the tensile stress along the axis of the rod. This simple stress system enables us to obtain a particularly simple expression for the thermoelastic internal friction of thin rods in transverse vibrations.

When the x axis is taken to lie parallel to the axis of the rod, this tensile stress is denoted by X_x. We consider X_x, as well as the strain e_{xx} and temperature fluctuation ΔT, to be a harmonic function of time. Hence by substituting

$$X_x=(\partial X_x/\partial e_{xx})_T e_{xx}+(\partial X_x/\partial T)_{e_{xx}}\Delta T$$

in the expression for the energy loss per cycle per unit length,

$$\Delta E=\nu^{-1}\text{ time average of }\int X_x(de_{xx}/dt)d\sigma,$$

we obtain

$$\Delta E=\nu^{-1}\zeta\text{ time average of }\int\Delta T(de_{xx}/dt)d\sigma.$$

In the partial derivative,

$$\zeta=(\partial X_x/\partial T)_{e_{xx}},$$

as well as in all the partial derivatives in this paragraph, the stresses Y_y and Z_z are held constant. The integration is over the cross section of the rod. The temperature fluctuation ΔT is completely determined by the diffusion equation

$$\partial\Delta T/\partial t=D\nabla^2\Delta T+\eta(\partial e_{xx}/\partial t),$$

and by the appropriate boundary condition. D is the thermal diffusion coefficient of the material, and

$$\eta=(\partial T/\partial e_{xx})_Q.$$

Corresponding to the physical condition that no heat flow across the surface of the rod, this boundary condition specifies that the normal component of the gradient of ΔT vanish at the surface.

The energy of vibration per unit length is equal to the maximum strain energy per unit length, E. We may write this energy in the form

$$\tfrac{1}{2}\epsilon\int e_{xx}^2 d\sigma. \tag{4}$$

The modulus ϵ may be called the effective Young's modulus. It is the adiabatic modulus E_s for rapid vibrations, the isothermal modulus E_T for slow vibrations. Since these two moduli differ from one another by less than one percent, very little error is made in

$$Q^{-1}=(1/2\pi)(\Delta E/E)$$

by replacing ϵ by either E_S or E_T throughout the entire frequency range.

By using the evaluation of ΔE given in the appendix, and by replacing E by (4), we obtain

$$Q^{-1}=(\zeta\eta/\epsilon)\sum f_k[\nu_k\nu/(\nu_k^2+\nu^2)], \tag{5}$$

with $$\sum f_k=1.$$

The constants f_k and ν_k are obtained from the eigenfunctions and eigenwert of the differential equation (a-5). (See Appendix.) Both f_k and ν_k/D are functions only of the shape of the rod. On the other hand, the factor $(\zeta\eta/\epsilon)$ is independent of the shape of the cross section, but depends only upon the thermoelastic constants of the material. Explicit formulae will now be derived for this factor in terms of these constants, and tables will be given for interesting cases.

We first replace ϵ by the adiabatic modulus.

The factor $(\zeta\eta/\epsilon)$ may then be written explicitly as

$$(\partial X_z/\partial T)_{\epsilon_{zz}}(\partial T/\partial e_{zz})_S/(\partial X_z/\partial e_{zz})_S,$$

or in the obviously equivalent form

$$(\partial X_z/\partial T)_{\epsilon_{zz}}(\partial T/\partial X_z)_S. \tag{6}$$

This expression may now be transformed in two ways. One transformation leads to the elegant expression $(E_S-E_T)/E_S$, the other leads to an expression containing only experimentally known constants.

Since only two of the four variables T, X_z, e_{zz}, S are independent, we may apply to Eq. (6) the following standard formula in partial differentiation:

$$(\partial x_1/\partial x_2)_{x_4}(\partial x_2/\partial x_1)_{x_3}=1-\frac{(\partial x_2/\partial x_3)_{x_1}}{(\partial x_2/\partial x_3)_{x_4}}.$$

Correlating x_1, x_2, x_3, x_4 with T, X_z, e_{zz}, S respectively, we obtain

$$(\zeta\eta/\epsilon)=(E_S-E_T)/E_S. \tag{7}$$

Again, we may transform (6) using the second law of thermodynamics. In the type of vibrations here considered, X_z is the only nonvanishing stress. Hence the total static energy density $\mathcal{E}$, as well as $X_z\,e_{zz}$, is a single valued function of any two of the variables T, X_z, e_{zz}, S. A small increment in $\mathcal{E}-X_z e_{zz}$, namely

$$T\,dS-e_{zz}dX_z,$$

is thus a perfect differential. It follows that

$$(\partial T/\partial X_z)_S=-(\partial e_{zz}/\partial S)_{X_z}=-(T/C_p)(\partial e_z/\partial T)_{X_z}.$$

Substituting this equation into (6), and replacing

$$(\partial X_z/\partial T)_{\epsilon_{zz}} \quad \text{by} \quad -(\partial X_z/\partial e_{zz})_T(\partial e_{zz}/\partial T)_{X_z},$$

we obtain

$$(\zeta\eta/\epsilon)=TE_T\alpha^2/C_p. \tag{8}$$

Here α is the linear thermal expansion coefficient, E_T is the isothermal Young's modulus, both *measured along the axis of the rod*. C_p is the specific heat, at constant pressure, per unit volume. Comparing Eqs. (7) and (8), we obtain the well-known formula

$$(E_S-E_T)/E_S=TE_T\alpha^2/C_p. \tag{9}$$

If the rod is isotropic, still another expression for $(\zeta\eta/\epsilon)$ may be obtained. When ϵ is replaced by the isothermal modulus, the appendix of reference 1 shows that

$$(\zeta\eta/\epsilon)=\tfrac{1}{3}(1-2\sigma)(C_p-C_v)/C_v,$$

where σ is here Poisson's ratio.

Table I gives the ratio $(E_S-E_T)/E_S$ for various polycrystalline metals, calculated from Eq. (9). Since E_T is affected by fiber structure, which is always present to some extent in cold worked specimens, the ratio for any particular sample may vary considerably from Table I. Since $(E_S-E_T)/E_S$ varies as the square of α, it is especially small in those alloys with small coefficients of thermal expansion, such as invar.

In rods of single crystals, $(E_S-E_T)/E_S$ will depend upon the relative orientation of the crystal with respect to the axis of the rod. In single metal crystals with cubic symmetry, α is independent of orientation. Young's modulus is greatest along the [111] axes, least along the [100] axes.[5] Table II has been constructed by substituting into Eq. (9) the maxima and minima values of E_T given in reference 5.

In single metal crystals with hexagonal symmetry, both α and E_T depend only upon the angle θ between the principal axis of the crystal

TABLE I. *Values of* $(E_S-E_T)/E_S$ *for polycrystalline metals at* 20°C.

METAL	$(E_S-E_T)/E_S$	METAL	$(E_S-E_T)/E_S$
invar	0.00002	Ni	0.0029
W	.0008	Cu	.0030
Bi	.0014	Ag	.0034
Pl	.0015	Sn	.0040
Au	.0017	Al	.0046
Sb	.0018	Mg	.0050
Pd	.0020	Zn	.0080
Pb	.0024	Cd	.010
Fe	.0024		

TABLE II. *Values of* $(E_S-E_T)/E_S$ *at* 20°C *when crystal axes* [111] *and* [100] *are parallel to axis of rod.*

METAL	DIRECTION PARALLEL TO ROD [111]	[100]
Cu	0.0046	0.0016
Ag	.0050	.0019
Au	.0028	.0010
Al	.0060	.0050
Fe(α)	.0024	.0011

[5] E. Schmid and W. Boas, *Kristallplastizität* (Springer, 1935), p. 202.

TABLE III. *Variation of* $10^3\,(E_S-E_T)/E_S$ *with* θ *in zinc.*

T \ θ	0°	10°	20°	30°	40°	50°	60°	70°	80°	90°
100°K	6.6	6.6	6.4	5.8	5.0	3.4	1.82	0.64	0.16	0.04
200°K	11.2	11.4	11.2	10.6	9.6	7.6	5.2	2.6	1.4	1.0
300°K	15.4	15.8	15.6	15.2	14.0	11.8	8.2	5.0	3.0	2.4

TABLE IV. *Variation of* $10^3(E_S-E_T)/E_S$ *with* θ *in cadmium.*

T \ θ	0°	10°	20°	30°	40°	50°	60°	70°	80°	90°
100°K	5.7	5.6	5.4	4.9	4.2	3.3	2.4	1.6	1.2	1.0
200°K	9.5	9.3	8.9	8.2	7.3	6.0	4.7	3.4	2.6	2.4
300°K	12.0	12.0	11.6	11.0	10.2	9.1	7.8	6.2	5.3	5.0

and the axis of the rod. Taking the data for E_T from reference 6, and the data for α from reference 7, we have constructed Table III for zinc and Table IV for cadmium. In a zinc rod whose axis is normal to the principal axis of the crystal, $(E_S-E_T)/E_S$ disappears slightly below 100°K. This is because the linear thermal expansion coefficient normal to the principal axis changes sign at this temperature.

The constants f_k and ν_k in Eq. (5) have already been evaluated for a rod of rectangular cross section (reed) in reference 1. If d is the width of the rod in the plane of vibration,

$$f_0, f_1, f_2\cdots = 0.986,\ 0.012,\ 0.0016,\ \cdots \qquad (10)$$
$$\nu_0,\ \nu_1\cdots = (\pi/2)Dd^{-2},\ (9\pi/2)Dd^{-2},\ \cdots.$$

We shall now evaluate these constants for a rod of circular cross section (wire) of radius a.

Following the analysis given in the appendix, we must first find the eigenfunctions U_k and the eigenwert ν_k of the differential equation (a-5), where in the present case ∇^2 is the two dimensional Laplace operator. These eigenfunctions must satisfy the boundary condition

$$(\partial/\partial r)U_k = 0 \quad \text{at} \quad r=a. \qquad (11)$$

We next expand e_{zz} in terms of these eigenfunctions. f_k is then given by

$$\left(\int e_{zz}U_k d\sigma\right)^2 \Big/ \int e_{zz}^2 d\sigma \int U_k^2 d\sigma.$$

The eigenfunctions of Eq. (a-5) and of the boundary condition (11) are of the form

$$\cos(m\varphi)J_m\{(2\pi\nu/D)^{\frac{1}{2}}r\},$$

where m is an integer, and where ν is one of the roots of the equation

$$J_m'\{(2\pi\nu/D)^{\frac{1}{2}}a\} = 0.$$

Since $$e_{xx} = e_0 r\cos\varphi,$$

only those eigenfunctions contribute to the summation in (5) for which $m=1$. From tables[8] of Bessel functions we find the first few roots of

$$(d/dq)J_1(q) = 0$$

to be $$q_0, q_1, q_2\cdots = 1.84,\ 5.33,\ 8.53\cdots. \qquad (12)$$

Setting $q=(2\pi\nu/D)^{\frac{1}{2}}a$, we find the first few allowed values of ν to be

$$\nu_0,\ \nu_1,\ \cdots = 0.539Da^{-2},\ 4.53Da^{-2}\cdots.$$

We may now write f_k explicitly as

$$f_k = \frac{\left(\int_0^a r^2 J_1(q_k r/a)dr\right)^2}{\int_0^a r^3 dr \int_0^a r J_1^2(q_k r/a)dr}.$$

With the aid of the formulae[9]

$$\int q^2 J_1(q)dq = q^2 J_2(q)$$

and $$\int q J_1^2(q)dq = \tfrac{1}{2}q^2\{J_1^2(q) - J_0(q)J_2(q)\},$$

we obtain

$$f_k = \frac{8J_2^2(q_k)}{q_k^2\{J_1^2(q_k) - J_0(q_k)J_2(q_k)\}}.$$

We now obtain the numerical value of f_k by substituting into this equation the values of q_k given by Eq. (12). The $J_0(q_k)$ and $J_1(q_k)$ can be obtained with sufficient accuracy by interpolation from the usual tables of Bessel functions, $J_2(q_k)$ from the tables in reference 9, p. 252. We obtain

$$f_0, f_1, f_2, \cdots = 0.988,\ 0.010,\ 0.0013\cdots.$$

Hence with a circular wire, as with a reed, we are justified in replacing f_0 by unity, and all the other f_k's by zero. This approximation, which

[6] E. Gruneisen and E. Goens, Zeits. f. Physik **26**, 245 (1924).
[7] E. Gruneisen and E. Goens, Zeits. f. Physik **29**, 147, 148 (1924).
[8] E.g., G. N. Watson's *Theory of Bessel Functions* (Cambridge Press, 1922), pp. 666–695.
[9] E. Jahnke and F. Emde, *Funktionentafeln* (Teubner, 1933) pp. 213–214.

eliminates all except the first term in the summation of Eq. (5), will probably be valid for all rods with a regular cross section.

§3. General Theory

In the expression for the internal friction of a solid,

$$Q^{-1}=(1/2\pi)(\Delta E/E), \tag{13}$$

ΔE may be interpreted either as the mechanical work ΔW required per cycle to keep the solid in steady vibration, or as the increment per cycle of the heat content ΔQ. We shall investigate ΔE from both points of view, directly calculating both ΔW and ΔQ.

Consider the vibrations of the solid to be a simple harmonic function of time. In each element of volume dv a set of coordinate axes may then be found with respect to which the shearing strains e_{yz}, e_{zx}, e_{xy} remain zero. The work performed upon an element of volume by giving the three tensile strains small increments is

$$dwdv=(X_x de_{xx}+Y_y de_{yy}+Z_z de_{zz})dv.$$

dw/dt will be equal to the sum of three terms of the type $X_x de_{xx}/dt$. The net work performed upon the element of volume during one cycle is thus equal to the sum of three terms of the type

$$\nu^{-1}\text{ time average of }X_x(de_{xx}/dt)dv.$$

In order to evaluate these time averages, express each stress as the sum of two terms. The first term is the value the stress would have if the temperature remained constant at its average value T_0. This term is in phase with the strains, and hence contributes nothing to the above time average. The second term is due to the deviation ΔT of the temperature from its average value. In the time average the stress X_x may thus be replaced by $(\partial X_x/\partial T)\Delta T$, where in the partial derivative it is understood that all the strains are kept constant. We now introduce a simplification by assuming that the elastic and thermal constants of the element of volume have cubic symmetry. This assumption not only limits us to solids with cubic symmetry, but also to solids which have no internal strains other than that due to vibrations. This simplification enables us to replace each of the three derivatives of the type $(\partial X_x/\partial T)$ by $-(\partial p/\partial T)_\theta$, where p refers to a hydrostatic pressure, and θ refers to the dilatation, $e_{xx}+e_{yy}+e_{zz}$. We now obtain the net work performed upon the whole solid per cycle by integrating $dwdv$ over the solid.

$\Delta W=-\nu^{-1}(\partial p/\partial T)_\theta$ time average of

$$\int \Delta T(d\theta/dt)dv. \tag{14}$$

The temperature fluctuation ΔT is completely determined by the differential equation

$$d\Delta T/dt=D\nabla^2\Delta T+(\partial T/\partial\theta)_Q(d\theta/dt) \tag{15}$$

and by the boundary condition that the normal component of the gradient of ΔT vanish at the surface of the solid.

We shall now calculate the rise in heat content per cycle, ΔQ, using only thermodynamical considerations. The rate at which the entropy of an elementary volume dv changes with time is equal to T^{-1} times the rate at which heat flows into the element of volume:

$$T^{-1}\sigma\nabla^2 T dv,$$

where σ is the thermal conductivity of the substance. Since the fluctuations in temperature are very small, we may write ΔQ as $T_0^{-1}\Delta S$, where ΔS is the entropy change of the whole solid per cycle. Summing the entropy changes in all the elementary volumes, we obtain

$$\Delta Q=\nu^{-1}\sigma T_0\text{ time average of }\int T^{-1}\nabla^2 T dv.$$

In the integrand T^{-1} is now replaced by $T_0^{-1}-T_0^{-2}\Delta T$. Eq. (15), valid only for solids with cubic symmetry, is now used to replace $\nabla^2 T$ in the integrand by

$$D^{-1}\{d(\Delta T)/dt-(\partial T/\partial\theta)_Q d\theta/dt\}.$$

The only term in the integrand which does not vanish upon taking the time average is $T_0^{-2}\Delta T(\partial T/\partial\theta)_Q d\theta/dt$. Using the relation

$$\sigma/D=C_v,$$

where C_v is the specific heat per unit volume, and using the thermodynamic formula

$$T^{-1}C_v(\partial T/\partial\theta)_Q=-(\partial p/\partial T)_\theta,$$

we obtain finally

$$\Delta Q = -\nu^{-1}(\partial p/\partial T)_\theta \text{ time average of } \int \Delta T(d\theta/dt)dv. \quad (16)$$

We have, from thermodynamical considerations, obtained an expression for ΔQ which is identical with the ΔW obtained from mechanical considerations.

On comparing Eq. (14) or (16), and Eq. (15) with the integral solved in the appendix, we find for $\Delta E(=\Delta W=\Delta E)$

$$\Delta E = -\pi(\partial p/\partial T)_\theta(\partial T/\partial\theta)_Q \int \Theta^2 dv \times \sum f_k[\nu_k\nu/(\nu_k^2+\nu^2)],$$

with $$\sum f_k = 1.$$

Here Θ is the maximum value of the dilation θ during a cycle. The energy associated with this maximum dilation is

$$-\tfrac{1}{2}(\partial p/\partial\theta)_T \int \Theta^2 dv.$$

This expression is exact only for slow isothermal vibrations. However, only very little error is made by using the isothermal differential for all frequencies. Let $\mathfrak{R}$ denote the ratio of this maximum strain energy associated with dilation to the maximum of the total strain energy, ΔE. We obtain

$$\Delta E/E = 2\pi\{(\partial p/\partial T)_\theta(\partial T/\partial\theta)_Q/(\partial p/\partial\theta)_T\}\mathfrak{R} \times \sum f_k[\nu_k\nu/(\nu_k^2+\nu^2)].$$

In the appendix of reference 1 it is shown that the bracketed expression is equal to $(C_p-C_v)/C_v$. Since $\Delta E/E = 2\pi Q^{-1}$, we obtain finally

$$Q^{-1} = [(C_p-C_v)/C_v]\mathfrak{R}\sum f_k[\nu_k\nu/(\nu_k^2+\nu^2)]. \quad (17)$$

§4. Internal Friction Caused by Small Cavities

In this paragraph Eq. (17) is used to calculate the internal friction caused by stress inhomogeneities about a spherical cavity in a vibrating isotropic solid. In this calculation the description of the strains about a spherical cavity is taken from Love.[10]

Since a general strain may be represented as the superposition of a pure dilation and of a pure shear, we need only consider the two special cases where the medium, in the absence of the cavity, has a pure dilation, and where it has a pure shear. When a spherical cavity in a medium of infinite extent is subjected to hydrostatic pressure, the strains about the cavity are pure shears, the dilation being exactly zero (reference 10, p. 185). One thus concludes that when a small spherical cavity is placed in a medium with pure dilation, the only strains introduced by the cavity are pure shears. Hence such cavities give rise to no thermoelastic damping of vibrations composed only of dilations.

On the other hand, a spherical cavity placed in a medium containing only pure shears introduces local strains which have dilation. From the strain given in reference 10, p. 256, we find this dilation Θ to be

$$\Theta = [-5\mu s/(9\lambda+14\mu)] \times (a/r)^2 \sin^2\theta\cos\varphi\sin\varphi. \quad (18)$$

Here a is the radius of the cavity; μ and λ are elastic constants related to Poisson's ratio σ and Young's modulus E by Eqs. (24), p. 101 of reference 10; s is the shear at large distances from the cavity.

As a first step in calculating the contribution of this cavity to the Q^{-1} of the solid, one obtains the ratio $\mathfrak{R}$ of the strain energy of dilation to the total strain energy. Now the strain energy of dilation is

$$\tfrac{1}{2}K\int \Theta^2 dv,$$

where K is the bulk modulus. The total strain energy per unit volume is $\frac{1}{2}\mu s^2$, neglecting the small contribution due to the cavity. The Q^{-1} of the solid due to one cavity per unit volume is obtained by setting

$$\mathfrak{R} = \tfrac{1}{2}K\int \Theta^2 dv/\tfrac{1}{2}\mu s^2.$$

Replacing μ, λ by their equivalents in σ and E,

[10] A. E. H. Love, *Mathematical Theory of Elasticity* (Cambridge Press, 1920).

TABLE V.

Poisson's ratio, σ	0	0.05	0.10	0.15	0.20	0.25	0.30	0.35	0.40	0.45	0.50
$p(\sigma)$	1.0	1.92	1.05	1.01	0.98	0.93	0.84	0.73	0.55	0.32	0

and denoting the volume of the cavity by v, we obtain

$$\Re = (10v/1764)p(\sigma),$$

where $p(\sigma) = (1-2\sigma)(1+\sigma)/(1-5\sigma/7)^2$,

and is given in Table V as a function of σ.

After the finding of the ratio $\Re$, the next step is to find the constants f_k and ν_k under the summation in Eq. (17). Following the analysis given in the appendix, we must first find those solutions of Eq. (a-5) whose normal derivatives vanish at the surface of a sphere of radius a, and also the associated eigenfunctions. In order that these solutions be quadratically integrable, we shall impose the second boundary condition that the solutions vanish at the surface of a large sphere of radius R, where $R \gg a$. We then expand Θ, given by Eq. (18), in terms of these eigenfunctions. f_k is then given by

$$f_k = \Theta_k^2 \Big/ \int \Theta^2 dv,$$

where Θ_k is the k'th coefficient in this expansion. In the final expression for Q^{-1}, we shall let the radius R approach infinity. The summation then passes into an integration.

The eigenfunctions of Eq. (a-5) may be written as the product of a surface harmonic and of a function of r. Only those eigenfunctions will enter into the expansion of Θ whose surface harmonics are given by $\sin^2\theta \cos\varphi \sin\varphi$. The radial dependence of these eigenfunctions is given by

$$[d/dy\{y^{-\frac{1}{2}}J_{-5/2}(y)\}]_{y=q}y^{-\frac{1}{2}}J_{5/2}(y) - [d/dy\{y^{-\frac{1}{2}}J_{5/2}(y)\}]_{y=q}y^{-\frac{1}{2}}J_{-5/2}(y).$$

Here $y = qr/a$,

and $q^2 = 2\pi\nu_k a^2/D$.

The derivative of this function automatically vanishes at $r=a$ for all values of q. The condition that this function vanish at $r=R$ is however satisfied by only a discrete set of q's. The normalization of these eigenfunctions, the evaluation of the coefficients Θ_k, and the passing to the limit $R\to\infty$, involves lengthy but only standard mathematics, and so will not be here reproduced.

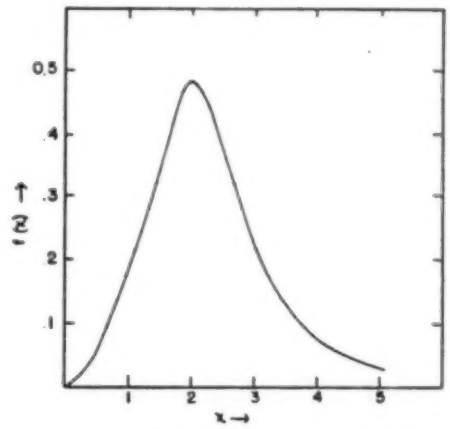

FIG. 2. Plot of $f(x) = 18x^2/(81+9x^2-2x^4+x^6)$.

The result of this calculation is that the summation

$$\sum f_k[\nu_k\nu/(\nu_k^2+\nu^2)]$$

is replaced by the integration

$$\int_0^\infty f(x)[\nu(x)\nu/(\nu^2(x)+\nu^2)]dx.$$

The function $f(x)$ is given by

$$f(x) = \frac{18x^2}{81+9x^2-2x^4+x^6},$$

and is plotted in Fig. 2. It satisfies of course the normalization condition

$$\int_0^\infty f(x)dx = 1.$$

The function $\nu(x)$ is given by

$$\nu(x) = (D/2\pi a^2)x^2.$$

§5. INTERNAL FRICTION DUE TO RANDOM ORIENTATION OF CRYSTALLITES

As mentioned in the introduction, the stress in a vibrating polycrystalline solid will vary from crystallite to crystallite. This stress fluctuation gives rise to heat currents between adjacent crystallites, which in turn give rise to internal

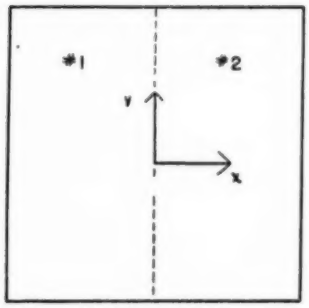

FIG. 3.

friction. The precise dependence of this internal friction upon frequency of vibration cannot be calculated without a detailed knowledge of the grain structure. However, we can predict the frequency ν_0 at which Q^{-1} is a maximum, and we can also predict the area beneath the curve of Q^{-1} plotted against $\log \nu = x$. From the diffusion equation, one can readily see that

$$\nu_0 \approx D/L^2,$$

where L is the mean diameter of the crystallites. From the relation

$$\int_{-\infty}^{\infty} \mathfrak{B}(x)dx = \pi \log_{10} e = 1.36,$$

and from Eq. (3), we obtain

$$\int_{-\infty}^{\infty} Q^{-1}dx = 0.68\mathfrak{R}(C_p - C_v)/C_v. \qquad (19)$$

In this integral the effect of the detailed structure no longer appears. The factor $(C_p - C_v)/C_v$ may be calculated from the well-known formula

$$(C_p - C_v)/C_v = T\alpha^2/C\chi,$$

where C is the specific heat, for constant volume, per unit volume, α is the volume coefficient of thermal expansion, and χ is the compressibility. There follows an estimate of that fraction $\mathfrak{R}$ of the total strain energy, in cubic metals, which is associated with fluctuations in dilation.

In cubic metals a macroscopic pure dilation implies a uniform dilation of all the crystallites. Hence we need consider only macroscopic pure shears.

In order to estimate that fraction of the energy of a macroscopic pure shear which is associated with microscopic fluctuations in dilation, consider a small cube divided in half. Each half is a crystallite, orientated at random. This system, together with a specification of the coordinate axes, is shown in Fig. 3. By compressing the block along the y axis by a small amount, and extending it along the x axis by the same small amount, a strain is produced which, on the average, has no net dilation. Using superscripts to distinguish the two crystallites, we obtain the following equations for the strains in the two halves of the cube

$$\begin{aligned} \tfrac{1}{2}(e_{zz}^{1} + e_{zz}^{2}) &= e, \\ e_{yy}^{1} = e_{yy}^{2} &= -e, \\ e_{zz}^{1} = e_{zz}^{2} &= 0, \end{aligned}$$

all shearing strains $= 0$. Denoting by Θ the dilation of the first crystallite, we may write the first equation of the above set as

$$e_{zz}^{1} = e + \Theta; \quad e_{zz}^{2} = e - \Theta.$$

A solution for Θ is obtained by substituting the stress-strain relations

$$X_x^{k} = C_{11}^{k} e_{zz}^{k} + C_{12}^{k} e_{yy}^{k}, \quad k = 1, 2,$$

in the equation of equilibrium

$$X_x^{1} = X_x^{2},$$

and by using the above expressions for the strains. The solution is

$$\Theta = Pe,$$

where

$$P = \frac{(C_{11}^{2} - C_{11}^{1}) - (C_{12}^{2} - C_{12}^{1})}{C_{11}^{1} + C_{11}^{2}}. \qquad (20)$$

The ratio $\mathfrak{R}_0$ for the cube is given by

$$\tfrac{1}{2}K\Theta^2/\tfrac{1}{2}G(2e)^2.$$

Here K is the microscopic as well as the macroscopic bulk modulus, and G is the macroscopic modulus of rigidity. On expressing K and G in

TABLE VI. *Effect of elastic anisotropy in cubic crystals.*

METAL	Pb	Cu	Ag	Au	Fe	Al	W
$\mathfrak{R}$	0.065	0.031	0.031	0.014	0.022	0.0009	10^{-4}
$(C_p - C_v)/C_v$	0.67	0.028	0.040	0.038	0.016	0.046	0.006
$10^3 \times \int Q^{-1}dx$	3.0	0.59	0.57	0.36	0.24	0.028	10^{-5}

terms of Young's modulus and Poisson's ratio σ, we find

$$\Re_0=\frac{1}{6}\frac{1+\sigma}{1-2\sigma}P^2.$$

A good estimate of the ratio $\Re$ for the solid would be obtained by averaging $\Re_0$ over all orientations of the two crystallites. Since, however, we are at present interested primarily in orders of magnitude, only the following rough average will be performed. The principal axes of the first crystallite are chosen to coincide with the coordinate axes. Further, one of the principal axes of the second crystallite is chosen to coincide with the z axis. Let θ be the angle which one of the other axes makes with the x axis. Then (see p. 151 of reference 10)

$$\begin{aligned} C_{11}^2-C_{11}^1&=4\Delta C_{44}\sin^2\theta\cos^2\theta,\\ C_{12}^2-C_{12}^1&=-4\Delta C_{44}\sin^2\theta\cos^2\theta,\\ C_{11}^2+C_{11}^1&=2C_{11}+4\Delta C_{44}\sin^2\theta\cos^2\theta. \end{aligned} \tag{21}$$

Here ΔC_{44} is a measure of the elastic anisotropy of the metal. It is defined by

$$\Delta C_{44}=C_{44}-\tfrac{1}{2}(C_{11}-C_{12}).$$

We now substitute Eqs. (21) in Eq. (20), and average $\Re_0$ over θ. We obtain

$$\Re=\frac{4}{45}\frac{1+\sigma}{1-2\sigma}\left(\frac{\Delta C_{44}}{C_{11}}\right)^2.$$

Values of this ratio are given in Table VI for various metals. In constructing this table, ΔC_{44} for Pb is taken from reference 11, ΔC_{44} for the other metals is taken from reference 5, p. 21.

Appendix

In the text we must evaluate the following type of integral:

$$\Delta E=\beta\nu^{-1}\text{ time average of }\int\Delta T(dG/dt)d\tau. \tag{a-1}$$

Here G is a harmonic function of time t, with frequency ν, and is an arbitrary function of the coordinates. ΔT is also a harmonic function of time, but its dependence upon the coordinates is determined by the equation

$$d(\Delta T)/dt=D\nabla^2\Delta T+\gamma dG/dt, \tag{a-2}$$

and by the condition that the normal component of the gradient of ΔT vanish at the boundary of the region.

The variable t is eliminated from Eqs. (a-1) and (a-2) by the introduction of complex quantities:

$$\begin{aligned} \Delta T(\mathbf{r},t)&=\text{Real part of }\mathfrak{T}(\mathbf{r})e^{2\pi i\nu t},\\ G(\mathbf{r},t)&=\text{Real part of }\mathfrak{G}(\mathbf{r})e^{2\pi i\nu t}. \end{aligned}$$

We choose the origin of time so as to make $\mathfrak{G}$ real. Then $\mathfrak{T}$ is in general complex. Eqs. (a-1) and (a-2) may now be rewritten as

$$\Delta E=-i\pi\beta\int\mathfrak{G}(\text{imaginary part of }\mathfrak{T})d\tau, \tag{a-3}$$

$$(D\nabla^2-2\pi i\nu)\mathfrak{T}+2\pi i\nu\gamma\mathfrak{G}=0. \tag{a-4}$$

The complex function $\mathfrak{T}$ may formally be expanded in any complete set of normalized functions. We shall choose that particular set of functions U_0, U_1, U_2 $\cdots$ which satisfy the differential equation

$$(D\nabla^2+2\pi\nu_k)U_k=0, \tag{a-5}$$

and also the same boundary condition that $\mathfrak{T}$ satisfies, namely the vanishing of the normal component of their gradients at the surface. By so choosing this boundary condition, we automatically make that expansion which satisfies Eq. (a-4) also satisfy the proper boundary condition.

In the expansion

$$\mathfrak{T}=\sum\mathfrak{E}_jU_j \tag{a-6}$$

the constants $\mathfrak{E}_j$ are in general complex. They are determined by substituting the expansion in Eq. (a-4), multiplying to the left by U_k, and integrating over all the solid. Using Eq. (a-5), and the notation

$$G_k=\int\mathfrak{G}U_kd\tau, \tag{a-7}$$

we obtain

$$\mathfrak{E}_k=\beta G_k\nu/(\nu_k+i\nu). \tag{a-8}$$

Now substitute the expansion (a-6) in Eq. (a-3), using the coefficients given by Eq. (a-8). Since

Imaginary part of $\mathfrak{E}_k=i\beta G_k\nu_k\nu/(\nu_k^2+\nu^2)$, we obtain

$$\Delta E=\pi\beta\gamma\sum G_k\nu_k\nu/(\nu_k^2+\nu^2). \tag{a-9}$$

Since the functions U_0, U_1, U_2 $\cdots$ form a complete orthogonal set, the following relation is satisfied[12]

$$\sum(G_k^2/\int G^2d\tau)=1. \tag{a-10}$$

By rewriting Eq. (a-9) as

$$\Delta E=\pi\beta\gamma(\int G^2d\tau)\sum\frac{G_k^2}{\int G^2d\tau}\cdot\frac{\nu_k\nu}{\nu_k^2+\nu^2},$$

we make the sum of the coefficients of $\nu_k\nu/(\nu_k^2+\nu^2)$ equal to unity.

[11] E. Goens, Wiss. Abhandl. Physik. Techn. Reichsanhalt **20**, 63 (1936).

[12] R. Courant and D. Hilbert, *Methoden der Mathematischen Physik*, (Springer, 1924) p. 36.

Internal Friction in Solids

III. Experimental Demonstration of Thermoelastic Internal Friction

C. ZENER,* W. OTIS† AND R. NUCKOLLS‡
Wayman Crow Hall of Physics, Washington University, St. Louis, Missouri
(Received July 13, 1937)

In order to demonstrate the presence of thermoelastic internal friction, the authors measured the internal friction of a copper reed over a wide frequency range (50 to 4000 cycles/sec.). They obtained a maximum precisely at the predicted frequency. The observed variation of internal friction with frequency proves that, over a wide frequency range, the internal friction due to the flow of heat back and forth across a reed is of a larger order of magnitude than that due to all other causes. Independent experiments of Bennewitz and Rötger on wires of silver, aluminum, brass, steel, and glass are shown to furnish an equally striking demonstration of thermoelastic internal friction.

IN a previous paper[1] one of the authors predicted that the internal friction of a reed vibrating transversely has a high maximum at the frequency

$$\nu_0 = (\pi/2)Dd^{-2}, \qquad (1)$$

where D is the thermal diffusion constant of the material, and d is the width of the reed in the plane of vibration. Although the literature on the internal friction of reeds is very extensive, a thorough search failed to find measurements made over a sufficiently wide range to test this prediction. In fact, all experiments with metal reeds had been made at frequencies of the order of one cycle per second. We therefore designed an experiment to measure the internal friction of a reed over a wide frequency band. This band was so chosen as to include the frequency ν_0 at which a maximum was expected.

The method adopted for the measurement of internal friction was that developed by Wegel and Walther,[2] namely the measurement of the width, $\Delta\nu$, at half-maximum of a resonance curve (plot of square of amplitude against frequency). A measure of internal friction at each resonance frequency is then given by

$$Q^{-1} = \Delta\nu/\nu.$$

Our measurements were made on copper reeds 3 mm wide cut from a cold rolled sheet 0.45 mm thick. Preliminary measurements showed that the lower the frequency, the greater was the care necessary to avoid energy loss through supports. Hence at lower frequencies the reed (30.0 cm long) was suspended at its center by a silk thread, only those types of vibration being investigated which had nodes at the center. At higher frequencies we used a shorter reed (13.0 cm long) soldered onto a massive block of brass.

Our measured values of Q^{-1} are given in Fig. 1, the crossed circles representing observations on the long reed, the full circles observations on the short reed. The full line curve gives the theoretical dependence upon frequency of that part of the internal friction which arises from the thermoelastic effect.[1] The theoretical and experimental maxima occur at precisely the same frequency.

While this experiment was in progress Benne-

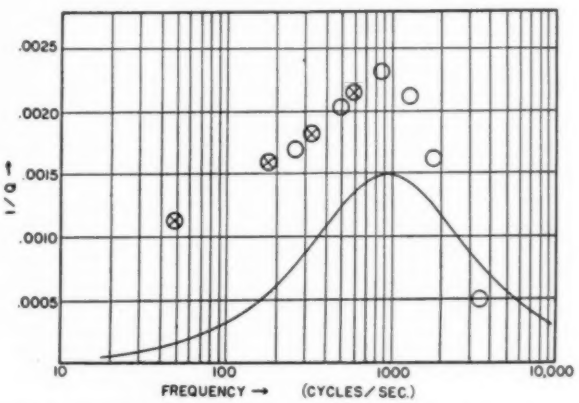

FIG. 1. Internal friction of vibrating reeds. Solid curve, calculated values. Open circles, reed 13 cm long, one end clamped. Circles with crosses, reed 30.5 cm long, both ends free.

* Now at the College of the City of New York.
† Now with the Southwestern Bell Telephone Co., St. Louis, Mo.
‡ Now at the University of Michigan.
[1] C. Zener, Phys. Rev. **52**, 230 (1937).
[2] R. L. Wegel and H. Walther, Physics **6**, 141 (1935).

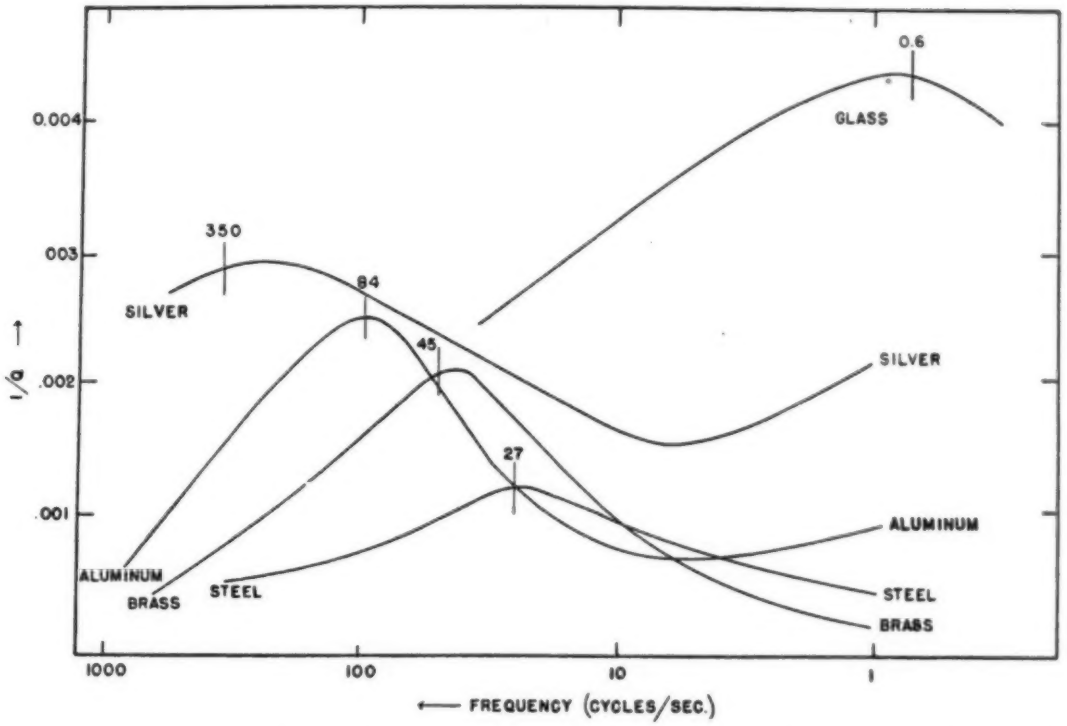

FIG. 2. Internal friction measured by Bennewitz and Rötger. The calculated values of the maxima are marked by vertical lines.

witz and Rötger[3] published the results of their experiments on the internal friction of wires vibrating transversely. Fig. 2 gives the curves which they fitted to their observations. While Bennewitz and Rötger correctly interpreted the maximum in each curve as due to a relaxation phenomenon, they did not realize the nature of this relaxation phenomenon.

We naturally suspected the maxima in these curves to be due to the thermoelastic effect. We thereupon calculated the position of each maximum by the theoretical formula

$$\nu_0 = 0.539 D/a^2$$

of the preceding paper, where a is the radius of the wire. The calculated value of ν_0 for each wire is shown as a vertical line in Fig. 2. In each case the calculated ν_0 practically coincides with the position of the observed maximum. The slight displacement to lower frequencies of the observed ν_0's for the metal wires with respect to the calculated ν's may be explained by an abnormal low thermal conductivity of the drawn metal wires.

A detailed comparison of these experiments with theory is given in Table I. As in the authors' experiment with a reed, the observed heights of the maxima are larger than the theoretical value $\frac{1}{2}(E_S - E_T)/E_S$. This discrepancy may also be due to the cold working of the samples. The curves for the soft wires of silver and aluminum show an unexpected rise in the low frequency range. Such a rise is also indicated by the curve for our copper reed. Since that part of internal friction which is due to plastic flow is larger the lower the frequency, this unexpected rise at low frequencies is probably due to plastic flow.

TABLE I. *Comparison of observed and calculated frequencies for maximum internal friction.*

Type of wire $2a$, in mm	glass 1.25	steel 1.0	brass 1.25	Al 1.5	Ag 1.01
ν_0, observed	0.66	25	40	83	240
$0.539 \times Da^{-2}$	0.5–0.6	27	45	84	350
†Obs. max. $\times 2 \times 10^3$	8.7	2.6	4.4	5.2	6.0
$10^3(E_S - E_T)/E_T$		2.4	3.2	4.6	3.4

† The observed maximum has been obtained by multiplying the λ_{max} of B. and R. by $2(\log_e 10)/\pi = 1.46$.

[3] K. Bennewitz and H. Rötger, Physik. Zeits. **37**, 578 (1936). These authors describe the internal friction by a logarithmic decrement λ, which is related to the Q^{-1} here used by the relation $Q^{-1} = (\log_e 10)\pi^{-1}\lambda$.

LETTERS TO THE EDITOR

Prompt publication of brief reports of important discoveries in physics may be secured by addressing them to this department. Closing dates for this department are, for the first issue of the month, the eighteenth of the preceding month, for the second issue, the third of the month. Because of the late closing dates for the section no proof can be shown to authors. The Board of Editors does not hold itself responsible for the opinions expressed by the correspondents.

The Penetrating Cosmic-Ray Particles

Data on range-curvature relations, and direct measurements of energy loss published by Anderson and the writer[1, 2] have been understandable on the assumption of the existence of particles whose mass is intermediate between that of an electron and a proton. Some of the range-curvature relations indicate that the mass is of the order of a hundred times the mass of the electron,[3, 4] but there are also reasons for believing that the mass may not be unique[4] and that many masses, ranging from a few times the electron mass up to very large values, may exist.

A basis for the existence of such particles can be found in a simple extension of de Broglie's first fundamental assumption, *viz.*, that an electron at rest may possess instead of just one normal mode, an indefinite number of them, whose frequencies are related in some way to the fundamental, which would itself be just the de Broglie proper frequency m_0c^2/h. De Broglie's second postulate would then lead to a set of proper masses, each mass being connected with its frequency by the usual quantum relationship. If then we make the further assumption that for each proper mass there exists an independent set of filled negative energy states, and that the Dirac equation applies, then it should be possible to calculate from the results of Oppenheimer-Plessett and Bethe-Heitler the probability that a photon will create a pair of particles of a given proper mass, provided that mass can exist.

The cross section per nucleus for creation of a pair of electrons by a photon of energy ξm_0c^2 may be written in the form $\Phi_1=\Phi^*f(\xi)$, where $\Phi^*=Z^2e^4/137\ m_0^2c^4$, and $f(\xi)$ is a function found by Bethe and Heitler.[5] The cross section for creation of a pair of particles of any allowed mass, km_0, would then be $\Phi_k=\Phi^*f(\xi/k)/k^2$; and the total cross section would be $\Phi=\Sigma\Phi_k$, summed over all permitted values of k. Without a new theory there is no way of deciding what masses would be permitted, but if we allow k to take all positive integral values we should obtain something close to an upper limit to what might reasonably be expected for the over-all cross section. Some approximate values of Φ_k/Φ_1 for various k's and photon energies (for absorption in lead) are listed in the table, along with the total cross section to be expected if all integral k's are allowed. At high energies Φ/Φ_1 will be slightly smaller for light materials.

TABLE I. *Relative cross sections for creation of pairs of mass km.*

ξ	k	Φ_k/Φ_1	$\sum_1^{k\,\max}\Phi_k/\Phi_1$
20	1	1.000	
	2	0.128	
(10 Mev)	3	0.029	
	4	0.011	
	5	0.002	1.17
34	1	1.000	
	2	0.144	
(17 Mev)	3	0.047	
	4	0.018	
	5	0.010	
	>5	Sum =0.01	~1.23
2000	k	$1/k^2$	1.64

The above hypothesis provides a mechanism for the production of penetrating particles which may be capable of accounting for the departure, at the lower altitudes, of the ionization difference curve, observed by Bowen, Millikan and Neher,[6] from the one calculated theoretically by Carlson and Oppenheimer on the basis of the Bethe-Heitler theory. It is clear, as pointed out by Bowen, Millikan and Neher, that the sea-level ionization must be produced by penetrating particles which are mainly secondaries of the incoming radiation; and the fact that there is approximate equality between particles of positive and negative charge suggests that they are created in pairs in the same way as are ordinary electrons. It is probable that the cross section found above by the assumption of all integral masses is somewhat too high to fit the observed ionzation curve. There is, however, no reason for this particular quantization, and the choice that is made must be indicated by detailed calculations and by further experiments.

Table I shows that if particles of mass only a few times the electron mass can be created in pairs, then they should be present among the pairs observed from the bombardment of lead by 17 Mev γ-rays. A simple calculation shows that the observed $H\rho$ distributions would be only inappreciably altered by the presence of such pairs; for example, the summed $H\rho$ values for a pair of mass 4 would be lower than for a pair of electrons by from 3 to 10 percent, depending on how the energy were divided between the components of the pair. It is quite certain that masses of 3 or lower would be difficult to detect by the ionization along their cloud-tracks without using special precautions to facilitate the counting of drops. If masses 4 and 5 exist, they should be present in a total amount of about 3 percent, of which about a fifth to a tenth might be expected to lie in an energy range where their presence could be detected easily from the observed track density. An examination of the pair photographs obtained by Delsasso, Fowler and Lauritsen, and kindly loaned to the writer, has revealed no instances of an ionization definitely greater than could be attributed to an electron. About 3 such

tracks could have been expected, although it is difficult to make a very good estimate.

The only real experimental evidence against the suggestion given here appears to lie in the above authors' determination of the absorption coefficient of 17 Mev γ-rays in lead.[7] This comes out lower instead of higher than the theoretical value, the latter lying just within the estimated probable error. However, the choice of odd masses, for example, instead of all integral ones would lower the expected excess absorption from 23 percent to only 6 percent, or about half the probable error. The foregoing hypothesis, then, offers a possible interpretation of the "new particle" difficulty, which has yet to be examined adequately by experiment.

SETH H. NEDDERMEYER
California Institute of Technology,
Pasadena, California,
December 14, 1937.

[1] Anderson and Neddermeyer, Phys. Rev. **50**, 270 (1936).
[2] Neddermeyer and Anderson, Phys. Rev. **51**, 884 (1937).
[3] Street and Stevenson, Phys. Rev. **52**, 1003 (1937); see also Corson and Brode, Abstract No. 27, Stanford Meeting of the Physical Society, December 18, 1937.
[4] Paper to be published.
[5] Heitler, *Quantum Theory of Radiation*, p. 201.
[6] Bowen, Millikan and Neher. (In press.)
[7] Delsasso, Fowler and Lauritsen, Phys. Rev. **51**, 398 (1937).

Multivibrator Geiger Counter Circuit

The mechanism for extinguishing the arc produced in a Geiger counter discharge resulting from the passage through it of an ionizing particle is simply the lowering of the voltage across the tube to a value below that necessary to maintain the arc. A condition of stability is that the duration of the lowering of the voltage be long enough to permit the removal of the ions produced in the discharge. The standard procedure has been to use a resistance in series with the tube sufficiently large (10^8 to 10^{10} ω) to produce the necessary drop. The relatively slow recovery is insured by the time needed to charge up the counter through so large a resistance.

Neher and Harper[1] have described a much more efficient circuit which possesses the characteristics that it is extraordinarily fast, but has the cathode of the counter at a high impedance above ground, and in addition requires the first vacuum tube to stand the entire voltage of the counter. Another fast circuit has been described by Libby, Lee, and Ruhen.[2]

The circuit here suggested employs a multivibrator so biased that it cannot oscillate. The circuit possesses the novel feature that the length of the pulse is limited by the vacuum tube circuit and not by the counter. The mechanism may be described by stating that the counter momentarily upsets the stability of the circuit by varying the voltage on one of the grids of the multivibrator so that one pulse takes place.

Alternatively, the action may be described as follows. The passage of the ionizing particle causes a sudden lowering of the voltage on the wire electrode and hence of the grid of the first tube. The change is twice amplified, and the amplified pulse of correct phase is fed back to the counter producing a regenerative effect. Whereas the initial lowering of the grid, resulting from the counter current through the megohm resistor, would not have been

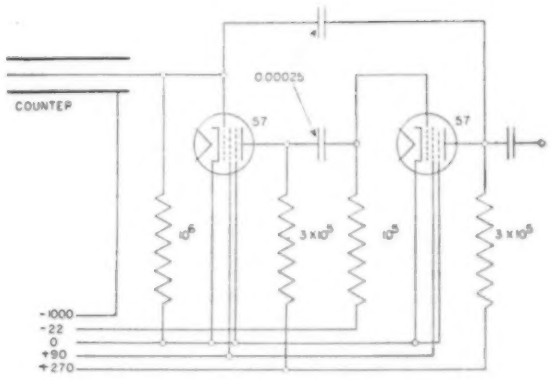

FIG. 1. Diagram of counter circuit.

sufficient to extinguish the arc, the regenerative effect of the coupling throws the entire available voltage drop of the vacuum tube circuit on the wire electrode. The recovery of the circuit is fixed by the resistances and capacities of the circuit, compared to which the capacity of the counter is negligible. The shape of the pulse is rectangular, the wave shape being fixed by the multivibrator.

With small counters, the length of the pulse has been reduced to as much as 10^{-4} second, but only at a loss of the voltage range of the counter itself. With the constants shown on Fig. 1, the circuit will count as many as 2,000 random counts per second. It should be pointed out, however, that the statistics of this counter are entirely different from those of previous circuits.[3] Here the maximum counting rate is the oscillation frequency of the multivibrator, independent of the Geiger counter. The passage of an ionizing particle while the wire is on the crest of the rectangular pulse has no appreciable effect because the counter is below its critical voltage and because the grid of the first tube is already so negative that the first tube cannot respond to any further small pulses were they forthcoming.

The advantages of the circuit are: (1) the highest resistor ever needed is 10^6 ω; (2) the outside electrode of the counter is insensitive to pick-up as it is connected directly to the high potential; (3) different counters may be used without altering the resolving time of the circuit; (4) all tubes are used within the manufacturer's ratings; (5) the pulse on the counter wire can be studied with an oscilloscope by connecting it directly through a reasonably large condenser; and (6) either sign pulses may be taken off by connecting either to the first or to the second tube. A disadvantage of the circuit is that the high potential must be turned on rapidly to prevent a continuous discharge. This results from the condenser coupling between the tubes of the multivibrator.

The author is indebted to Professor Street for helpful discussions.

I. A. GETTING*
Research Laboratory of Physics,
Harvard University,
Cambridge, Massachusetts,
December 9, 1937.

* Society of Fellows, Harvard University.
[1] Neher and Harper, Phys. Rev. **49**, 940 (1936).
[2] Libby, Lee and Ruhen, Rev. Sci. Inst. **8**, 38 (1937).
[3] Schiff, Phys. Rev. **50**, 88 (1936).

Radioactive Isotopes of Zinc and Cobalt

Professor E. O. Lawrence gave to one of us some copper filings of the Berkeley cyclotron's tank. The filings came from the deflecting plate which is submitted to strong deuteron and neutron bombardment and showed an intense radioactivity. Three months at least elapsed between the ending of the bombardment and the beginning of the measurements. In spite of this the filings showed a strong activity due to P^{32} which is an ever-present surface contamination of the samples we received from Berkeley. This isotope was chemically separated and used in some biological investigations.[1]

The copper filings were carefully analyzed. Even commercial copper is generally very pure and we assume that any activity, but for surface contaminations, is due to transmutation of Cu into radioactive isotopes.

The analysis was carried on with standard methods[2] and the following elements were definitely tested by addition to the original solution of the radioactive copper and subsequent separation: (1) arsenic, cadmium, aluminum, iron, manganese, lithium, gallium, carbon, nickel, calcium, copper, barium, sulphur; (2) sodium, cobalt, zinc, phosphorus.

The elements of the first group were found to be inactive, also many other elements which are not mentioned can be ruled out as carriers of any activity. To take into account surface contaminations we made a test by combustion of carbon with negative result, whereas P^{32} was separated as we have already pointed out. A weak radioactivity was found in sodium. This is possibly due to Na^{22},[3] but on account of its smallness we did not follow this activity. The elements enumerated above were chosen partially for chemical reasons in order to rule out as many elements as possible, and partially because they were suspected of being active.

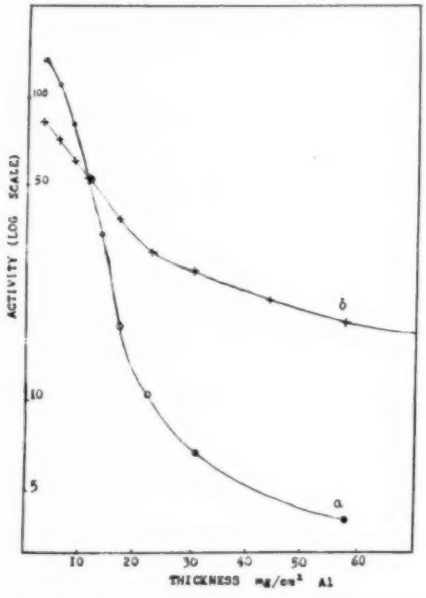

FIG. 1. Absorption curves of cobalt (a) and zinc radiation.

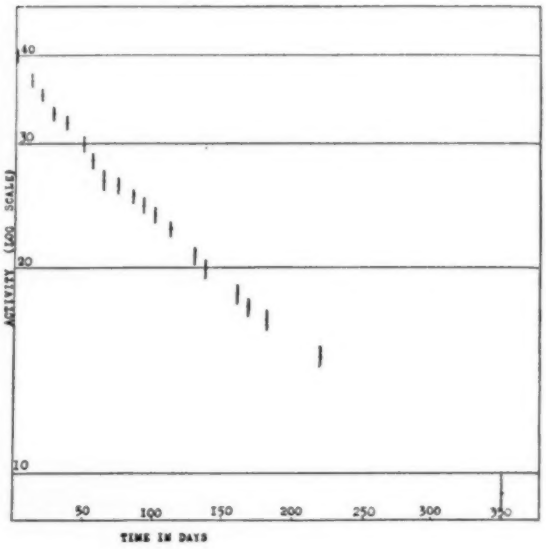

FIG. 2. Decay curve of cobalt.

Fairly strong activities were found in cobalt and zinc precipitates.

Cobalt and zinc, nickel and manganese were precipitated together in the ammonium sulphide group after having been added to the original solution.

Nickel and cobalt were separated by diacetylglioxime and α-nitroso-β-naphthol, or first by precipitation of nickel with diacetylglioxime and subsequent precipitation of cobalt with sulphuretted hydrogen.

Zinc and cobalt were separated by the method of Cl. Zimmermann[2] and by the method of Smith and Brunner.

Manganese was separated from nickel and cobalt with sulphuretted hydrogen in acetic solution. Zinc sulphide was also dissolved and reprecipitated as ammonium zinc phosphate.

From the pure precipitates we deposited zinc electrolytically from a sodic solution according to Spitzer, and cobalt from an ammoniacal solution according to Gibbs.

Zinc. The activity of zinc was measured on a thin electrolytic deposit and on zinc sulphide; the decay curves agree within the limits of experimental error. They were taken both on an ionization chamber closed by an aluminum foil of 0.1 mm thickness filled with CO_2 at three atmospheres pressure and on an ionization chamber closed by two aluminum foils of 0.001 mm thickness.

As a result of four of such curves measured for about 300 days a half-value period of 245 days was found. The decay curves are simple exponentials within experimental error.

The absorption curve of the radiation is given in Fig. 1, curve *b*.

Copper has two stable isotopes Cu^{63} and Cu^{65}. By the usual (D, n) reaction these isotopes would give rise to Zn^{64} and Zn^{66} both of which are stable. With the rather unusual (D, γ) reaction one would get Zn^{65} or Zn^{67}. The latter is known as a stable isotope; Zn^{65} according to Livingood[4] is radioactive with a period of one hour. It does not seem

possible to explain the existence of our radioactive zinc without assuming that it is isomeric with some nucleus already known. With this assumption all masses 64, 65, 66, 67 become possible. The possibility that the activity is due to neutron bombardment must also be borne in mind, though no zinc could be formed from copper by the usual primary neutron processes.

Cobalt. The activity of cobalt was examined by the same means as that of zinc. Electrolytic metallic cobalt, cobalt sulphide and the precipitate by α-nitroso-β-naphthol were examined. The decay curves show an indication of a bending; this bending seems to be present in all curves. Fig. 2 gives an example of such curves. The shape of the curve can be accounted for by admitting two radioactive cobalt isotopes. The longest period can be rather accurately determined and is of about 215 days. The shorter and, in our case, much weaker one is of the order of magnitude of one month. The absorption curve of the radiation is shown in Fig. 1, curve *a*. Two such curves were taken at about a six months interval. However, they do not show any remarkable difference in shape.

Magnetic deflection experiments show that the particles emitted are mostly electrons. There is also a γ-radiation.

We separated nickel from old cobalt preparations in order to see if cobalt decaying produced any radioactive nickel. No activity was found in nickel.

The formation of radioactive cobalt from copper under deuteron bombardment is not easily explained. Possibly radioactive cobalt is formed from copper under the bombardment of the neutrons always present in the cyclotron. In this case the processes would be $Cu^{63}(n, \alpha)\ Co^{60}$ or $Cu^{65}(n, \alpha)\ Co^{62}$.

If one of our activities is to be identified with an already known long period of cobalt[5] the mass 60 for the radioactive isotope seems to be most probable.

We have tried to find a radioactive cobalt by bombarding copper with neutrons of 500 mC of Rn+Be for several weeks and separating cobalt chemically. No activity was found in this way, but of course the neutron bombardment of the cyclotron is much more intense than ours can have been. Decisive evidence showing that the primary process is due to neutrons could be had by taking copper of a part of the tank which is not hit by deuterons.

Our warmest thanks are due to Professor E. O. Lawrence and to the Radiation Laboratory of the University of California (Berkeley) who by their invaluable gift made this investigation possible.

C. Perrier
M. Santangelo
E. Segrè

Royal University,
Palermo, Italy,
December 6, 1937.

[1] C. Artom, G. Sarzana, C. Perrier, M. Santangelo and E. Segrè, Nature **139**, 836, 1105 (1937)
[2] For all these methods see e.g. Treadwell's *Analytic Chemistry*.
[3] L. Jackson Laslett, Phys. Rev. **52**, 529 (1937).
[4] Livingood, Phys. Rev. **50**, 425 (1936).
[5] Sampson, Ridenour and Bleakney Phys. Rev. **50**, 382 (1936); Risser, ibid. **58**, 768 (1937).

Demagnetization Coefficient of Oblate Spheroids

The demagnetization coefficient N for an oblate (disk-like) spheroid in a direction normal to the axis of rotation is generally given in the form

$$N=2\pi\left[\frac{(1-e^2)^{\frac{1}{2}}}{e^3}\sin^{-1}e-\frac{1-e^2}{e^2}\right], \qquad (1)$$

where e is the eccentricity. In terms of m, the ratio of the major to the minor axis, this becomes

$$N=\frac{2\pi}{m(1-1/m^2)}\left[\frac{1}{(1-1/m^2)^{\frac{1}{2}}}\sin^{-1}(1-1/m^2)^{\frac{1}{2}}-\frac{1}{m}\right]. \qquad (2)$$

Neither form lends itself to rapid calculation, but it happens that an empirical equation can be used which is not only simple, but exceedingly accurate as well. A plot of $1/N$ against m results in a very straight line, except for values of m near 1. The equation of this line is

$$1/N=0.1013m+0.127. \qquad (3)$$

An idea of its accuracy can be obtained from the following comparison:

m	$1/N$ (Eq. (1))	$1/N$ (Eq. (3))
1	0.239	0.228
5	0.638	0.634
10	1.143	1.140
20	2.153	2.153
50	5.200	5.192
100	10.26	10.26

This empirical equation should prove useful in connection with magnetization and torque measurements on oblate spheroids, and it is also applicable to a flat disk, insofar as a disk can be said to have a definite demagnetizing coefficient.

L. P. Tarasov

Research Laboratory,
General Electric Company,
Schenectady, New York,
November 15, 1937.

The Zeeman Effect of the p^5d Configurations of Neon and Argon

We are just completing an investigation of the Zeeman effect in neon and argon, using a capillary discharge at high frequency in a field of about 28,000 gauss.

In the case of neon, a few members of the $2p^53d$, all of the $2p^54d$, and some of the members of $2p^55d$ and $2p^56d$ configurations are sufficiently resolved to allow the determination of the g factors. The agreement between the values thus found and the values calculated from Sampson's[1] and Shortley's[2] values is extremely satisfactory.

The results for argon also show very good agreement with the values computed from Sampson's parameters, although the agreement for the $3p^55d$ configuration is more satisfactory for $j=2$ than for $j=1$. Argon also shows an anomaly for the $j=2$ levels of the $3p^54d$ and $3p^55d$. While the levels called s_1'' and s_1'''' have practically identical g values ($g=1.00$) for the $3p^54d$, the values for $3p^55d$ are 1.2 and 0.8, showing that $5d$ is very much smaller for the $3p^54d$ than for the $3p^55d$.

Neon shows several interesting examples of the Paschen-Back effect in the p^5d configurations. The patterns have been calculated using the matrix mechanics and the computations are in good agreement with the observations.

A complete report will be published in the very near future.

J. B. Green
J. A. Peoples, Jr.
B. Fried

Mendenhall Laboratory of Physics,
Ohio State University,
Columbus, Ohio,
December 13, 1937.

[1] Sampson, Phys. Rev. **52**, 1157 (1937).
[2] Shortley, Phys. Rev. **44**, 671 (1933).

Heavy Particles and the Neutrino

In a previous letter the writer[1] has suggested that the x particle may be produced by the absorption of a photon by an ordinary electron. Corson and Brode[2] give the rest mass of a heavy particle as 350 m_0, while Street and Stevenson[3] give 130 m_0. (m_0 is the rest mass of the ordinary electron. See previous letter for definitions.) To produce a rest mass of p_2m_0 a photon of energy $(p_2^2-1)m_0c^2/2$ is needed. When $p_2=350$, this energy is 31,000 Mev. The values 130 and 350 for p_2 and still other values are consistent with the writer's idea.

If a photon of α_1 greater than $(p_2^2-1)/2$ strikes an ordinary electron ($p_1=1$) at rest ($\beta_1=0$), an energy $\alpha'm_0c^2$, where $\alpha'=(p_2^2-1)/2$, is absorbed from the photon, giving rise to a particle of mass p_2m_0 with a velocity $\beta'c=c(p_2^2-1)/(p_2^2+1)$ in the direction of the photon. The remaining energy $(\alpha_1-\alpha')m_0c^2$ is treated as that of a primary photon which is to be scattered in the direction θ according to the principles of the Compton effect by an electron of rest mass p_2m_0 traveling with an original speed $\beta'c$ in the direction of the primary photon.

Perhaps heavy particles other than the heavy electron may be produced according to Eqs. (1) and (2) of the previous letter. To produce a heavy particle of mass p_2m_0 from a particle of mass p_1m_0 which is at rest a photon

$$h\nu_1=m_0c^2(p_2^2-p_1^2)/2p_1 \tag{1}$$

is needed. The kinetic energy produced by complete absorption of this photon is

$$T_2=m_0c^2(p_2-p_1)^2/2p_1. \tag{2}$$

So, to produce a heavy proton with kinetic energy 940 Mev, a photon of energy 2260 Mev is needed. From (2), $p_2=2.414p_1$.

In a β-ray radioactive transformation the β-rays are found to have a continuous spectrum of speeds up to a certain maximum speed β_0c, such that the energy relation

$$M_1c^2=M_2c^2/(1-\beta_2^2)^{\frac{1}{2}}+m_0c^2/(1-\beta_0^2)^{\frac{1}{2}} \tag{3}$$

holds, where M_1 and M_2 are the rest masses of the parent and product atoms, respectively, and β_2c is the recoil velocity of M_2. The writer suggests that the energies of all β-rays in the spectrum are the same but that different β-rays have different rest masses pm_0 and different velocities βc, such that

$$m_0c^2/(1-\beta_0^2)^{\frac{1}{2}}=pm_0c^2/(1-\beta^2)^{\frac{1}{2}}. \tag{4}$$

From (4), it is seen that, as p increases from unity to $1/(1-\beta_0^2)^{\frac{1}{2}}$, β decreases from β_0 to zero. Allowing the expelled β-particle to have a variable rest mass thus removes the need for postulating the neutrino. The kinetic energy distribution curves for β-rays have been calculated on the basis of the rest mass always being m_0. According to the writer's suggestion, variation of $H\rho$ implies variation of p. From the distribution curve with respect to $H\rho$ for the β-particles from RaE, it is estimated that more than 90 percent of the electrons have a rest mass greater than $2m_0$ and a kinetic energy less than half the maximum kinetic energy, 2.06 m_0c^2. The average kinetic energy for all the electrons is less than one-third of the maximum. This is in agreement with Meitner and Ortheim's calorimetric experiment[4] on RaE, provided that the life of the heavy electron is long compared with the duration of the experiment, or that the γ-radiation which the heavy electron ultimately emits in returning to m_0 was not recorded in Meitner and Ortheim's experiments.

G. E. M. Jauncey

Wayman Crow Hall of Physics,
Washington University,
St. Louis, Missouri.
December 15, 1937.

[1] Jauncey, Phys. Rev. **52**, 1256(L) (1937).
[2] Corson and Brode, Bull. Am. Phys. Soc., December 2 (1937).
[3] Street and Stevenson, Phys. Rev. **52**, 1004 (1937).
[4] Meitner and Ortheim, Zeits. f. Physik **60**, 143 (1930).

Proceedings of the Metropolitan Section of the American Physical Society

MEETING OF OCTOBER 29, 1937

THE first meeting of the Metropolitan Section of the American Physical Society for the season 1937–1938 was held on Friday, October 29, 1937 in the Pupin Physics Laboratories of Columbia University. The following papers were presented:

The Measurement of the Elastic Constants of Crystalline Sodium at Low Temperatures. S. L. QUIMBY.
Semi-Conductors. W. H. BRATTAIN.
Order and Disorder Theory as Applied to Alloys. W. SHOCKLEY.
Ferromagnetic Anisotropy. J. H. VAN VLECK.

W. S. GORTON,
Secretary-Treasurer

Proceedings of the New England Section of the American Physical Society

MINUTES OF THE WELLESLEY MEETING

October 23, 1937

THE eleventh regular meeting of the New England Section was held at Wellesley College on October 23, 1937. The morning session was devoted to contributed papers, a business meeting, and a colloquium on the College Entrance Examination Board requirement in physics led by R. S. Bartlett and A. T. Waterman. At the business meeting the following officers were elected for the ensuing year:

LOUISE S. MCDOWELL, *Chairman*
K. S. VAN DYKE, *Vice Chairman*
J. C. BOYCE, *Secretary-Treasurer*
K. T. BAINBRIDGE AND G. F. HULL, *members of Program Committee.*

A rising vote of thanks was extended to Professor McDowell and to her colleagues of the Physics Department of Wellesley College for their generous hospitality.

The afternoon session consisted of two invited papers, "Cosmic Rays and the Earth's Magnetic Field" by M. S. Vallarta and "Review of the Evidence for the Existence of a New Particle" by J. C. Street.

Eighty-five persons were present at the morning session and 100 at the afternoon session. The Wellesley physics laboratories were open for inspection throughout the day.

The winter meeting will be held at New Haven, Connecticut, on January 15, 1938.

Abstracts of the contributed papers are given below.

J. C. BOYCE, *Secretary-Treasurer,*
New England Section

ABSTRACTS

1. An Acoustical Study of the Intake Process in an Internal-Combustion Engine. HARRY SCHECTER AND PHILIP M. MORSE, *Massachusetts Institute of Technology.*—An investigation has been made of the dynamics of the intake system of a four-stroke single-cylinder engine, with particular reference to the effect of a long intake pipe. A mathematical analysis has been developed, based on a study of the forced motion of the air in the valve port, with the periodic cylinder intake as the driving force. The motion is assumed to be controlled essentially by the stiffness of the air in the cylinder. Experimental measurements have been made, of the instantaneous pressure at the valve port and of the power of the engine, with varying lengths of intake pipe. Comparison of theory and experiment shows that the reaction of the standing waves back on the flow through the valve is an important factor. When

this reaction is included in the driving force, the theoretical results show good agreement with experiment. In general, a supercharging effect is obtained when the fundamental frequency of the intake pipe (considered as closed at one end) is about 3, 4 or 5 times the engine cycle frequency. The corresponding increase in power is about 15 to 20 percent, and may be as much as 40 percent.

2. Acoustics of the Combustion Chamber. C. S. DRAPER, *Massachusetts Institute of Technology.*—Instruments and methods are discussed for studying the pressure waves produced by detonation in the cylinder of an internal combustion engine. It has been shown that a system of standing waves accompanies detonation. In order to study these waves photographic records of the rate of change of pressure are taken simultaneously at two points in the engine cylinder. Amplitude and phase data taken from these records makes it possible to determine the modes of vibration which are excited in a given case. Electromagnetic pick-up units of very high natural frequency are used for detecting the pressure waves. The output of these units is coupled to two cathode-ray oscillograph tubes by means of special amplifiers. The apparatus is described and a sample detonation record is shown.

3. Surface Magnetization of Cobalt. W. C. ELMORE, *Massachusetts Institute of Technology.*—The magnetic powder patterns of cobalt crystals have been studied in an attempt to identify the magnetic structure responsible for them. Suitable cuts of selected grains in a small cobalt ingot were prepared by careful sawing followed by metallurgical or electrolytic polishing. Patterns were formed (for observation with microscope) by depositing colloidal γ-Fe_2O_3 onto the polished ingot. On all cuts of the crystals two reciprocal patterns (i.e. with spaces and deposits interchanged) and an intermediate pattern were found, corresponding to plus, minus and no applied normal field. The basal plane patterns possessed considerable detail in places suggesting hexagonal symmetry. They were relatively insensitive to moderate increases in applied field. On cuts approximately perpendicular to the basal plane were found patterns of narrow no-field lines, spaced about 60μ apart, running parallel to the principal axis. Depending on its sign a small applied normal field spread the colloid into one or the other set of alternate bands between these lines. Further increase in field caused the bands to widen and finally to merge together. These and other features can be interpreted in terms of a simple model of magnetized prisms, traversing the entire crystal, but subdividing near crystal boundaries and exposed surfaces.

4. The Effect of Tension on the Electrical Resistance of Single Tetragonal Tin Crystals. MILDRED ALLEN, *Mount Holyoke College.*—The adiabatic tension coefficient of resistance of single tetragonal tin crystals has been determined for various orientations. Bridgman's theory, as modified by Cookson, has been extended to the tetragonal case and the experimental points found to lie within experimental error on the curves computed according to this theory. Without correction for strain, the tension coefficients depend both on the primary and secondary orientations of the crystal; for $\theta=90°$ they depend on the secondary orientation which is contrary to what has been found in the case of the trigonal crystals studied. When corrected for strain, the tension coefficients are found to be independent of the secondary orientation whatever the primary orientation, again contrary to what holds for trigonal crystals.

5. The Crystal Structure of Uranium. C. W. JACOB AND B. E. WARREN, *Massachusetts Institute of Technology.*—X-ray powder patterns were made of uranium using Cu $K\alpha$ radiation. By a method involving orthogonal nets in the reciprocal lattice, the pattern was indexed in terms of an orthorhombic cell with axes; $a=2.852$, $b=5.865$, $c=4.945$. From the density there are 4 atoms per unit cell. The space group is $V_h^{17}Cmcm$ and the atoms are in position $4c$. The parameter is determined from the intensities as $y=0.105 \pm 0.005$. The structure can be considered as a deformed hexagonal close packed structure with 4 nearest neighbors at about 2.8A and 8 next nearest at 3.3A. The 4 closest neighbors indicate a tendency to form covalent bonds. The uranium structure is not that of a true metal. The material should be considered as a pseudo-metal such as antimony or gallium. The high electrical resistivity of uranium is in keeping with the structure deduced. Uranium does not belong in the Cr, Mo, W group.

6. A New Ether-Drift Interferometer of High Efficiency. W. B. CARTMEL, *Université de Montréal.*—In an interferometer of obliquity Ω the angle between the end mirror normals is $(\pi/2-\Omega)$. For an oblique interferometer the writer has deduced the formula

$$F=(2l/\lambda)\sin\Omega(v^2/c^2)\sin 2(\theta\pm\tfrac{1}{2}\Omega).$$

Since Ω equals zero in a rectangular interferometer, no second order fringe shift is to be expected with a perfectly rectangular interferometer, and according to the above formula an interferometer has a maximum efficiency for ether-drift measurement when Ω equals 45°. Preliminary measurements with a 45° interferometer 70.2 cm long, have shown a displacement of a few hundredths of a fringe, whereas with a velocity of 200 km/sec., more than a fringe was expected. I find that there are two solutions to Miller's astronomical calculations based on Fig. 17, p. 223 of his paper,[1] one of which yields the values $\delta=-72°\ 15'$, $V=202$ km/sec. which agrees closely with what Professor Miller finds, but the other solution gives us $\delta=+22°\ 26'$, $V=44.7$ km/sec. The displacement expected with this new value of V, is 0.0476 of a fringe. My experiments have not yet been carried to the point where an exact comparison may be made, but there seems to be more than 0.0478 of a fringe, part of which is no doubt due to the first order effect.

[1] Dayton C. Miller, Rev. Mod. Phys. **5**, 203 (1933).

7. Preliminary Report on the Analysis of the Spectrum of Singly Ionized Cerium, Ce II. WALTER ALBERTSON AND GEORGE R. HARRISON, *Massachusetts Institute of Technology.*—A preliminary attack on the analysis of Ce II

made several years ago with the Harrison interval sorter[1] showed that more accurate wave-length values would be required for satisfactory application of the combination principle. A new description of the cerium spectrum made on the M.I.T.-W.P.A. wave-length program is now available, and application to this data of the interval sorter and of a newly designed interval recorder, to be described, has resulted in a rapidly growing quadratic array. 430 lines have thus far been classified as resulting from combinations between 24 low levels and 40 mid-lying levels. The average deviation between observed and calculated term values is less than 0.02 cm^{-1}, and 44 percent of the lines fit the array to 0.01 cm^{-1}. Most wave-length values appear accurate to within 0.002A. Relative J values of the levels have been determined, and absolute J values are known to within one unit. Unresolved Zeeman patterns confirm the analysis to the extent of showing proper pattern types for classified lines. Our results are not in agreement with those of Haspas,[2] who has published the results of a previous attack on this spectrum.

[1] Harrison, Rev. Sci. Inst. **4**, 581 (1933).
[2] Haspas, Zeits. f. Physik **96**, 410 (1935).

8. The Ultraviolet Absorption of Simple Hydrocarbons. IV. Unsaturated Cyclic Hydrocarbons in the Schumann Region. EMMA P. CARR AND HILDEGARD STÜCKLEN. *Mt. Holyoke College.*—The absorption spectra of cyclohexene, cyclopentene, 1-3-cyclohexadiene, and benzene have been examined in vapor phase in the region $\lambda = 2300$A to 1600A and the results are presented in the form of graphs. The spectra of these cyclic hydrocarbons show sharp narrow bands in contrast with the diffuse bands of all of the olefins except cis- and transbutene-2 and isobutene. The electronic excitation responsible for the first bands in this region is practically independent of the cyclic structure of the molecule since the wave-number of the first absorption band for each compound agrees closely with that obtained for olefins having the same number and arrangement of hydrogen atoms around the double bond. Vibrational frequencies associated with the C=C and C−H bonds have been identified in the long wave portion of the spectra of all except cyclopentene. The electronic excitation for cyclopentene shows only a series of equally spaced narrow bands of increasing intensity, although bond separations of the order of the C=C and C−H vibrations are evident in a higher electronic level. The spectrum of cyclohexene indicates the existence of from 4–5 different electronic levels. The spectrum of cyclohexadiene is characterized by a series of more than fifty narrow bands with an average separation of 100 $cm.^{-1}$ superimposed upon diffuse bands which show separations corresponding to characteristic vibrational frequencies. On the basis of the general characteristics of the spectra of benzene, cyclohexene, and 1-3-cyclohexadiene and their analogy to the spectra of the ethylene derivatives, the excitation responsible for the absorption beginning about 48,000 cm^{-1} has tentatively been ascribed to the transition $^1A_1 \rightarrow {}^1B_1$ as in the olefins.

9. The Isotopic Constitution of Xe, Kr, As, Cs, I and Be. ALFRED O. NIER, *National Research Fellow, Harvard University.*—A mass spectrometer will be described which has been constructed for the purpose of making accurate determinations of relative abundances of isotopes. Xenon was found to consist of the isotopes 136, 134, 132, 131, 130, 129, 128, 126 and 124 present in amounts proportional to the numbers 33.2, 39.1, 100.0, 78.5, 15.1, 97.3, 7.06, 0.327 and 0.347, respectively. A search was made for other possible isotopes. The following upper limits can be set for their abundances relative to Xe^{132}: Xe^{128}, Xe^{127}, Xe^{125}, and Xe^{123}, 1/15,000; Xe^{127}, 1/30,000; Xe^{125}, Xe^{123} and Xe^{122}, 1/60,000. Krypton was found to consist of the isotopes 86, 84, 83, 82, 80, and 78 present in amounts proportional to the numbers 30.6, 100.0, 20.2, 20.2, 3.52, and 0.608, respectively. The following upper limits relative to Kr^{84} can be set for the abundance of other possible isotopes: Kr^{88}, 1/50,000; Kr^{87} and Kr^{85}, 1/25,000; Kr^{81}, Kr^{79}, Kr^{77} and Kr^{76}, 1/50,000. Arsenic, caesium, and iodine were shown to be single to a very high degree. A search for Be^9 revealed that if it existed it must be less than 1/100,000 of Be^9.

10. Artificial Radioactivity of Tantalum. O. OLDENBERG, *Radiation Laboratory, University of California and Harvard University.*—Radioactivity has been induced in tantalum by slow neutrons, fast neutrons, and fast deuterons. (1) Slow neutron capture leads to Ta^{182} with a lifetime of 97 days. (2) Fast neutron bombardment excites, in addition, an 8.2 hour period with the emission of electrons, K radiation of Ta, and γ-rays. The process responsible for these effects is probably the capture of one neutron with the ejection of two neutrons. The product nucleus, Ta^{180}, goes over to Hf^{180} largely by K electron capture; in this process either γ-rays are emitted or, by their internal conversion, extranuclear electrons ejected. (3) Deuteron bombardment of tantalum leads to a decay curve affected to such an extent by impurities that the tantalum activity cannot be observed clearly.

11. Colloquium on the College Board Examination in Physics. RUSSELL S. BARTLETT, *Exeter Academy,* AND ALAN T. WATERMAN, *Yale University.*

12. Cosmic-Rays and the Earth's Magnetic Field. M. S. VALLARTA, *Massachusetts Institute of Technology.*

13. Review of the Evidence for the Existence of a New Particle. J. C. STREET, *Harvard University.*